SYNTHESIS AND BIOLOGICAL EVALUATION OF INDOLOAZEPINE AND ITS ANALOGS AS AN INHIBITOR OF CHK2

Ву

Thu Ngoc Thi Nguyen

A DISSERTATION

Submitted to
Michigan State University
In partial fulfillment of the requirements
For the degree of

DOCTOR OF PHILOSOPHY

Chemistry

2011

ABSTRACT

SYNTHESIS AND BIOLOGICAL EVALUATION OF INDOLOAZEPINE AND ITS ANALOGS AS AN INHIBITOR OF CHK2

By

Thu Ngoc Thi Nguyen

This dissertation is focused on two objectives. The first objective comprises the improvement of the synthesis of (Z)-5-(2-amino-4-oxo-1H-imidazol-5(4H)-ylidene)-2,3,4,5-tetrahydroazepino[3,4-b]indol-1(10H)-one, also referred to as indoloazepine. The second objective is to evaluate indoloazepine as a cellular inhibitor of checkpoint kinase 2 and its use as an adjuvant drug for cancer therapy. The first chapter identifies checkpoint kinase 2 (Chk2) as a viable adjuvant drug target for cancer therapies. The second chapter discusses the improvement in a previously reported synthesis of indoloazepine. The third chapter describes the biological evaluation and the cellular inhibition of Chk2 by indoloazepine. Finally, the fourth chapter describes the use of indoloazepine as a potential chemosensitizer via the nuclear factor-kappa B (NF-κB) pathway.

DNA damage induced by ionizing radiation activates the ataxia telangiectasia mutated pathway, resulting in apoptosis or DNA repair. The serine/threonine checkpoint kinase, Chk2 is an important transducer of this DNA damage signaling pathway and mediates the ultimate fate of the cell. Chk2 is an advantageous target for the development of adjuvant drugs for cancer therapy; because inhibition of Chk2 allows normal cells to enter cell cycle arrest and carry out DNA repair, whereas many tumors bypass cell cycle checkpoints. Chk2 inhibitors may thus have a radioprotective affect on normal cells. Previously, our research group reported the synthesis of hymenialdisine-

derived indoloazepine and its ability to inhibit the kinase activity of Chk2 using purified kinase.

The previous synthesis of indoloazepine reported by the Tepe research group yielded indoloazepine in 12%. The synthetic route utilized steps that resulted in unstable intermediates that were difficult to isolate with the final step requiring purification twice by column chromatography. The improved synthesis reported here increased the overall yield to 30% utilizing a thiohydantoin derivative, which also facilitated the isolation of the indoloazepine. In addition, this route gave rise to new analogs of indoloazepine which were evaluated as inhibitors of Chk2.

Indoloazepine was evaluated in cell culture and was found to be non-cytotoxic to cells. Indoloazepine increased survival in normal cells following IR-induced DNA damage, but not in tumor cells with mutated p53. Additionally, indoloazepine was directly inhibited Chk2 in cells by inhibition of cis-autophosphorylation of Ser516 of Chk2. Chk2 also plays a significant role in the inhibition of IR-induced G_2 arrest. The data suggests that inhibition of Chk2 in normal cells protects cells exposed to IR as well as induce rapid progression into G_1 so that cells initiate DNA repair following IR-induced DNA damage.

This disserta	tion is dedicated	to my mother	⁻ . Nam Nguver	n. and mv granc	lmother. Lieu
Nguyen. educations, th	Although they d ney taught me m an I could ever fi	id not have the ore lessons a	e opportunities bout life, faith,	s to advance in to perseverance a	their own and hard work

ACKNOWLEDGEMENTS

I would like to acknowledge my advisor, Prof. Jetze Tepe and to thank him for being incredibly patient with my many, many struggles in my research. My determination and perseverance along with his patience have carried me through my research. I did not realize that graduate school would teach me so many things about life, and have so much influence on my character. I would not have learned these without my advisor. Thank you, Jetze.

Additionally, I would like to acknowledge Prof. Babak Borhan, my second reader. After taking his CEM 845 course for a few weeks, I really thought he enjoyed picking on me and mocking me (this might still be true). However, I like to think that his intentions were good and that he was pushing me to be a better student. He has always been an invaluable resource to me. I would like to acknowledge my committee members, Professors J. Justin McCormick and Kevin Walker for being a wealth information as well as guidance throughout my graduate career.

Doing biochemistry surrounded by synthetic organic chemists proved to be challenging. I would like to thank Dr. Sandra O'Reilly, Dr. Elizabeth McNeil and Dr. Louis King for all the help with my irradiations and flow cytometry experiments and intellectual discussions. In addition to these people, Teri Lansdell has also been a tremendous resource for learning different biological techniques, trouble shooting and helpful discussions.

I most genuinely want to thank staff in MSU Chemistry including Nancy Lavrik, Bob Rasico, Melissa Parsons, Bill Flick, Beth McGaw, and Karen Maki. The chemistry department is unbelievably lucky to have such a hard-working staff that is always willing to help. They are an invaluable asset to this department.

I cannot have come as far as I have as a scientist and teacher without the influence and friendships of the past and present Tepe group members. I have met remarkable people and made lifelong friends in this lab. It has been an honor and a privilege to have become such good friends with my lab mates including, Chris, Nicole, Stacy, Amanda and especially Adam.

I never expected that I would come to graduate school and meet somebody who would someday become my husband. I want to thank Adam for being there. He has always been a wonderful source of scientific discussions throughout my graduate school career and provided infinite support. He has survived all of my empty stomach mood swings and somehow he still stuck around. Thanks Adam.

I want to thank my mother for coming to America so that her children could have a better life. She is an amazing woman who worked two jobs in order to raise her 5 children. She's always been supportive of me achieving my goals. My family and has incredibly supportive and has always offered a prayer when I needed it. I have been truly blessed to have been surrounded by such good people.

TABLE OF CONTENTS

LIST OF 1	ΓABLES	viii
LIST OF F	FIGURES	ix
LIST OF S	SCHEMES	xiii
LIST OF A	ABBREVIATIONS	xv
CHAPTER	R I. CHECKPOINT KINASE 2 AS A TARGET FOR ADJUVANT (
I.A		
I.B	Chemotherapy	6
I.C	Radiation therapy	9
I.D	DNA damage and cell cycle checkpoints	13
I.E	Activation of the ATR and ATM pathways	16
I.F	Checkpoint kinase 2	18
I.G	The role of Chk2 and p53	20
I.H	Cell cycle response pathways	26
1.1	Chk2 as a drug target candidate	30
I.J	Validation of Chk2 as a drug target	31
I.K	Purified drug target and X-ray crystal structure	33
I.L	Current Chk2 Inhibitors	34
I.M	Chk2 binding pocket properties	41
I.N	Goals of project	45
I.O	References	46
CHAPTEF	R II. IMPROVEMENT OF A SYNTHETIC METHOD FOR THE PREPARATION OF (Z)-5-(2-AMINO-IMIDAZOL-5(4H)-YLIDE TETRAHYDROAZEPINO[3,4-b]INDOLE-1(10H)-ONE, A	-
11 A	HYMENIALDISINE ANALOG	
II.A	, ,	
II.B	Synthesis of hymenialdisine and debromohymenialdisine	/ 3

	II.C	Synthesis of marine sponge alkaloids through a common bicyclic pyrrocoupling to 2-aminoimidazole	
	II.D	Synthesis of axinohydantoins	84
	II.E	Synthesis of hymenialdisine and analogs through thiols	86
	II.F	Synthesis of indole analogs of hymenialdisine	92
	II.G	Synthesis of 2-aminoimidazolone ring through phenyloxazalone	
	II.H	Hymenialdisine analog synthesis via Heck reaction	97
	11.1	Improvement of the synthetic route to indoloazepine II-70	. 100
	II.J	General experimental information	. 109
	II.K	References	. 124
CHA	PTER I	II. EVALUATION OF INDOLOAZEPINE AS AN INHIBITOR OF CHECKPOINT KINASE 2	. 129
	III.A	Biological target of natural product and hypothesis for activity	. 129
	III.B	In vitro evaluation of Chk2 inhibitors	. 130
	III.C	In vitro evaluation of the effect of indoloazepine in the DNA pathway .	. 136
	III.D	In vitro evaluation of the cell cycle with indoloazepine	. 140
	III.E	Cellular evaluation of indoloazepine	. 147
	III.F	Indoloazepine as a radioprotecting agent	. 153
	III.G	In vivo evaluation of indoloazepine	. 163
	III.H	Inhibition of Chk2 as a strategy for chemosensitization	. 172
	III.I	Conclusions	. 174
	III.J	General experimental information and procedures	. 175
	III.K	References	. 184
СНА	PTER I	V. EVALUATION OF INDOLOAZEPINE AS AN INHIBITOR OF NF-κΒ	189
	IV.A	Introduction to the NF-кВ pathway	. 189
	IV.B	Targets for inhibition of NF-кВ	. 193
	IV.C	Evaluation of II-70 and analogs as an inhibitor of NF-кВ-mediated gen transcription.	
	IV.D	Evaluation of II-70 as an inhibitor of IL-1β induced TNF-α production in human whole blood	า
	IV.E	Evaluation of II-70 as an inhibitor of NF-кВ <i>in vitro</i>	
	IV.F	General experimental Information	
	III.H	References	

LIST OF TABLES

Table I-1.	FDA-approved kinase inhibitors9
Table I-2.	Some of the possible damage in mammalian cell nucleus following 1 Gy IR13
Table II-1.	Nitrogen protecting group variations for indole aldisine 94
Table II-2.	Scope of the Suzuki and Stille coupling for indole aldisine 95
Table II-3.	Attempted conditions for cyclization
Table III-1.	Kinase profiling data for indoloazepine II-1, II-2 and II-70 130
Table III-2.	Summary of IC ₅₀ values for kinase inhibition by analogs II-70, II-84, II-99, III-1 and III-2
Table III-3.	Statistically significant differences in cell cycle distribution of untreated Chk2 +/+ versus II-70 treated cells, and unt reated Chk2 +/+ versus Chk2 -/- cells
Table III-4.	Results of NCI-60 cell line screen with II-70 152
Table III-5.	Statistically analysis of vehicle compared to II-70 whole body irradiated Balb-C mice
Table III-6.	Log values, standard error of log values and IC ₅₀ values 178
Table III-7.	Mean and standard deviation of IC ₅₀ values of Chk1 and Chk2
Table III-8.	Summary of GI ₅₀ values of cells treated with II-70
Table IV-1.	Kinase inhibition by hymenialdisine-derived analogs 201

LIST OF FIGURES

Figure I-1.	Representation of replication of normal and mutated cells 2		
Figure I-2.	Representation of uncontrolled growth of cancer cells		
Figure I-3.	Causes of cancer4		
Figure I-4.	DNA damage by IR12		
Figure I-5.	Schematic representation of some types of DNA damage in double-stranded DNA caused by IR12		
Figure I-6.	Components of the DNA damage checkpoint pathway 15		
Figure I-7.	Representation of Chk2		
Figure I-8.	Upstream signaling of p53 after IR-induced DNA damage 22		
Figure I-9.	Control of the cell division cycle by cyclins and Cdks and their regulation by cell cycle checkpoints27		
Figure I-10.	The G ₁ /S and G ₂ /M checkpoint regulation network following upstream ATM/ATR activation		
Figure I-11.	Survival rates of Chk2 -/-, Chk2 +/- and Chk2 +/+ mice after 8 Gy whole body ionizing radiation		
Figure I-12.	Illustration of Chk2 and crystal structure of kinase domain 34		
Figure I-13.	Squaric acid derivatives and indazoles as Chk2 inhibitors 35		
Figure I-14.	Structures of NSC 109555 and PV1019		
Figure I-15.	Structure of carboxamide Chk2 inhibitors		
Figure I-16.	Structure of arylbenzimidazole and non-benzimidazole inhibitors of Chk2		
Figure I-17.	Structures of aminopyrimidine inhibitors of Chk2		
Figure I-18.	Structure of CCT24153339		
Figure I-19.	Structure of natural product staurosporine and analog UCN-01.		
Figure I-20.	Structure of debromohymenialdisine and its analog indoloazepine41		
Figure I-21.	Debromohymenialdisine inside the Chk2 active site, top view. 42		

Figure I-22.	Debromohymenialdisine inside the Chk2 active site, bottom view
Figure I-23.	Indoloazepine modeled in the Chk2 catalytic site 44
Figure II-1.	Structures (Z)-debromohymenialdisine and (Z)-hymenialdisine70
Figure II-2.	Structures of the axinohydantoins and (Z)-debromohymenialdisine and (Z)-hymenialdisine71
Figure II-3.	Structure of hymenin and stevensine73
Figure II-4.	Azafulvene intermediate to be coupled to 2-aminoimidazole II-2078
Figure II-5.	Structure of 1-benzoyl-2-methylsulfanyl-1,5-dihydroimidazol-4-one87
Figure II-6.	Structure of phenyloxazolone96
Figure II-7.	General scaffold for hymenialdisine analogs 100
Figure III-1.	Structure of hymenialdisine and hymenialdisine-derived indoloazepine II-1 , II-2 and II-70
Figure III-2.	Illustration of radio-active kinase protocol
Figure III-3.	Structures of analogs II-84, II-99, III-1 and III-2
Figure III-4.	Inhibition of $[\gamma^{-33}P]$ -ATP phosphorylation by Chk1 or Chk2 133
Figure III-5.	Natural product hymenialdisine in Chk2 catalytic site 135
Figure III-6.	Compounds II-70, III-1 and III-2 modeled in the Chk2 catalytic site with PyMol
Figure III-7.	Western blot analysis of 184B5 (normal, p53 WT) whole cell extracts
Figure III-8.	Western blot analysis of MDA-MB-231 (tumor, p53 mut) whole cell extracts
Figure III-9.	Western blot analysis of 184B5 whole cell untreated (control) or treated with vehicle or with compounds III-1 and III-1 for 2 hours prior to IR (10 Gy)
Figure III-10.	Cell cycle histograms of HCT116 Chk2 +/+ or Chk2 -/- cells untreated (control) or pretreated for 2 hours with II-70 (30 µM) followed by IR (0-5 Gy)
Figure III-11.	DNA frequency histograms of HCT116 Chk2 +/+ or Chk2 -/- cells in G ₂ 143

Figure III-12.	The abbreviated G ₁ /S and G ₂ /M checkpoint regulation network following upstream ATM/ATR activation		
Figure III-13.	DNA frequency histograms of HCT116 Chk2 +/+ or Chk2 -/- cells in G_1		
Figure III-14.	Results of trypan blue exclusion test in breast cell lines 148		
Figure III-15.	Results of trypan blue exclusion test in colon cancer cell lines.		
Figure III-16.	Microscopic cell images of HCT116 cell lines following treatment with II-70 for 24 hours of continuous exposure		
Figure III-17.	Clones of 184B5 (normal) cells untreated (top panel) or pretreated with II-70 for 30 minutes (bottom panel) followed by IR (0-7.5 Gy) and seeded at the indicated cloning density 154		
Figure III-18.	Cloning survival of 184B5 (normal) cells untreated or pretreated with II-70 for 30 minutes followed by IR (0-7.5 Gy)		
Figure III-19.	Microscopic images (20X) of normal cell colonies (184B5) treated with II-70 followed by 0 or 10 Gy IR		
Figure III-20.	Cloning survival of 184B5 normal cells with various treatment times. A) Cells post-treated 30 minutes following IR (0-7.5 Gy); B) Cells pretreated for 2 hours and post-treated for 4 hours after IR (0-7.5 Gy)		
Figure III-21.	Cloning survival of 184B5 and MDA-MB-231 cells 158		
Figure III-22.	Clones of MDA-MB-231 (tumor, p53 mutant) cells untreated (top panel) or pretreated with II-70 for 30 minutes (bottom panel) followed by IR (0-7.5 Gy) and seeded at the indicated cloning density		
Figure III-23.	Microscopic images (20X) of tumor cell colonies (MDA-MB-231) treated with II-70 followed by 0 or 10 Gy IR		
Figure III-24.	Cloning survival of HCT116 cell lines		
Figure III-25.	Comparison of cloning survival of HCT116 treated with II-70 versus HCT116 Chk2 -/- cells following IR		
Figure III-26.	LC/MS quantification of biologically available II-70 in mice 166		
Figure III-27.	Cytotoxicity of mice treated with varying doses of II-70 by IP.167		
Figure III-28.	Mouse irradiation chamber used for whole body IR 169		
Figure III-29.	Effect of pre-treatment with II-70 (10, 1 or 0.1 mg/kg) for 30 minutes prior to whole body IR with 7.3 Gy on survival of male Balb-C mice		

Figure III-30.	70173		
Figure III-31.	Trypan blue exclusion assay of OVCAR-3 cells treated with II-70 in combination with 0.5 µM Topotecan		
Figure IV-1.	NF-кВ signal cascade190		
Figure IV-2.	IкВ Kinase inhibitors		
Figure IV-3.	IKKβ inhibitors		
Figure IV-4.	Structures of GSK-3 Inhibitors		
Figure IV-5.	Structures of II-70 , II-84 , II-100		
Figure IV-6.	Structures of IV-1 – IV-4		
Figure IV-7.	Dose-response activity of II-70 in inhibition of luciferase production in HeLa-NF-κB-luc cells		
Figure IV-8.	Dose-response activity of II-70 in inhibition of TNF-α production in IL-1β stimulated human blood		
Figure IV-9.	Western blot of TNF-α induced p65 after 30 minutes in HeLa-NF-κB-luc cells		
Figure IV-10.	Western blot of HeLa cells with TNF-α induced p-p65 after 30 minutes		
Figure IV-11.	EMSA Assay for NF-κB Activation by TNF-α (10 ng/mL) 206		

LIST OF SCHEMES

Scheme I-1.	DNA damage by UV	. 10
Scheme II-1.	Synthetic route toward II-1 and II-2 of intermediate II-11	. 74
Scheme II-2.	Synthetic route toward II-1 and II-2 of intermediate II-14	. 75
Scheme II-3.	Synthesis of II-17 toward II-1 and II-2	. 76
Scheme II-4.	Completed synthesis of II-1 and II-2.	. 77
Scheme II-5.	Synthesis of azafulvene intermediate II-19a	. 78
Scheme II-6.	Synthesis of hymenin and debromohymenin	. 79
Scheme II-7.	Synthesis of intermediates II-25 and II-26	. 80
Scheme II-8.	Synthesis of stevensine II-7	. 81
Scheme II-9.	Synthesis of II-7 from II-6.	. 82
Scheme II-10.	Synthesis of II-1 and II-2 from intermediate II-29 and II-28	. 83
Scheme II-11.	Synthesis of II-2 using a one-pot, two-step synthesis	. 84
Scheme II-12.	Synthesis of II-3c, II-4c, II-36 and II-37 from intermediate I	I-35
		. 85
Scheme II-13.	Synthesis of axinohydantoins II-3b and II-4b from II-3c and II	-4c
		. 86
Scheme II-14.	Synthesis of II-2 via thiohydantoin II-39.	
Scheme II-15.	Improved synthesis of II-11a	. 88
Scheme II-16.	Synthesis of II-1 and II-2 utilizing II-41	. 89
Scheme II-17.	Conversion of II-44 to II-2 under microwave conditions	. 90
Scheme II-18.	Synthetic route for II-3a, II-3b and II-4a, II-4b	. 91
Scheme II-19.	Synthesis of endo-pyrrole analogs	. 92

Scheme II-20.	Toward the synthesis of indole analogs of hymenialdisine	93
Scheme II-21.	Synthesis of mono- and di-triflate protected indole aldisines.	94
Scheme II-22.	Synthesis of indoloazepine II-70	97
Scheme II-23.	Synthesis of intermediate II-74 for ring closure via Heck reac	tion
		98
Scheme II-24.	Unsuccessful Heck reaction approach to II-70	99
Scheme II-25.	Synthesis of II-82 via hydantoin II-79.	101
Scheme II-26.	Hydantoin coupling to II-68.	102
Scheme II-27.	Attempted HWE synthesis to form II-84	102
Scheme II-28.	Alternate synthesis to II-84.	102
Scheme II-29.	Synthesis of intermediate II-95.	104
Scheme II-30.	Synthesis of II-41	106
Scheme II-31.	Synthesis of intermediate II-98	107
Scheme II-32.	Synthesis of II-70 and analogs II-84 and II-99.	108

LIST OF ABBREVIATIONS

184B5 normal, breast cell line

5-FU fluorouracil

Abl tyrosine kinase enzyme

ABI arylbenzimidazole, Chk2 Inhibitor II

ACN acetonitrile

ADP adenosine diphosphate

AP apyrimidic/apurinic

ARS acute radiation syndrome

Asn asparagine

ATM ataxia telangiectasia mutated

ATP adenosine triphosphate

ATR ataxia telangiectasia and Rad3-related

BRCA1 breast cancer type 1 susceptibility protein

BJ-hTERT foreskin fibroblasts

BM hematopoietic syndrome

Boc tert-butyl carbamate

¹³C NMR carbon nuclear magnetic resonance

c-Kit human proto-oncogene

c-Rel proto-oncogene protein encoded by Rel

Cdc2 cell division cycle 2

Cdc25A cell division cycle 25 homolog A

Cdc25C cell division cycle 25 homolog C

CD4+ cluster of differentiation 4

CD8+ cluster of differentiation 4

Cdk1 cyclin dependent kinase cyclin

Chk1 checkpoint kinase 1

Chk2 checkpoint kinase 2

CK1δ casein kinase 1

CK2 casein kinase 2

CML chronic myeloid leukemia

CNS central nervous system

DBH Debromohymenialdisine

DCM dichloromethane

DMAP dimethylaminopyridine

DMF dimethylformamide

DMSO dimethylsulfoxide

DNA deoxyribonucleic acid

DNA-PK DNA dependent protein kinase

DSB double-strand break

Dex Dexamethasone

(E) entgegen, trans double bond

EDCI 1-ethyl-3-(3-dimethylaminopropyl) carbodiimide

EGFR epidermal growth factor receptor

EMSA Electrophoretic mobility shift assay

EtOAc ethyl acetate

EtOH ethanol

eV electronvolt

FDA food and drug administration

FHA forkhead association domain

FLT3 receptor tyrosine kinase

Gap 1 phase

G₂ Gap 2 phase

GI gastrointestinal syndrome

GIST gastrointestinal stromal tumor

Glu gluatamate

GSK-3β glycogen synthase kinase -3 beta

Gy Gray, SI unit of absorbed radiation

¹H NMR proton nuclear magnetic resonance

HOAc acetic acid

H2AX gene that codes for histone H2A

HC hepatocellular carcinoma

HCT116 colon cancer cell line

Her-2 human epidermal growth factor receptor 2

HWE Horner-Wadsworth-Emmons reaction

IBX 2-lodoxybenzoic acid

IC₅₀ half maximal inhibitor concentration

IFN-α interferon-α

ΙκΒ-α inhibitory kappa B-alpha protein

ΙΚΚα inhibitory kappa B kinase-alpha

ΙΚΚβ inhibitory kappa B kinase-beta

IL-# interleukin-#

IP intraperitoneal

IR Ionizing radiation

KHMDS Potassium bis(trimethylsilyl)amide

MCF-7 breast cancer cell line (Michigan Cancer Foundation 7)

MDA-MB-231 breast tumor, p53 mutant

MDM2 murine double minute 2 gene

MeCN acetonitrile

MEF mouse embryonic fibroblasts

MEK1 mitogen-activated protein kinase kinase/ERK1

MeOH methanol

Met methionine

MG-132 proteasome inhibitor

MRE11 meiotic recombination 11 homolog A

mRNA messenger ribonucleic acid

MSK1 mitogen- and stress-activated protein kinase-1

Myt1 myelin transcription factor

NaOAc sodium acetate

NBS N-bromosuccinimide

NBS1 nibrin, Nijmegen breakage syndrome 1

NCI National Cancer Institute

NES nuclear export signal

NLS nuclear localization signal

NF-κB nuclear factor-kappa B

NSCLC non-small cell lung cancer

OVCAR ovarian carcinoma

p21^{WAF1} cyclin-dependent kinase inhibitor

p53 protein p53, tumor protein supressor

PARP poly adenosine diphosphate ribose polymerase

PDGFRa platelet-derived growth factor receptor, alpha polypeptide

PDGFRb platelet-derived growth factor receptor, beta polypeptide

Ph phenyl

PIKK phosphoinositide 3-kinase related kinases

PKCα protein kinase C-alpha

PKCβII protein kinase C-alpha

PPA polyphosphoric acid

RA rheumatoid arthritis

Rad50 DNA repair protein

Rb retinoblastoma protein

RCC renal cell carcinoma

RelA v-rel reticuloendotheliosis viral oncogene homolog A

RelB v-rel reticuloendotheliosis viral oncogene homolog B

RHD Rel homology domain

RNA ribonucleic acid

RNAi ribonucleic acid interfernce

RPA Replication Protein A

RT-PCR real-time polymerase chain reaction

S synthesis phase

SAR structural activity relationship

SCD serine-glutamine/threonine-glutamine cluster domain

SEM [2-(trimethylsilyl)ethoxy]methyl ether

Ser serine

siRNA small interfering RNA

SRB sulforhodamide B

Src sarcoma

SQ/TQ serine-glutamine/threonine-glutamine region

SSB single-strand break

TADs transactivation domains

TBAF tetra butyl ammonium fluoride

TEA triethylamine

TFA trifluoroacetic acid

THF tetrahydrofuran

Thr threonine

TIPS triisopropylsilyl ether

TNF- α tumor necrosis factor- α

U2OS human osteosarcoma cell line

VEGFR vascular endothelial growth factor

Wee1 cell division kinase inhibitor

UV ultra violet

X-ray X-radiation

(Z) zusammen, cis double bond

CHAPTER I

CHECKPOINT 2 KINASE AS A TARGET FOR ADJUVANT CANCER THERAPY

I.A. Introduction to cancer

Currently, one in four deaths in the United States is caused by cancer, making it one of the leading causes of death. Although there has been an increase in knowledge and advances in cancer therapies, the mortality rate due to cancer has not been greatly affected. However, from 1991 to 2006, US cancer death rates decreased 16% while rates for other chronic diseases including heart disease (36%), cerebrovascular (31%) and influenza (49%) decreased even more significantly. This is a major public health problem that plagues not only the United states, but many other parts of the world.

Cancer exists in over 100 different forms capable of manifesting in almost every tissue in the body. Cancer encompasses a group of diseases described by uncontrolled growth and spread of abnormal cells, frequently resulting in death.² Each human has trillions of cells that work together to form networks of tissue and organs. Normal cells have the ability to divide in a regulated and systematic way. These cells form new daughter cells allowing injured, mutated or dead cells to be replaced (Figure I-1).² Cells that cease to cooperate metabolically and structurally with neighboring cells can become transformed and eventually become tumor cells which may later result in cancer cells.²

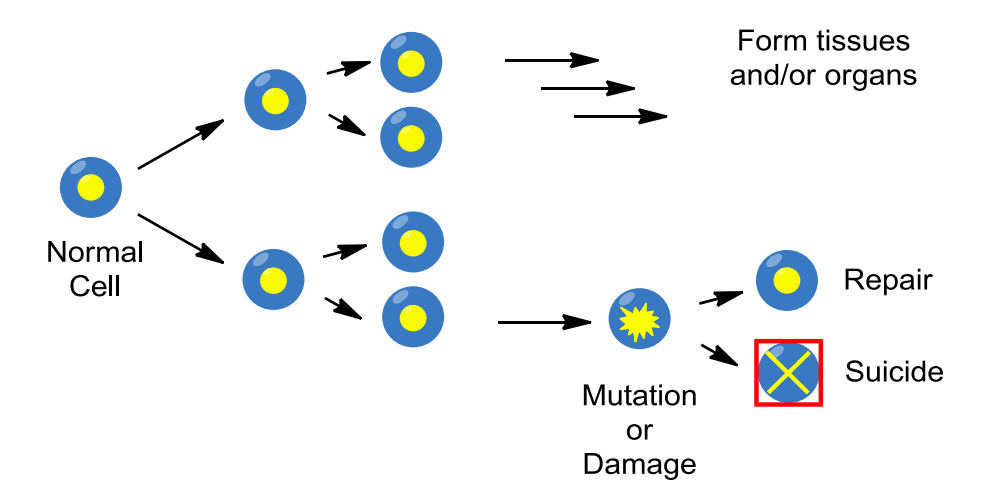


Figure I-1. Representation of replication of normal and mutated cells. For interpretation of the references to color in this and all other figures, the reader is referred to the electronic version of this dissertation.

Benign tumors belong to the first of the two classes of generic tumors. They are most often enclosed in a protective capsule of tissue^{3, 4} and do not spread to other parts of the body.⁵ In general, benign tumors are not lethal, unless they exert pressure against critical organs or tissue, leading to death.²

Malignant tumors make up the second, more dangerous class of tumors. These tumors are capable of destroying a part of the body in which they originate, as well as neighboring tissue. Malignant tumors can also metastasize to other parts of the body, initiating the growth of new secondary tumors. These secondary tumors can continue to destroy additional tissues and organs, distinguishing them from benign tumors, which do not spread to other parts of the body. ^{2, 5}

As mentioned above, malignant tumor cells (cancer cells), can cause destruction in the tissue of origin, as well as surrounding and neighboring tissues.^{2, 5} Unlike normal cells, cancer cells divide and grow rapidly, piling up into a mass or tumor as illustrated in

Figure I-2. ^{2-4, 8, 9} These cancer cells can spread and metastasize to distant tissue and can eventually destroy it.^{2, 5} Cancer cells from the primary tumor can travel through the bloodstream or lymphatic system, spreading to sites near to and far away from the original tumor.^{2, 5}

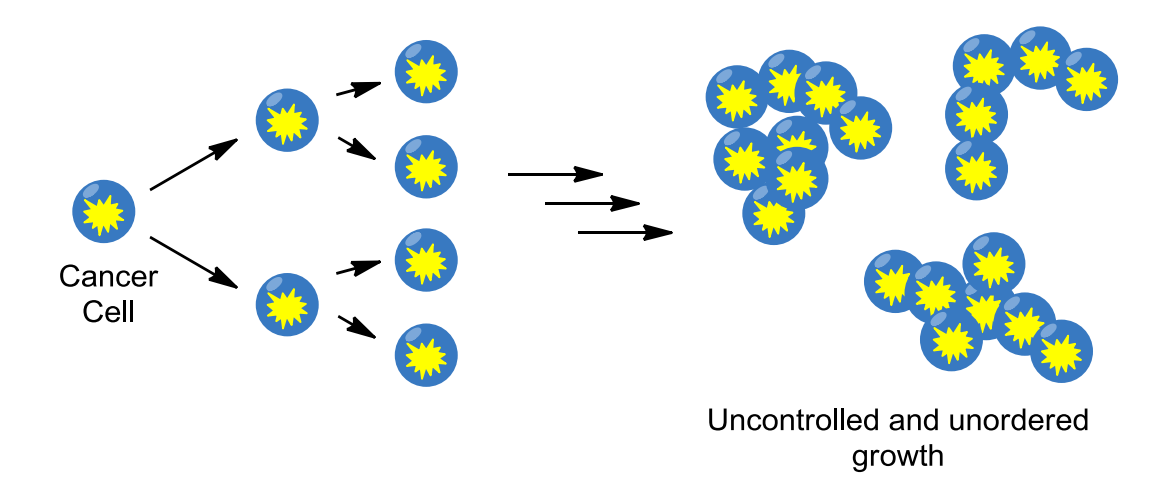


Figure I-2. Representation of uncontrolled growth of cancer cells.

Malignant tumors are comprised of different types including carcinomas, sarcomas, leukemias and lymphomas. Carcinomas make up 92% of human tumors. These tumors develop in tissue that line the surfaces of organs such as the lung, liver, skin, and breast.² Sarcomas originate from mesenchymal cells, including cells from bone, cartilage, fat, connective tissues and muscle. Leukemias are malignant tumors that affect white blood cells. Sarcomas and leukemias combined make up 8% of the total human tumors.² Lymphomas develop in the lymphatic system and represent the smallest percentage of human tumors, developing in the lymphatic system.²

Because there are so many different types of cancers, there are also several causes, or factors that contribute to cancer. There are endogenous factors (hormones), and exogenous factors (occupational and environmental carcinogens) that can

contribute to the development of human cancer.² The major causes include tobacco smoke and related tobacco products (30%), hormones (30%), diet (15%), viruses (10%), drugs, x-rays, and ultra violet light (UV) (10%) as well as occupational carcinogens (5%) (Figure I-3).²

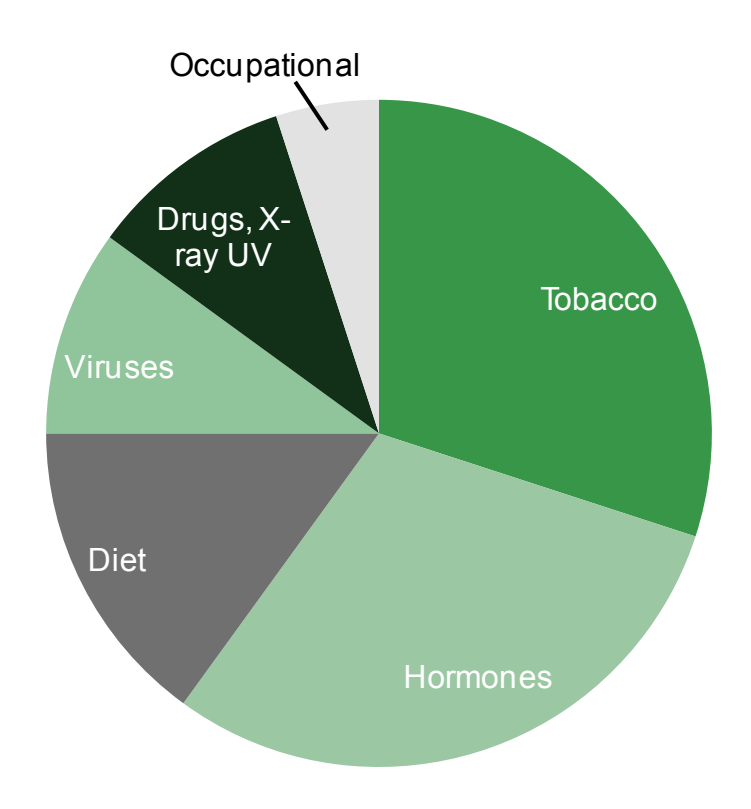


Figure I-3. Causes of cancer.²

Several cancers thought to be induced by tobacco smoke exposure include lung cancer, bladder cancer, pancreatic cancer, liver cancer, cervical cancer, laryngeal cancer, cancer of the lip, stomach cancer, kidney cancer, and colon cancer. ¹⁰

The influence of hormones is believed to be the cause of about 30% of new cases of cancer.² Estrogens without progestogens cause endometrial cancer and estrogen can also cause breast cancer (progesterone can increase the effect).^{2, 10}

Ovarian cancer can be brought on by the hormone changes involved in ovulation. ¹⁰ The effects of testosterone or its metabolites can be responsible for the onset of prostate cancer. ^{2, 10}

Dietary factors are a second major contributor to the induction of human cancer.^{2,}

10-13 Two factors that are believed to contribute to the induction of cancer are excess caloric content and a diet high in red meats. A diet including more green-leafy and yellow vegetables protect against various types of cancers, while a diet lacking these has been correlated with a higher cancer incidence. 10-14 These, along with other dietary factors are thought to account for 15% of human cancers. 2, 10-13

Other contributing causes of cancer include oncogenic viruses (about 10%) such as hepatitis B virus leading to liver cancer. ^{10, 15} In addition, 10% of human cancer can be due to medical drugs, exposure to radiations such as medical and dental x-rays or UV light. ¹⁰ This also encompasses "secondary tumors induced by specific chemotherapeutic agents, skin tumors induced by UV light, and tumors induced by specific drugs."

Lastly, 5% of human cancer can be attributed to by exposure to carcinogens in the workplace. These include asbestos (lung cancer and mesothelioma), benzene (acute myelogenous leukemia), and hexavalent chromium (nasal and respiratory cancer). 9, 16-18

Nearly half (45%) of all human cancer causes can be traced to exposure to chemical carcinogens and radiation. It is astounding that 60% of all human cancers are theoretically preventable. Eliminating exposure to tobacco and tobacco products

would reduce human cancer by 30%. In addition, having a proper diet with controlled caloric and fiber intake, including increasing vegetables and limiting intake of animal fat could help to reduce risks of cancer exposure. Avoiding excess exposure to specific drugs, x-rays and UV light can also prevent human cancer.^{2, 10, 11, 13, 19, 20}

I.B Chemotherapy

Cancer in its many forms of uncontrolled cell growth can lead to solid tumors (with the exception of a few cases such as leukemia), but can be treated using different types of therapy. Surgery, when applicable is a viable option to remove solid tumors, however it does not completely remove the cancer. Chemotherapy and/or radiation therapy or the combination of them can be used as a treatment method. ²¹⁻³⁵ There are several types of chemotherapeutic agents available including alkylating, topoisomerase II inhibitors, antimetabolic, biological, hormonal and tubulin-targeting agents. ³⁶

Alkylating agents are polyfunctional compounds that can substitute alkyl groups for hydrogen ions. Most of these compounds can react with phosphate, amino, hydroxyl, sulfhydryl, carboxyl, and imidazole groups. Alkylations, which most often occur at the N-7 position of guanine, leads to abnormal base pairing and interference with DNA replication, transcription of RNA as well as the disruption of nucleic acid function. Alkylating agents can lead to disruptions in the normal cell functions in both cancerous and normal tissues. The alkylating agents are divided into five classes: bischloroethylamines (nitrogen mustards), aziridines, nitrosoureas and non-classical alkylating agents.

Topoisomerase inhibitors are a class of compounds that interact with topoisomerase I and topoisomerase II enzymes by assisting in the unwinding of DNA

during the replication process. Topoisomerase I can reversibly cleave a single strand of DNA in order to allow relaxation of the coil, then reseal the cleaved strand after unwinding. Topoisomerase I inhibitors include camptothecin, topotecan and irinotecan. Topoisomerase II has a function similar to topoisomerase I, however it completes a reversible double stranded DNA cleavage to aid in the unwinding of DNA for replication, then reseals the cleaved strands. Topoisomerase II inhibitors include etoposide, doxorubicin and daunorubicin. Doxorubicin belongs to a class of anthracyclines that intercalate between base pairs of DNA causing a distortion that prevents DNA replication process. The metabolism of this process with compounds like doxorubicin can also lead to free radical formation that can cause oxidative damage to DNA. Additionally, the reactive intermediates formed from the radicals can form covalent adducts with DNA, again repeating the overall replication process.

Antimetabolites constitute a large group of anticancer drugs that are able to interfere with metabolic processes necessary for the proliferation of cancer cells. The major classes of the antimetabolites include the antifols, purine analogs, and pyrimidine analogs. ^{36, 38, 41-43} Nearly all of the antimetabolites in clinical use function as an inhibitor of the synthesis of purine or pyrimidine nucleotides or directly inhibit enzymes involved in DNA replication. ³⁶ Newer antimetabolites include gemcitabine and the 5-fluorouracil (5-FU) prodrug, capecitabine.

Biologic agents or biologic therapy utilizes agents that evoke immune responses, directly target receptor or signaling pathways, modify the stroma of the tumor, or elicit tumor regression.³⁶ This class of therapy includes recombinant cytokines, some of

which have immunomodulatory and antitumor activity, including interleukin-2 and interferon- α (IFN- α). Other cytokines have been evaluated including tumor necrosis factor- α (TNF- α), interferon- γ , IL-1, IL-4, and IL-12.

Hormonal reagents play a significant role in regulating the growth and development of their target organs. There have been different hormonal reagents used in treating tumors originating from the breasts, uterus, ovary and prostate. Estrogens, androgens and progestins function via their respective receptors. Following high-affinity binding to the receptors, the steroids can then modify the configuration of the receptor molecules and allow them to bind to a segment of the DNA template (hormone response element). Once the steroid is bound to the hormone response element, it can regulate gene transcription and control cellular growth and function. 44

Tubulins are critical in eukaryotic biology during both cell division as well as nonmitotic phases of the cell cycle. Tubulin-binding drugs play a part in chromosomal separation during mitosis, making them desirable targets for antitumor drugs. This class of drugs is made up of a large family of heterogeneous compounds that include the vinca alkaloids, taxanes, and estramustine phosphate. 45

Kinases have become an attractive and challenging target in cancer drug discovery as researchers have revealed more information about cancer. Many groups have researched the development of kinase inhibitors; however few have been approved by the FDA in the last decade (Table I-1).

Table I-1. FDA-approved kinase inhibitors²⁸

U.S. Brand Name	Year Approved	Cancer type	Company	Target kinase
Gleevec	2001	CML	Novartis	Abl, c-Kit, PDGFRa, PDGFRb
Iressa	2003	NSCLC	AstraZeneca	EGFR
Tarceva	2004	NSCLC, P	Genetech, OSIP	EGFR
Nexavar	2005	HC, RCC	Bayer, Onyx	c-Kit, VEGFR, PDGFR, FLT3
Sutent	2006	GIST, RCC	Pfizer	Abl, c-Kit, PDGFR, Src
Sprycel	2006	CML	BMS	Abl, c-Kit, PDGFR, Src
Tasigna	2007	CML	Novartis	Abl, c-KIT, PDGFRb, Src, Ephthrin
Tykerb	2007	BC	GSK	EGFR, Her-2

CML = chronic myeloid leukemia; NSCLC = non-small cell lung cancer; P = pancreatic; HC = hepatocellular carcinoma; RCC = renal cell carcinoma; GIST = gastrointestinal stromal tumor; BC= breast cancer

I.C Radiation therapy

Although a large variety of chemotherapeutic agents are available for cancer treatment, radiation continues to be a method of therapy for nearly half of all cancer patients. Radiation therapy uses high-energy radiation in order to reduce tumor sizes by causing instability in the form of DNA damage leading to cell death.^{22, 31, 46} There are a variety of methods in which radiation can be delivered. The first method involves the delivery of x-rays or γ-rays⁴⁶ outside of the body using external-beam radiation therapy. A patient receiving radiation therapy for breast cancer could be exposed to 45-60 Gray (Gy) of radiation over a period of weeks.⁴⁷ The radiation therapy is administered in fractionated doses in which the patient receives 1-2 Gy/day for 5 days/week.⁴⁷ 1 Gy of

radiation is approximately equivalent to the radiation exposure of 200,000 dental X-rays or 140 chest X-rays.⁴⁷ Internal radiation therapy can be administered by placing radioactive material in the body near cancer cells, also referred to as brachytherapy. Systemic radiation therapy uses substances such as radioactive iodine 131 to treat thyroid cancers. The radioactivity can travel in the blood stream and accumulate in the thyroid, killing cancer cells in this region.⁴⁶

Ultraviolet radiation is lower in energy and the majority of DNA damage results from the formation of photoproducts. An example of a photoproduct resulting from UV damage is a pyrimidine dimer (Scheme I-4). The dimer can inhibit transcription of DNA and the replication machinery which can ultimately lead to cell death. 48

Scheme I-1. DNA damage by UV.

lonizing radiation (IR) has been previously reported as a cause of cancer among other adverse effects. It is a human carcinogen that is among the most extensively studied, accounting for nearly 3% of all cancers. ⁴⁹ IR can remove electrons from atoms resulting in changes in the molecular structures of the cells. The DNA damage incurred from the ionizing radiation is capable of causing the development of cancer. ⁴⁹ This DNA damage could also be used as a tool in cancer therapy.

IR is among the various agents that are capable of creating free radicals that induce DNA damage.³¹ DNA damage resulting from •OH are the predominant source of damage when DNA is irradiated in dilute aqueous media. In an aqueous DNA solution, only ~0.5% of the energy of IR is actually absorbed by DNA following γ-irradiation. The remaining ~99.5% of the energy of IR is absorbed by water. The majority of the free-radical damage to DNA is caused by the free-radicals produced via the radiolysis of water. An almost negligible amount of free-radicals come from the energy absorbed by DNA.³¹

On average, ~100 eV of energy is deposited per ionization event when highenergy electrons are absorbed by water following IR. A water radical cation and an electron are generated during this process (Figure I-4, Reaction (1)). The water radical cation can further cause ionizations in the surrounding areas. The areas which contain further ionizations and sometimes electronic excitations events are referred to as spurs (Figure I-4, Reaction (2)). The small pockets containing spurs can lead to the formation of clustered lesions which can be amplified resulting in more than one damaged site caused from just one *OH radical.³¹ The radicals can cause nucleotide damage, crosslinking and strand breaks. Figure I-4 shows an example of a strand cleavage reaction that could occur following IR.³¹

$$H_2O \xrightarrow{IR} H_2O^{+} + e^{\bigcirc}$$
 (1)

$$H_2O \xrightarrow{IR} H_2O^*$$
 (2)

P = phosphate

Figure I-4. DNA damage by IR.

The main types of damage that can be formed in DNA include base damage, apyrimidic/apurinic (AP) site, single-strand break (SSB), double-strand break (DSB), tandem lesions and various clustered lesions. These types of damage are summarized in Figure I-5. With enzymatic treatments, Figure I-5a, b and e could potentially turn into an SSB, while f and g could lead to a DSB (Figure I-5).

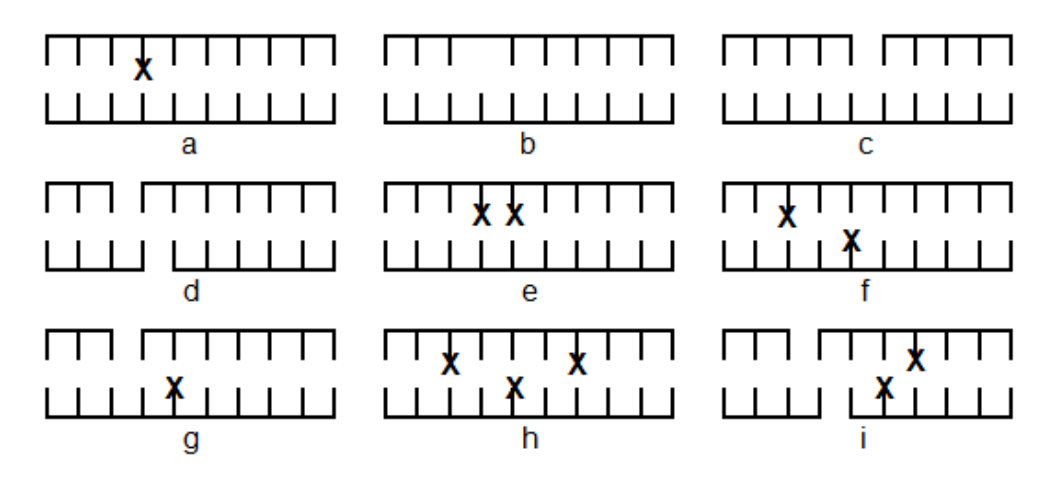


Figure I-5. Schematic representation of some types of DNA damage in double-stranded DNA caused by IR: a) base damage; b) AP site; c) SSB; d) DSB from two close-by SSBs; e) tandem lesion; f) clustered lesion with two damaged bases at opposite strands; g) SSB with damaged base on opposite strand; h) clustered lesion with three damaged bases; i) clustered lesion with a DSB (from two close-by SSBs) and two damaged bases.³¹

Although one site of damage can cause other sites of damage, it is important to note that a one single strand or double strand break does not necessarily constitute damage that is lethal.³¹ Cellular repair enzymes in the DNA damage repair pathway can often efficiently repair the simple lesions. Lethal DNA damage is commonly the result of more complex lesions. ³¹ Table I-2 lists the possible damage as a result of 1 Gy of IR ranging from a simple, repairable lesion, to more complex lesions.

Table I-2. Some of the possible damage in a mammalian cell nucleus following 1 Gy IR. ^{50, 51}

Initial phsyical damage	# of events
Ionizations in the cell nucleus	~ 100,000
Ionizations directly in DNA	~ 2,000
Excitations directly in DNA	~ 2000
Selected biochemical damage	
SSBs	1,000
8-oxo-A (a typical single-base damage)	700
DSBs	40
DNA-protein cross-links	150
Selected cellular events	
Lethal events	~0.2-0.8
Chromosome abberations	~1

I.D DNA damage and cell cycle checkpoints

DNA damage arises from several sources including UV, IR, background radiation, environmental mutagens and chemical substances that attack DNA. ^{52, 53} Cells have evolved complex mechanisms to protect their genomes from the damage. DNA damage responses function to correct the damage or minimize the probability of lethal

or permanent genetic damage.⁵³ The cellular responses to DNA damages are made up of several repair mechanisms and checkpoint responses which can delay the progression of the cell cycle or modulate DNA replication. These responses are pivotal in maintaining stability of the genome.⁵³

DNA checkpoint pathways act as an anticancer barrier to maintain the genetic integrity from one cell to the next.⁵⁴ The pathways were initially observed when chemotherapeutic agents induced damage to DNA which led to an inhibition of the cell cycle that subsequently allowed cellular repair.^{55, 56} A similar control of cell cycle progression was observed in *Saccharomyces cerevisiae* and was then termed a "checkpoint. ^{57, 58} The original view was that checkpoint pathways functioned only as regulators of the cell cycle transitions. The current accepted view is that checkpoints are part of a cascade of signals that are responsible for DNA damage response processes. ^{59, 60} The damage responses are capable of removing the damaged DNA sites in addition to restoring the DNA duplex. Arresting the cell cycle temporarily permits repair and prevention of further replication of damaged DNA or its transcriptional response. ⁵⁷ Cells that have been heavily damaged or seriously deregulated can undergo apoptosis or terminal cell cycle arrest. ^{59, 61, 62}

The checkpoint pathways consists of three major groups of proteins that work together (Figure I-6):⁶³ a) sensor proteins that recognize damaged DNA and signal the presence of abnormalities, initiating the signal cascade;⁶³ b) transducer proteins, often protein kinases that relay and amplify the damage signal obtained from the sensors and phosphorylating other kinases or downstream targets;⁶³ and c) effector proteins, which

consist of the most downstream targets of the transducer protein kinases, and are consequently regulated by phosphorylation to prevent cell cycle progression. ^{63, 64}

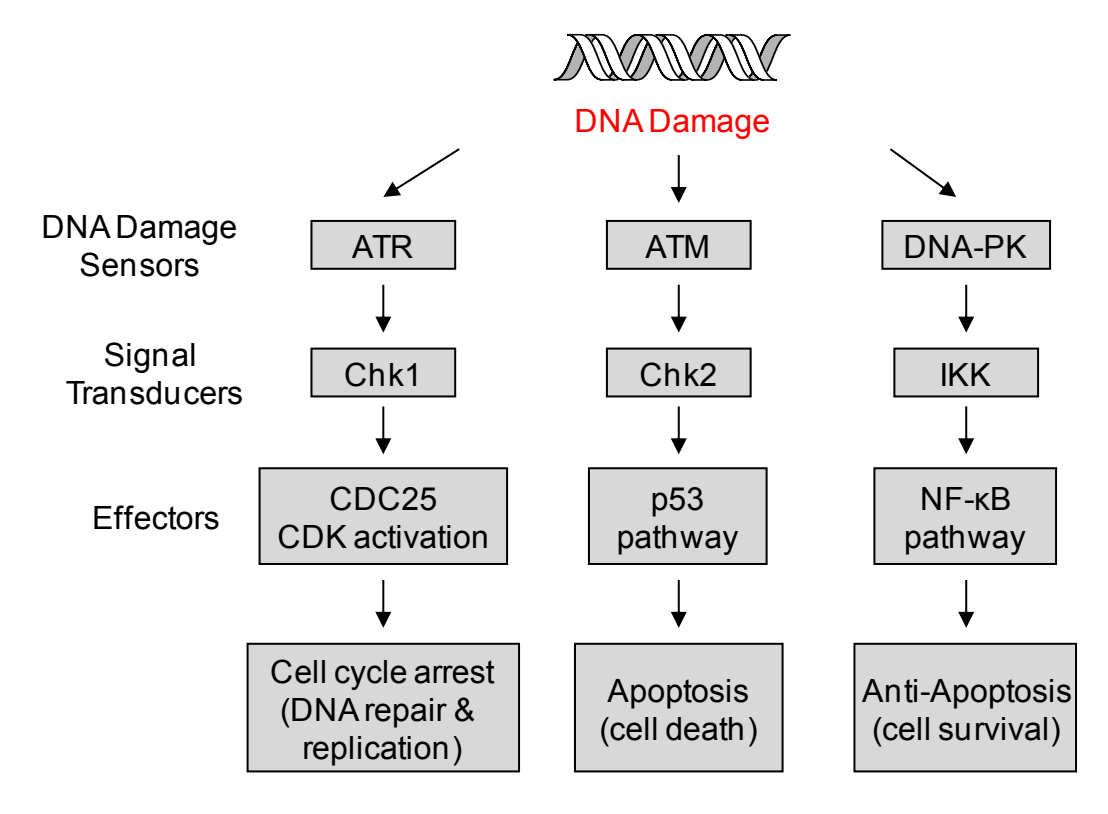


Figure I-6. Components of the DNA damage checkpoint pathway.

In the initial stages of checkpoint activation, DNA damage sensors relay information to members of a family of phosphoinositide 3-kinase related kinases (PIKK). Three of the main sensors belong to the PIKK family and include the: ataxia telangiectasia mutated (ATM), ataxia telangiectasia and Rad3-related (ATR) proteins and DNA-PK, all of which play pivotal roles in early signal transmission through cell cycle checkpoints. DNA-PK activates the NF-kB signaling pathway and will be described in further detail in Chapter 4. ATM and ATR are large serine-threonine kinases with a molecular weight of 350 kDa that phosphorylate different substrates in the DNA damage response signaling networks.

After DNA damage, sensor proteins such as ATR/ATM initiate the signal cascade and the effect is amplified by phosphorylation of the signal transducers checkpoint kinase 1 (Chk1) and checkpoint kinase 2 (Chk2), respectively. Chk1 and Chk2 are serine-threonine kinases required for cell cycle arrest in response to DNA damage and can further phosphorylate downstream targets. The effector components, Cdc25 and p53, are phosphorylated by Chk1 and Chk2, leading to cell cycle arrest and apoptosis, respectively. The series of the signal transducers checkpoint kinase 1 (Chk1) and Chk2 are serine-threonine kinases required for cell cycle arrest to DNA damage and can further phosphorylated by Chk1 and Chk2, leading to cell cycle arrest and apoptosis, respectively. The series of the signal transducers checkpoint kinase 2 (Chk2), respectively. The signal transducers checkpoint kinase 2 (Chk2) (Chk2), respectively. The signal transducers checkpoint kinase 2 (Chk2) (Chk2), respectively. The signal transduce

I.E. Activation of the ATR and ATM pathways

ATR and ATM respond to different forms of DNA damage. ATR is activated by tracts of single strand breaks in conjunction with its partner protein ATR-interacting protein (ATRIP). ATM is recruited and activated by DSBs in association with the MRE11:Rad50:NBS1 (MRN) sensor complex. Because ATM and ATR have a sequence homology, they often have overlapping functions and substrate specificities. ATM has been observed to respond to DNA damage in the early stages and ATR then responds in the late stages.

ATR is activated most strongly when DNA replication is interrupted, such as nucleotide depletion or replication-blocking DNA damage lesions often induced by UV light. ^{53, 64} Replication-blocking causes DNA polymerases to become uncoupled from the replicative helicase, ⁷⁵ which generates SSBs and quickly gets coated with a trimeric ssDNA-binding protein complex, Replication Protein A (RPA). ATR is then recruited and activated at the single strand breaks with its partner ATRIP. ^{53, 72} The activation of ATR does not require autophosphorylation or posttranslational modification. ⁶⁴

Once ATR is activated, it phosphorylates its downstream effector Chk1 at both Ser345 and Ser317, in response to UV DNA damage. ^{76, 77} Phosphorylation at Ser345 is essential for Chk1 biological activity, although the exact modifications that are required for regulation of the Chk1 catalytic activity are poorly understood. ^{53, 78} Phosphorylation of Chk1 regulates its subcellular localization and therefore translocates to centrosomers and inhibits premature activation of Cdk1 (Cdc2)-Cyclin B1 through inhibition of Cdc25C. ⁷⁸⁻⁸⁰ Chk1 can also be phosphorylated by ATM in response to IR-induced replication stress, contributing to the degradation of Cdc25A following IR. ⁸¹ Chk1 and Chk2 possess overlapping functions of Chk1 and Chk2 despite their lack of structural similarity. ⁸²⁻⁸⁴

The ATM pathway is activated by IR and genotoxins that induce DSBs. They can also be activated only weakly, if at all, by agents that block DNA replication without inducing damage. When DNA damage is not present, ATM is believed to exist as inactive homodimers. When DSBs occur, the inactive ATM homodimers are quickly induced to autophosphorylate *in trans*, causing them to dissociate to form partially active monomers. The first autophosphorylation site identified is Ser1981. This residue is not necessary for ATM function, however its modification is linked to the activation of ATM. The monomers of ATM are recruited to DSBs via interactions with the MRN sensor complex, which fully activates ATM allowing it to act on downstream substrates. These substrates include the variant histone, H2AX, forming the DNA damage-associated γ-H2AX histone mark, the MRN complex and Chk2.

form, Chk2 can phosphorylate several substrates that control cell cycle progression and DNA repair as well apoptosis. ⁹⁰

The difference in functionalities of ATR and ATM was confirmed utilizing their respective null mice. The ATM null mice were viable, however had a phenotype that was characterized by infertility and growth retardation. ^{91, 92} ATR null mice, however, died early in embroygenesis, demonstrating a phenotype similar to that of mitotic catastrophe. ^{93, 94} This illustrates how essential ATR is for life, likely because of its functions in monitoring DNA replication. ⁹⁵

I.F Checkpoint kinase 2

The first example of the "Chk2 family" of checkpoint kinases was first discovered in 1994 as Rad53, which was a kinase involved in multiple checkpoint responses in budding yeast. Homologues of Rad53 were later identified in fission yeast and higher eukaryotes. Five laboratories reported identification of the human homologue sand the human gene Chk2 was cloned and named by the Elledge group. The overall structure of the Chk2 protein is similar in all eukaryotes. Although all eukaryotes share a structural homology and share a role as transducers of cell cycle checkpoints, there are functional differences between the Chk2 homologues. The yeast homologues are needed for different forms of DNA damage as well as replication blocks, The while the mammalian Chk2 responds primarily to DSBs. The properties of the checkpoint of the checkpo

The amino-terminal domain of Chk2 contains a series of serine or threonine residues followed by glutamine serine-glutamine/threonine-glutamine (SQ/TQ)-rich motif or SCD (Figure I-7a). These are reported to be the preferred sites for phosphorylation

by ATM/ATR.¹⁰⁷ Another key domain of Chk2 is the fork-head associated (FHA) domain, which seems to bind phospho-threonine residues. It is also thought to be involved in protein-protein interactions triggered by phosphorylation of proteins recognized by FHA partners such as Chk2.⁹⁷ The kinase domain comprises nearly the entire carboxy-terminal half of Chk2, and the main functional elements including the activation loop (Figure I-7a).⁹⁸

In response to DSBs, ATM is activated and subsequently phosphorylates Chk2 at Thr68 in the SQ/TQ motif of one Chk2 molecule. This results in recognition by the phosphopeptide-binding FHA domain of another molecule (Figure I-7b) and leads to transient homodimerization, intermolecular activation loop autophosphorylation on Thr383 and Thr387 and *cis*-autophosphorylation ^{108, 109} on Ser516, and full activation. ¹¹⁰⁻¹¹²

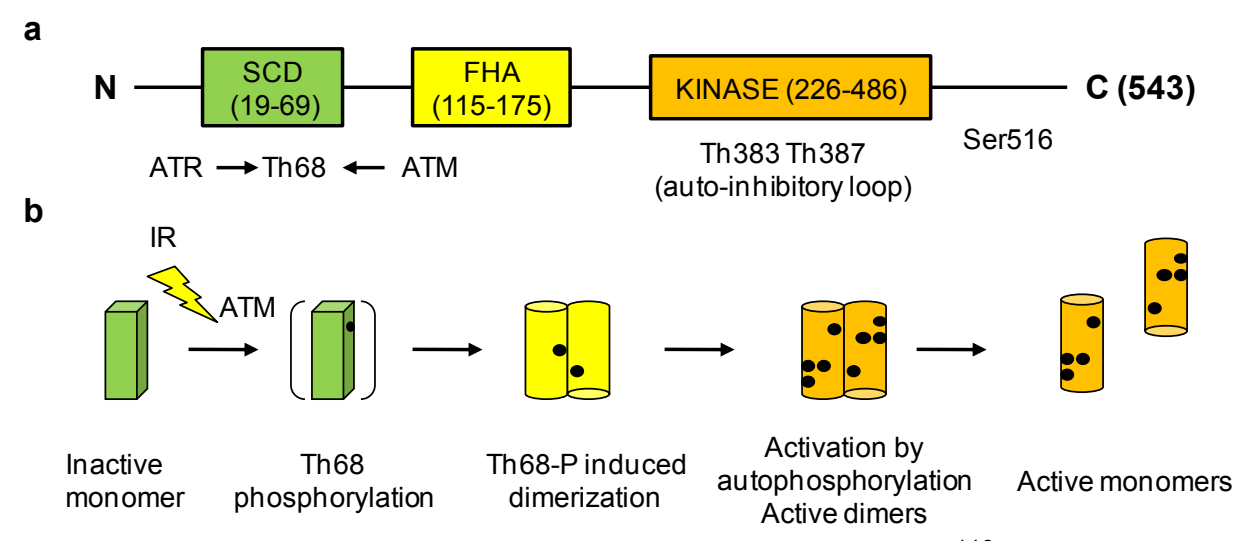


Figure I-7. Representation of Chk2. a) Functional domain of Chk2; 113 b) Model of Chk2 activation.

Following activation, Chk2 is believed to dissociate from sites of damage in its monomeric form to act on multiple substrates resulting in cell cycle arrest, activation of

DNA repair, and apoptosis.^{53, 89} Substrates of Chk2 *in vivo* include, but are not limited to, p53, BRCA1, Cdc25A and Cdc25C.⁹⁷ Phosphorylation of p53 by Chk2 and/or Chk1 stabilizes the p53 protein, ¹¹⁴⁻¹¹⁶ which increases the potential to positively regulate the factors involved in DNA repair, cell death and cell-cycle control.^{117, 118}

BRCA1 is another substrate of Chk2¹¹⁹ and is a key checkpoint controlling protein that is responsible for regulating homologous recombination repair, transcription-coupled repair, the cell cycle, chromatin remodeling and possible, and cell death. ¹²⁰⁻¹²² Chk2 phosphorylates BRCA1 at Ser988, which is required for the release of BRCA1 from its complex with Chk2. This event is important for cell survival following DNA damage. ¹¹⁹

I.G The role of Chk2 and p53

Chk2 has been associated with mediating cell cycle arrest in pathways through p53. p53 is a short-lived transcription factor that has attracted extensive research in its ability to mediate tumor suppression. 117, 123, 124 Evidence has suggested that p53 is not responsible for the rate of tumor initiation or mutation. Instead, p53 prevents the progression of malignant tumor cells. 125-128 It regulates cell growth through activation of cell-cycle arrest and apoptosis following chemotherapeutic or radiation induced DNA damage. 129-131 p53 is highly expressed in several normal tissues (lymphoid, hematopoietic organs, intestinal epithelia, etc.), which are severely damaged during chemotherapeutic treatment and IR. 132 There is a high level of p53 mutations in cancerous tissue (> 50% of all cancer contain p53 mutations). 133 In nearly half of these

tumors, p53 is inactivated directly resulting from mutations in the p53 gene. ¹¹⁷ In the majority of the remaining tumors, p53 is inactivated indirectly through viral proteins or from alterations in genes whose products interact with or transmit information to p53. ¹¹⁷

The p53 network can be activated by the ATM-Chk2 and the ATR-Chk1 pathway, ¹¹⁷ which inhibit degradation of p53, therefore stabilizing high concentrations of p53. The activated form of p53 can bind to particular DNA sequences and activate transcription of nearby genes which can ultimately lead to inhibition of cell division or cell death.

The levels of p53 in cells are dependent on its degradation rate which is regulated by ubiquitin-mediated proteolysis. The MDM2 protein is an enzyme that is involved in the attaching ubiquitin to p53, labeling it for degradation. This process is regulated by a negative feedback loop (Figure I-8). 134 p53 binds to the regulatory region of MDM2 and stimulates gene transcription to mRNA and subsequent translation into protein. 117 The MDM2 binds to p53 forming a complex, which allows ubiquitinylation and subsequent degradation of p53. 117, 126 The degradation of p53 reduces the amount of p53 and also reduces transcription of MDM2, closing the feedback loop and consequently allowing p53 levels to increase. Upstream phosphorylation of p53 occurs in the N-terminal region (Ser15, Thr18, Ser20, Ser37), 116, 135-138 where MDM2 binds. This affects the interaction with MDM2 in vitro, leading to stabilization of p53. 116, 135-138

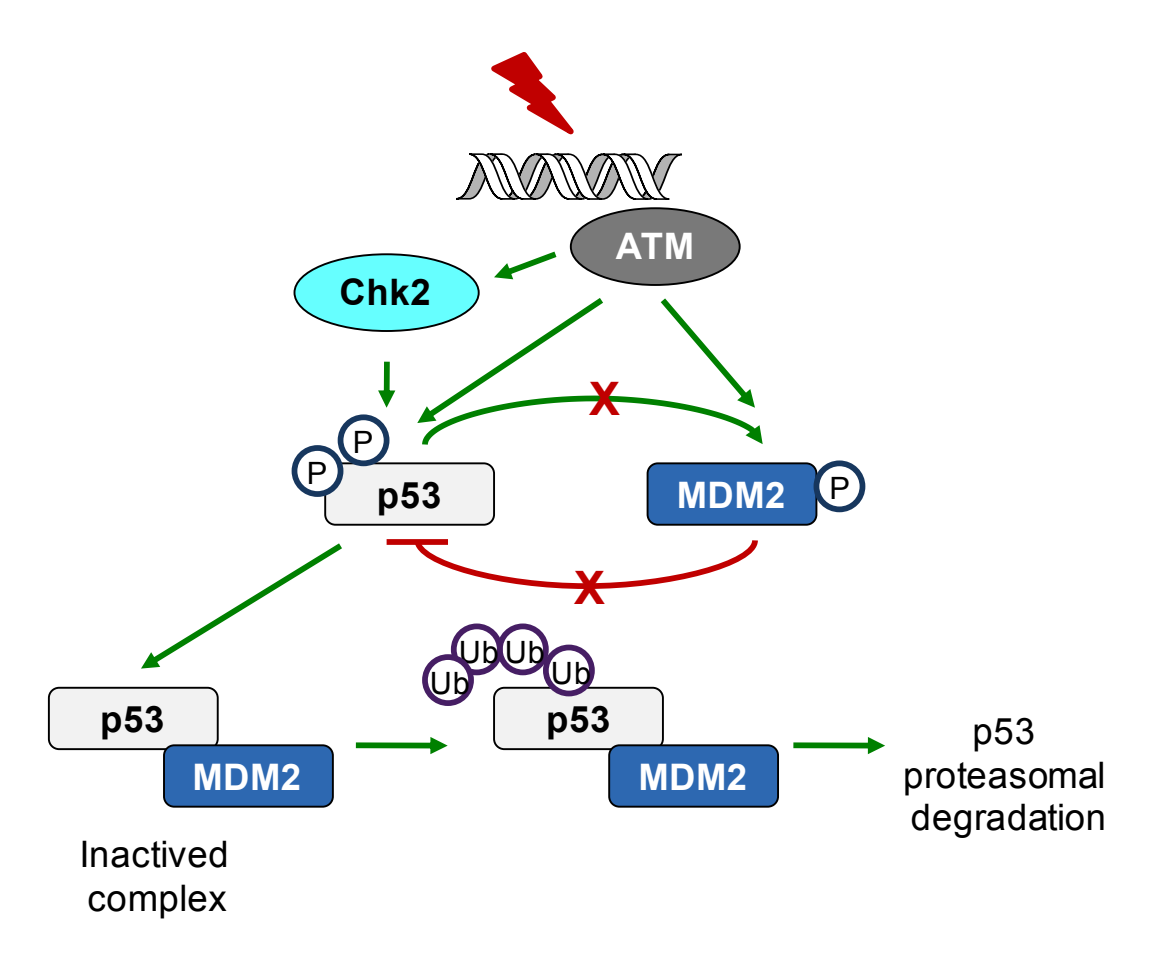


Figure I-8. Upstream signaling of p53 after IR-induced DNA damage. Phosphorylation of p53 and MDM2 disrupt the interaction between the two proteins.

ATM and Chk2 are capable of phosphorylating p53 within the MDM2 region, which has lead to much controversy over the connection between Chk2 and p53. Chk2 has been placed immediately upstream of p53 through studies involving Chk2 knockout mice as well as in vivo and in vitro experiments. ^{89, 114-116, 139-142} Chk2 was found to phosphorylate p53 at Ser20 thereby regulating p53 levels in response to DSBs. ^{114, 115, 140, 143} A kinase defective form of Chk2 prevented stabilization and phosphorylation of Ser20 in co-transfected p53 after DNA damage. ¹¹⁶ U2OS cells having a dominant negative Chk2 were incapable of stabilizing or phosphorylating endogenous p53 at

Ser20 and induced a p53 dependent G₁ checkpoint. In further support of the connection between Chk2 and p53, it was reported that Chk2 was capable of phosphorylating p53 at Ser20 *in vitro* and was capable of disrupting pre-complexed p53 and Mdm2. A different study reported that IR-activated immunoprecipitated Chk2 was able to phosphorylate p53. When Chk2 was silenced using engineered zinc finger transcription factors, decreased p53 transcriptional activation of the MDM2 gene and reduced p53 Ser20 phosphorylation were observed.

Conversely, evidence has also weakened the view that Chk2 regulates p53. Chk2 that was purified from tumor cell lines prior to and following DNA damage was unable to phosphorylate various forms of truncated or full-length p53 despite being markedly activated to phosphorylate the domain of Cdc25C containing Ser216. ¹⁴⁵ Other experiments *in vivo* have also challenged the relationship of Chk2 and p53. Chk1 and Chk2 knockout by siRNAs or RNAi of several human tumor cell lines resulted in partial or no defects in the DNA damage induced phosphorylation and stabilization of p53 Ser20 phosphorylation or transcriptional activity despite preventing Ser216 phosphorylation of Cdc25C. ^{140-142, 145, 146} Additionally, homozygous deletion of Chk2 in HCT116 colon carcinoma cells yielded no phenotype with respect to p53, G₁ or G₂ cell cycle arrest, and apoptosis. ^{113, 146}

The region of p53 spanning Ser20 does not share the homology with the consensus motif, L-X-R-X-X-S/T which is present in other known substrates of Chk2. Consequently, the peptide covering the p53 Ser20 region is a poor Chk2 substrate, which weakens the Chk2-p53 link. However, there are two regions of p53, amino

acids 117-132 and 272-288, that were proposed as Chk2 docking sites that could potentially regulate the kinase activity toward p53 allosterically. The purified Chk2 supplemented with these docking-site motifs was able to phosphorylate a Ser20 peptide (P-L-S-Q-E-T-F-S-D-L-D-L-W-K-L-K-K)¹⁴⁷ in a kinase assay. This study showed that Chk2 could modulate p53 specifically with a protein kinase docking site instead of by a consensus sequence.

Chk2 knockout mice have been generated independently by two groups which both support a role for Chk2 in the regulation of p53, however the proposed mechanisms did not agree. The first reported Chk2 null mouse generated from Hirao and colleagues 140 demonstrated that thymocytes, splenic T cells, and MEFs lacking Chk2 were unable to stabilize p53 following y-IR. When Chk2 was reintroduced, the defect was corrected. The cells were highly resistant to apoptosis consistent with a defect in p53 signaling. 140 A follow up study showed that Chk2 knockout mice were highly resistant to apoptosis in multiple tissue compartments by whole body IR experiments. These mice also developed chemically-induced skin tumors more rapidly. 141 At low doses of γ-IR, the G₁/S checkpoint of these mice was compromised, however, the cells arrested normally at doses above 5 Gy. 141 Another group used MEFs from these same mice, however did not observe a defect in G₁/S arrest at even low Xray doses. 149 Chk2 knockout mice generated by another research group was reported yielding different results. 142 The second generation of mice had many tissues that were resistant to apoptosis induced by y-IR, which was in agreement with the original Chk2 null mice, strongly supporting the role of Chk2 in DNA damage induced apoptosis. 142

These authors observed a deficient G_1/S arrest consistent with impaired p53 signaling. Unlike results reported by Hirao et al, only a 30-50% reduction in p53 stabilization and human p53 introduced into Chk2 -/- MEFs was phosphorylated normally on Ser20 after IR. These results indicated that Chk2 in murine tissue made only a partial contribution to p53 stabilization and that other factors contributed to the stabilization. Only a partial p53 stabilization defect was observed upon analysis of five p53 targets genes by quantitative RT-PCR in thymocytes and MEF"s. There was no upregulation of mRNA observed in the Chk2 -/- cells after IR, possibly providing a mechanistic explanation for the G_1/S arrest and apoptotic defects in the cells. 142

The relationship between Chk2 and p53 is likely to be stimuli- as well as cell type-specific as cell death in primary neuronal cultures induced by etoposide or camptothecin was shown to be ATM-dependent but Chk2 independent. 113, 150 It is evident that Chk2 plays a pivotal role in γ-IR induced apoptosis, however the exact mechanism remains unclear. Chk2 can regulate p53 transcriptional activity independently of Ser20 phosphorylation and stabilization in murine tissues after IR. 113 It is important to consider that many types of cellular stresses that activate p53 do not activate Chk2 and can subsequently signal to p53 normally even in the absence of Chk2. 113 Chk2 also has molecular targets other than p53, in the event that p53 or Chk2 is not present, the other protein remains a participant in other checkpoint pathways. Chk1 has been observed to undergo activation compensating for the absence of Chk2. 142 These features could support why Chk2 deletion or mutation does not affect p53 inactivation in human cancer cells. 141 Although the DNA damage pathway in

response to DSBs is not a linear pathway, cancer cells defective in Chk2 are under pressure to inactivate p53, which is consistent with the observed concomitant mutations of p53 and Chk2 in some tumors. 139, 151-153

I.H Cell cycle response pathways

Checkpoints function by arresting or delaying the progression of the cell cycle in response to DNA damage. ⁹³ The DNA damage response can operate in several ways: it regulates cell cycle arrest, activates DNA repair mechanisms, induces cell cycle death by apoptosis, regulates telomere length and activates pivotal transcriptional programs. ^{64, 154} Checkpoint genes have also been demonstrated to be necessary for the survival of organisms, causing embryonic lethality in mice when particular genes are knocked out. ^{76, 155} This provides strong evidence that checkpoint genes are critical for regulation of DNA damage, and more importantly, essential for functions in cellular survival. ⁵²

Cell cycle division in mammals is controlled by numerous cyclin-dependent kinase (Cdk) complexes (Figure I-9). Cdk4/6-Cyclin D complexes are active in the early phase of the G₁ phase of the cell cycle. Entry into and progression of cells through the S-phase are regulated by Cdk-2-Cyclin E and Cdk2-Cyclin A, respectively. Whether or not cells proceed into mitosis is governed by Cdk1 (Cdc2)-Cyclin B. The activities of the Cdk"s can be inhibited by several cyclin-dependent kinase inhibitors, such as p21 WAF1. In addition to the existing cell cycle phases G1, S, G2 and mitosis, there are also transitional points: G1/s, G2/M as well as intra-S phase and the mitotic checkpoint, which are all tightly controlled checkpoints. 61, 156 A key function of Chk1 and Chk2

following activation by ATR and ATM centers around the inactivation of members of the Cdc25 family by phosphorylation. This results in inhibition of cell cycle progression after DNA damage in the G_1/S phase or the G_2/M phase.⁵²

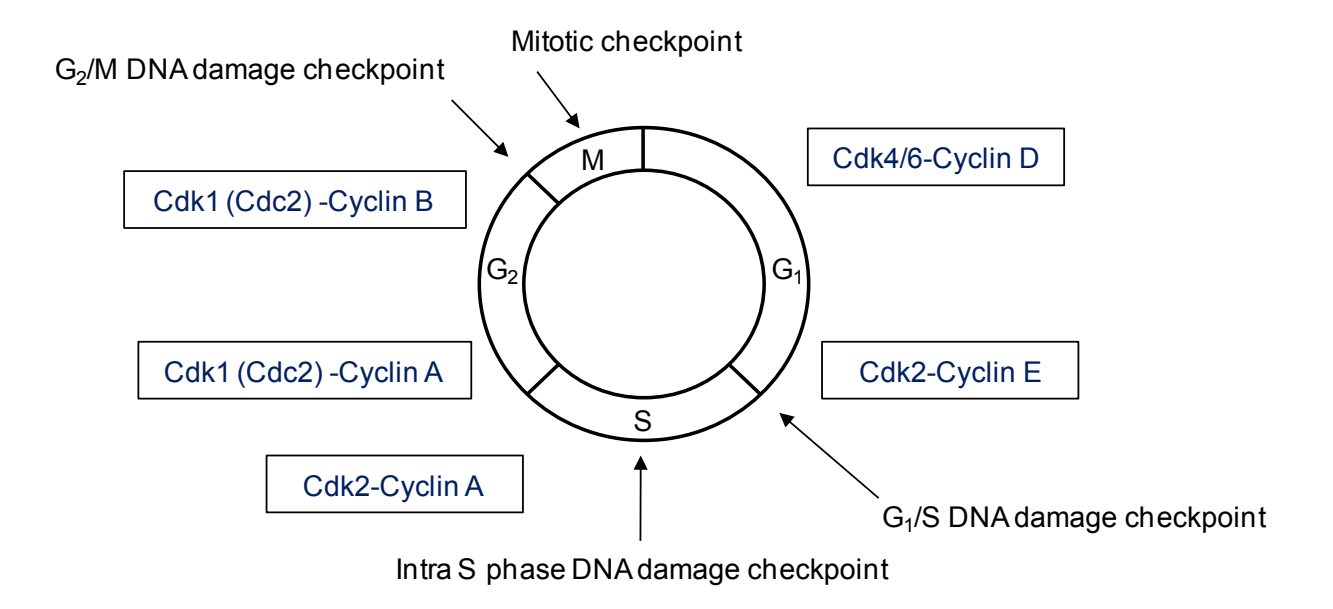


Figure I-9. Control of the cell division cycle by cyclins and Cdks and their regulation by cell cycle checkpoints.

Progression of the G_1/S checkpoint is dependent upon the Chk1/Chk2-Cdc25A-Cdk2 pathway (Figure I-10, pathway A). When active, Cdc25A is unphosphorylated and functions as a phosphatase for the Cdk2-Cyclin E complex. The Cdk2-Cyclin E complex remains active and allows the cell cycle to progress from G_1 to S_1 . In response to DNA damage, Chk1 and Chk2 can phosphorylate Cdc25A resulting in its degradation. The degradation of Cdc25A causes the Cdk2-Cyclin E complex to stay in its inactive hyperphosphorylated form and halts the G_1/S progression. S_2

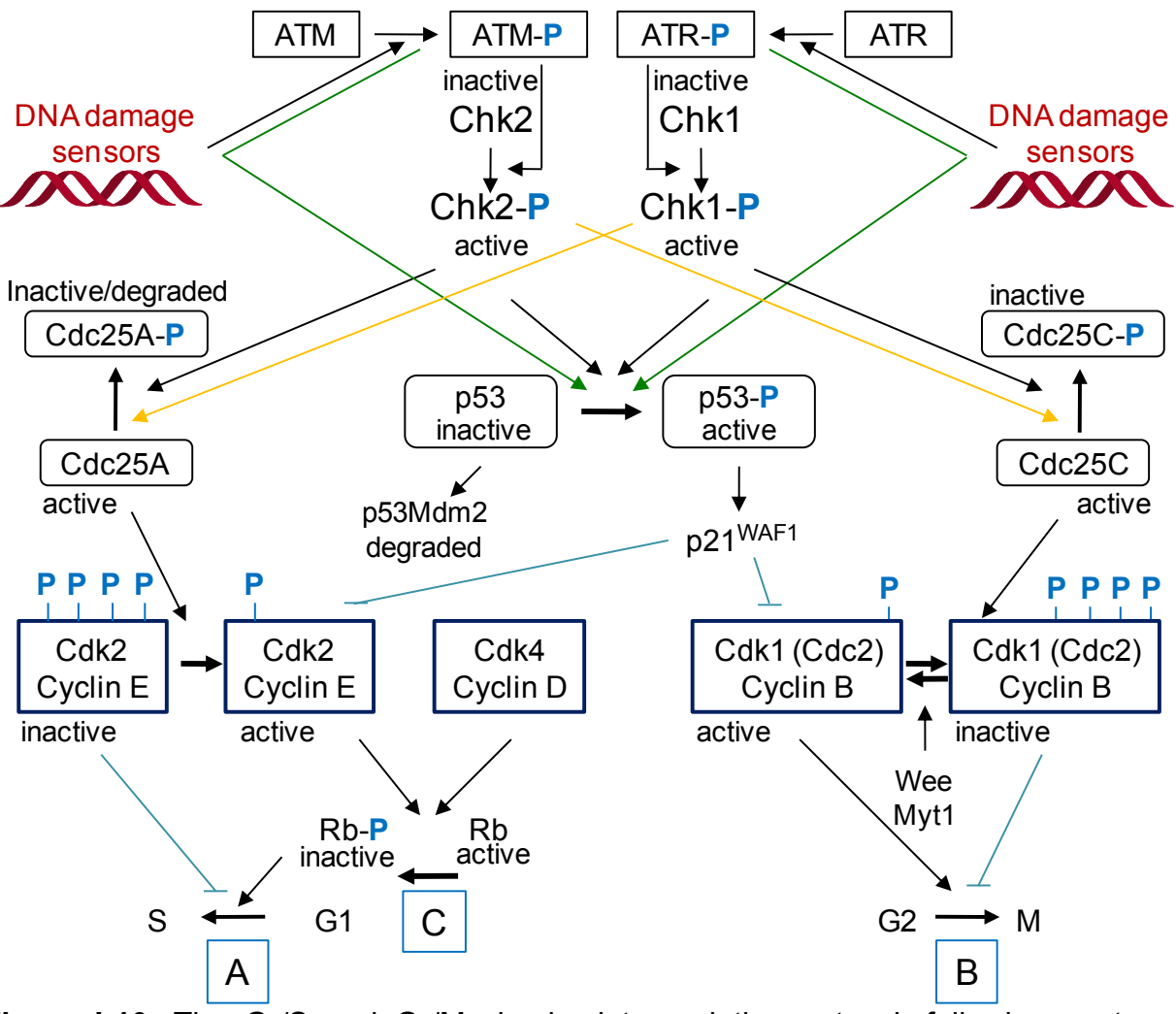


Figure I-10. The G_1/S and G_2/M checkpoint regulation network following upstream ATM/ATR activation. ⁵²

The G₂/M checkpoint relies on the Chk1/Chk2-Cdc25C-Cdk1 pathway (Figure I-10, pathway B). Activation of Cdk1-Cyclin B1 can subsequently activate Cdc25C, creating a positive feedback loop allowing progression into mitosis. ^{157, 158} The Cdk1-Cyclin B1 complex can also inactivate Wee1, which would result in two positive feedback loops. ¹⁵⁹ Mitosis that is triggered by Cdk1 is the most attractive target of the G₂ regulation. Cdk1 is phosphorylated at two sites by protein kinases Wee1 and Myt1 then subsequently dephosphorylated by Cdc25C phosphatase. ⁵² Increased amounts of phosphorylation of Cdk1 by Wee1/Myt1, or inhibition of dephosphorylation by Cdc25C

activated by Chk1 results in G_2/M DNA damage checkpoint arrest.⁵² The Cdk1-Cyclin B1 complex when inactive blocks entry into mitosis. Consequently, Chk1 and Chk2 can inhibit the cell cycle by controlling the Cdk1-Cyclin B1 complex via Cdc25C following DNA damage (Figure I-10, pathway B).⁵²

The Chk1/Chk2 pathway involving p53 regulates the G_1/S checkpoint (Figure I-10, pathway B, C). p53 can be phosphorylated at many sites by various protein kinases following DNA damage $^{160,\ 161}$ and is catalyzed by ATM, ATR, DNA-PK, and Chk1/Chk2. The phosphorylated form of p53 reduces the ability of MDM2 to bind to p53, which increases accumulation of p53 as well as its phosphorylation after DNA damage as mentioned above. $^{135,\ 162}$ The activation of p53 upregulates several target genes involved in the DNA damage response, one of which his p21 WAF1 . Build up of p21 WAF1 downregulates Cdk2-Cyclin E, resulting in G_1 arrest (Figure I-10, pathway C). 163 Inhibition of the G_1/S phase is a result of preventing phosphorylation of Rb by inhibiting Cdk2. 52 Activated p53 can also play a role in the G_2/M checkpoint by inducing p21 WAF1 , which blocks the formation of Cdk1-Cyclin B1 and therefore inhibiting its activity (Figure I-10, pathway B). $^{164-166}$

Checkpoint control following DNA damage can be influenced by p53 which is phosphorylated directly by ATM or ATR, $^{69, 162, 167, 168}$ or indirectly by ATM and ATR via Chk1 and Chk2. $^{114, 140}$ The Chk2 gene can have cancer-related mutations which prevents p53 from being phosphorylated. $^{139, 169}$ Cancer cells are dependent on the S and G_2 checkpoints in order to repair DNA damage. This is in part due to the defective G_1 checkpoint mechanisms. The S-phase checkpoint does not arrest in response to

DNA damage, instead it slows the progression of the cell cycle, then arrests at G_2 . Consequently, the G2 checkpoint is the key regulator of cancer cells and hence has been an attractive target for cancer therapy. Arresting cancer cells at G_2 prevents them from repairing DNA damage and forces them into mitotic catastrophe and apoptosis.¹⁷⁰

I.I Chk2 as a drug target candidate

Radiation and genotoxic chemotherapies remain primary methods of conventional cancer treatment and are likely to remain so. These therapies are imperfect often incurring severe side effects. Consequently, there has been interest focused on understanding how normal and tumor cells respond to DNA damage and determining whether the responses to DNA damage could be used for therapeutic purposes. 53 Based on the described DNA damage pathways above, it is possible that inhibiting the checkpoint kinases could be used to augment the effects of chemotherapeutics by sensitizing cancer cells, or desensitizing normal cells. 171-174 It is believed that inhibiting Chk1 sensitizes tumor cells by blocking the ability of cells to initiate DNA repair, resulting in DNA damage beyond repair. 171 175-177 Inhibition of Chk2 could selectively inhibit apoptosis in p53 wild type or normal cells, therefore desensitizing them from cell death during chemotherapeutic treatment. 173, 178 Inhibition of Chk2 is not anticipated to have effects on apoptosis in cells containing mutated p53 (> 50% of cancer cells). 133 Efforts have been focused on developing Chk2 inhibitors in order to desensitize normal cells toward IR and thus widen the therapeutic window of treatment.

I.J Validation of Chk2 as a drug target

Chk2 has become an attractive target for cancer therapy given its pivotal role in the regulation of the cell cycle, apoptosis and DNA repair following DNA damage. ^{179, 180} Ionizing radiation and DNA damaging chemotherapeutics continue to be the conventional form of cancer therapy often resulting in severe side effects. Inhibiting the DNA damage checkpoints could potentially augment the current chemo- or radiation therapies by sensitizing cancer cells to the cytotoxic effects of the therapy. Conversely, checkpoint inhibition could potentially allow an enhancement in survival of normal cells by desensitizing normal cells from IR or DNA damaging agents. ²

Chk2 inhibition is involved in eliciting radio- or chemoprotection of normal tissue via the inhibition of p53-dependent apoptosis. 179, 180 Most tumor cells bypass normal cell cycle responses following DNA damage if p53 is mutated. 181 In normal cells, p53 is activated by Chk2 following IR, resulting in cell cycle arrest and apoptosis. 182-184 Thus, inhibition of Chk2 in normal cells may prevent p53-mediated apoptosis, DNA repair and potential cell survival. This hypothesis was supported by a study in which Chk2 -/-transgenic mice showed a reduction in p53-dependent apoptotic responses. 142 Increased survival of the Chk2 -/- mice was observed following exposure to whole body IR as compared to Chk2 +/+ mice (Figure I-11). 142 Inhibition of Chk2 in mouse thymocytes 185 and isolated CD4+ and CD8+ human lymphocytes 186 also showed a decrease in apoptosis in response to IR. These and other elegant studies 66, 185-189 therefore indicate that inhibition of Chk2 in normal cells, may increase survival following IR by selectively reducing p53-mediated cell death.

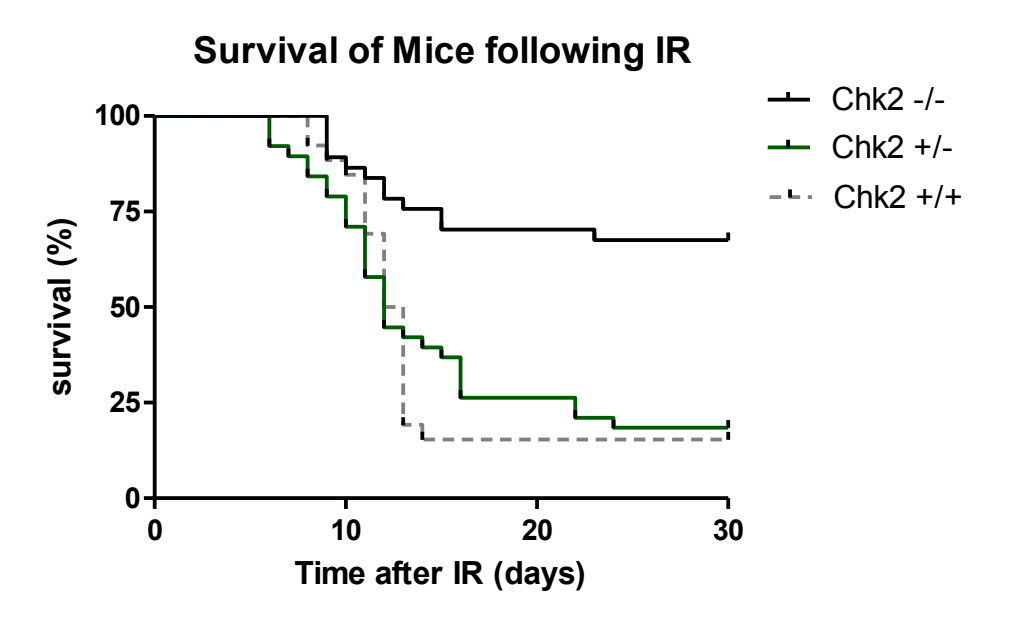


Figure I-11. Survival rates of Chk2 -/-, Chk2 +/- and Chk2 +/+ mice after 8 Gy whole body ionizing radiation. ¹⁴²

In addition to the radioprotective affects in normal cells, Chk2 inhibitors have been shown to enhance the effects of cytotoxic drugs¹⁹⁰⁻¹⁹² Transfection of MCF-7 cells with Chk2 siRNA¹⁴⁵ was found to enhance the effect of paclitaxel.¹⁹² Chk2 inhibition augmented the levels of mitotic catastrophe when used together with doxorubicin¹⁹³ or cisplatin¹⁹⁴ by releasing mitochondrial pro-apoptotic proteins. Additionally, small molecule Chk2 inhibitors have shown potentiation of DNA-damaging agents topotecan and camptothecin in OVCAR-4 and OVCAR-5 human tumor cells.¹⁹⁵

Recent studies also demonstrate that inhibition of Chk2 without an additional genotoxic agent may also be advantageous for therapeutic development in tumors possessing increased levels of activated Chk2. 180, 195, 196 Tumor cells in which Chk2 is constitutively activated have plausibly adapted a Chk2 dependence in order to survive.

A recent study by Pommier et al demonstrated the antiproliferative activity of a Chk2 inhibitor (discussed further in Chapter I.L) and Chk2 siRNA in cancer cell lines that were over-expressed in Chk2. 195

The use of Chk2 inhibitors for potentiating DNA-damage agents continues to be exciting albeit somewhat controversial 179, 180, 197 as not all inhibitors of Chk2 demonstrate these effects. 185, 188 There are only a few small molecule inhibitors of Chk2 that have been reported in the literature, thus interest in discovering a potent and selective inhibitor remains high. Of these reported inhibitors, high-throughput screening has proven to be very useful resulting in the identification of several ATP-competitive Chk2 inhibitors including 2-arylbenzimidazole-5-carboxamides (ABI), 186, 187 isothiazole carboxamidines 185, 188 and bis-guanylhydrazones (discussed further in Chapter I.L). 66,

I.K Purified drug target and X-ray crystal structure

It can be important and beneficial to have information about the purified drug target as a tool in developing inhibitors. Oliver et al. were able to crystallize the kinase domain of Chk2 (Figure I-12) offering an enormous amount of information toward the development of Chk2 inhibitors. Several Chk2 inhibitors have since been co-crystallized within the Chk2 binding domain. 111, 196, 198-200

The top of Figure I-12 illustrates the linear representation of the whole Chk2 protein. Chk2 is a 543 long amino acid protein that consists of three domains which were described in Chapter I.F. Briefly, The first domain is known as the SQ/TQ cluster domain (SCD), which is the substrate of the upstream protein ATM. The second domain

is the FHA which has been implicated in the modulation of protein-protein interactions. The last domain, which was crystallized, is the kinase domain which is responsible for performing the phosphorylation of substrates. The information the Chk2 crystal structure has provided has been invaluable toward the discovery of new Chk2 inhibitors and progress toward an adjuvant drug for chemo- and radiation therapy.

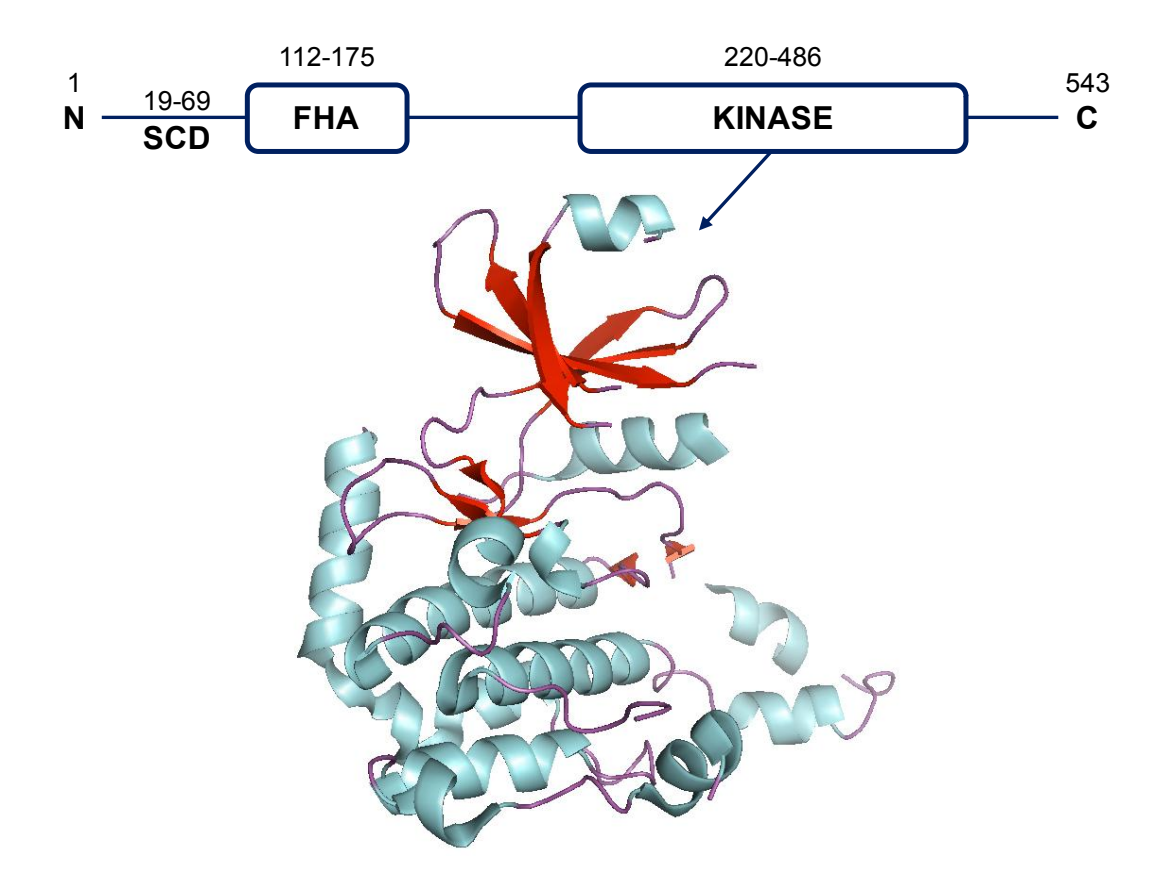


Figure I-12. Illustration of Chk2 and crystal structure of kinase domain.

I.L Current Chk2 Inhibitors

Although there has been an increase in the synthesis and discovery of Chk2 inhibitors within the last decade, few potent and selective Chk2 inhibits were reported until recently. Some of these inhibitors remain highly confidential such as XL844, developed by Excelixis, which is currently in clinical trials. 201-203 While the structure of

XL844 is not publicly known, other inhibitors have been hidden in patents such as the indazole and squaric acid derivatives shown in Figure I-13, and have not been highly publicized. ²⁰⁴⁻²⁰⁶

Figure I-13. Squaric acid derivatives and indazoles as Chk2 inhibitors.

An increasing number of novel Chk2 inhibitors have been reported through high throughput screening of compound collections and combinatorial libraries. ^{66, 185-188, 195,} A bis-quanylhydrazone (NSC 109555) was identified after a high throughput screen of over 100,000 compounds (Figure I-14) and was co-crystallized in the Chk2 binding pocket. 199 The compound was found to be an ATP competitive inhibitor of Chk2 with an IC₅₀ of 240 nM. NSC 109555 was relatively selective for Chk2 showing at least 6.5 times selectivity over other kinases. When evaluated in cellular studies, NSC 109555 was unable to inhibit topotecan-induced autophosphorylation of Chk2 at Ser516 as well as abrogation of the G₂/M block induced by camptothecin.⁶⁶ The lack of cellular inhibition was possibly due to pharmacokinetics or DNA binding interference of the polyamine. 66 A further SAR study of the bis-guanylhydrazones produced a derivative of NSC 109555, which demonstrated similar potent inhibition of Chk2 in vitro. PV1019 was at least 75 times more selective for Chk2 when evaluated against a screen of 50 kinases. 195 PV1019 inhibited Chk2 autophosphorylation in

addition to its downstream substrates. Chk2 inhibitor PV1019 protected normal mouse thymocytes against IR-induced apoptosis and showed synergistic antiproliferative activity with chemotherapeutics in tumor cell lines. Inhibition of Chk2 with PV1019 alone in cancer cells with high Chk2 expression resulted in antiproliferative activity.

Figure I-14. Structures of NSC 109555 and PV1019.

A series of isothiazole carboxamidine compounds were described by Wu and Carlessi as novel and selective and potent inhibitors of Chk2 (IC₅₀ = 120 nM to 40 μM). ¹⁸⁵ Of these, VRX0466617 (Figure I-15) was found to be the most potent and selective, exhibiting radioprotection in BJ-hTERT cells and mouse thymocytes. VRX0466617 did not modify the cytotoxicity of anticancer drugs, nor did it have a significant effect on G₂/M arrest. However, VRX0466617 did show cellular inhibition of Chk2 at Ser 19 and Ser 33-25 in addition to other downstream substrates. ¹⁸⁵ Zabludoff et al. introduced a thiophene carboxamide, AZD7762, which is currently in phase I clinical trials in combination with gemcitabine and IR in pancreatic tumor models. ^{207, 209} AZD7762 has been shown in multiple assays to inhibit DNA damage-induced cell cycle checkpoints. This Chk2 inhibitor has been evaluated extensively and has demonstrated its ability to increase the response to multiple DNA-damaging agents in several tumor cell lines. Although AZD7762 is an equally potent inhibitor of Chk1 and Chk2, the

cellular studies performed point to mechanisms targeted at Chk1 *in vivo* and not Chk2. 207, 209 AZD7762 inhibited Chk1 autophosphorylation (Ser296), stabilized Cdc25A and increased ATR/ATM-mediated Chk1 phosphorylation (Ser345). 209 AZD7762 showed radio- and chemosensitizing properties comparable to those observed by Chk1 inhibitors PD-321852 and PF-00477736 (100-fold more selective for Chk1 than Chk2). 210-212

Figure I-15. Structure of carboxamide Chk2 inhibitors.

Researchers at Johnson and Johnson developed a new class of benzimidazoles as inhibitors of Chk2. A high-throughput screening of purified human Chk2 led to a novel series of 2-arylbenzimidazoles which demonstrated potent and selective inhibition of Chk2. The most potent inhibitor is illustrated in Figure I-16, resulting in an IC $_{50}$ value of 2 nM and showing excellent selectivity for Chk2 over 35 kinases evaluated. The 2-arylbenzimidazole inhibitor also showed effective radioprotection of human T-cells against IR with EC $_{50}$ values between 3-7.6 μ M. Additionally, isolated CD4+ and CD8+ human lymphocytes also showed a decrease in apoptosis. $^{186,\ 187}$

An SAR study was performed with a series of non-benzimidazole Chk2 inhibitors (Figure I-16). The IC $_{50}$ values for the new inhibitors ranged from 5.8 μ M-16 nM. 187

Studies with these inhibitors evaluating the potentiation of cytotoxic abilities with current cancer therapeutics have not yet been performed.^{57, 187}

Figure I-16. Structure of arylbenzimidazole and non-benzimidazole inhibitors of Chk2.

Hilton et al. identified a class of 3,5-diaryl-2-aminopyridine inhibitors through high throughput screening of a kinase-focused compound library. Over 60 compounds were synthesized and characterized in addition to displaying the interaction of the compounds using co-crystallization with Chk2. Many of these compounds were reported to be Chk2 inhibitors. Of the many nanomolar inhibitors, three compounds (Figure I-17) showed selectivity toward Chk2 and demonstrated cellular inhibition of autophosphorylation of Chk2 at Ser516. 198

Figure I-17. Structures of aminopyrimidine inhibitors of Chk2.

Structure-based design was used to optimize a new class of 2-(quinazoline-2-yl)phenols in order to generate potent and selective inhibitors of Chk2. 196 The SAR

study gave rise to nearly 50 compounds which were screened for Chk2/Chk1 potency and selectivity. The most potent compound (IC $_{50}$ = 3 nM), CCT241533 (Figure I-18), had a 63-fold selectivity of Chk2 over Chk1 and demonstrated cellular inhibition of autophosphorylation of Ser516. 196 Additionally, CCT241533 enhanced the cytotoxicity of PARP inhibitors in p53-deficient cell lines and inhibited etoposide-induced biomarkers of Chk2 activity in human tumor cell lines. 213 CCT241533 showed a dose dependent decrease in apoptosis of mouse thymocytes when treated before IR. 196 Caldwell et al were also able to identify minor differences in the Chk1 and Chk2 binding pockets, however were unable to determine if these changes were significant. 196

Figure I-18. Structure of CCT241533.

Natural products and analogs of natural products have contributed to the number of current Chk2 inhibitors. Staurosporine and its analog UCN-01 (Figure I-19) were shown to be potent inhibitors of Chk2, however, did not demonstrate selectivity for the checkpoint kinase. $^{66,\ 214,\ 215}$ UCN-01 showed potent inhibition of Chk2 (IC₅₀ = 10 nM) 214 and an ability to potentiate the anticancer activity of a variety of therapeutics including cis-platin, mitomycin and IR. $^{216-219}$ Additionally, UCN-01 has been found to

augment the cytotoxicity of chemotherapeutic agents in human glioblastoma cells.²²⁰ The use of UCN-01 has been questionable due to its promiscuity as a kinase inhibitor. The structure of UCN-01 also contains pharmacokinetic disadvantages such as its strong binding to human plasma protein and its low bioavailability.²²¹⁻²²³

Figure I-19. Structure of natural product staurosporine and analog UCN-01.

Debromohymenialdisine (Figure I-20) is a natural product that inhibited Chk1 and Chk2 (IC $_{50}$ = 3 and 3.5 μ M, *in vitro*). ^{176, 224} Debromohymenialdisine also exhibited moderate cytotoxicity (25 μ M) and inhibition of the G $_2$ checkpoint at 8 μ M *in vivo*. ¹⁷⁶ Despite the moderate inhibition, its lack of selectivity for Chk2 over other kinases limits the use of debromohymenialdisine as a Chk2 inhibitor. ⁵⁷

$$\begin{array}{c} H_2N \longrightarrow N \\ HN \longrightarrow NH \\ H \longrightarrow NH \\ H$$

Figure I-20. Structure of debromohymenialdisine and its analog indoloazepine.

A debromohymenialdisine-derived analog, indoloazepine, was developed in our laboratory and has been shown to be a potent and selective inhibitor of Chk2. An *in vitro* assay identified an IC₅₀ = 8 nM for Chk2 inhibition by indoloazepine, which was also ~30 fold more selective over Chk1 and other purified kinases. Indoloazepine is a potent and selective inhibitor in the kinase assay, however, we wanted to further evaluate the drug to determine if it also showed cellular inhibition of Chk2, which is the foundation of my project.

I.M Chk2 binding pocket properties

Crystallization of the kinase domain of Chk2 by Oliver et al. 112 allowed exploration and examination within the binding pocket. Debromohymenialdisine (DBH) was successfully crystallized within the binding pocket making it possible to identify possible residues important for binding purposes. Important hydrogen bonding interactions can be seen between DBH and the Chk2 (Figure I-21) using PyMol to visualize the active site. 225

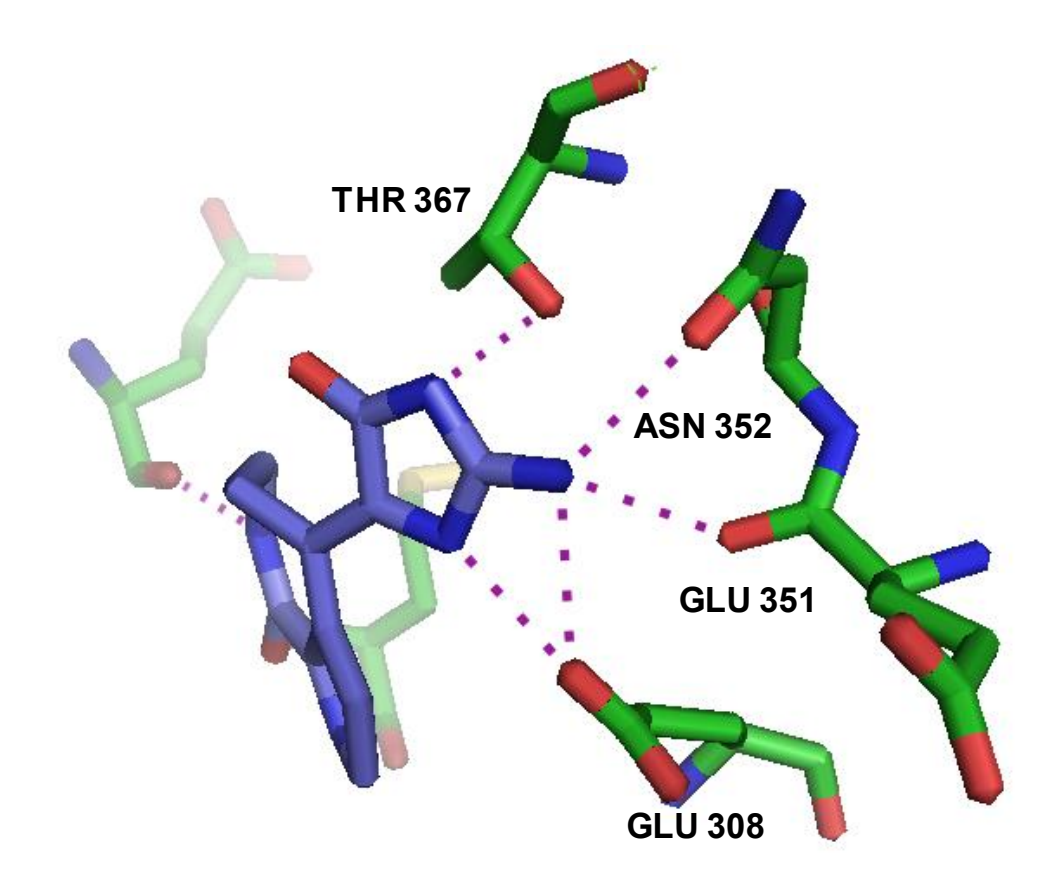


Figure I-21. Debromohymenial disine inside the Chk2 active site, top view.

DBH is shown in the center of Figure I-21 in blue, and the purple dashed lines represent hydrogen bonding interactions made with the side chains and main chain of Chk2. The potent inhibition of DBH can be attributed to the hydrogen binding interactions to the glycocyamidine portion, which include threonine, asparagine and glutamic acid residues. Additional hydrogen bonding interactions were observed in the southern portion of DBH as shown in Figure I-22. The interactions are made between the amide functional group of the seven-membered ring to glutamine and methionine residues, contributing further to the potency of DBH.

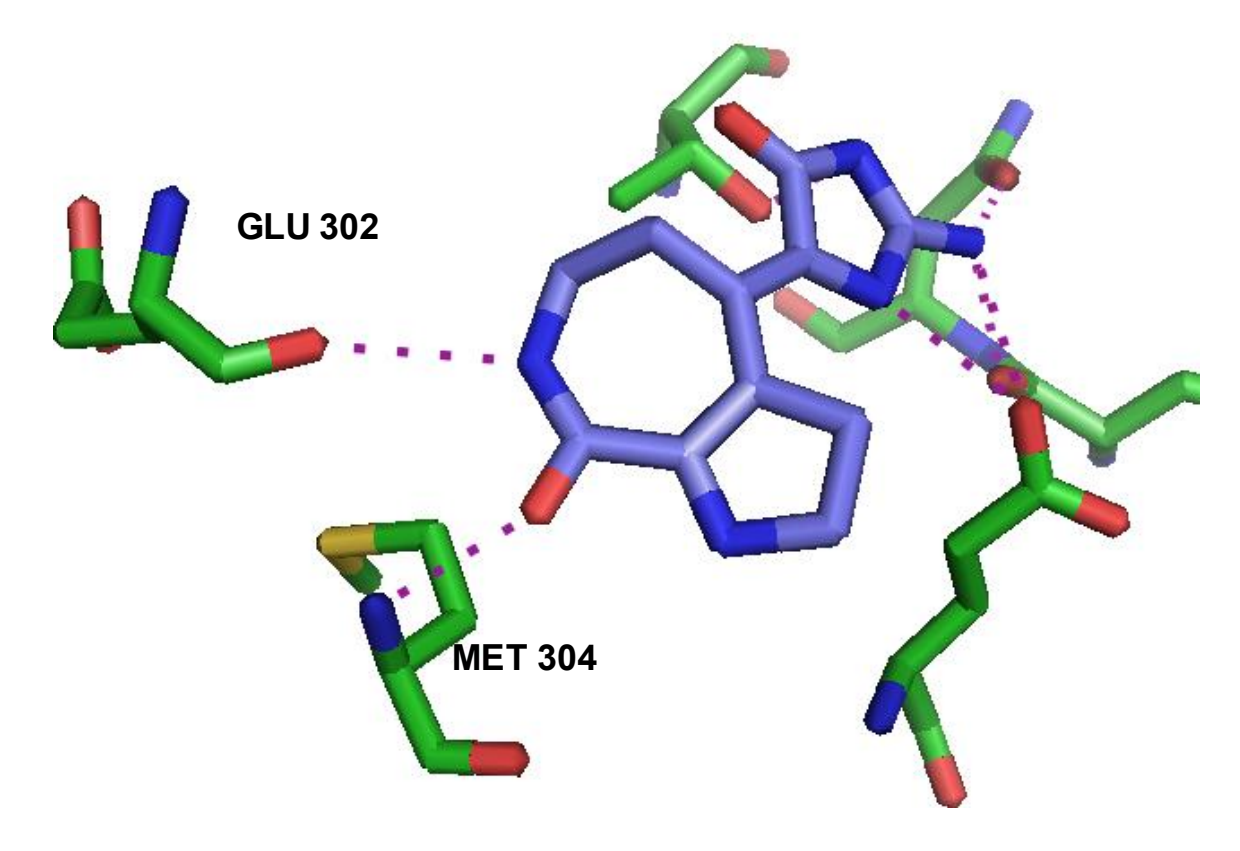


Figure I-22. Debromohymenialdisine inside the Chk2 active site, bottom view.

Information obtained from DBH and Chk2 was applied to the DBH analog, indoloazepine, which could have similar binding interactions within Chk2. Figure I-23 shows the potential binding interactions could be very similar to those of DBH. The hydrogen bonding interactions between the glycocyamidine ring of indoloazepine and the residues surrounding it could interact to help hold indoloazepine in the active site. The seven-membered ring of indoloazepine could also form hydrogen binding interactions between the amide and those residues that held DBH in the active site.

The exact binding nature of indoloazepine in the active site of Chk2 remains unknown, however it can be hypothesized based on the binding properties of a closely related structure (DBH).

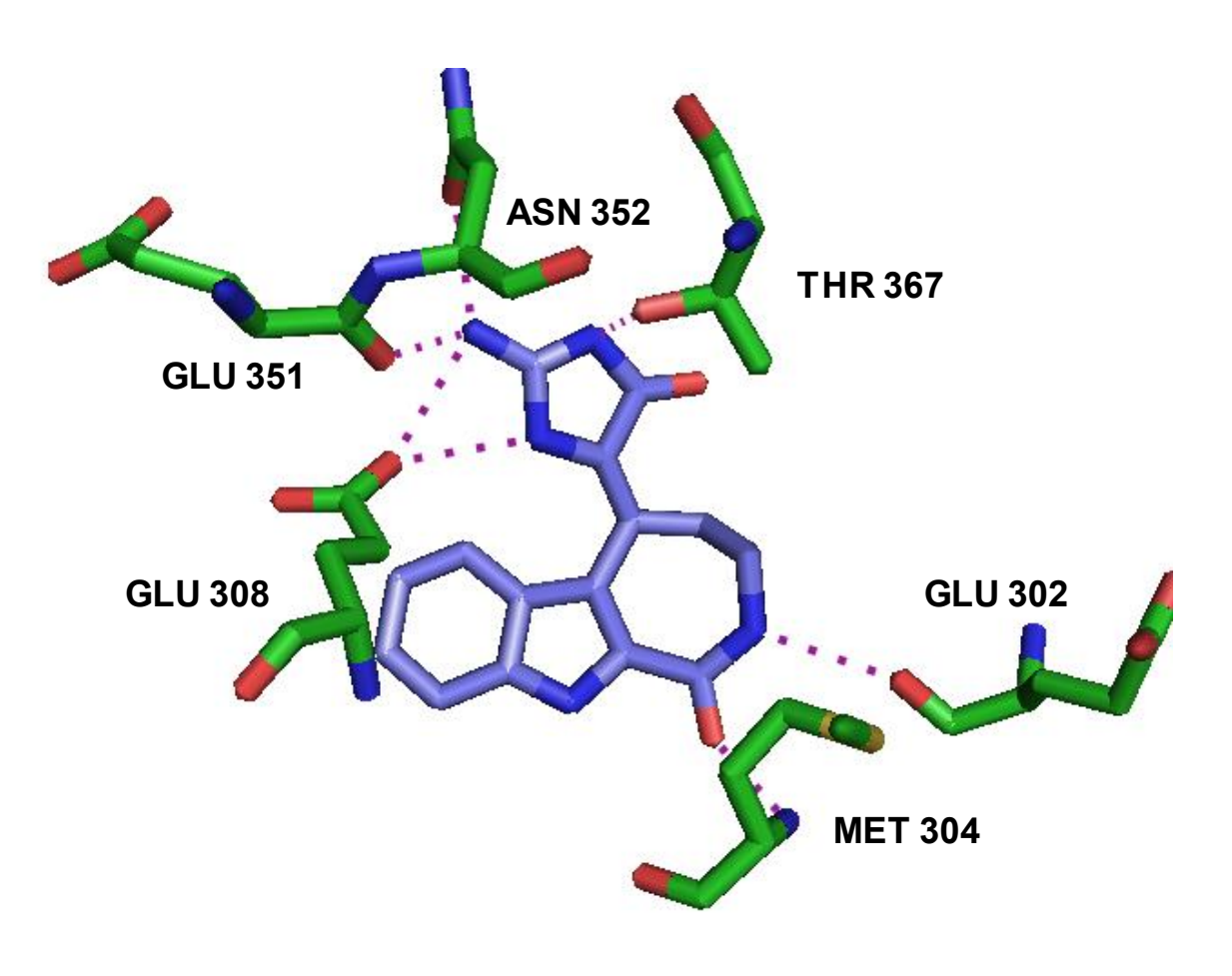


Figure I-23. Indoloazepine modeled in the Chk2 catalytic site.

I. N Goals of project

The first goal of this project was directed toward optimizing a scale up synthesis of indoloazepine, which would allow for further biological evaluation. The synthetic route previously synthesized in our lab produced indoloazepine in 12% total yield. ^{224, 226} In the interest of obtaining a more potent/selective inhibitor, analogs were synthesized to assist in understanding the importance of the free amine moiety of the glycocyamidine ring in the ATP binding pocket.

Chk2 was inhibited by indoloazepine in an *in vitro* kinase assay, however Chk2 had not been confirmed as the target of indoloazepine in cell culture. The second goal of the project was to elucidate cellular mechanisms and radioprotection abilities.

REFERENCES

I.O References

- 1. Jemal, A.; Siegel, R.; Ward, E.; Hao, Y.; Xu, J.; Murray, T.; Thun, M. J., Cancer statistics, 2008. *CA Cancer J. Clin.* **2008**, *58* (2), 71-96.
- Warshawsky, D.; Landolph, J. R. J., Molecular Carcinogenesis and the Molecular Biology of Human Cancer. CRC Taylor & Francis Group, LLC: Boca Raton, 2006; p 576.
- 3. Harris, C. C., Chemical and physical carcinogenesis: advances and perspectives for the 1990s. *Cancer Res.* **1991**, *51* (18 Suppl), 5023s-5044s.
- 4. Yuspa, S. H., Overview of carcinogenesis: past, present and future. *Carcinogenesis* **2000**, *21* (3), 341-344.
- 5. Yokota, J., Tumor progression and metastasis. *Carcinogenesis* **2000**, *21* (3), 497-503.
- 6. Atit, R. P.; Mitchell, K.; Nguyen, L.; Warshawsky, D.; Ratner, N., The neurofibromatosis type 1 (Nf1) tumor suppressor is a modifier of carcinogen-induced pigmentation and papilloma formation in C57BL/6 mice. *J. Invest. Dermatol.* **2000**, *114* (6), 1093-1100.
- 7. Kerbel, R. S., Tumor angiogenesis: past, present and the near future. *Carcinogenesis* **2000**, *21* (3), 505-515.
- 8. Barinaga, M., Is apoptosis key in Alzheimer's disease? *Science* **1998**, *281* (5381), 1303-1304.
- 9. Landolph, J. R.; Verma, A.; Ramnath, J.; Clemens, F., Molecular biology of deregulated gene expression in transformed C3H/10T1/2 mouse embryo cell lines induced by specific insoluble carcinogenic nickel compounds. *Environ. Health Perspect.* **2002**, *110 Suppl 5*, 845-850.
- 10. Henderson, B. E.; Ross, R. K.; Pike, M. C., Toward the primary prevention of cancer. *Science* **1991**, *254* (5035), 1131-1138.

- 11. Goldin, B. R.; Adlercreutz, H.; Gorbach, S. L.; Warram, J. H.; Dwyer, J. T.; Swenson, L.; Woods, M. N., Estrogen excretion patterns and plasma levels in vegetarian and omnivorous women. *N. Engl. J. Med.* **1982**, *307* (25), 1542-1547.
- 12. Hatch, F. T.; MacGregor, J. T.; Zeiger, E., Review: Putative mutagens and carcinogens in food. VII. Genetic toxicology of the diet. A summary of a satellite symposium of the Fourth International Conference on Environmental Mutagens. Copenhagen, June 19-22, 1985. Abstracts. *Environ. Mutagen.* **1986**, *8* (3), 467-484.
- 13. Ames, B. N., Dietary carcinogens and anticarcinogens. Oxygen radicals and degenerative diseases. *Science* **1983**, *221* (4617), 1256-1264.
- 14. Cohen, L. A., Diet and cancer. *Sci. Am.* **1987**, *257* (5), 42-48.
- 15. Butel, J. S., Viral carcinogenesis: revelation of molecular mechanisms and etiology of human disease. *Carcinogenesis* **2000**, *21* (3), 405-426.
- Biedermann, K. A.; Landolph, J. R., Role of valence state and solubility of chromium compounds on induction of cytotoxicity, mutagenesis, and anchorage independence in diploid human fibroblasts. *Cancer Res.* 1990, 50 (24), 7835-7842.
- 17. Biedermann, K. A.; Landolph, J. R., Induction of anchorage independence in human diploid foreskin fibroblasts by carcinogenic metal salts. *Cancer Res.* **1987**, *47* (14), 3815-3823.
- 18. Landolph, J. R., Molecular mechanisms of transformation of C3H/10T1/2 C1 8 mouse embryo cells and diploid human fibroblasts by carcinogenic metal-compounds. *Environ. Health Perspect.* **1994,** *102*, 119-125.
- 19. Lew, E. A.; Garfinkel, L., Variations in mortality by weight among 750,000 men and women. *J. Chron. Dis.* **1979,** *32* (8), 563-576.
- 20. Hatch, F. T.; Macgregor, J. T.; Zeiger, E., Putative mutagens and carcinogens in foods. 7. Genetic toxicology of the diet review. *Environ. Mutag.* **1986**, *8* (3), 467-484.

- 21. Aletras, V.; Hadjiliadis, D.; Hadjiliadis, N., On the Mechanism of Action of the Antitumor Drug cis-Platin (cis-DDP) and its Second Generation Derivatives. *Met. Based Drugs* **1995**, *2* (3), 153-185.
- 22. Bernier, J.; Hall, E. J.; Giaccia, A., Radiation oncology: a century of achievements. *Nat. Rev. Cancer* **2004**, *4* (9), 737-747.
- 23. Bikker, J. A.; Brooijmans, N.; Wissner, A.; Mansour, T. S., Kinase domain mutations in cancer: implications for small molecule drug design strategies. *J. Med. Chem.* **2009**, *52* (6), 1493-1509.
- 24. Ghoshal, K.; Jacob, S. T., An alternative molecular mechanism of action of 5-fluorouracil, a potent anticancer drug. *Biochem. Pharmacol.* **1997**, *53* (11), 1569-1575.
- 25. Hande, K. R., Etoposide: four decades of development of a topoisomerase II inhibitor. *Eur. J. Cancer* **1998**, *34* (10), 1514-1521.
- 26. Katsoulas, A.; Rachid, Z.; Brahimi, F.; McNamee, J.; Jean-Claude, B. J., Cytokinetics and mechanism of action of AKO4: a novel nitrogen mustard targeted to bcr-abl. *Leuk. Res.* **2005**, *29* (5), 565-572.
- 27. Kumar, G. S.; Lipman, R.; Cummings, J.; Tomasz, M., Mitomycin C-DNA adducts generated by DT-diaphorase. Revised mechanism of the enzymatic reductive activation of mitomycin C. *Biochemistry* **1997**, *36* (46), 14128-14136.
- 28. Rothenberg, M. L., Topoisomerase I inhibitors: review and update. *Ann. Oncol.* **1997,** *8* (9), 837-55.
- 29. Rowinsky, E. K.; Donehower, R. C., Paclitaxel (taxol). *N. Engl. J. Med.* **1995**, 332 (15), 1004-14.
- 30. Sahasranaman, S.; Howard, D.; Roy, S., Clinical pharmacology and pharmacogenetics of thiopurines. *Eur. J. Clin. Pharmacol.* **2008**, *64* (8), 753-767.
- 31. von Sonntag, C., *Free-Radical-Induced DNA Damage and Its Repair*. Springer-Verlag: Berlin, 2006; p 523.

- 32. Krohn, K., *Topics in Current Chemistry; Anthracycline Chemistry and Biology II; Mode of Action, Clinical Aspects and New Drugs.* Springer-Verlag: 2008; Vol. 283, p 222.
- 33. Thorburn, A.; Frankel, A. E., Apoptosis and anthracycline cardiotoxicity. *Mol. Cancer Ther.* **2006**, *5* (2), 197-9.
- 34. Trevino, A. V.; Woynarowska, B. A.; Herman, T. S.; Priebe, W.; Woynarowski, J. M., Enhanced topoisomerase II targeting by annamycin and related 4-demethoxy anthracycline analogues. *Mol. Cancer Ther.* **2004**, *3* (11), 1403-1410.
- 35. DeVita, V. T. J.; Lawrence, T. S., *Cancer: Principles and Practice of Oncology*. 8th ed.; Lippincott Williams and Wilkins: Philadelphia, 2008.
- 36. Kirkwood, J. M.; Lotze, M. T.; Yasko, J. M., *Current Cancer Therapeutics*. 4th ed.; Current Medicine, linc: Philadelphia, 2001; p 490.
- 37. Calabresi, P.; Rall, T.; Nies, A.; Palmer, T., *Goodman and Gilman's The Pharmalogical Basis of Therapeutics*. 8 ed.; Pegamon Press: New York, 1990.
- 38. Chabner, B.; Collins, J., *Cancer Chemotherapy: Principles and Practice*. JB Lippincott: Philadelphia, 1990.
- 39. Black, D. J.; Livingston, R. B., Antineoplastic drugs in 1990 A review. 1. *Drugs* **1990**, 39 (4), 489-501.
- 40. Black, D. J.; Livingston, R. B., Antineoplastic drugs in 1990 A review. 2. *Drugs* **1990,** 39 (5), 652-673.
- 41. Chen, A. P.; Grem, j. L., Antimetabolites. *Curr. Opin. Oncol.* **1992,** *4* (6), 1089-1098.
- 42. Cheson, B. D., New antimetabolites in the treatment of human malignancies. *Semin. Oncol.* **1992,** *19* (6), 695-706.
- 43. Clarke, S. J.; Jackman, A. L.; Harrap, K. R., Antimetabolites in cancer-chemotherapy. *Purine and Pyrimidine Metabolism in Man Vii, Pt A* **1991,** 309, 7-13.

- 44. Baxter, J. D.; Funder, J. W., Hormone receptors. *N. Engl. J. Med.* **1979,** 301 (21), 1149-1161.
- 45. Rowinsky, E. K.; Tolcher, A. W., Antimicrotubule drugs. In *Cancer, Principles and Practice of Oncology*, DeVita, V. T. J.; Hellman, S.; Rosenberg, S. A., Eds. Lippincott-Raven: Philadelphia, 2000.
- 46. Lawrence, T. S.; Ten Haken, R. K.; Giaccia, A., Principles of Radition Oncology. In *Cancer: Principles of Oncology*, 8th ed.; DeVita, V. T. J.; Lawrence, T. S.; Rosenberg, S. A., Eds. Lippincott Williams and Wilkins: Philadelphia, 2008.
- 47. Tobias, J. S., Clinical practice of radiotherapy. *Lancet* **1992**, 339 (8786), 159-63.
- 48. Batista, L. F. Z.; Kaina, B.; Meneghini, R.; Menck, C. F. M., How DNA lesions are turned into powerful killing structures: Insights from UV-induced apoptosis. *Mutat. Res. Rev. Mutat. Res.* **2009**, *681* (2-3), 197-208.
- 49. Health Effects of Exposure to Low Levels of Ionizing Radiation (Beir IV). Sciences, N. A. o., Ed. National Academies Press: Washington, D.C., 1990.
- 50. Ward, J. F., DNA damage produced by ionizing-radiation in mammalian-cells-identities, mechanisms of formation, and repairability. *Prog. Nucleic Acid Res. Mol. Biol.* **1988**, *35*, 95-125.
- 51. Goodhead, D. T., Initial events in the cellular effects of ionizing-radiations clustered damage in DNA. *Int. J. Radiat. Biol.* **1994**, *65* (1), 7-17.
- 52. Poehlmann, A.; Roessner, A., Importance of DNA damage checkpoints in the pathogenesis of human cancers. *Pathol. Res. Pract.* 206 (9), 591-601.
- 53. Smith, J.; Mun Tho, L.; Xu, N.; A. Gillespie, D.; George, F. V. W.; George, K., The ATM-Chk2 and ATR-Chk1 Pathways in DNA Damage Signaling and Cancer. In *Adv Cancer Res*, Academic Press: Vol. Volume 108, pp 73-112.
- 54. Melo, J.; Toczyski, D., A unified view of the DNA-damage checkpoint. *Curr. Opin. Cell Biol.* **2002**, *14* (2), 237-245.

- 55. Zhou, B. B.; Bartek, J., Targeting the checkpoint kinases: chemosensitization versus chemoprotection. *Nat. Rev. Cancer* **2004**, *4* (3), 216-225.
- 56. Tobey, R. A., Different drugs arrest cells at a number of distinct stages in G2. *Nature* **1975**, *254* (5497), 245-247.
- 57. Sharma, V.; Hupp, C. D.; Tepe, J. J., Enhancement of chemotherapeutic efficacy by small molecule inhibition of NF-kappaB and checkpoint kinases. *Curr. Med. Chem.* **2007**, *14* (10), 1061-1074.
- 58. Weinert, T. A.; Hartwell, L. H., The RAD9 gene controls the cell-cycle response to DNA damage in saccharomyces-cerevisiae. *Science* **1988**, *241* (4863), 317-322.
- 59. Zhou, B. B.; Elledge, S. J., The DNA damage response: putting checkpoints in perspective. *Nature* **2000**, *408* (6811), 433-439.
- 60. Elledge, S. J., Cell cycle checkpoints: preventing an identity crisis. *Science* **1996**, 274 (5293), 1664-1672.
- 61. Sancar, A.; Lindsey-Boltz, L. A.; Unsal-Kacmaz, K.; Linn, S., Molecular mechanisms of mammalian DNA repair and the DNA damage checkpoints. *Annu. Rev. Biochem.* **2004**, *73*, 39-85.
- 62. Khanna, K. K.; Lavin, M. F.; Jackson, S. P.; Mulhern, T. D., ATM, a central controller of cellular responses to DNA damage. *Cell Death Differ.* **2001**, 8 (11), 1052-1065.
- 63. Nyberg, K. A.; Michelson, R. J.; Putnam, C. W.; Weinert, T. A., Toward maintaining the genome: DNA damage and replication checkpoints. *Annu. Rev. Genet.* **2002,** *36*, 617-656.
- 64. Abraham, R. T., Cell cycle checkpoint signaling through the ATM and ATR kinases. *Genes Dev.* **2001**, *15* (17), 2177-2196.
- 65. Tibbetts, R. S.; Abraham, R. T., PI3K-related kinase: Roles in cell-cycle regulation and DNA damage responses. In *Signaling networks and cell cycle control: The molecular basis of cancer and other diseases*, Gutkind, J., Ed. Humana Press: Totowa, NJ, 2000; pp 267-301.

- 66. Jobson, A. G.; Cardellina, J. H.; Scudiero, D.; Kondapaka, S.; Zhang, H.; Kim, H.; Shoemaker, R.; Pommier, Y., Identification of a bis-guanylhydrazone [4,4 'diacetyldiphenylurea-bis(guanylhydrazone); NSC 109555] as a novel chemotype for inhibition of Chk2 kinase. *Mol. Pharmacol.* **2007**, 72, 876-884.
- 67. Bakkenist, C. J.; Kastan, M. B., DNA damage activates ATM through intermolecular autophosphorylation and dimer dissociation. *Nature* **2003**, *421* (6922), 499-506.
- 68. Bakkenist, C. J.; Kastan, M. B., Initiating cellular stress responses. *Cell* **2004**, *118* (1), 9-17.
- 69. Banin, S.; Moyal, L.; Shieh, S. Y.; Taya, Y.; Anderson, C. W.; Chessa, L.; Smorodinsky, N. I.; Prives, C.; Reiss, Y.; Shiloh, Y.; Ziv, Y., Enhanced phosphorylation of p53 by ATN in response to DNA damage. *Science* **1998**, *281* (5383), 1674-1677.
- 70. Dart, D. A.; Adams, K. E.; Akerman, I.; Lakin, N. D., Recruitment of the cell cycle checkpoint kinase ATR to chromatin during S-phase. *J. Biol. Chem.* **2004**, *279* (16), 16433-16440.
- 71. Lupardus, P. J.; Byun, T.; Yee, M. C.; Hekmat-Nejad, M.; Cimprich, K. A., A requirement for replication in activation of the ATR-dependent DNA damage checkpoint. *Genes Dev.* **2002**, *16* (18), 2327-2332.
- 72. Zou, L.; Elledge, S. J., Sensing DNA damage through ATRIP recognition of RPA-ssDNA complexes. *Science* **2003**, *300* (5625), 1542-1548.
- 73. Lee, J. H.; Paull, T. T., ATM activation by DNA double-strand breaks through the Mre11-Rad50-Nbs1 complex. *Science* **2005**, *308* (5721), 551-554.
- 74. Suzuki, K.; Kodama, S.; Watanabe, M., Recruitment of ATM protein to double strand DNA irradiated with ionizing radiation. *J. Biol. Chem.* **1999**, *274* (36), 25571-25575.
- 75. Byun, T. S.; Pacek, M.; Yee, M. C.; Walter, J. C.; Cimprich, K. A., Functional uncoupling of MCM helicase and DNA polymerase activities activates the ATR-dependent checkpoint. *Genes Dev.* **2005**, *19* (9), 1040-1052.

- 76. Liu, Q. H.; Guntuku, S.; Cui, X. S.; Matsuoka, S.; Cortez, D.; Tamai, K.; Luo, G. B.; Carattini-Rivera, S.; DeMayo, F.; Bradley, A.; Donehower, L. A.; Elledge, S. J., Chk1 is an essential kinase that is regulated by Atr and required for the G(2)/M DNA damage checkpoint. *Genes Dev.* **2000**, *14* (12), 1448-1459.
- 77. Zhao, H.; Piwnica-Worms, H., ATR-mediated checkpoint pathways regulate phosphorylation and activation of human Chk1. *Mol. Cell. Biol.* **2001**, *21* (13), 4129-4139.
- 78. Niida, H.; Katsuno, Y.; Banerjee, B.; Hande, M. P.; Nakanishi, M., Specific role of Chk1 phosphorylations in cell survival and checkpoint activation. *Mol. Cell. Biol.* **2007**, *27* (7), 2572-2581.
- 79. Kramer, A.; Mailand, N.; Lukas, C.; Syljuasen, R. G.; Wilkinson, C. J.; Nigg, E. A.; Bartek, J.; Lukas, J., Centrosome-associated Chk1 prevents premature activation of cyclin-B-Cdk1 kinase. *Nat. Cell Biol.* **2004,** *6* (9), 884-89.
- 80. Jackman, M.; Lindon, C.; Nigg, E. A.; Pines, J., Active cyclin B1-Cdk1 first appears on centrosomes in prophase. *Nat. Cell Biol.* **2003**, *5* (2), 143-148.
- 81. Bartek, J.; Lukas, J., Chk1 and Chk2 kinases in checkpoint control and cancer. *Cancer Cell* **2003**, 3 (5), 421-429.
- 82. Gatei, M.; Sloper, K.; Sorensen, C.; Syljuasen, R.; Falck, J.; Hobson, K.; Savage, K.; Lukas, J.; Zhou, B. B.; Bartek, J.; Khanna, K. K., Ataxia-telangiectasia-mutated (ATM) and NBS1-dependent phosphorylation of Chk1 on Ser-317 in response to ionizing radiation. *J. Biol. Chem.* **2003**, *278* (17), 14806-14811.
- 83. Sorensen, C. S.; Syljuasen, R. G.; Falck, J.; Schroeder, T.; Ronnstrand, L.; Khanna, K. K.; Zhou, B. B.; Bartek, J.; Lukas, J., Chk1 regulates the S phase checkpoint by coupling the physiological turnover and ionizing radiation-induced accelerated proteolysis of Cdc25A. *Cancer Cell* **2003**, *3* (3), 247-258.
- 84. Zaugg, K.; Su, Y. W.; Reilly, P. T.; Moolani, Y.; Cheung, C. C.; Hakem, R.; Hirao, A.; Elledge, S. J.; Mak, T. W., Cross-talk between Chk1 and Chk2 in double-mutant thymocytes. *Proc. Natl. Acad. Sci. U. S. A.* **2007**, *104* (10), 3805-3810.
- 85. Matsuoka, S.; Rotman, G.; Ogawa, A.; Shiloh, Y.; Tamai, K.; Elledge, S. J., Ataxia telangiectasia-mutated phosphorylates Chk2 in vivo and in vitro. *Proc. Natl. Acad. Sci. U. S. A.* **2000,** *97* (19), 10389-10394.

- 86. Pellegrini, M.; Celeste, A.; Difilippantonio, S.; Guo, R.; Wang, W. D.; Feigenbaum, L.; Nussenzweig, A., Autophosphorylation at serine 1987 is dispensable for murine Atm activation in vivo. *Nature* **2006**, *443* (7108), 222-225.
- 87. Lee, J. H.; Paull, T. T., Activation and regulation of ATM kinase activity in response to DNA double-strand breaks. *Oncogene* **2007**, *26* (56), 7741-7748.
- 88. Fernandez-Capetillo, O.; Lee, A.; Nussenzweig, M.; Nussenzweig, A., H2AX: the histone guardian of the genome. *DNA Repair* **2004**, *3* (8-9), 959-967.
- 89. Lukas, C.; Falck, J.; Bartkova, J.; Bartek, J.; Lukas, J., Distinct spatiotemporal dynamics of mammalian checkpoint regulators induced by DNA damage. *Nat Cell Biol* **2003**, *5* (3), 255-260.
- 90. Falck, J.; Mailand, N.; Syljuasen, R. G.; Bartek, J.; Lukas, J., The ATM-Chk2-Cdc25A checkpoint pathway guards against radioresistant DNA synthesis. *Nature* **2001**, *410* (6830), 842-847.
- 91. Barlow, C.; Hirotsune, S.; Paylor, R.; Liyanage, M.; Eckhaus, M.; Collins, F.; Shiloh, Y.; Crawley, J. N.; Ried, T.; Tagle, D.; WynshawBoris, A., Atm-deficient mice: A paradigm of ataxia telangiectasia. *Cell* **1996**, *86* (1), 159-171.
- 92. Elson, A.; Wang, Y. Q.; Daugherty, C. J.; Morton, C. C.; Zhou, F.; CamposTorres, J.; Leder, P., Pleiotropic defects in ataxia-telangiectasia protein-deficient mice. *Proc. Natl. Acad. Sci. U. S. A.* **1996**, *93* (23), 13084-13089.
- 93. Brown, E. J.; Baltimore, D., ATR disruption leads to chromosomal fragmentation and early embryonic lethality. *Genes Dev.* **2000**, *14* (4), 397-402.
- 94. de Klein, A.; Muijtjens, M.; van Os, R.; Verhoeven, Y.; Smit, B.; Carr, A. M.; Lehmann, A. R.; Hoeijmakers, J. H. J., Targeted disruption of the cell-cycle checkpoint gene ATR leads to early embryonic lethality in mice. *Curr. Biol.* **2000**, *10* (8), 479-482.
- 95. Cimprich, K. A.; Cortez, D., ATR: an essential regulator of genome integrity. *Nat. Rev. Mol. Cell Biol.* **2008**, 9 (8), 616-627.

- 96. Allen, J. B.; Zhou, Z.; Siede, W.; Friedberg, E. C.; Elledge, S. J., The SAD1/RAD53 protein-kinase controls multiple checkpoints and DNA damage-induced transcription in yeast. *Genes Dev.* **1994**, *8* (20), 2401-2415.
- 97. Bartek, J.; Falck, J.; Lukas, J., CHK2 kinase--a busy messenger. *Nat. Rev. Mol. Cell Biol.* **2001**, *2* (12), 877-886.
- 98. Matsuoka, S.; Huang, M.; Elledge, S. J., Linkage of ATM to cell cycle regulation by the Chk2 protein kinase. *Science* **1998**, *282* (5395), 1893-1897.
- 99. Blasina, A.; Van de Weyer, I.; Laus, M. C.; Luyten, W.; Parker, A. E.; McGowan, C. H., A human homologue of the checkpoint kinase Cds1 directly inhibits Cdc25 phosphatase. *Curr. Biol.* **1999**, *9* (1), 1-10.
- 100. Brown, A. L.; Lee, C. H.; Schwarz, J. K.; Mitiku, N.; Piwnica-Worms, H.; Chung, J. H., A human Cds1-related kinase that functions downstream of ATM protein in the cellular response to DNA damage. *Proc. Natl. Acad. Sci. U. S. A.* 1999, 96 (7), 3745-3750.
- 101. Tominaga, K.; Morisaki, H.; Kaneko, Y.; Fujimoto, A.; Tanaka, T.; Ohtsubo, M.; Hirai, M.; Okayama, H.; Ikeda, K.; Nakanishi, M., Role of human Cds1 (Chk2) kinase in DNA damage checkpoint and its regulation by p53. *J. Biol. Chem.* **1999**, *274* (44), 31463-31467.
- 102. Chaturvedi, P.; Eng, W. K.; Zhu, Y.; Mattern, M. R.; Mishra, R.; Hurle, M. R.; Zhang, X. L.; Annan, R. S.; Lu, Q.; Faucette, L. F.; Scott, G. F.; Li, X. T.; Carr, S. A.; Johnson, R. K.; Winkler, J. D.; Zhou, B. B. S., Mammalian Chk2 is a downstream effector of the ATM-dependent DNA damage checkpoint pathway. *Oncogene* 1999, 18 (28), 4047-4054.
- 103. Carr, A. M., Control of cell cycle arrest by the Mec1(sc)/Rad3(sp) DNA structure checkpoint pathway. *Curr. Opin. Genet. Dev.* **1997,** *7* (1), 93-98.
- 104. Rhind, N.; Russell, P., Chk1 and Cds1: linchpins of the DNA damage and replication checkpoint pathways. *J. Cell Sci.* **2000**, *113* (22), 3889-3896.
- 105. Murakami, H.; Okayama, H., A kinase from fission yeast responsible for blocking mitosis in S-phase. *Nature* **1995**, *374* (6525), 817-819.

- 106. Ahn, J. Y.; Schwarz, J. K.; Piwnica-Worms, H.; Canman, C. E., Threonine 68 phosphorylation by ataxia telangiectasia mutated is required for efficient activation of Chk2 in response to ionizing radiation. *Cancer Res.* **2000**, *60* (21), 5934-5936.
- 107. Kastan, M. B.; Lim, D. S., The many substrates and functions of ATM. *Nat. Rev. Mol. Cell Biol.* **2000**, *1* (3), 179-186.
- 108. Wu, X.; Chen, J., Autophosphorylation of checkpoint kinase 2 at serine 516 is required for radiation-induced apoptosis. *J. Biol. Chem.* **2003**, 278 (38), 36163-36168.
- 109. Schwarz, J. K.; Lovly, C. M.; Piwnica-Worms, H., Regulation of the Chk2 protein kinase by oligomerization-mediated cis- and trans-phosphorylation. *Mol. Cancer Res.* **2003**, *1* (8), 598-609.
- 110. Ahn, J.; Prives, C., Checkpoint kinase 2 (Chk2) monomers or dimers phosphorylate Cdc25C after DNA damage regardless of threonine 68 phosphorylation. *J. Biol. Chem.* **2002**, 277 (50), 48418-48426.
- 111. Cai, Z.; Chehab, N. H.; Pavletich, N. P., Structure and Activation Mechanism of the CHK2 DNA Damage Checkpoint Kinase. *Mol. Cell* **2009**, *35* (6), 818-829.
- 112. Oliver, A. W.; Paul, A.; Boxall, K. J.; Barrie, S. E.; Aherne, G. W.; Garrett, M. D.; Mittnacht, S.; Pearl, L. H., Trans-activation of the DNA-damage signalling protein kinase Chk2 by T-loop exchange. *EMBO J.* **2006**, *25* (13), 3179-3190.
- 113. Ahn, J.; Urist, M.; Prives, C., The Chk2 protein kinase. *DNA Repair (Amst)* **2004**, 3 (8-9), 1039-1047.
- 114. Shieh, S. Y.; Ahn, J.; Tamai, K.; Taya, Y.; Prives, C., The human homologs of checkpoint kinases Chk1 and Cds1 (Chk2) phosphorylate p53 at multiple DNA damage-inducible sites. *Genes Dev.* **2000**, *14* (3), 289-300.
- 115. Chehab, N. H.; Malikzay, A.; Stavridi, E. S.; Halazonetis, T. D., Phosphorylation of Ser-20 mediates stabilization of human p53 in response to DNA damage. *Proc. Natl. Acad. Sci. U. S. A.* **1999**, *96* (24), 13777-13782.

- 116. Chehab, N. H.; Malikzay, A.; Appel, M.; Halazonetis, T. D., Chk2/hCds1 functions as a DNA damage checkpoint in G(1) by stabilizing p53. *Genes Dev.* **2000**, *14* (3), 278-88.
- 117. Vogelstein, B.; Lane, D.; Levine, A. J., Surfing the p53 network. *Nature* **2000**, *408* (6810), 307-310.
- 118. Ryan, K. M.; Phillips, A. C.; Vousden, K. H., Regulation and function of the p53 tumor suppressor protein. *Curr. Opin. Cell Biol.* **2001**, *13* (3), 332-337.
- 119. Lee, J. S.; Collins, K. M.; Brown, A. L.; Lee, C. H.; Chung, J. H., hCds1-mediated phosphorylation of BRCA1 regulates the DNA damage response. *Nature* **2000**, *404* (6774), 201-204.
- 120. Wang, Y.; Cortez, D.; Yazdi, P.; Neff, N.; Elledge, S. J.; Qin, J., BASC, a super complex of BRCA1-associated proteins involved in the recognition and repair of aberrant DNA structures. *Genes Dev.* **2000**, *14* (8), 927-939.
- Xu, B.; Kim, S. T.; Kastan, M. B., Involvement of Brca1 in S-phase and G(2)phase checkpoints after ionizing irradiation. *Mol. Cell. Biol.* 2001, 21 (10), 3445-3450.
- 122. Scully, R.; Livingston, D. M., In search of the tumour-suppressor functions of BRCA1 and BRCA2. *Nature* **2000**, *408* (6811), 429-432.
- 123. Lowe, S. W.; Cepero, E.; Evan, G., Intrinsic tumour suppression. *Nature* **2004**, *432* (7015), 307-315.
- 124. Vousden, K. H.; Lane, D. P., p53 in health and disease. *Nat. Rev. Mol. Cell Biol.* **2007**, *8* (4), 275-283.
- 125. Chen, Z. B.; Trotman, L. C.; Shaffer, D.; Lin, H. K.; Dotan, Z. A.; Niki, M.; Koutcher, J. A.; Scher, H. I.; Ludwig, T.; Gerald, W.; Cordon-Cardo, C.; Pandolfi, P. P., Crucial role of p53-dependent cellular senescence in suppression of Ptendeficient tumorigenesis. *Nature* **2005**, *436* (7051), 725-730.
- 126. Meek, D. W., Tumour suppression by p53: a role for the DNA damage response? *Nat. Rev. Cancer* **2009**, *9* (10), 714-723.

- Kemp, C. J.; Donehower, L. A.; Bradley, A.; Balmain, A., Reduction of p53 gene dosage does not increase initiation or promotion or promotion but enhances malignant progression of chemically-induced skin tumors. *Cell* 1993, 74 (5), 813-822.
- 128. Sands, A. T.; Suraokar, M. B.; Sanchez, A.; Marth, J. E.; Donehower, L. A.; Bradley, A., p53 defficiency does not affect the accumulation of point mutations in a transgene target. *Proc. Natl. Acad. Sci. U. S. A.* 1995, 92 (18), 8517-8521.
- 129. Sionov, R. V.; Haupt, Y., Apoptosis by p53: mechanisms, regulation, and clinical implications. *Springer Semin. Immunopathol.* **1998**, *19* (3), 345-362.
- 130. Sionov, R. V.; Haupt, Y., The cellular response to p53: the decision between life and death. *Oncogene* **1999**, *18* (45), 6145-6157.
- 131. Meek, D. W., The p53 response to DNA damage. *DNA Repair (Amst)* **2004,** *3* (8-9), 1049-56.
- 132. Rogel, A.; Popliker, M.; Webb, C. G.; Oren, M., p53 cellular tumor antigen: analysis of mRNA levels in normal adult tissues, embryos, and tumors. *Mol. Cell Biol.* **1985**, *5* (10), 2851-2855.
- 133. Hollstein, M.; Sidransky, D.; Vogelstein, B.; Harris, C. C., p53 mutations in human cancers. *Science* **1991**, *253* (5015), 49-53.
- 134. Momand, J.; Wu, H. H.; Dasgupta, G., MDM2 master regulator of the p53 tumor suppressor protein. *Gene* **2000**, *242* (1-2), 15-29.
- 135. Shieh, S. Y.; Ikeda, M.; Taya, Y.; Prives, C., DNA damage-induced phosphorylation of p53 alleviates inhibition by MDM2. *Cell* **1997**, *91* (3), 325-334.
- 136. Sakaguchi, K.; Saito, S.; Higashimoto, Y.; Roy, S.; Anderson, C. W.; Appella, E., Damage-mediated phosphorylation of human p53 threonine 18 through a cascade mediated by a casein 1-like kinase Effect on Mdm2 binding. *J. Biol. Chem.* **2000**, 275 (13), 9278-9283.
- 137. Lai, Z. H.; Auger, K. R.; Manubay, C. M.; Copeland, R. A., Thermodynamics of p53 binding to hdm2(1-126): Effects of phosphorylation and p53 peptide length. *Arch. Biochem. Biophys.* **2000**, *381* (2), 278-284.

- 138. Dornan, D.; Hupp, T. R., Inhibition of p53-dependent transcription by BOX-I phospho-peptide mimetics that bind to p300. *EMBO Rep.* **2001**, *2* (2), 139-144.
- 139. Falck, J.; Lukas, C.; Protopopova, M.; Lukas, J.; Selivanova, G.; Bartek, J., Functional impact of concomitant versus alternative defects in the Chk2-p53 tumour suppressor pathway. *Oncogene* **2001**, *20* (39), 5503-5510.
- 140. Hirao, A.; Kong, Y. Y.; Matsuoka, S.; Wakeham, A.; Ruland, J.; Yoshida, H.; Liu, D.; Elledge, S. J.; Mak, T. W., DNA damage-induced activation of p53 by the checkpoint kinase Chk2. *Science* **2000**, *287* (5459), 1824-1827.
- 141. Hirao, A.; Cheung, A.; Duncan, G.; Girard, P. M.; Elia, A. J.; Wakeham, A.; Okada, H.; Sarkissian, T.; Wong, J. A.; Sakai, T.; De Stanchina, E.; Bristow, R. G.; Suda, T.; Lowe, S. W.; Jeggo, P. A.; Elledge, S. J.; Mak, T. W., Chk2 is a tumor suppressor that regulates apoptosis in both an ataxia telangiectasia mutated (ATM)-dependent and an ATM-independent manner. *Mol. Cell Biol.* 2002, 22 (18), 6521-6532.
- 142. Takai, H.; Naka, K.; Okada, Y.; Watanabe, M.; Harada, N.; Saito, S.; Anderson, C. W.; Appella, E.; Nakanishi, M.; Suzuki, H.; Nagashima, K.; Sawa, H.; Ikeda, K.; Motoyama, N., Chk2-deficient mice exhibit radioresistance and defective p53-mediated transcription. *EMBO J.* **2002**, *21* (19), 5195-205.
- 143. Craig, A.; Scott, M.; Burch, L.; Smith, G.; Ball, K.; Hupp, T., Allosteric effects mediate CHK2 phosphorylation of the p53 transactivation domain. *EMBO Rep.* **2003**, *4* (8), 787-792.
- 144. Tan, S. Y.; Guschin, D.; Davalos, A.; Lee, Y. L.; Snowden, A. W.; Jouvenot, Y.; Zhang, H. S.; Howes, K.; McNamara, A. R.; Lai, A.; Ullman, C.; Reynolds, L.; Moore, M.; Isalan, M.; Berg, L. P.; Campos, B.; Qi, H.; Spratt, S. K.; Case, C. C.; Pabo, C. O.; Campisi, J.; Gregory, P. D., Zinc-finger protein-targeted gene regulation: Genomewide single-gene specificity. *Proc. Natl. Acad. Sci. U. S. A.* 2003, 100 (21), 11997-12002.
- 145. Ahn, J.; Urist, M.; Prives, C., Questioning the role of checkpoint kinase 2 in the p53 DNA damage response. *J. Biol. Chem.* **2003**, *278* (23), 20480-20489.
- 146. Jallepalli, P. V.; Lengauer, C.; Vogelstein, B.; Bunz, F., The Chk2 tumor suppressor is not required for p53 responses in human cancer cells. *J. Biol. Chem.* **2003**, 278 (23), 20475-20479.

- 147. O'Neill, T.; Giarratani, L.; Chen, P.; Iyer, L.; Lee, C. H.; Bobiak, M.; Kanai, F.; Zhou, B. B.; Chung, J. H.; Rathbun, G. A., Determination of substrate motifs for human Chk1 and hCds1/Chk2 by the oriented peptide library approach. *J. Biol. Chem.* **2002**, 277 (18), 16102-16115.
- 148. Seo, G. J.; Kim, S. E.; Lee, Y. M.; Lee, J. W.; Lee, J. R.; Hahn, M. J.; Kim, S. T., Determination of substrate specificity and putative substrates of Chk2 kinase. *Biochem. Biophys. Res. Commun.* **2003**, *304* (2), 339-343.
- 149. Jack, M. T.; Woo, R. A.; Hirao, A.; Cheung, A.; Mak, T. W.; Lee, P. W., Chk2 is dispensable for p53-mediated G1 arrest but is required for a latent p53-mediated apoptotic response. *Proc. Natl. Acad. Sci. U. S. A.* **2002**, *99* (15), 9825-9829.
- 150. Keramaris, E.; Hirao, A.; Slack, R. S.; Mak, T. W.; Park, D. S., Ataxia telangiectasia-mutated protein can regulate p53 and neuronal death independent of Chk2 in response to DNA damage. *J. Biol. Chem.* **2003**, *278* (39), 37782-37789.
- 151. Bell, D. W.; Varley, J. M.; Szydlo, T. E.; Kang, D. H.; Wahrer, D. C.; Shannon, K. E.; Lubratovich, M.; Verselis, S. J.; Isselbacher, K. J.; Fraumeni, J. F.; Birch, J. M.; Li, F. P.; Garber, J. E.; Haber, D. A., Heterozygous germ line hCHK2 mutations in Li-Fraumeni syndrome. *Science* **1999**, *286* (5449), 2528-2531.
- 152. Reddy, A.; Yuille, M.; Sullivan, A.; Repellin, C.; Bell, A.; Tidy, J. A.; Evans, D. J.; Farrell, P. J.; Gusterson, B.; Gasco, M.; Crook, T., Analysis of CHK2 in vulval neoplasia. *Br. J. Cancer* **2002**, *86* (5), 756-760.
- 153. Sullivan, A.; Yuille, M.; Repellin, C.; Reddy, A.; Reelfs, O.; Bell, A.; Dunne, B.; Gusterson, B. A.; Osin, P.; Farrell, P. J.; Yulug, I.; Evans, A.; Ozcelik, T.; Gasco, M.; Crook, T., Concomitant inactivation of p53 and Chk2 in breast cancer. *Oncogene* **2002**, *21* (9), 1316-1324.
- 154. Nasmyth, K., Viewpoint: putting the cell cycle in order. *Science* **1996,** *274* (5293), 1643-1645.
- 155. Takai, H.; Tominaga, K.; Motoyama, N.; Minamishima, Y. A.; Nagahama, H.; Tsukiyama, T.; Ikeda, K.; Nakayama, K.; Nakanishi, M.; Nakayama, K., Aberrant cell cycle checkpoint function and early embryonic death in Chk1(-/-) mice. *Genes Dev.* **2000**, *14* (12), 1439-1447.

- 156. Bartek, J.; Lukas, J., Mammalian G1- and S-phase checkpoints in response to DNA damage. *Curr. Opin. Cell Biol.* **2001**, *13* (6), 738-747.
- 157. Roshak, A. K.; Capper, E. A.; Imburgia, C.; Fornwald, J.; Scott, G.; Marshall, L. A., The human polo-like kinase, PLK, regulates cdc2/cyclin B through phosphorylation and activation of the cdc25C phosphatase. *Cell Signal* **2000**, *12* (6), 405-411.
- 158. Reagan-Shaw, S.; Ahmad, N., Silencing of polo-like kinase (Plk) 1 via siRNA causes induction of apoptosis and impairment of mitosis machinery in human prostate cancer cells: implications for the treatment of prostate cancer. *FASEB J.* **2005**, *19* (1), 611-613.
- 159. Watanabe, N.; Arai, H.; Nishihara, Y.; Taniguchi, M.; Hunter, T.; Osada, H., M-phase kinases induce phospho-dependent ubiquitination of somatic Wee1 by SCF beta-TrCP. *Proc. Natl. Acad. Sci. U. S. A.* **2004,** *101* (13), 4419-4424.
- 160. Milczarek, G. J.; Martinez, J.; Bowden, G. T., p53 phosphorylation: Biochemical and functional consequences. *Life Sci.* **1996**, *60* (1), 1-11.
- 161. Meek, D. W., Posttranslational modification of p53. Semin. Cancer Biol. **1994,** 5 (3), 203-210.
- 162. Tibbetts, R. S.; Brumbaugh, K. M.; Williams, J. M.; Sarkaria, J. N.; Cliby, W. A.; Shieh, S. Y.; Taya, Y.; Prives, C.; Abraham, R. T., A role for ATR in the DNA damage-induced phosphorylation of p53. *Genes Dev.* **1999**, *13* (2), 152-157.
- 163. Bartek, J.; Lukas, J.; Bartkova, J., DNA damage response as an anti-cancer barrier Damage threshold and the concept of 'conditional haploinsufficiency'. *Cell Cycle* **2007**, *6*, 2344-2347.
- 164. Stark, G. R.; Taylor, W. R., Control of the G(2)/M transition. *Mol. Biotechnol.* **2006**, *32* (3), 227-248.
- 165. Taylor, W. R.; Stark, G. R., Regulation of the G2/M transition by p53. *Oncogene* **2001**, *20* (15), 1803-1815.
- 166. Stewart, N.; Hicks, G. G.; Paraskevas, F.; Mowat, M., Evidence for a 2nd cell-cycle block at G2/M by p53. *Oncogene* **1995**, *10* (1), 109-115.

- 167. Canman, C. E.; Lim, D. S., The role of ATM in DNA damage responses and cancer. *Oncogene* **1998**, *17* (25), 3301-3308.
- 168. Hammond, E. M.; Denko, N. C.; Dorie, M. J.; Abraham, R. T.; Giaccia, A. J., Hypoxia links ATR and p53 through replication arrest. *Mol. Cell. Biol.* **2002**, 22 (6), 1834-1843.
- Jazayeri, A.; Falck, J.; Lukas, C.; Bartek, J.; Smith, G. C. M.; Lukas, J.; Jackson, S. P., ATM- and cell cycle-dependent regulation of ATR in response to DNA double-strand breaks. *Nat. Cell Biol.* 2006, 8 (1), 37-45.
- 170. Bucher, N.; Britten, C. D., G2 checkpoint abrogation and checkpoint kinase-1 targeting in the treatment of cancer. *Br. J. Cancer* **2008**, *98* (3), 523-528.
- 171. Zhou, B. B.; Anderson, H. J.; Roberge, M., Targeting DNA checkpoint kinases in cancer therapy. *Cancer Biol. Ther.* **2003**, *2* (4 Suppl 1), S16-S22.
- 172. Suganuma, M.; Kawabe, T.; Hori, H.; Funabiki, T.; Okamoto, T., Sensitization of cancer cells to DNA damage-induced cell death by specific cell cycle G2 checkpoint abrogation. *Cancer Res.* **1999**, *59* (23), 5887-5891.
- 173. Tenzer, A.; Pruschy, M., Potentiation of DNA-damage-induced cytotoxicity by G2 checkpoint abrogators. *Curr. Med. Chem. Anti-Canc. Agents* **2003**, *3* (1), 35-46.
- 174. Sausville, E. A., Cyclin-dependent kinase modulators studied at the NCI: preclinical and clinical studies. *Curr. Med. Chem. Anti-Canc. Agents* **2003**, 3 (1), 47-56.
- 175. Zhou, B. B.; Sausville, E. A., Drug discovery targeting Chk1 and Chk2 kinases. *Prog. Cell Cycle Res.* **2003**, *5*, 413-421.
- 176. Curman, D.; Cinel, B.; Williams, D. E.; Rundle, N.; Block, W. D.; Goodarzi, A. A.; Hutchins, J. R.; Clarke, P. R.; Zhou, B. B.; Lees-Miller, S. P.; Andersen, R. J.; Roberge, M., Inhibition of the G2 DNA damage checkpoint and of protein kinases Chk1 and Chk2 by the marine sponge alkaloid debromohymenialdisine. *J. Biol. Chem.* **2001**, 276 (21), 17914-17919.
- 177. Prudhomme, M., Novel checkpoint 1 inhibitors. *Recent Pat. Anti-Cancer Drug Discovery* **2006**, *1* (1), 55-68.

- 178. Lukas, C.; Bartkova, J.; Latella, L.; Falck, J.; Mailand, N.; Schroeder, T.; Sehested, M.; Lukas, J.; Bartek, J., DNA damage-activated kinase Chk2 is independent of proliferation or differentiation yet correlates with tissue biology. *Cancer Res.* **2001**, *61* (13), 4990-4993.
- 179. Pommier, Y.; Sordet, O.; Rao, V. A.; Zhang, H. L.; Kohn, K. W., Targeting Chk2 kinase: Molecular interaction maps and therapeutic rationale. *Curr. Pharm. Des.* **2005**, *11* (22), 2855-2872.
- 180. Antoni, L.; Sodha, N.; Collins, I.; Garrett, M. D., CHK2 kinase: cancer susceptibility and cancer therapy two sides of the same coin? *Nat. Rev. Cancer* **2007**, *7*, 925-936.
- 181. Levesque, A. A.; Eastman, A., p53-based cancer therapies: is defective p53 the Achilles heel of the tumor? *Carcinogenesis* **2007**, *28* (1), 13-20.
- 182. Iliakis, G.; Wang, Y.; Guan, J.; Wang, H. C., DNA damage checkpoint control in cells exposed to ionizing radiation. *Oncogene* **2003**, *22* (37), 5834-5847.
- 183. Kruse, J. P.; Gu, W., Modes of p53 Regulation. *Cell* **2009**, *137* (4), 609-622.
- 184. Bernhard, E. J.; Maity, A.; Muschel, R. J.; McKenna, W. G., Effects of ionizing-radiation on cell-cycle progression A review. *Radiat. Environ. Biophys* **1995**, *34* (2), 79-83.
- 185. Carlessi, L.; Buscemi, G.; Larson, G.; Hong, Z.; Wu, J. Z.; Delia, D., Biochemical and cellular characterization of VRX0466617, a novel and selective inhibitor for the checkpoint kinase Chk2. *Mol. Cancer Ther.* **2007**, *6* (3), 935-944.
- 186. Arienti, K. L.; Brunmark, A.; Axe, F. U.; McClure, K.; Lee, A.; Blevitt, J.; Neff, D. K.; Huang, L.; Crawford, S.; Pandit, C. R.; Karlsson, L.; Breitenbucher, J. G., Checkpoint kinase inhibitors: SAR and radioprotective properties of a series of 2-arylbenzimidazoles. J. Med. Chem. 2005, 48 (6), 1873-1885.
- 187. McClure, K. J.; Huang, L. M.; Arienti, K. L.; Axe, F. U.; Brunmark, A.; Blevitt, J.; Breitenbucher, J. G., Novel non-benzimidazole chk2 kinase inhibitors. *Bioorg. Med. Chem. Lett.* **2006**, *16* (7), 1924-1928.

- 188. Larson, G.; Yan, S.; Chen, H.; Rong, F.; Hong, Z.; Wu, J. Z., Identification of novel, selective and potent Chk2 inhibitors. *Bioorg. Med. Chem. Lett.* **2007,** *17* (1), 172-175.
- 189. Hilton, S.; Naud, S.; Caldwell, J. J.; Boxall, K.; Burns, S.; Anderson, V. E.; Antoni, L.; Allen, C. E.; Pearl, L. H.; Oliver, A. W.; Wynne Aherne, G.; Garrett, M. D.; Collins, I., Identification and characterisation of 2-aminopyridine inhibitors of checkpoint kinase 2. *Bioorg. Med. Chem.* 18 (2), 707-718.
- 190. Yu, Q.; La Rose, J. H.; Zhang, H. L.; Pommier, Y., Antisense inhibition of Chk2/hCds1 expression attenuates DNA damage-induced S and G2 checkpoints and enhances apoptotic activity in HEK-293 cells. *FEBS Lett.* **2001,** *505* (1), 7-12.
- 191. Ghosh, J. C.; Dohi, T.; Raskett, C. M.; Kowalik, T. F.; Altieri, D. C., Activated checkpoint kinase 2 provides a survival signal for tumor cells. *Cancer Res.* **2006**, 66 (24), 11576-11579.
- 192. Chabalier-Taste, C.; Racca, C.; Dozier, C.; Larminat, F., BRCA1 is regulated by Chk2 in response to spindle damage. *Biochimica Et Biophysica Acta-Molecular Cell Research* **2008**, *1783* (12), 2223-2233.
- 193. Castedo, M.; Perfettini, J. L.; Roumier, T.; Valent, A.; Raslova, H.; Yakushijin, K.; Horne, D.; Feunteun, J.; Lenoir, G.; Medema, R.; Vainchenker, W.; Kroemer, G., Mitotic catastrophe constitutes a special case of apoptosis whose suppression entails aneuploidy. *Oncogene* **2004**, *23* (25), 4362-4370.
- 194. Vakifahmetoglu, H.; Olsson, M.; Tamm, C.; Heidari, N.; Orrenius, S.; Zhivotovsky, B., DNA damage induces two distinct modes of cell death in ovarian carcinomas. *Cell Death Differ.* **2008**, *15* (3), 555-566.
- 195. Jobson, A. G.; Lountos, G. T.; Lorenzi, P. L.; Llamas, J.; Connelly, J.; Cerna, D.; Tropea, J. E.; Onda, A.; Zoppoli, G.; Kondapaka, S.; Zhang, G. T.; Caplen, N. J.; Cardellina, J. H.; Yoo, S. S.; Monks, A.; Self, C.; Waugh, D. S.; Shoemaker, R. H.; Pommier, Y., Cellular Inhibition of Checkpoint Kinase 2 (Chk2) and Potentiation of Camptothecins and Radiation by the Novel Chk2 Inhibitor PV1019 [7-Nitro-1H-indole-2-carboxylic acid {4-[1-(guanidinohydrazone)-ethyl]-phenyl}-amide]. J. Pharmacol. Exp. Ther. 2009, 331 (3), 816-826.
- 196. Caldwell, J. J.; Welsh, E. J.; Matijssen, C.; Anderson, V. E.; Antoni, L.; Boxall, K.; Urban, F.; Hayes, A.; Raynaud, F. I.; Rigoreau, L. J. M.; Raynham, T.; Aherne,

- G. W.; Pearl, L. H.; Oliver, A. W.; Garrett, M. D.; Collins, I., Structure-Based Design of Potent and Selective 2-(Quinazolin-2-yl)phenol Inhibitors of Checkpoint Kinase 2. *J. Med. Chem.* **2010**, *54* (2), 580-590.
- 197. Pommier, Y.; Weinstein, J. N.; Aladjem, M. I.; Kohn, K. W., Chk2 molecular interaction map and rationale for Chk2 inhibitors. *Clin. Cancer Res.* **2006**, *12* (9), 2657-2661.
- 198. Hilton, S.; Naud, S.; Caldwell, J. J.; Boxall, K.; Burns, S.; Anderson, V. E.; Antoni, L.; Allen, C. E.; Pearl, L. H.; Oliver, A. W.; Aherne, G. W.; Garrett, M. D.; Collins, I., Identification and characterisation of 2-aminopyridine inhibitors of checkpoint kinase 2. *Bioorg. Med. Chem.* 18 (2), 707-718.
- 199. Lountos, G. T.; Tropea, J. E.; Zhang, D.; Jobson, A. G.; Pommier, Y.; Shoemaker, R. H.; Waugh, D. S., Crystal structure of checkpoint kinase 2 in complex with NSC 109555, a potent and selective inhibitor. *Protein Sci.* **2009**, *18* (1), 92-100.
- 200. Li, J.; Lee, G. I.; Van Doren, S. R.; Walker, J. C., The FHA domain mediates phosphoprotein interactions. *J Cell Sci* **2000**, *113 Pt 23*, 4143-4149.
- Matthews, D. J., In vitro and in vivo potentiation of cytotoxic therapy by XL844, an orally bioavailable inhibitor of Chk1 and Chk2. *Mol. Cancer Ther.* 2007, 6 (12), 3504S-3505S.
- 202. Matthews, D. J.; Yakes, F. M.; Chen, J.; Tadano, M.; Bornheim, L.; Clary, D. O.; Tai, A.; Wagner, J. M.; Miller, N.; Kim, Y. D.; Robertson, S.; Murray, L.; Karnitz, L. M., Pharmacological abrogation of S-phase checkpoint enhances the anti-tumor activity of gemcitabine in vivo. *Cell Cycle* 2007, 6 (1), 104-110.
- 203. Tse, A.; Yazji, S.; Naing, A.; Matthews, D.; Schwartz, G.; Lawhorn, K.; Kurzrock, R., Phase I study of XL844, a novel Chk1 and Chk2 kinase inhibitor, in combination with gemcitabine in patients with advanced malignancies. *EJC Suppl* **2008**, *6* (12), 124-124.
- 204. Janetka, J. W.; Ashwell, S., Checkpoint kinase inhibitors: a review of the patent literature. *Expert Opin. Ther. Pat.* **2009**, *19* (2), 165-197.
- 205. Preparation of 3-aminoindazoles as Chk1/Chk2 kinase inhibitors. 2007. DE200610005179 20060206

- 206. Mederski, W.; Gericke, R.; Klein, M.; Beier, N.; Lang, F. Preparation of 3-oxoindazolyl-substituted squaric acid derivatives as Chk1, Chk2 and or SGK kinase inhibitors. 03/01/2007, 2007. WO2006EP07650 20060802
- 207. Zabludoff, S. D.; Deng, C.; Grondine, M. R.; Sheehy, A. M.; Ashwell, S.; Caleb, B. L.; Green, S.; Haye, H. R.; Horn, C. L.; Janetka, J. W.; Liu, D.; Mouchet, E.; Ready, S.; Rosenthal, J. L.; Queva, C.; Schwartz, G. K.; Taylor, K. J.; Tse, A. N.; Walker, G. E.; White, A. M., AZD7762, a novel checkpoint kinase inhibitor, drives checkpoint abrogation and potentiates DNA-targeted therapies. *Mol. Cancer Ther.* 2008, 7 (9), 2955-2966.
- 208. Neff, D. K.; Lee-Dutra, A.; Blevitt, J. M.; Axe, F. U.; Hack, M. D.; Buma, J. C.; Rynberg, R.; Brunmark, A.; Karlsson, L.; Breitenbucher, J. G., 2-Aryl benzimidazoles featuring alkyl-linked pendant alcohols and amines as inhibitors of checkpoint kinase Chk2. *Bioorg. Med. Chem. Lett.* **2007**, *17* (23), 6467-6471.
- 209. Morgan, M. A.; Parsels, L. A.; Zhao, L.; Parsels, J. D.; Davis, M. A.; Hassan, M. C.; Arumugarajah, S.; Hylander-Gans, L.; Morosini, D.; Simeone, D. M.; Canman, C. E.; Normolle, D. P.; Zabludoff, S. D.; Maybaum, J.; Lawrence, T. S., Mechanism of radiosensitization by the Chk1/2 inhibitor AZD7762 involves abrogation of the G2 checkpoint and inhibition of homologous recombinational DNA repair. Cancer Res. 2010, 70 (12), 4972-4981.
- 210. Morgan, M. A.; Parsels, L. A.; Maybaum, J.; Lawrence, T. S., Improving Gemcitabine-Mediated Radiosensitization Using Molecularly Targeted Therapy: A Review. *Clin. Cancer Res.* **2008**, *14* (21), 6744-6750.
- 211. Parsels, L. A.; Morgan, M. A.; Tanska, D. M.; Parsels, J. D.; Palmer, B. D.; Booth, R. J.; Denny, W. A.; Canman, C. E.; Kraker, A. J.; Lawrence, T. S.; Maybaum, J., Gemcitabine sensitization by checkpoint kinase 1 inhibition correlates with inhibition of a Rad51 DNA damage response in pancreatic cancer cells. *Mol. Cancer Ther.* 2009, 8 (1), 45-54.
- 212. Blasina, A.; Hallin, J.; Chen, E. H.; Arango, M. E.; Kraynov, E.; Register, J.; Grant, S.; Ninkovic, S.; Chen, P.; Nichols, T.; O'Connor, P.; Anderes, K., Breaching the DNA damage checkpoint via PF-00477736, a novel small-molecule inhibitor of checkpoint kinase 1. *Mol. Cancer Ther.* 2008, 7 (8), 2394-2404.
- 213. Anderson, V. E.; Walton, M. I.; Eve, P. D.; Boxall, K. J.; Antoni, L.; Caldwell, J. J.; Aherne, W.; Pearl, L. H.; Oliver, A. W.; Collins, I.; Garrett, M. D., CCT241533 Is a

- Potent and Selective Inhibitor of CHK2 that Potentiates the Cytotoxicity of PARP Inhibitors. *Cancer Res.* **2011**, *71* (2), 463-472.
- 214. Yu, Q.; La Rose, J.; Zhang, H.; Takemura, H.; Kohn, K. W.; Pommier, Y., UCN-01 inhibits p53 up-regulation and abrogates gamma-radiation-induced G(2)-M checkpoint independently of p53 by targeting both of the checkpoint kinases, Chk2 and Chk1. *Cancer Res.* **2002**, *62* (20), 5743-5748.
- 215. Kohn, E. A.; Yoo, C. J.; Eastman, A., The protein kinase c inhibitor Go6976 is a potent inhibitor of DNA damage-induced S and G(2) cell cycle checkpoints. *Cancer Res.* **2003**, *63* (1), 31-35.
- 216. Akinaga, S.; Nomura, K.; Gomi, K.; Okabe, M., Enhancement of antitumoractivity of mitomycin-C in vitro and in vivo by UCN-01, a selective inhibitor of protein-kinase-C. *Cancer Chemother. Pharmacol.* **1993**, *32* (3), 183-189.
- 217. Wang, Q. Z.; Fan, S. J.; Eastman, A.; Worland, P. J.; Sausville, E. A.; Oconnor, P. M., UCN-01, a potent abrogator of G(2) checkpoint function in cancer cells with disrupted p53. *J. Nat. Cancer Inst.* **1996**, *88* (14), 956-965.
- 218. Hu, B. C.; Zhou, X. Y.; Wang, X.; Zeng, Z. C.; Iliakis, G.; Wang, Y., The radioresistance to killing of A1-5 cells derives from activation of the Chk1 pathway. *J. Biol. Chem.* **2001**, *276* (21), 17693-17698.
- 219. Pollack, I. F.; Kawecki, S.; Lazo, J. S., Blocking of glioma proliferation in vitro and in vivo and potentiating the effects of BCNU and cisplatin: UCN-01, a selective protein kinase C inhibitor. *J. Neurosurg.* **1996**, *84* (6), 1024-1032.
- 220. Hirose, Y.; Berger, M. S.; Pieper, R. O., Abrogation of the Chk1-mediated G(2) checkpoint pathway potentiates temozolomide-induced toxicity in a p53-independent manner in human glioblastoma cells. *Cancer Res.* **2001**, *61* (15), 5843-5849.
- 221. Fuse, E.; Kuwabara, T.; Sparreboom, A.; Sausville, E. A.; Figg, W. D., Review of UCN-01 development: A lesson in the importance of clinical pharmacology. *J. Clin. Pharmacol.* **2005**, *45* (4), 394-403.
- 222. Fuse, E.; Tanii, H.; Kurata, N.; Kobayashi, H.; Shimada, Y.; Tamura, T.; Sasaki, Y.; Tanigawara, Y.; Lush, R. D.; Headlee, D.; Figg, W. D.; Arbuck, S. G.; Senderowicz, A. M.; Sausville, E. A.; Akinaga, S.; Kuwahara, A.; Kobasashi, S.,

- Unpredicted clinical pharmacology of UCN-01 caused by specific binding to human alpha(1)-acid glycoprotein. *Cancer Res.* **1998**, *58* (15), 3248-3253.
- 223. Sausville, E. A.; Arbuck, S. G.; Messmann, R.; Headlee, D.; Bauer, K. S.; Lush, R. M.; Murgo, A.; Figg, W. D.; Lahusen, T.; Jaken, S.; Jing, X. X.; Roberge, M.; Fuse, E.; Kuwabara, T.; Senderowicz, A. M., Phase I trial of 72-hour continuous infusion UCN-01 in patients with refractory neoplasms. *J. Clin. Oncol.* **2001**, *19* (8), 2319-2333.
- 224. Sharma, V.; Tepe, J. J., Potent inhibition of checkpoint kinase activity by a hymenialdisine-derived indoloazepine. *Bioorg. Med. Chem. Lett.* **2004,** *14* (16), 4319-4321.
- 225. DeLano, W. L. The PyMol Molecular Graphics System., 2009.
- 226. Sharma, V.; Lansdell, T. A.; Jin, G.; Tepe, J. J., Inhibition of Cytokine Production by Hymenialdisine Derivatives. *J. Med. Chem.* **2004**, *47* (14), 3700-3703.

CHAPTER II

IMPROVEMENT OF A SYNTHETIC METHOD FOR THE PREPARATION OF (Z)-5-(2-AMINO-4-OXO-1*H*-IMIDAZOL-5(4*H*)-YLIDENE-2,3,4,5-TETRAHYDROAZEPINO[3,4-b]-1(10*H*)-ONE, A HYMENIALDISINE ANALOG

II.A Isolation and characterization of hymenialdisine and analogs

Debromohymenialdisine (structure II-1), shown in Figure II-1, was first isolated from the Great Barrier Reef sponge *Phakellia* sp. in 1980. Natural products from this sponge have been known to possess antimicrobial activities. The structure was originally elucidated with HNMR, UV and chemical degradation. Hymenialdisine (structure II-2) was later extracted from the Red Sea sponge *Acanthella* sp. and the Mediterranean sponge *Axinella* sp. in 1982 as well as the from *Hymeniacidon* sp. in 1983, and characterized by X-ray crystallography. Several pyrrolic metabolites in addition to II-1 and II-2 were isolated and confirmed in X-ray studies from *Pseudaxinyssa* sp. in 1985. II-1 was reported to be slightly cytotoxic against murine p388 lymphocytic cells, and had no antimicrobial activity. II-2 was found to be moderately cytotoxic in PV₄ cells (32.5% at 100 μg/mL).

(Z)-Debromohymenialdisine **II-1** (Z)-Hymenialdisine **II-2**

Figure II-1. Structures (*Z*)-debromohymenialdisine and (*Z*)-hymenialdisine.

II-1 and II-2 are structurally similar compounds, differing only by the presence of bromine at the C2 position. Both compounds contain a pyrroloazepine ring that is connected to a glycocyamidine ring through a double bond between C10 and C11. Endocyclic torsion angles for the azepine group suggests a distorted boat conformation.⁴ Although the pyrrole ring is planar, the adjacent amide bond at C6 is not planar due to a slight rotation in the amide carbonyl and nitrogen,⁴ forming a 43.80° dihedral angle between the pyrroloazepine plane and the glycocyamidine ring.⁶

$$\begin{array}{c} & & & & & \\ & & & & \\ & & & & \\ & & \\ & & & \\ & & & \\ & & \\ & & & \\ & & & \\ & & & \\ & & & \\ & & & \\ & & & \\ & & & \\ & &$$

 R_1 = Br, R_2 = H, (E)-axinohydantoin **II-3a** R_1 = R_2 = H, (E)-debromohydantoin **II-3b** R_1 = R_2 = Br, (E)-bromoaxinohydantoin **II-3c**

 R_1 = Br, R_2 = H, (Z)-axinohydantoin **II-4a** R_1 = R_2 = H, (Z)-debromohydantoin **II-4b** R_1 = R_2 = Br, (Z)-bromoaxinohydantoin **II-4c**

R = Br, (E)-Debromohymenialdisine **II-5a** R = H, (E)-Hymenialdisine **II-5b**

Figure II-2. Structures of the axinohydantoins and (Z)-debromohymenialdisine and (Z)-hymenialdisine.

Axinohydantoins **II-3** and **II-4**, illustrated in Figure II-2 are structurally related to **II-2** consisting of the same fused pyrroloazepine ring. Instead of the glycocyamidine ring,

the pyrroloazepine ring is bonded to a hydantoin ring via a (Z) or (E) double bond. (E)axinohydantoin II-3a was isolated in 1990 from the sponge Axinella sp. and the structure was determined by X-ray crystallography. (Z)-axinohydantoin II-4a¹⁰ and the bromine derivatives **II-4b** and **II-4c**¹¹ were isolated and characterized in 1997 and 1998, respectively. 10, 11 Like the axinohydantoins, II-2 and II-1 have also been isolated as the (E) isomers II-5a and II-5b, 12 although the (Z) isomer is predominant due to its thermodynamic stability. 13, 14 Isolation of crystalline samples of the free bases of II-2 and II-1 produced two sets of ¹H and ¹³C NMR signals, which were determined to be the (10E)- and (10Z)-isomers of both II-2 and II-1. Higher concentrations of the (10E)and (10Z)- isomers resulted in a single set of signals, while dilution of the sample caused the signals to revert back to two sets. The NH protons in the compounds were found to act as a base in the tautomerization. As was expected, addition of any protic solvent to the NMR sample also resulted in a single set of signals matching that of the (*Z*)-isomer. 12

Hymenin **II-6** (Figure II-3) was isolated from an Okinawan sponge *Hymeniacidon* sp. in 1984 and characterized by NMR.¹⁵ Unlike **II-2**, hymenin contains two bromines on the pyrrole ring and contains a single bond to a 2-aminoimidazole ring instead of a glycocyamidine ring. Stevensine **II-7** (Figure II-3) isolated from *Pseudaxinyssa* sp. in 1985,^{7, 16} is another natural product similar to hymenin, but contains an additional unsaturation site between C9 and C10.^{7, 16}

$$H_2N$$
 H_2N
 H_2N
 H_3N
 H_4N
 H_5N
 H_7N
 H_7N

Figure II-3. Structure of hymenin and stevensine.

II.B SYNTHESIS OF HYMENIALDISINE AND DEBROMOHYMENIALDISINE

II-2 and **II-1** were first synthesized by Annoura and Tatsuoka in 1995. ¹⁷ This synthetic route sought an efficient way to make the 2-amino-4-oxo-2-imidazoline-5-(Z)-disubstituted -ylidine ring system. The synthesis began with treatment of pyrrole-2-carboxylic acid **II-8** with SOCl₂ and catalytic DMF in toluene at 60°F, followed by condensation with β-alanine methylester, as seen in Scheme **II-1**. Bromination of 2-pyrrole derivative **II-9** was accomplished using NBS, resulting in **II-10**. Formation of the aldisine ring **II-11** was synthesized with a Friedel-Craft acylation with PPA following hydrolysis of the methyl ester **II-10**.

1.
$$SOCl_2$$
, $cat.DMF$ $PhCH_3$, $60^{\circ}C$, 1 h $PhCH_3$, $63^{\circ}M$ $PhCH_3$, $90^{\circ}M$ $PhCH_3$, 9

Scheme II-1. Synthetic route toward **II-1** and **II-2** of intermediate **II-11**.

The rings **II-11a** and **II-11a**' were formed in 65% yield as a mixture of isomers. This may have resulted from a 1,2-migration of the bromine atom, which was likely caused by the strong acidic environment. The bromine isomers **II-11a** and **II-11a**' were not easily isolated until after the pyrrole and amide nitrogen were protected with SEM group to yield **II-12a**, **II-12a**' (Scheme II-2). Aldisine **II-11b** was also SEM protected to give **II-12b**. The Horner-Wadsworth-Emmons (HWE) reaction proceeded with ethyl diethylphosphonoacetate giving a mixture of α,β and β,γ -unsaturated esters **II-13**. The ester **II-13** was subsequently deprotonated with KHMDS to generate ester anions, which then reacted with 2-benzenesulfonyl-3-phenyloxaziridine to give the α - β -unsaturated esters **II-14** as a single regioisomer.

Scheme II-2. Synthetic route toward **II-1** and **II-2** of intermediate **II-14**.

Reacting **II-14** with guanidine and AlMe₃ as a Lewis acid resulted in the hydantoin derivative **II-17** as seen in Scheme II-3. Experimentation with intermediate **II-16** (not isolated) under various conditions did not result in cyclization to form the glycocyamidine ring.

Scheme II-3. Synthesis of II-17 toward II-1 and II-2.

In order to avoid formation of the hydantoin, compound **II-14** was mesylated under basic conditions to yield **II-15** quantitatively (Scheme II-4). Treatment of **II-15** with guanidine cyclized to form the glycocyamidine ring followed by isomerization of the double bond into conjugated system to give **II-18a** and **II-18b** in 42% and 52% yield, respectively. The NMR data of the products were compared with those of the natural products and the Z-stereochemistry was confirmed. The SEM groups were deprotected followed by purification over silica gel to give **II-1** 70% and **II-2** 75%. Annoura and Tatsuoka demonstrated an efficient route to the synthesis of **II-2** and **II-1**. As we will see in the next few sections, other groups have found different, perhaps more versatile

methods for the synthesis of the above mentioned natural products as well as their unnatural analogs.

Scheme II-4. Completed synthesis of **II-1** and **II-2**.

II.C SYNTHESIS OF MARINE SPONGE ALKALOIDS THROUGH A COMMON BICYCLIC PYRROLE COUPLING TO 2-AMINOIMIDAZOLE

Horne, D.A. et al discovered a methodology to synthesize hymenialdisine, debromohymenialdisine, hymenin and stevensine from a common bicyclic pyrrole[2,3-c]azepine-8-one ring system.^{13, 14, 19} The key step in the synthesis of these compounds was coupling the azafulvene unit **II-19** to 2-aminoimidazole **II-20** (Figure **II-4**) under acidic conditions to form the carbon-carbon bond between the two rings of the natural products.¹³

Figure II-4. Azafulvene intermediate to be coupled to 2-aminoimidazole

One obstacle to the synthesis of hymenin was to prevent or suppress the dimerization of the monomer with the azafulvene unit, resulting in the formation of II-22 as seen in Scheme II-5. Several acidic conditions did not result in the coupling of II-20 with II-19a.

Scheme II-5. Synthesis of azafulvene intermediate **II-19a**.

However, when bromine was introduced to the pyrrole **II-19b**, it functioned in blocking the nucleophilic site and prevented the dimerization and formation of **II-22** (Scheme II-6). After forming the fused bicyclic pyrrole, coupling **II-20** with **II-19b** went smoothly in methanesulfonic acid (23°C, 7 d) to give racemic hymenin **II-6**. Further hydrogenation of **II-6** over Pd/C and NaOAc in methanol gave (±)-2,3-debromohymenin **II-23** in quantitative yield. Wan et. al utilized the same synthetic strategy to synthesize **II-2** as well as indolo- analogs of **II-2**, which will be discussed later. ²⁰

Scheme II-6. Synthesis of hymenin and debromohymenin.

Intermediate II-19a proved to be useful toward the synthesis of stevensine II-7 and its analogs. Recalling that II-7 is saturated at C9-C10, it is possible to visualize the formation of an alkene through halogen elimination. An addition of bromine to pyrroloazepine II-19a was performed in methanol to give II-24 (Scheme II-7). When the elimination was performed in methanesulfonic acid, II-25 was obtained in 46% yield along with the bromo olefin II-26 (20%).

III-19a
$$\xrightarrow{Br_2, MeOH}$$
 \xrightarrow{Br} $\xrightarrow{Br$

Scheme II-7. Synthesis of intermediates **II-25** and **II-26**.

In order to synthesize II-7 from II-25, elimination of HBr was necessary. Acid catalysis was used to facilitate the syn elimination, which otherwise proved to be challenging under basic conditions (Scheme II-8). Heating II-25 in methanesulfonic acid in a sealed tube gave two analogs of II-7: II-27 and II-28. The formation of these two products eliminated HBr initially to give II-7. HBr then acted as a reducing agent causing protodebromination of the β-pyrrole position to produce olefin II-27, which, when combined with the molecular bromine present, afforded II-28. Horne et al found that eliminating the HBr and molecular bromine by leaving the flask unsealed, prevented II-7 from going on to II-27 and II-28.

Scheme II-8. Synthesis of stevensine II-7.

Alternatively, scheme **II-9** illustrates how **II-7** can be obtained in two steps from **II-6**. Although a direct oxidation of **II-6** to **II-7** was not possible, treatment with bromine in trifluoroacetic acid gave the expected 4'-bromohymenin **II-29** in 95% yield. When the bromination is performed in methanesulfonic acid, the reaction gave **II-29** as a product as well as 5-bromostevensine **II-30** and starting material. ^{13, 21} **II-7** could not be directly obtained from hymenin, however, debromination of **II-29** in methanesulfonic acid gave **II-7** in 20% yield. ¹³

Br₂, TFA
rt, 95%
Br
$$H_2N$$
 H_1
 H_2N
 H_2
 H_1
 H_2
 H_2
 H_2
 H_2
 H_2
 H_3
 H_2
 H_3
 H_4
 H_4
 H_5
 H_5
 H_7
 H_8
 H_8

Scheme II-9. Synthesis of II-7 from II-6.

In addition to the chemistry of protodebromination and transbromination, hydrolysis was also used in synthesizing II-1 and II-2 from intermediate II-29. As shown in Scheme II-10, II-29 was heated in HBr forming II-2 directly in 40% yield along with 2,3-debromostevensine II-31 (21% yield). Under the same conditions, II-1 was not formed due to the competitive nature of the hydrolysis and protodebromination. There was not a direct way to obtain II-1 from precursor II-29, however, milder conditions using a mixture of 1:1 H₂O/CH₃CO₂H gave the hydrolysis product II-32. A selective protodebromination in methanesulfonic acid in a sealed tube produced II-1 and II-2 in 33% and 27% yield, respectively. II-1 could also be formed in 65% yield as the major product by hydrolyzing II-28 in aqueous acetic acid (Scheme II-10). 13

Scheme II-10. Synthesis of II-1 and II-2 from intermediate II-29 and II-28.

In an effort to streamline the syntheses, Sosa et al ¹⁴ designed a one-pot, two-step procedure to synthesize **II-6** from **II-33** in Scheme **II-11**. The first reported syntheses of (*Z*)-3-bromohymenialdisine was obtained, while further hydrogenation gives debromohymenialdisine. ¹⁴ In a one-pot reaction, acid-catalyzed deprotection of acetal **II-33** and cyclization of the resultant aldehyde occurred to give intermediate **II-19b** without isolation. Intermediate **II-19b** was then coupled in the same pot to **II-20** to give **II-6**. The overall reaction was performed on a multi-gram scale giving **II-6** in 60% overall yield. Oxidation of **II-6** cleanly gave (Z)-3-bromohymenialdisine **II-34** followed by hydrogenation to give **II-2**. ¹⁴

Scheme II-11. Synthesis of **II-2** using a one-pot, two-step synthesis.

II.D SYNTHESIS OF AXINOHYDANTOINS

The first reported synthesis of axinohydantoins was reported by Sosa et al in $2002.^{19}$ The authors had envisioned synthesizing these compounds using hymenin analog **II-19b**. However, accessing a hydantoin nucleus from an imidazolone precursor was problematic and an intramolecular cyclization was instead utilized to remedy problems associated with the use of **II-19b** as seen in Scheme **II-12**. This key step formed the tricyclic pyrroloazepinone framework present in the axinohydantoins. Thus, **II-35** was treated with trifluoroacetic acid to form **II-36**. Cyclizations of α -debromopyrrole analogs were observed to have a higher yield than cyclization of α -bromopyrrole analogs, which underwent hydrolysis to form a spirolactam (not shown). Utilizing protodebromination conditions developed for the other marine alkaloid syntheses 13, 14, **II-3c** and **II-4c** were synthesized from **II-36**.

Scheme II-12. Synthesis of II-3c, II-4c, II-36 and II-37 from intermediate II-35.

Hydrogenation of **II-3c** and **II-4c** afforded debromoaxinohydantoins as seen in Scheme **II-13**. Hydrogenation of **II-4c** gave **II-4b** in 80% yield, however, the reduction of the (E)-isomer **II-3c** gave a 1:1.3 mixture of expected (E)-debromoaxinohydantoin **II-3b**, and the unexpected mono-reduction product, (E)-isoaxinohydantoin **II-38**. Compound **II-3b** was found to isomerize slowly at room temperature in DMSO- d_6 to the (Z)-isomer. Similar observations were seen with **II-38**.

Scheme II-13. Synthesis of axinohydantoins II-3b and II-4b from II-3c and II-4c.

II.E SYNTHESIS OF HYMENIALDISINE AND ANALOGS THROUGH THIOLS

In an effort to improve the synthesis of hymenialdisine, a few groups considered alternative heterocyclic coupling partners, such as thiohydantoin II-39 as seen in Scheme II-14. Portevin et al repeated the synthesis as performed by Horne (Scheme II-11), however, the cyclization to form II-19b followed by coupling of II-19b to 2-aminoimidazole II-20 occurred slowly, requiring 4 and 5 days, respectively. Although II-2 was obtained, there was room for improvement in the synthesis. The improved synthesis began with the same aldisine precursor II-11b, which was coupled with thiohydantoin II-39 using BF3•OEt2 (Scheme II-14). Using TiCl4 as a coupling reagent only gave the product in trace amounts, whereas the use of BF3•OEt2 under unoptimized reaction conditions gave 31% of II-40. Reacting II-40 with aqueous

ammonium hydroxide in the presence of *tert*-butylhydroperoxide gave optimal results affording **II-2** in 74% yield.²²

Scheme II-14. Synthesis of II-2 via thiohydantoin II-39.

Alternatively, Papeo et al synthesized II-1 as well as II-2 using II-41, an S-methylated, N-benzoylated thiohydantoin, as seen in Figure II-5.²³ The syntheses of II-1 and II-2 involved a condensation between II-11b and II-41, which was synthesized readily from N-benzoylthiohydantoin on a gram scale.

Figure II-5. Structure of 1-benzoyl-2-methylsulfanyl-1,5-dihydroimidazol-4-one.

Before the condensation, Papeo et al improved the overall yield of the Friedel-Craft cyclization **II-11a**¹⁷ to 53% as illustrated in Scheme **II-15**. Carboxylic acid **II-10** was reacted with phosgene to give the acyl chloride, and in the same one-pot process, AlCl₃ and 4 Å molecular sieves were added as an acid scavenger.²³ Using this method, **II-11a**

was prepared without the problematic 1,2-bromine migration that was observed in Annoura's synthesis.¹⁷

Br
$$\stackrel{H}{\stackrel{N}{\stackrel{}}}$$
 CO_2H $\frac{1.(COCI)_2$, DMF cat DCE, rt $\frac{1}{2}$. AlCI₃, 4 Å MS, rt (57%)

Scheme II-15. Improved synthesis of II-11a.

Scheme II-16 illustrates the condensation of II-41 with II-11 to give II-42. Intermediate II-42 was discovered to be sensitive to nucleophilic ring-opening as well as chromatography and the synthesis proceeded without isolation of II-42. Ammonia in dioxane was used to displace the methylthio group, giving compound II-43. However these conditions were not successful in displacing the benzoyl-protecting group, even after 2 days. Evaporation of dioxane and exposure to 7 N NH₃ in methanol removed the benzoyl protecting group and gave II-1 and II-2.

Scheme II-16. Synthesis of II-1 and II-2 utilizing II-41.

In the case of **II-43b**, *endo*-isomer **II-44** was also formed in 10%, however, this was easily converted to the more thermodynamically stable exo-(Z)-isomer²⁵ with diluted aqueous ammonia using microwave conditions (Scheme **II-17**).²³

Scheme II-17. Conversion of II-44 to II-2 under microwave conditions.

The same intermediate **II-2a** and **II-42b** were also used in the first total synthesis of (Z)-axinohydantoin **II-4a** (seven steps, 8% yield overall) following demethylation under acidic conditions and cleavage of the N-benzoyl protecting group using NH₂NH₂•H₂O (Scheme **II-18**). The stereoselective synthesis also afforded (Z)-debromoaxinohydantoin as well as the (E) isomers **II-3a**, **II-3b**) as the minor product as seen in Scheme **II-15**. ²⁶

Scheme II-18. Synthetic route for II-3a, II-3b and II-4a, II-4b.

Scheme **II-19** shows that 2-substituted *endo*-analogs of hymenialdisine can be synthesized using analogs of **II-46** as was demonstrated by Papeo.^{23, 24} The synthesis of this series of analogs began with either pyrrole derivatives or alkylated carboxylic acid derivatives of pyrrole (synthesis not shown).²⁴ Compound **II-46** was obtained following procedures similar to the previous syntheses of hymenialdisine.^{13, 14, 17, 22, 23} The expected *exo*-isomer was not obtained following reaction with ammonia, instead the *endo*-isomer was observed. Converting the isomers from *endo* to *exo* under microwave conditions (Scheme **II-17**) did not afford the exo-isomer. It was reported that having substituents in the 2-position on the pyrrole ring likely require higher energy in order to isomerize than unsubstituted pyrroles.²⁴

Scheme II-19. Synthesis of endo-pyrrole analogs.

II.F SYNTHESIS OF INDOLE ANALOGS OF HYMENIALDISINE

2-substituted hymenialdisine analogs are accessible as well as fused indole-pyrrole analogs of hymenialdisine.²⁷ The synthesis of the indole-aldisine intermediate began with the coupling of indole-2-carboxyllic acid with β -alanine ethyl ester in the presence of DMAP and EDCI to afford **II-50a** as seen in Scheme **II-20**²⁷ N-methylation of **II-50a**, followed by hydrolysis under mild conditions yielded **II-50c** which subsequently was cyclized to **II-51** using PPA and P₂O₅.^{27, 28}

Scheme II-20. Toward the synthesis of indole analogs of hymenialdisine.

The amide nitrogen was protected with various groups as seen in Table II-1. Following protection, indoloaldisine II-52 was reacted under basic conditions with trifluoromethanesulfonic anhydride (Scheme II-21). Utilizing II-52a and II-52e, three compounds were isolated: the expected triflate II-53 (21% yield from II-53a and 53% yield from II-53e), the monotriflate II-54 with unprotected amide (30% yield from II-53a and 20% from II-53e), and ditriflate II-55 (13% yield from II-53a and 23% yield from II-53e) (Scheme II-21).

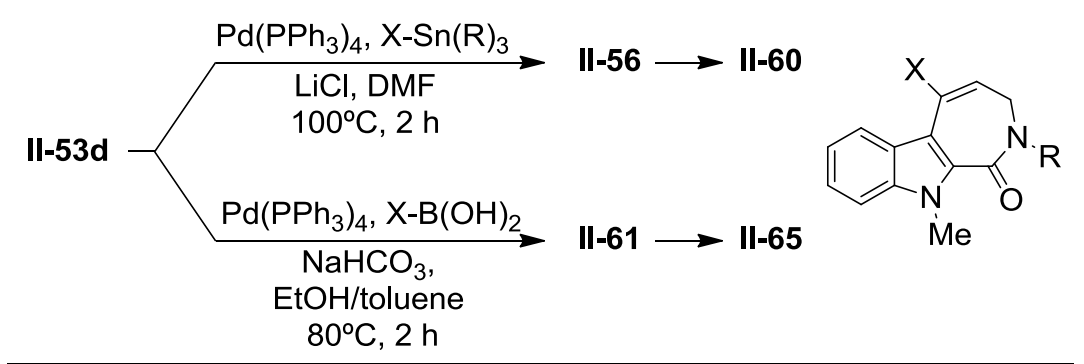
Table II-1. Nitrogen protecting group variations for indole aldisine.

Product	R	Conditions	Yield (%)
a	Ac	Ac ₂ O, pyr reflux, 2 h	85
b	Boc	Boc ₂ O, DMAP, MeCN, 24 h	40
С	Me	MeI, NaH, DMF, 0°C, 15 min	60
d	Bn	BnCl, NaH, DMF, 0°C, 30 min	72
е	PMB	PMBCl, NaH, DMF, 0°C, 40 min	78
f	SO ₂ Ph	PhSO₂Cl, NaH, DMF, 0°C, 1 h	90

Scheme II-21. Synthesis of mono- and di-triflate protected indole aldisines.

II-53d was the most reactive of the series with the added benefit of the ability to deprotect the amide nitrogen easily.²⁷ Thus, the indole-hymenialdisine analogs were prepared from **II-53d** using either Stille conditions or Suzuki conditions (Table **II-2**).

Table II-2. Scope of the Suzuki and Stille coupling for indole aldisine.



Product	Х	R	Yield (%)
II-56		Bn	90
II-57	Me	Bn	99
II-58	EtO	Bn	92
II-59	0	Bn	74
II-60	S	н	71
II-61	S	Bn	90
II-62	S	Bn	99
II-63		Bn	86
II-64	S	PMB	86
II-65	Me	SO_2Ph	76

II.G SYNTHESIS OF 2-AMINOIMIDAZALONE RING THROUGH PHENYLOXAZALONE

Sharma et al synthesized an indolo- analog of hymenialdisine, which was obtained via a condensation with phenyloxazolone **II-66** and indoloaldisine **II-67** or **II-51**, following a displacement with S-benzylthiourea (Figure **II-6**).

Figure II-6. Structure of phenyloxazolone.

The syntheses of **II-70a** and **II-70b** were achieved initially by amidation of indole-2-carboxylic acid with β -alanine ethyl ester in the presence of DMAP and EDCI (Scheme **II-22**). Compound **II-68** was obtained via hydrolysis of **II-67** and **II-50c**. Friedel-Craft cyclization was completed using P_2O_5 and methanesulfonic acid instead of PPA. Compound **II-68** and **II-51** underwent a TiCl₄ mediated aldol condensation with **II-66** to obtain the key intermediate **II-69**. Intermediate **II-69** was treated with S-benzylthiourea under basic conditions to give **II-70a** and **II-70b** in modest yields (Scheme **II-22**).

Scheme II-22: Synthesis of indoloazepine II-70.

II.H HYMENIALDISINE ANALOG SYNTHESIS VIA HECK REACTION

Another route of synthesis of the compound **II-70a** was proposed combining the Wittig reaction as well as the Heck reaction to close the 7-membered azepine ring. 31-33 Synthesis of the glycocyamidine ring was modeled after Annoura and Tatsuoka's synthesis. The Shown in Scheme **II-23**, indole-2-carboxylic acid **II-49**, was reacted with iodine to give I-substituted **II-71**. Compound **II-71** was subsequently coupled with (*E*)-5-amino-2-pentoate hydrochloride **II-72** in the presence of EDCI and DMAP in

dichloromethane to produce II-73.^{33} Boc protection of the free nitrogen atoms followed to give $\text{II-74.}^{31,\,33}$

Scheme II-23. Synthesis of intermediate II-74 for ring closure via Heck reaction.

With **II-74** in hand, it was possible to perform the catalytic Heck cyclization to form the indole-azepine ring under optimized conditions giving **II-75** (Scheme **II-24**). 31, 33 Dihydroxylation of **II-75** followed by dehydration afforded allyl alcohol **II-77**, which subsequently was converted to an allylic chloride **II-78**. Additionally, several attempts to obtain **II-70a** from **II-78** through reaction with guanidine in DMF were unsuccessful. 31

Scheme II-24. Unsuccessful Heck reaction approach to II-70.

The natural and unnatural analogs of hymenialdisine described here have a similar fused bicyclic pyrroloazepine ring system bonded to another 5-membered ring. With the exception of the indole analogs, these have in common with the marine sponge alkaloids a $C_{11}N_5$ core. Figure II-7 illustrates the scaffolds and positions that were modified to create analogs.²⁰ Using this scaffold, Wan et al were able to synthesize over 50 analogs for biological evaluation.

Figure II-7. General scaffold for hymenialdisine analogs.

II.I IMPROVEMENT OF THE SYNTHETIC ROUTE TO INDOLOAZEPINE II-70.

As more information about the biological activity of **II-70** became available, greater quantities of the compound was needed to perform *in vitro* studies. The original synthesis of **II-70** as performed in the Tepe group afforded the desired final product in a 28% yield (Scheme II-22) as the free amine. When the same synthesis was repeated as originally proposed, only 8% yield was obtained in the final step. Although this method provided material temporarily for biological testing, there was much room for improvement in the synthetic route.

Various attempts were made in the last step to replace the thiourea with a reagent that would introduce the guanidine portion of the imidazolone in higher yields. However, this method proved to be unfruitful with the phenylazlactone remaining intact. With the phenylazlactone remaining seemingly untouched, it was thought that perhaps the phenylazlactone was the troublesome portion of the molecule. Replacing the

phenylazlactone with a hydantoin had potential for providing higher yields of **II-70**. A previously reported total synthesis of a marine alkaloid from the Tunicate Dendrodoa in the Tepe group demonstrated that the imidazolone could be accessed via the hydantoin (Scheme **II-25**).³⁴ This route could allow access to the imidazolone with the free amine using ammonium hydroxide instead of dimethyl amine. Use of dimethyl amine however, would facilitate access to an additional analog of **II-70**.

Scheme II-25. Synthesis of II-82 via hydantoin II-79.

With the possibility of transforming a hydantoin into the glycocyamidine ring, efforts were put into coupling a hydantoin with aldisine **II-68**. Coupling **II-68** to hydantoin with TiCl₄ did not yield the desired compound **II-84** (Scheme **II-26**). Instead, hydantoin

was recovered along with starting materials. Protecting the amines of hydantoin did not improve the coupling efforts to **II-68**.

Scheme II-26. Hydantoin coupling to II-68.

Due to lack of success in a direct coupling of hydantoin to **II-68**, a Horner-Wadsworth Emmons (HWE) approach was instead pursued. Phosphonate **II-85** was synthesized as previously reported by Cativiela et al (Scheme **II-27**). The HWE reaction was performed under various previously reported conditions, however did not yield the desired product **II-84**. 35, 36

Scheme II-27. Attempted HWE synthesis to form **II-84**.

With several unsuccessful attempts at synthesizing **II-84**, another route was proposed as seen in Scheme **II-28**. The proposed route begins with iodination at C3 of indole-2-carboxylic acid to give **II-87**. **II-87** was then coupled with **II-88** and the resulting alcohol **II-89** was protected with TIPSCI to yield **II-90**. 27, 31-33

Scheme II-28. Alternate synthesis to II-84.

In Scheme **II-29**, the nitrogens of aldehyde **II-90** were Boc protected before the TIPS group was removed. **II-92** was oxidized to the aldehyde with IBX before coupling to **II-85** utilizing conditions for a similar reaction previously published.³⁷ Following coupling, Boc protection of remaining nitrogens and a Heck reaction would give the desired compound.

Scheme II-29. Synthesis of intermediate II-95.

Cyclization of **II-95** (R=H and R=Boc) was attempted under various conditions involving halogen-metal exchange (Table II-3). It was envisioned that a lithium ion would exchange with the iodine and perform an intramolecular conjugate addition in order to close the ring (entry 1). However, this did not occur. Attempts at forming a Grignard intermediate (entry 2) to perform the ring closure also failed. Formation of a cuprate in situ (entry 3) was unsuccessful in producing the hydantoin analog **II-84**. Entry 4 shows an attempted Heck reaction using conditions optimized for a similar substrate. ^{32, 33} This reaction gave decomposition products upon filtration. The salts contained starting

material. When Pd(OAc)₂ was used in molar quantities as well as in excess, there was still no cyclized product observed. It was speculated that there was not enough base and triphenylphosphine to get to Palladium(0). These amounts were increased and there was still no observance of the cyclized product.

Table II-3. Attempted conditions for cyclization.

Entry	Conditions	Temperature	Solvent
1	t-BuLi (10 eq)	-100°C to RT	THF
2	t-BuLi (10 eq) MgBr-OEt (4.5 eq)	-100°C to RT	THF
3	t-BuLi (10 eq) Cul (2.5 eq)	-100°C to RT	THF
4	Pd(OAc) ₂ , AgCO ₃ , KCl, PPh ₃ ,	90°C, 6 hr	DMF

The Heck reaction was also attempted using Pd(PPh₃)₄. The desired product was not observed. Different methods of work up were also performed, however, the product was not isolated. Sterics very likely played a major role in the reaction not producing the **II-84**. There were several bulky Boc groups that although could assist in orienting the chain to cyclize, could also provide enough bulkiness to inhibit the ring closure.

After several various failed attempts at closing the ring on **II-95**, another method was attempted. An improved synthesis was found utilizing Papeo's thiohyandantoin **II-41** was easily synthesized on a multigram scale from hippuric acid and ammonium thiocyanate (Scheme II-30).

Scheme II-30. Synthesis of II-41.

With **II-41** in hand, a TiCl₄ coupling was possible with indoloaldisine **II-68** which was synthesized as previously reported (Scheme II-22).^{28, 29} The resultant product (**II-97**) of the coupling was prone to decomposition during purification over silica, so was debenzoylated without further purification. **II-98b** was isolated cleanly using silica chromatography.

Scheme II-31. Synthesis of intermediate II-98.

Intermediate **II-98b** was a stable compound that proved synthetically advantageous, providing easy access to three compounds. Upon reaction with ammonia in a sealed tube, **II-70** resulted as a precipitate which was filtered and washed with 10% HCl before being filtered again (Scheme II-32). The resultant bright yellow solid was collected as HCl salt form of **II-70** in 67% yield, a vast improvement from the previously reported 28% yield and nearly 10-fold greater yield when repeated in the lab. A dimethylamino analog **II-99** was synthesized substituting dimethylamine for ammonia. This reaction mixture formed a similar precipitate, which was filtered, washed with 10% HCl, then filtered again. To form the hydantoin analog **II-84**, intermediate **II-98a** or **II-98b** was refluxed with NaOH in a 1:1 H₂O/THF mixture overnight. Unlike **II-70** or **II-99**, this compound required column chromatography over silica in order to isolate **II-100** from impurities.

Scheme II-32. Synthesis of II-70 and analogs II-99 and II-84.

The improved synthetic route employed in Scheme II-32 provided more facile access to II-70 in which was precipitated out of the reaction. Column chromatography was not required to isolate the compound from impurities. Multiple grams of II-70 was obtained using this synthesis which was then taken on to be examined as a checkpoint kinase 2 (Chk2) inhibitor *in vitro* and *in vivo* (discussed in Chapter 3).

II.J General experimental information of procedures and characterization

Reactions were carried out in flame-dried glassware under nitrogen atmosphere. All reactions were magnetically stirred and monitored by TLC with 0.25 µm pre-coated silicaa gel plates using either UV light or iodine to visualize compounds. Column chromatography was carried out on Silica Gel 60 (2330-400 mesh) supplied by EM Science. Yields refer to chromatographically and spectroscopically pure compounds unless otherwise noted. Infrared spectra were recorded on a Nicolet IR/42 spectrometer. ¹H NMR and ¹³C NMR spectra were recorded on a Varian Unity Plus-500 spectrometer or a Varian Inova-300, as noted in the experimental for each compound. Chemical shifts are reported relative to the residue peaks for the solvent (CDCI₃: 7.24 ppm for ¹H and 77.0 ppm for ¹³C); (DMSO-d₆: 2.49 ppm for ¹H and 39.5 ppm for ¹³C); (Acetone-d₆: 2.09 ppm for ¹H and 30.60 for ¹³C). The following abbreviations are used to denote the multiplicities in ¹H NMR: s = singlet, d = doublet, dd = doublet of doublets, t = triplet, m = multiplet, g = quartet. HRMS were obtained with a Micromass Q-Tof Ultima API LC-MS/MS mass spectrometer. Elemental analysis data were obtained on a Perkin Elmer 2400 Series II CHNS/O analyzer. Purity of compound, whose elemental analyses were above the ACS tolerated 0.4% deviation, were confirmed by ¹H NMR and ¹³C NMR. Melting points were obtained using an Electrothermal® capillary melting point apparatus and are uncorrected. Reagents and solvents were purchased from commercial suppliers and used without further purification. Anhydrous methylene chloride was dispensed from a delivery system which passes solvents through a column

packed with dry neutral alumina. Anhydrous tetrahydrofuran was distilled over sodium and benzophenone.

1-benzoyl-2-(methylthio)-1H-imidazol-4(5H)-one (II-41). Compound II-97 (10.0 g, 45.4 mmol) was dissolved in dichloromethane (500 mL) in a flame-dried RBF. To this mixture was added iodomethane (8.5 mL, 136.2 mmol), dimethylaminopyridine (553 mg, 4.54 mmol), and N,N-diisopropylethylamine (40 mL, 227 mmol) and the mixture was stirred at room temperature for 3 hours. 1% HCl was added to the reaction mixture and stirred for 10 minutes. The organics were then extracted and dried with anhydrous Na₂SO₄ and concentrated. The product was crystallized from ethyl acetate to yield white crystals (10.4 g, >99%). The spectral data matches that previously reported in the literature. HNMR (500 MHz, DMSO-d₆) δ 2.53 (s, 3H), 4.48 (s, 2H), 7.40-7.72 (m, 5H). NMR (128.2 MHz, DMSO-d₆) δ 16.1, 55.0, 127.7, 128.7, 132.0, 133.6, 166.8, 182.5, 186.1. MS: m/z calcd for C₁₁H₁₁N₂O₂S [M+H], 235.0541; found [M+H] 235.0551.

Ethyl 3-(1H-indole-2-carboxamido)propanoate (II-50a). This reaction was performed according to the known procedure. ²⁹ To a mixture of 2-indolecarboxylic acid (2.41 g, 14.9 mmol) and 4-(dimethylamino)pyridine (3.24 g, 26.4 mmol) in 75 mL of CH_2Cl_2 was added N-(3-dimethylaminopropyl)-N-ethylcarbodiimide hydrochloride (EDCI·HCI) (3.46 g, 18 mmol) and β-alanine ethyl ester hydrochloride (2.91 g, 18 mmol) at 0°C. The mixture was then stirred at 0°C for 4 hours and allowed to warm to room temperature for 20 hours. The solution was washed with water (25 mL) and 10% HCI (25 mL). The organics were dried over anhydrous Na_2SO_4 , filtered and concentrated to

dryness *in vacuo* to give a white solid (3.52g, 93%) which was recrystallized in methanol. The spectral data matches that previously reported in the literature. 28 m.p. $^{158-160^{\circ}}$. 1 H NMR (500 MHz, CDCl₃) δ 1.17 (t, J = 7.5 Hz, 3H), 2.58 (t, J = 6.5 Hz, 1H), 3.67 (q, J = 6.0 Hz, 2H), 4.08 (q, J = 7 Hz, 2H), 6.81 (s, 1H), 7.01 (t, J = 7.5 Hz, 1H), 7.09 (s, 1H), 7.14 (t, J = 7 Hz, 1H), 7.35 (d, J = 8.5 Hz, 1H), 7.52 (d, J = 8.5 Hz, 1H), 9.86 (s, 1H). 13 C NMR (74.47 MHz, CDCl₃) δ 13.9, 33.9, 35.0, 60.6, 102.3, 111.9, 120.3, 121.7, 124.2, 127.5, 130.6, 136.4, 161.7, 172.3. IR (NaCl): 3377, 3352, 1715, 1624, 1550, 1320, 1200, 750 cm⁻¹.

3-(1H-indole-2-carboxamido)propanoic acid (II-67). This reaction performed according to the known procedure.²⁸ A mixture of **II-50a** (1.38 g, 5.3 mmol) and LiOH·H₂O (0.70 g, 10.6 mmol) was dissolved in ethanol (100 mL) and stirred at room temperature for 20 hours. The ethanol was evaporated to dryness in vacuo. The residue was dissolved in water (15 mL), and the solution was acidified to pH = 3 with concentrated HCl to form a white solid. The mixture was allowed to stand at 0°C for 30 min, and the precipitate was isolated by filtration. The resulting solid was washed with water (20 mL) and recrystallized with a minimal amount of methanol to give 1.201 g, 97%. The spectral data matches that previously reported in the literature. ²⁸ m.p. 232°C. ¹H NMR (300 MHz, d⁶-DMSO) δ 2.55 (t, 2H, J = 7.2 Hz), 3.47 (g, J = 6.9 Hz, 2H), 7.01, (t, J = 7.2 Hz, 1H), 7.04 (s, 1H), 7.13 (t, J = 7.2 Hz, 1H), 7.41 (d, J = 8.1 Hz, 1H), 7.57 $(d, J = 8.1 \text{ Hz}, 1H), 8.52(s, 1H), 11.55 (s, 1H); ^{13}C NMR (74.47 MHz, d^6-DMSO) \delta 34.6,$ 35.9, 103.2, 112.9, 120.3, 122.1, 123.9, 127.8, 132.4, 137.1, 161.8, 173.4, IR (NaCl): 3420, 3268, 1750, 1702, 1640, 1545, 1415, 1340, 1249, 740 cm⁻¹.

3,4-dihydroazepino[3,4-b]indole-1,5(2H,10H)-dione (II-68). This reaction was performed according to the known procedure. ²⁸ **II-67** (6 g, 26.6 mmol) was added to a clear solution of P₂O₅ (4.1 g, 32 mmol) in MeSO₃H (300 g) at 60°C. The reaction mixture was heated to 110°C and stirred for 1.5 hours, then cooled to room temperature. The mixture was poured into ice water and stirred for 30 min. The purplecolored solid was then filtered. The solid was set aside. The filtrate was extracted with ethyl acetate (3 x 150 mL), dried with anhydrous Na₂SO₄ and concentrated in vacuo. The solid from filtration was dissolved in acetone, filtered again and the filtrate was combined with the organics of the extraction and concentrated. The light brown solid was purified further by column chromatography (20% acetone in CH₂Cl₂) on silica gel to yield the desired product (4.6 g, 81%). The spectral data matches that previously reported in the literature. ²⁸ m.p. 257-260°C. ¹H NMR (300 MHz, d⁶-DMSO) δ 2.80-2.85 (m, 2H), 3.40-3.46 (m, 2H), 7.22-7.38 (m, 2H), 7.51 (d, J = 9.0 Hz, 1H), 8.28 (d, J = 9.0 Hz,Hz, 1H), 8.72 (m, 1H), 12.41 (s, 1H). ¹³C NMR (74.47 MHz, d⁶-DMSO) δ 36.5, 44.0, 112.6, 113.7, 122.6, 122.7, 124.7, 126.0, 134.5, 135.6, 162.3, 195.0. IR (KBr-pellet): 3160, 1660, 1620, 1530, 1430, 1400 cm⁻¹.

(Z)-4-(1-oxo-1,2,3,4-tetrahydroazepino[3,4-b]indol-5(10H)-ylidene)-2-phenyloxazol-5(4H)-one (II-69). This reaction was performed according to the known procedure. A 1 mM solution of TiCl₄ in CH₂Cl₂ (19 mL, 19 mmol) was added to THF (150 mL) at -10°C. II-68 (1.07 g, 5 mmol) and 2-phenylazlactone (1.46 g, 9 mmol) were subsequently added and allowed to stir at 0°C for 1 hour. Pyridine (3.2 mL, 40 mmol) was then added over a 30 min period. The reaction mixture was stirred at 0°C for an

additional 2 hours and then the reaction was allowed to stir overnight at room temperature. NH₄Cl (80 mL saturated solution in water) was added, and the mixture was stirred for 10 min and subsequently extracted with ethyl acetate (3 x 80 mL). The organic extracts were combined, dried with anhydrous Na₂SO₄ and concentrated *in vacuo*. The residue was purified using column chromatography on silica gel (7% MeOH/43% Hexanes/50% EtOAc) to give 1.02 g, 57% yield as a reddish-yellow solid. The spectral data matches that previously reported in the literature. ^{28, 29} m.p. 247-250°C. ¹H NMR (300 MHz, d⁶-DMSO) δ 3.36-3.47 (m, 4H), 7.14 (t, J = 8.1 Hz, 1H), 7.30 (t, J = 9.0 Hz, 1H), 7.49-7.58 (m, 4H), 7.81-7.87 (m, 3H), 8.45-8.56 (m, 1H), 12.11 (s, 1H); ¹³C NMR (74.47 MHz, d⁶-DMSO) δ 37.7, 38.6, 112.9, 115.3, 121.0, 125.1, 125.3, 126.5, 127.4, 129.0, 133.2, 134.0, 136.9, 146.3, 158.4, 165.0, 166.1. IR (KBr-pellet): 3350, 3190, 1750, 1650, 1640, 1450 cm⁻¹.

(Z)-5-(2-amino-4-oxo-1H-imidazol-5(4H)-ylidene)-2,3,4,5-tetrahydroazepino [3,4-b]indol-1(10H)-one (II-70). Compound II-98b was dissolved in THF (10 mL) and stirred with ammonium hydroxide (30 mL) at 90°C in a sealed tube for 24 hours. The reaction mixture was allowed to cool to room temperature at which point the precipitate was filtered from the reaction mixture. The solid was collected and washed in 10% HCl and filtered a second time. The bright yellow solid was filtered and dried in vacuo (617 mg, 69.2%). Further purification of II-70, if necessary can also be performed with silica column chromatography with a gradient elution system of 15% MeOH: 85% CH₂Cl₂ followed by 4% TEA:20%MeOH: 76% CH₂Cl₂. Washing the resulting solid with 10% HCl yields II-70 after filtration and drying in vacuo. m.p.: decomposes over 260°C. ¹H NMR.

(500 MHz, DMSO-d₆) δ 3.32-3.39 (br, 4H), 7.19 (t, 1H, J = 7.9 Hz), 7.31 (t, 1H, J = 7.9 Hz), 7.52-7.57 (m, 2H), 8.36 (br, 2H), 9.05 (br, 1H) 10.31 (br, 1H), 12.45 (s, 1H); ¹³ C NMR (128.2 MHz, DMSO-d₆) δ 36.6, 39.2, 112.7, 113.6, 121.9, 122.4, 122.9, 124.6, 125.0, 128.9, 132.9, 132.9, 137.0, 154.6, 165.5. IR: (KBr-pellet) 3209, 1701, 1618, 1529, 1469, 1250. HRMS (ESI): m/z calcd for $C_{15}H_{12}N_5O_2$ [M+H], 296.1069; found, 296.1144.

(Z)-5-(1-oxo-1,2,3,4-tetrahydroazepino[3,4-b]indol-5(10H)-

ylidene)imidazolidine-2,4-dione (II-84). Compound 10 (500 mg, 1.2 mmol) was dissolved in THF (50 mL) and added to a mixture of sodium hydroxide (233 mg, 5.8 mmol) in water, which was then stirred for 24 hours. The reaction mixture was cooled and neutralized with sat. NH₄Cl (50 mL). The organics were extracted with ethyl acetate (2 x 50 mL). The organics were then dried with Na₂SO₄ and concentrated. The product was isolated as a brown solid over silica with MeOH:CH₂Cl₂ (10:90). (R_f = 0.3) (240 mg, 60.7%). m.p. decomposes over 320°C. 1 H NMR. (500 MHz, DMSO-d₆) $\bar{\delta}$ 3.50-3.53 (m, 4H), 7.24 (t, J = 8 Hz, 1H), 7.45 (t, J = 8.2, 1H), 7.57 (d, J = 7.7 Hz, 1H), 7.99 (s, 1H), 8.09 (d, J = 8 Hz, 1H), 10.54 (s, 1H), 12.47 (s, 1H); 13 C NMR (128.2 MHz, DMSO-d₆) $\bar{\delta}$ 23.1, 38.6, 112.9, 114.2, 117.0, 120.5, 120.9, 122.26, 122.37, 122.4, 126.2, 130.5, 139.4, 154.0, 160.8. IR: (KBr-pellet) 3372, 3059, 1674, 1454, 1342, 1201. HRMS (ESI): m/z calcd. for C₁₅H₁₃N₄O₃, 297.0988; found 297.0979.

Diethyl (2,5-dioxoimidazolidin-4-yl)phosphonate (II-85). This reaction was performed according to the known procedure. ³⁵ To a 100 mL 3-neck round bottom flask was added acetic acid (18 mL) and hydantoin (4.01 g, 40 mmol). The reaction mixture

was heated to 100°C and bromine (2.2 mL, 43 mmol) was added drop-wise with an addition funnel and the mixture was allowed to stir for 45 minutes at 100°C. The mixture was then cooled to 30°C in an ice/water bath at which point triethyl phosphite (9.6 mL, 55.5 mmol) was added slowly to the reaction mixture while maintaining an internal temperature between 40-45°C. The reaction mixture was stirred an additional 90 minutes and the solvent was removed under high vacuum. The resultant residue was dissolved in ether (10 mL) and placed in the freezer to precipitate the product which was then filtered and washed with cold ether to yield a white solid (6.0 g, 63.7% yield). The spectral data matches that previously reported in the literature. $^{35~1}$ H NMR (500 MHz, d⁶-DMSO) δ 1.23 (t, J = 3.6 Hz, 6H), 4.08 (m, 4H), 4.75 (d, J = 14.6 Hz, 1H), 8.42 (s, 1H), 10.92 (s, 1H). 13 C NMR (148.9 MHz, d⁶-DMSO) δ 16.2, 55.6, 56.8, 62.9, 63.1, 157.5, 169.5.

3-iodo-1H-indole-2-carboxylic acid (II-87). Indole-2-carboxylic acid (1.05 g, 6.2 mmol) was dissolved in acetone (50 mL). In a separate flask, N-iodosuccinimide (1.4 g, 6.2 mmol) was dissolved in acetone (10 mL) and this mixture was added drop wise to the indole-2-carboxylic acid/acetone mixture. The reaction mixture was stirred for 1.5 hours at which time the solvent was removed *in vacuo*. The solid was filtered and washed with water to remove succinimide to give a brownish-orange solid (1.5 g, 85%). ¹H NMR (500 MHz, d⁶-acetone) δ 3.34 (s, 1H), 7.12 (t, J = 6 Hz, 1H), 7.30 (t, J = 6 Hz, 1H), 7.416 (t, J = 8 Hz, 2H), 12.16 (s, 1H), 13.2 (s, 1H); ¹³C NMR (148.9 MHz, d⁶-acetone) δ 64.97, 112.9, 120.9, 125.5, 127.9, 130.7, 136.8 161.8. IR (NaCl): 3400,

3270, 3125, 3050, 2950, 1700, 1510, 1470, 1422, 1400, 1220 cm $^{-1}$. HRMS (ESI): m/z calcd for C₉H₅INO₂ [M-H], 285.9370; found [M-H], 285.9362.

N-(3-hydroxypropyl)-3-iodo-1H-indole-2-carboxamide (II-89). Compound II-87 (9.98 g, 34.8 mmol) and 4-(dimethylamino)pyridine (6.49 g, 53 mmol) were dissolved in CH₂Cl₂ and stirred at 0°C for 5 minutes. N-(3-dimethylaminopropyl)-N-ethylcarbodiimide hydrochloride (EDCI·HCI) (7.6 g, 39.6 mmol) and 3-aminopropan-1-ol (3 mL, 39 mmol) were then added and stirred at 0°C for 4 hours, allowed to warm to room temperature and stirred overnight. The reaction mixture was washed with water (150 mL) and extracted. The mixture was washed with 10% HCl (150 mL) and stirred for 10-15 minutes. Organics were extracted and dried with anhydrous Na₂SO₄. ¹H NMR (500 MHz, d^6 -DMSO) δ 1.72 (quint, J = 6.5 Hz, 2H), 3.37 (q, J = 6.9 Hz, 2H), 3.54 (t, J = 6.2 Hz, 2H), 4.53 (bs, 1H), 7.14 (t, J = 7.7 Hz, 1H), 7.26 (t, J = 7.5 Hz, 1H), 7.35 (d, J = 7.9Hz, 1H), 7.41 (d, J = 8.1 Hz, 1H), 7.94 (s, 1H), 11.97 (s, 1H). 13 C NMR (148.9 MHz, 6 -DMSO) δ 32.1, 36.5, 58.6, 112.5, 120.7, 121.6, 124.4, 130.2, 132.1, 135.9, 160.5. IR (NaCl): 3300, 3952, 2873, 1620, 1550, 1420, 1330, 1282, 825 cm⁻¹. HRMS (ESI): m/z calcd for $C_{12}H_{14}IN_2O_2$ [M+H], 345.0100; found [M+H], 345.0107.

3-iodo-N-(3-((triisopropylsilyl)oxy)propyl)-1H-indole-2-carboxamide (II-90). In a flame dried RBF, II-89 (1.53 g, 4.4 mmol) and triisopropylsilyl chloride (1.2 g, 5.2 mmol) were dissolved in DMF (10 mL) and stirred for 10 minutes at room temperature. Imidazole (0.856 g, 11 mmol) was then added to the mixture and stirred at room temperature for an additional 16 hours. 1% HCl was then added to the mixture which was extracted with ethyl acetate (3 x 10 mL). The organics were dried over Na₂SO₄ and

solvent removed *in vacuo*. The resulting residue was purified using silica column chromatography with 15% EtOAc/85% hexanes to give a clear residue (1.8 g, 82% yield). 1 H NMR (500 Mhz, d 6 -DMSO) δ 1.01 (d, J = 8.0 Hz, 21H), 1.80 (quint, J = 6.5 Hz, 2H), 3.40 (dd, J = 6.9, 12.7 Hz, 2H), 3.78 (t, J = 6.3 Hz, 2H), 7.13 (ddd, J = 0.96, 7.0, 8.0 Hz, 1H), 7.25 (ddd, J = 1.2, 7.0, 8.2 Hz, 1H), 7.35 (d, J = 8.0 Hz, 1H), 7.41 (d, J = 8.2 Hz, 1H), 7.91 (t, J = 5.4 Hz, 1H), 11.96 (s, 1H). 13 C NMR (148.9 MHz, d 6 -DMSO) δ 11.4, 17.9, 32.3, 36.3, 59.6, 60.8, 112.5, 120.7, 124.5, 130.1, 132.1, 160.6. IR (KBr): 3400, 3250, 2950, 2875, 1630, 1560, 1470, 1422, 1400, 1240 cm $^{-1}$. MS: m/z calcd for $C_{21}H_{34}IN_2O_2ISI$ [M+H], 500.4; found [M+H] 457.1 [-CH₃CHCH₃]. HRMS (ESI): m/z calcd for $C_{21}H_{34}IN_2O_2SI$ [M+H], 501.1434; found, 501.1415.

tert-butyl 2-((tert-butoxycarbonyl)(3- ((triisopropylsilyl)oxy)propyl) carbamoyl) -3-iodo-1H-indole-1-carboxylate (II-91). In a flame dried RBF, **II-90** (1.8 g, 4 mmol), and di-*tert*-butyl-dicarbonate (2.2 g, 10 mmol) were dissolved in acetonitrile (125 mL) and stirred for 10 minutes. 4-dimethylaminopyridine (1.7 g, 12 mmol) was then added to the mixture which was stirred at room temperature for an additional 18 hours. Acetonitrile was then removed *in vacuo* and the reaction mixture was purified using silica chromatography in 10% EtOAc/90% hexanes to yield a light yellow foam. (2.7 g, 96% yield). ¹H NMR (500 Mhz, CDCl₃) δ 1.06 (d, J = 11.0, 21H), 1.11 (s, 9H), 1.58 (s, 9H), 2.02-2.08 (m, 2H), 3.83 (quint, J = 6.5 Hz, 2H), 4.07-4.15 (m, 2H), 7.24-7.58 (m, 4H), 8.09 (d, J = 8.3 Hz, 1H). ¹³C NMR: (148.9 MHz, CDCl₃) δ 11.98, 18.0, 27.6, 27.9, 31.1, 31.8, 42.5, 61.7, 64.99 83.5, 85.2, 109.7, 115.5, 121.6, 123.7, 126.1, 134.6, 151.5,151.7, 164.1. IR (KBr): 2975, 2850, 1730 1680, 1460, 1430 cm⁻¹. MS: m/z calcd

 $C_{31}H_{49}N_2O_6ISi~[M+H],~570.72,~found,~657.1~[-CH_3CHCH_3].~HRMS~(ESI):~m/z~calcd~for$ $<math>C_{31}H_{50}IN_2O_6Si~[M+H],~701.2483;~found,~701.2484.$

tert-butyl 2-((tert-butoxycarbonyl)(3-hydroxypropyl)carbamoyl)-3-iodo-1Hindole-1-carboxylate (II-92). In a flame-dried RBF, compound II-91 (4.4 g, 6.3 mmol), and tetrabutylammonium fluoride (12.6 mL, 12.6 mmol) was dissolved in anhydrous THF (100 mL). The reaction mixture was stirred at room temperature for 4 hours. Sat. NH₄Cl (100 mL) was then added and stirred for 10 minutes at which point the organics were extracted with EtOAc (3 x 75 mL). The organics were dried with Na₂SO₄ and solvent removed in vacuo. The alcohol was purified using silica chromatography with 10% acetone/90% dichloromethane to give a light yellow foam. (2.7 g, 79.4% yield). ¹H NMR (300 Mhz, CDCl₃) δ 1.06 (s, 9H), 1.60 (s, 9H), 1.96-2.02 (m, 2H), 2.68 (s, 1H), 3.78 (s, 2H), 3.89-3.98 (m, 1H), 4.13-4.21 (m, 1H), 7.38-7.40 (m, 3H), 8.05 (d, J = 9.15Hz, 1H). ¹³C NMR (74.47 MHz, CDCl₃) δ 27.4, 28.0, 31.0, 40.9, 59.3, 65.1, 83.9, 85.4, 115.4, 121.7, 123.9, 126.2, 130.8, 134.3, 136.4, 152.3, 164.4. IR (KBr): 3443, 2950, 2920, 1730, 1675, 1470, 1370, 1280, 1100 cm⁻¹. MS: m/z calcd for C₂₂H₂₉N₂O₆I [M+H], 544.11, found, 544.0. HRMS (ESI): m/z calcd for C₂₂H₃₀IN₂O₆ [M+H], 545.1149; found, 545.1155.

tert-butyl 2-((tert-butoxycarbonyl)(3-oxopropyl)carbamoyl)-3-iodo-1H-indole-1-carboxylate (II-93). In a flame-dried RBF, compound II-92 (2.25 g, 4.13 mmol) was dissolved in EtOAc (150 mL). IBX (2.31, 8.26 mmol) was added to the reaction mixture which was then refluxed for 20 hours. The mixture was filtered over celite and the filtrate concentrated *in vacuo*. The product was isolated using silica column

chromatography with 30% EtOAc/70% Hexanes to yield a clear residue (1.7 g, 75% yield). 1 H NMR (500 Mhz, CDCl₃) δ 1.05 (s, 9H), 1.56 (s, 9H), 2.94 (t, J = 7.6 Hz, 2H), 4.09 (dt, J = 7.29, 14.3, 2H), 4.33 (dt, J = 6.99, 13.6 Hz, 2H,), 7.30 (dd, J = 6.41, 15.55 Hz, 3H), 8.03 (d, J = 8.79 Hz, 1H), 9.84 (s, 1H). 13 C NMR (148.9 MHz, CDCl₃) δ 27.2, 27.7, 38.2, 42.2, 65.0, 83.6, 85.2, 115.2, 121.4, 123.7, 126.1, 130.5, 134.2, 136.0, 148.0, 151.1, 163.8, 200.0. IR (KBr): 2975, 2900 1725, 1730, 1675, 1450,1375 cm $^{-1}$. MS: m/z calcd for $C_{22}H_{27}N_2O_6I$ [M+H]; 542.11, found, 542.0.

2-((tert-butoxycarbonyl)(3-(2,5-dioxoimidazolidin-4-(Z)-tert-butyl ylidene)propyl)carbamoyl)-3-iodo-1H-indole-1-carboxylate (II-94). In a flame dried flask, compound **II-85** (739 mg, 3.13 mmol) and lithium bromide (326 mg, 3.76 mmol) were dissolved in anhydrous acetonitrile (75 mL) and stirred for 5 minutes. Triethylamine (0.43 mL, 3.76 mmol) was added to the mixture and stirred for 10 minutes followed by the addition of II-93 (1.7 g, 3.13 mmol). The reaction mixture was stirred 24 hours at room temperature. 1N HCl (50 mL) was added to the reaction mixture and stirred for 10 minutes. Organics were extracted with CH₂Cl₂ (3 x 100 mL), dried over Na₂SO₄ and concentrated to dryness in vacuo. The product was isolated from impuries with silica chromatography with 20% acetone/dichloromethane to yield a light yellow foam. (1.6g, 82% yield (2:1 Z:E)). ¹H NMR (500 Mhz, d⁴-Acetone) (mixture of isomers, not separated) δ 1.15 (s, 9H), 1.18 (s, 9H), 1.61 (s, 9H), 1.62 (s, 9H), 2.11 (dt, J = 1.46, 8.39, 8.28 Hz, 2H), 3.17-3.21 (m, 2H), 3.89-3.98 (m, 2H), 4.16-4.21 (m, 2H), 5.70 (t, J =8.05 Hz, 1H), 5.80 (t, J = 7.83 Hz, 1H), 7.49-7.39 (m, 5H), 8.14 (d, J = 8.33 Hz, 1H), 9.03 (s. 1H), 9.18 (s. 1H), 9.80 (s. 1H). 13 C NMR (148.9 MHz, 4 -Acetone) δ 25.7.

26.4, 27.7, 28.0, 43.8, 44.4, 64.8, 84.2, 86.2, 108.7, 114.3, 122.3, 124.8, 131.4, 131.9, 135.3, 149.0, 152.4, 154.9, 164.4. IR (KBr): 3250, 2975, 1730, 1450, 1350 cm $^{-1}$. MS: m/z calcd $C_{25}H_{29}N_4O_7I$ [M+H] 624.42; found [M+H], 524.0 [-Boc]. HRMS (ESI):m/z calcd for $C_{25}H_{30}IN_4O_7$ [M+H], 625.1159; found, 625.1166.

(Z)-di-tert-butyl 4-(3-(N,1-bis(tert-butoxycarbonyl)-3-iodo-1H-indole-2carboxamido)propylidene)-2,5-dioxoimidazolidine-1,3-dicarboxylate (II-95).Compound **II-94** (750 mg, 1.2 mmol) and di-tert-butyl-dicarbonate (654 mg, 3 mmol) were dissolved in anhydrous THF (35 mL) followed by the addition of 4dimethylaminopyridine (29.4 mg, 0.24 mmol). Triethylamine (140 µl, 1.2 mmol) was added to the mixture which was then stirred at room temperature for 3 hours at which time an additional portion of DMAP (0.98 g, 0.008 mmol) was added and the mixture stirred for an additional 20 hours. The mixture was then concentrated to dryness in vacuo and dissolved in CH₂Cl₂, and subsequently washed with 1 N HCl, saturated Na₂CO₃ and brine. The organics were dried with anhydrous Na₂SO₄ and concentrated in vacuo. The product was purified with silica chromatography with 25% EtOAc/Hexanes to yield a yellow foam (4.4 g, 98% yield). ¹H NMR (500 Mhz, CDCl₃) δ 1.08 (s, 9H), 1.55 (s, 18H), 1.56 (s, 9H), 3.19-3.39 (m, 1H), 3.32-3.42 (m, 1H), 3.92-4.01 (m, 1H), 4.18-4.27 (m, 1H), 7.16 (t, J = 7.93 Hz, 1H), 7.28 (t, J = 7.01 Hz, 1H), 7.34 (t, J = 7.1 Hz, 2H), 8.03 (d, J = 8.4 Hz, 1H). 13 C NMR (148.9 MHz, CDCl₃) δ 26.1, 27.5, 27.7, 27.9, 43.4, 65.0, 83.5, 85.2,85.5, 56.4, 115.4, 121.7, 123.7,124.6, 127.8, 145.3,145.7, 151.4, 157.3, 163.9. IR (KBr): 2980, 2950, 1720, 1690, 1490, 1450, 1270, 1160, 1050

cm⁻¹. MS: m/z calcd for $C_{35}H_{45}N_4O_{11}I$ [M+H] 824.66, found [M+H] 523.3 [-3 Boc]. HRMS (ESI): m/z calcd for $C_{35}H_{46}N_4O_{11}I$ [M-H], 823.2057; found, 823.2035.

1-benzoyl-2-thioxoimidazolidin-4-one (II-97). This reaction was performed according to the known procedure²³. Hippuric acid (8.0g, 44.6 mmol) and ammonium thiocyanate (8.5 g, 111.5 mmol) were thoroughly ground together in a mortar and suspended in a mixture of glacial acetic acid (4 mL) and acetic anhydride (36 mL). The reaction mixture was heated for one hour at 60° C and for an additional hour at 100° C. The red solution was cooled, diluted with cold water (200 mL) and stirred overnight for 18 hours. The reaction mixture was concentrated *in vacuo*. The crude residue was then crystallized from EtOH affording the product (8.07 g, 82%) as an orange solid. The spectral data matches that previously reported in the literature.²³ m.p. 156-158. ¹H NMR. (500 MHz, DMSO-d₆) δ 4.60 (s, 2H), 7.4-7.7 (m, 5H), 12.50 (bs, 1H). ¹³ C NMR (128.2 MHz, DMSO-d₆) δ 52.9, 127.9, 128.5, 131.7, 134.4, 169.0, 170.7, 182.6. MS: m/s calcd for C₁₀H₉N₂O₂S [M⁺] 221.0385; found [M⁺], 221.0383.

(Z)-5-(2-(methylthio)-4-oxo-1H-imidazol-5(4H)-ylidene)-2,3,4,5-

tetrahydroazepino[3,4-b]indol-1(10H)-one (II-98b). A 1 M solution of TiCl₄ in CH₂Cl₂ (1.9 mL, 1.9 mmol) was added to THF (25 mL) at -10°C. II-68 (200 mg, 0.5 mmol) and II-41 (219 mg, 0.93 mmol) were subsequently added and allowed to stir at 0°C for 30 minutes. Pyridine (0.3mL, 3.7 mmol) was then added drop wise over 30 minutes. The reaction mixture was stirred at 0°C for an additional 2 hours and allowed to stir overnight at room temperature. Sat. NH₄Cl (25 mL) was added, and the mixture was stirred for 10 min followed by subsequent extractions with ethyl acetate (3 x 25 mL). The

organic extracts were then washed with water (25 mL), followed by brine (25 mL). The organic extracts were then dried with anhydrous NaSO₄ and concentrated. The resultant residue (200 mg, 0.47 mmol) was dissolved in THF (10 mL) and stirred with sodium hydroxide (94 mg, 2.35 mmol) in water (10 mL) at room temperature for 20 hours. The mixture was neutralized with 1% HCl and extracted with ethyl acetate (50 mL). Organics were dried and concentrated. Product was isolated from impurities on silica with 5% methanol/dichloromethane to yield a reddish-yellow solid (161 mg, 53% overall yield). m.p. decomposes over 190°C. 1 H NMR (500 MHz, DMSO-d₆) 2.33 (s, 3H), 3.34-3.40 (m, 4H), 7.06 (t, J = 7.2 Hz, 1H), 7.21 (t, J = 7.0 Hz, 1H), 7.41 (d, J = 8.2 Hz, 1H), 8.33 (t, J = 5.1 Hz, 1H), 11.59 (s, 1H), 12.19 (s, 1H). 13 C NMR (128.2 MHz, DMSO-d₆) 5 11.9, 35.5, 38.9, 111.9, 115.3, 119.2, 123.8, 125.2, 125.9, 131.7, 134.8, 135.2, 135.9, 157.4, 164.7, 169.7. IR: (KBr-pellet) 3220, 1700, 1650, 1540, 1480. HRMS (ESI): m/z calcd for C₁₆H₁₆N₄O₂S [M+H], 327.0916; found, 327.0914.

(Z)-5-(2-(dimethylamino)-4-oxo-1H-imidazol-5(4H)-ylidene)-2,3,4,5-tetrahydroazepino[3,4-b]indol-1(10H)-one (2) (II-99). Compound II-98b (514 mg, 1.6 mmol) was added to a solution of dimethylamine (12 mL (2M in THF), 24 mmol). The mixture was heated to 90°C in a sealed tube for 24 hours. The reaction mixture was allowed to cool to room temperature and the resulting precipitate was filtered and washed with 10% HCl. The bright yellow solid was dried *in vacuo*. (212mg, 41.4%). m.p. decomposes over 250°C. 1 H NMR. (500 MHz, DMSO-d₆) δ 2.90 (s, 3H), 3.15 (s, 3H), 3.19 (s, 4H), 7.14 (t, 1H, J = 7.5 Hz), 7.29 (t, 1H, J = 7.6 Hz), 7.54 (d, 1H, J = 8.2 Hz), 8.43 (s, 1H), 10.35 (s, 1H), 12.49 (br, 1H); 13 C NMR (128.2 MHz, DMSO-d₆) δ 25.5,

35.9, 38.4, 67.0, 112.4, 112.9, 120.5, 122.1, 122.5, 124.1, 129.2, 132.4, 136.3, 153.1, 163.3, 164.7. IR: (KBr) 3385, 3224, 2940, 1676, 1603, 1441, 1287. HRMS (ESI): m/z calcd for $C_{17}H_{18}N_5O_2$ [M+H], 324.1460; found, 324.1463.

REFERENCES

II.K References

- 1. Sharma, G. M.; Buyer, J. S.; Pomerantz, M. W., Characterization of a Yellow Compound Isolated from the Marine Sponge Phakellia-Flabellata. *J. Chem. Soc. Chem. Comm.* **1980**, (10), 435-436.
- 2. Sharma, G.; Magdoff-Fairchild, B., Natural products of marine sponges. 7. The constitution of weakly basic guanidine compounds, dibromophakellin and monobromophakellin. *J. Org. Chem.* **1977**, *42* (25), 4118-24.
- 3. Sharma, G. M.; Schem, G. F.; Pastore, A. T., Natural products of marine sponges. VIII: Partial structure of a novel compound isolated from Phakellia flabellata. *Drugs Food Sea Myth Reality?* [Int. Symp.] **1978**, 199-202.
- 4. Mattia, C. A.; Mazzarella, L.; Puliti, R., 4-(2-Amino-4-Oxo-2-Imidazolin-5-Ylidene)-2-Bromo-4,5,6,7-Tetrahydropyrrolo-[2,3-C]Azepin-8-One Methanol Solvate a New Bromo Compound from the Sponge Acanthella-Aurantiaca. *Acta Crystallographica Section B-Structural Science* **1982**, *38* (Sep), 2513-2515.
- 5. Cimino, G.; De Rosa, S.; De Stefano, S.; Mazzarella, L.; Puliti, R.; Sodano, G., Isolation and x-ray crystal structure of a novel bromo compound from two marine sponges. *Tetrahedron Lett.* **1982**, *23* (7), 767-8.
- 6. Kitagawa, I.; Kobayashi, M.; Kitanaka, K.; Kido, M.; Kyogoku, Y., Marine natural products. XII. On the chemical constituents of the Okinawan marine sponge Hymeniacidon aldis. *Chem. Pharm. Bull.* **1983**, *31* (7), 2321-8.
- 7. Denanteuil, G.; Ahond, A.; Guilhem, J.; Poupat, C.; Dau, E. T. H.; Potier, P.; Pusset, M.; Pusset, J.; Laboute, P., Marine-Invertebrates from Neo-Caledonian Lagoons .5. Isolation and Identification of Metabolites from a New Species of Sponge, Pseudaxinyssa-Cantharella. *Tetrahedron* **1985**, *41* (24), 6019-6033.
- 8. Endo, M.; Nakagawa, M.; Hamamoto, Y.; Ishihama, M., Pharmacologically Active Substances from Southern Pacific Marine-Invertebrates. *Pure Appl. Chem.* **1986**, *58* (3), 387-394.
- 9. Pettit, G. R.; Herald, C. L.; Leet, J. E.; Gupta, R.; Schaufelberger, D. E.; Bates, R. B.; Clewlow, P. J.; Doubek, D. L.; Manfredi, K. P.; et al., Antineoplastic agents. 168. Isolation and structure of axinohydantoin. *Can. J. Chem.* **1990**, *68* (9), 1621-4.

- 10. Patil, A. D.; Freyer, A. J.; Killmer, L.; Hofmann, G.; Randall, K., Z-axinohydantoin and debromo-z-axinohydantoin from the sponge Stylotella aurantium: Inhibitors of protein kinase C. *Natural Product Letters* **1997**, *9* (3), 201-207.
- 11. Inaba, K.; Sato, H.; Tsuda, M.; Kobayashi, J., Spongiacidins A-D, new bromopyrrole alkaloids from Hymeniacidon sponge. *J. Nat. Prod.* **1998,** *61* (5), 693-695.
- 12. Williams, D. H.; Faulkner, D. J., Isomers and tautomers of hymenialdisine and debromohymenialdisine. *Nat. Prod. Lett. FIELD Full Journal Title:Natural Product Letters* **1996**, *9* (1), 57-64.
- 13. Xu, Y.-z.; Yakushijin, K.; Horne, D. A., Synthesis of C11N5 Marine Sponge Alkaloids: (+-)-Hymenin, Stevensine, Hymenialdisine, and Debromohymenialdisine. *J. Org. Chem.* **1997**, *62* (3), 456-464.
- 14. Sosa, A. C. B.; Yakushijin, K.; Horne, D. A., A Practical Synthesis of (Z)-Debromohymenialdisine. *J. Org. Chem.* **2000**, *65* (2), 610-611.
- 15. Kobayashi, J.; Ohizumi, Y.; Nakamura, H.; Hirata, Y.; Wakamatsu, K.; Miyazawa, T., Hymenin, a novel a-adrenoceptor blocking agent from the Okinawan marine sponge Hymeniacidon sp. *Experientia* **1986**, *42* (9), 1064-5.
- 16. Kobayashi, J.; Nakamura, H.; Ohizumi, Y., Alpha-Adrenoceptor Blocking Action of Hymenin, a Novel Marine Alkaloid. *Experientia* **1988**, *44* (1), 86-87.
- 17. Annoura, H.; Tatsuoka, T., Total syntheses of hymenialdisine and debromohymenialdisine: stereospecific construction of the 2-amino-4-oxo-2-imidazolin-5(Z)-disubstituted ylidene ring system. *Tetrahedron Lett* **1995**, *36* (3), 413-16.
- 18. Davis, F. A.; Vishwakarma, L. C.; Billmers, J. M.; Finn, J., Synthesis of Alpha-Hydroxy Carbonyl-Compounds (Acyloins) Direct Oxidation of Enolates Using 2-Sulfonyloxaziridines. *J. Org. Chem.* **1984,** *49* (17), 3241-3243.
- 19. Sosa, A. C. B.; Yakushijin, K.; Horne, D. A., Synthesis of Axinohydantoins. *J. Org. Chem.* **2002**, *67* (13), 4498-4500.

- 20. Wan, Y.; Hur, W.; Cho, C. Y.; Liu, Y.; Adrian, F. J.; Lozach, O.; Bach, S.; Mayer, T.; Fabbro, D.; Meijer, L.; Gray, N. S., Synthesis and target identification of hymenialdisine analogs. *Chem. Biol.* **2004**, *11* (2), 247-59.
- 21. Xu, Y. Z.; Yakushijin, K.; Horne, D. A., Transbromination of brominated pyrrole and imidazole derivatives: Synthesis of the C11N5 marine alkaloid stevensine. *Tetrahedron Lett.* **1996**, 37 (45), 8121-8124.
- 22. Portevin, B.; Golsteyn, R. M.; Pierre, A.; De Nanteuil, G., An expeditious multigram preparation of the marine protein kinase inhibitor debromohymenialdisine. *Tetrahedron Lett.* **2003**, *44* (52), 9263-9265.
- 23. Papeo, G.; Posteri, H.; Borghi, D.; Varasi, M., A new glycociamidine ring precursor: Syntheses of (Z)-hymenialdisine, (Z)-2-debromohymenialdisine, and (+/-)-endo-2-debromohymenialdisine. *Org. Lett.* **2005**, 7 (25), 5641-5644.
- 24. He, Q. F.; Chen, W.; Qin, Y., Synthesis of 2-substituted endo-hymenialdisine derivatives. *Tetrahedron Lett.* **2007**, *48* (11), 1899-1901.
- 25. Eder, C.; Proksch, P.; Wray, V.; Steube, K.; Bringmann, G.; van Soest, R. W. M.; Sudarsono; Ferdinandus, E.; Pattisina, L. A.; Wiryowidagdo, S.; Moka, W., New alkaloids from the Indopacific sponge Stylissa carteri. *J. Nat. Prod.* **1999,** *62* (1), 184-187.
- 26. Tutino, F.; Posteri, H.; Borghi, D.; Quartieri, F.; Mongelli, N.; Papeo, G., Stereoselective synthesis of (Z)-axino- and (Z)-debromoaxinohydantoin. *Tetrahedron* **2009**, *65*, 2372-2376.
- 27. Chacun-Lefevre, L.; Joseph, B.; Merour, J.-Y., Synthesis and reactivity of azepino[3,4-b]indol-5-yl trifluoromethanesulfonate. *Tetrahedron* **2000**, *56* (26), 4491-4499.
- 28. Sharma, V.; Lansdell, T. A.; Jin, G.; Tepe, J. J., Inhibition of Cytokine Production by Hymenialdisine Derivatives. *J. Med. Chem.* **2004**, *47* (14), 3700-3703.
- 29. Sharma, V.; Tepe, J. J., Potent inhibition of checkpoint kinase activity by a hymenialdisine-derived indoloazepine. *Bioorg. Med. Chem. Lett.* **2004,** *14* (16), 4319-4321.

- 30. Sharma, V.; Lansdell, T. A.; Peddibhotla, S.; Tepe, J. J., Sensitization of Tumor Cells toward Chemotherapy: Enhancing the Efficacy of Camptothecin with Imidazolines. *Chem. Biol.* **2004**, *11* (12), 1689-1699.
- 31. Montagne, C.; Laurent, N.; Joseph, B.; Merour, J. Y., Preparation and reactivity of 5-substituted azepino[3,4-b]indoles. *J. Heterocycl. Chem.* **2005**, *42* (7), 1433-1441.
- 32. Chacun-Lefevre, L.; Beneteau, V.; Joseph, B.; Merour, J.-Y., Ring closure metathesis of indole 2-carboxylic acid allylamide derivatives. *Tetrahedron* **2002**, *58* (51), 10181-10188.
- 33. Chacun-Lefevre, L.; Joseph, B.; Merour, J.-Y., Intramolecular Heck coupling of alkenyl 3-iodoindole-2-carboxamide derivatives. *Synlett* **2001**, (6), 848-850.
- 34. Hupp, C. D.; Tepe, J. J., Total synthesis of a marine alkaloid from the tunicate Dendrodoa grossularia. *Org. Lett.* **2008**, *10* (17), 3737-3739.
- 35. Cativiela, C.; Fraile, J. M.; Garcia, J. I.; Lafuente, G.; Mayoral, J. A.; Tahir, R.; Pallares, A., The use of Lewis acids in the synthesis of 5-arylhydantoins. *J. Catal.* **2004,** *226* (1), 192-196.
- 36. Meanwell, N. A.; Roth, H. R.; Smith, E. C. R.; Wedding, D. L.; Wright, J. J. K., Diethyl 2,4-dioxoimidazolidine-5-phosphonates: Horner-Wadsworth-Emmons reagents for the mild and efficient preparation of C-5 unsaturated hydantoin derivatives. *J. Org. Chem.* **1991**, *56* (24), 6897-904.
- 37. Shabica, A. C.; Howe, E. E.; Ziegler, J. B.; Tishler, M., Improved synthesis of 3-indolealdehyde. *J. Am. Chem. Soc.* **1946**, *68*, 1156-7.

CHAPTER III

EVALUATION OF INDOLOAZEPINE AS AN INHIBITOR OF CHECKPOINT KINASE 2

III.A Biological target of natural product and hypothesis for activity

As discussed in detail in Chapter 1, Chk2 has been the biological target from the start of this project. The function of Chk2 has been proposed to act as a barrier to tumorigenesis by preventing or delaying progression through the cell cycle following the activation of the DNA damage response in cancer lesions.^{1, 2} Activation of ATM-Chk2 by IR leads to phosphorylation of several downstream substrates involved in many cellular processes including cell cycle arrest, apoptosis and DNA repair.³⁻⁹

The use of Chk2 inhibitors for potentiating DNA-damage agents continues to be exciting but controversial 10-12 as not all inhibitors of Chk2 demonstrate a synergistic cytotoxic effect with chemotherapeutic drugs. 13 There are a few small molecule inhibitors of Chk2 that have been reported in the literature, and interest in discovering a potent and selective inhibitor remains high.

Figure III-1. Structure of debromohymenialdisine, hymenialdisine and hymenialdisine derived indoloazepine **II-70.**

Natural product debromohymenialdisine has some structural characteristics similar to indoloazepine **II-70** (Figure III-1). It has been hypothesized that the majority of the hydrogen bonding contacts believed to be important for the natural product are present in indoloazepine (See Figure I-20 - I-22). Cellular inhibition of debromohymenialdisine and hymenialdisine (Figure III-1) was reported by Roberge and co-workers showing inhibition of the G_2 checkpoint. Debromohymenialdisine inhibited Chk1 and Chk2 *in vitro* with an IC50 value of 3 and 3.5 μ M, respectively.

III.B In vitro evaluation of Chk2 inhibitors

In order to determine the selectivity of **II-70** for Chk2, *in vitro* kinase-profiling experiments were performed (Table III-1). The kinase listed in table III-1 were selected from a large panel of kinases known to be affected by the hymenial disines at low micromolar concentrations. ^{15, 16, 17}

Table III-1. Kinase profiling data for indoloazepine debromohymenialdisine, hymenialdisine and **II-70**. Values are reported at IC₅₀ values. Experiments were performed by Millipore KinaseProfiler Service using a radioactive assay method.

Kinase	debromohymenialdisine	hymenialdisine	II-70
Chk1 (nM)	725	1950	237
Chk2 (nM)	183	42	8
GSK-3β (nM)	NA	10	86
CK1δ(h) (nM)	NA	35 ^{15, 16}	1,352
CK2 (h) (nM)	NA	7000 ^{15, 16}	> 10,000
IKKα(h) (nM)	NA	NA	> 10,000
IKKβ(h) (nM)	NA	NA	> 10,000
MEK1(h) (nM)	824 ¹⁸	6 ¹⁸	89
PKCα(h) (nM)	NA	700 ^{15, 16}	2,539
PKCβII(h) (nM)	NA	1200 ^{15, 16}	3,381

The compounds were screened for multiple kinases so that insight into the selectivity against other kinases could be evaluated. The kinases screened are listed in Table III-1. An *in vitro* kinase assay was performed against the listed kinases with debromohymenialdisine, hymenialdisine and **II-70** as seen in Table III-1 (Millipore, Billerica, MA). A general illustration of the protocol used for the kinase screen is shown in Figure III-2. Briefly, a known substrate for the kinase is incubated with a compound, such as **II-70**, along with radio-labeled [γ -33P]-ATP and the kinase. The kinase phosphorylates the substrate with 33P-ATP (or not, if inhibited) and the amount of radio-activity bound to the negatively charged filter mat is directly related to the incorporation of 33P.

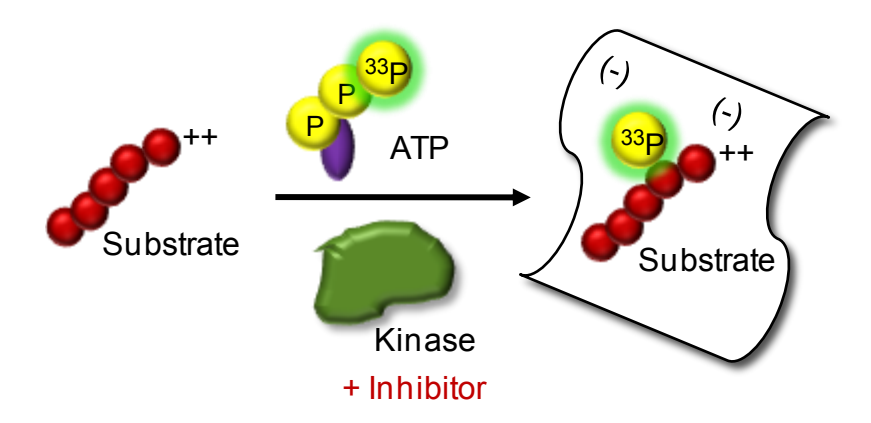


Figure III-2. Illustration of radio-active kinase protocol.

II-70 exhibited potent inhibition of Chk1 and Chk2 with IC₅₀ values of 237 nM and 8 nM, respectively. ¹⁷ II-70 showed a greater potency toward Chk2 compared to hymenialdisine. However, hymenialdisine was more selective for Chk2 than Chk1 (~45-fold selectivity) when compared to II-70 (~30-fold selectivity). II-70 also demonstrated

inhibition and at least 10-fold selectivity over GSK-3 β (IC₅₀ = 86 nM), MEK1 (IC₅₀ = 89 nM).

Figure III-3. Structures of analogs II-84, II-99, III-1 and III-2.

The Tepe lab reported the original synthesis of II-70,^{17, 19} and the improved synthesis was discussed in Chapter 2. With the newly acquired II-70 collected as the HCl salt, it was necessary to re-evaluate the inhibitor to ensure it was still able to inhibit Chk1 and Chk2. Two other hymenialdisine derived analogs III-1, and III-2 (Figure III-3) were synthesized by two members of the Tepe research group (Micah Luderer, Rahman Saleem, respectively). The analogs were synthesized in order to learn more about the structural requirements for Chk2 binding activity. At this time, analogs II-84, II-99, III-1 and III-2 (Figure III-3) were also evaluated for their ability to Chk1 and Chk2.

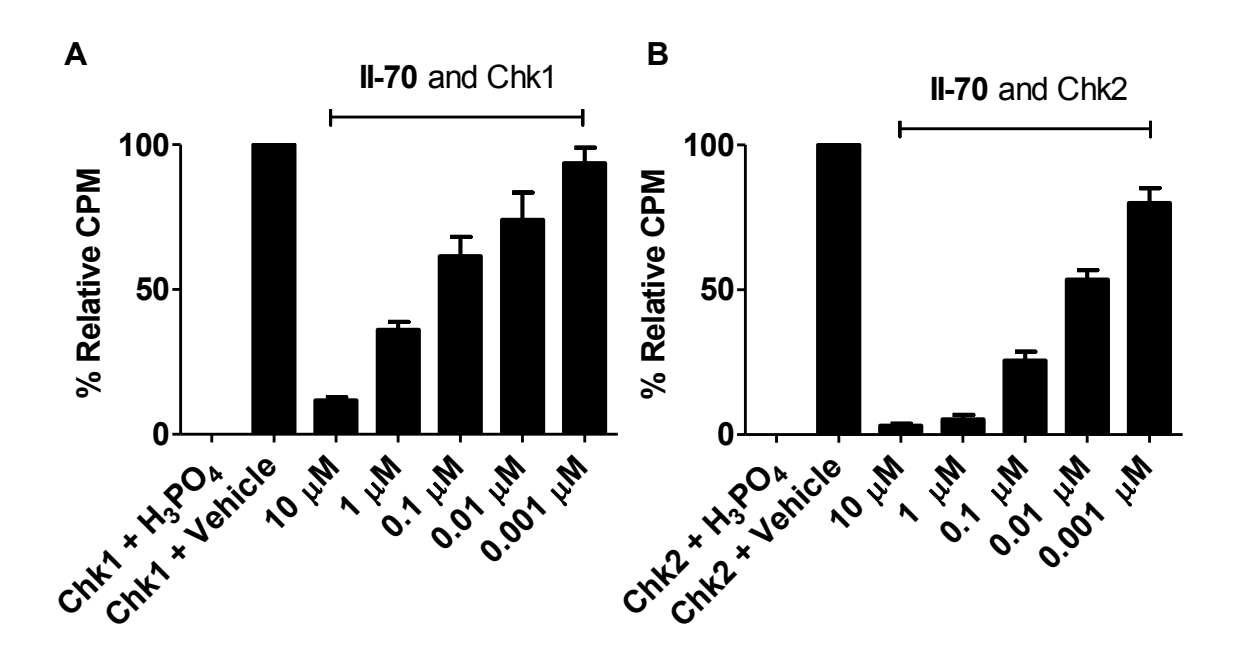


Figure III-4. Inhibition of $[\gamma^{-33}P]$ -ATP phosphorylation by Chk1 or Chk2. H₃PO₄ was used as a negative or untreated control. A) Inhibition of $[\gamma^{-33}P]$ -ATP phosphorylation of Chk1 by indoloazepine **II-70**. B) Inhibition of $[\gamma^{-33}P]$ -ATP phosphorylation of Chk2 by indoloazepine **II-70**.

The radio-labeled filter mat assay that was described above was used to evaluate II-70, II-84 II-99 and III-1 and III-2. The results of the inhibition of Chk1 and Chk2 are illustrated in Figure III-4. The graphs clearly indicate a dose dependent inhibition of Chk1 (Figure III-4A) and Chk2 (Figure III-4B) by II-70, and that II-70 was a more selective inhibitor of Chk2 than for Chk1. The values for IC $_{50}$ were calculated based on the phosphoric acid control and the vehicle control and found to be 220.4 nM and 13.5 nM for Chk1 and Chk2, respectively (Table III-2). Neither analogs II-84 or II-99 indicated any inhibition of Chk1 or Chk2 at relevant concentrations (IC $_{50}$ >10 μ M). However, compounds III-1 and III-2 were also found to be potent inhibitors of Chk2, albeit with somewhat less selectivity toward the related Chk1. The results of the Chk1 and Chk2 inhibition by these compounds are summarized in Table 1.

TABLE III-2. Summary of mean IC₅₀ values for kinase inhibition by analogs **II-70**, **II-84**, **II-99**, **III-1** and **III-2**.

Kinase	II-70	II-84	II-99	III-1	III-2
Chk1 (nM)	220.4	> 10,000	> 10,000	581.4	626.8
Chk2 (nM)	13.5	> 10,000	> 10,000	65.9	53.9

Replacement of the exocyclic amine with an oxygen (compound II-84) abrogated the ability of the indoloazepine analog to inhibit Chk1 or Chk2. The lack of Chk2 inhibition by compound II-99 suggests that the methyl groups add steric bulk to the exocyclic nitrogen of the glycocyamidine, which could prevent a proper fit in the active pocket of Chk2 and eliminate the hydrogen bonding interactions with ASN352, as seen in Figure III-5. 20 The lack of activity of compounds **III-84** and **III-99** indicates that the free amine group is necessary for binding and could also act as a hydrogen bond donor, consistent with the binding of hymenialdisine to Chk2. Compounds II-70, III-1 and III-2 all possess the free amine on the glycocyamidine ring allowing for the hydrogen bonding that is not present in II-84 and II-99 (Figure III-6). The decrease in potency of compound III-1 relative to II-70 (Figure III-6a) may potentially be explained by the location of the double bond of the glycocyamidine ring, which is not conjugated with the carbonyl in the ring, but instead is conjugated to the indoloaldisine portion, thus competing for hydrogen bonding with GLU308. The indole hydrogen could form an intramolecular hydrogen bond with the proximal nitrogen, potentially reducing hydrogen bond opportunities to the Chk2 catalytic site (Figure III-6b). The intramolecular hydrogen

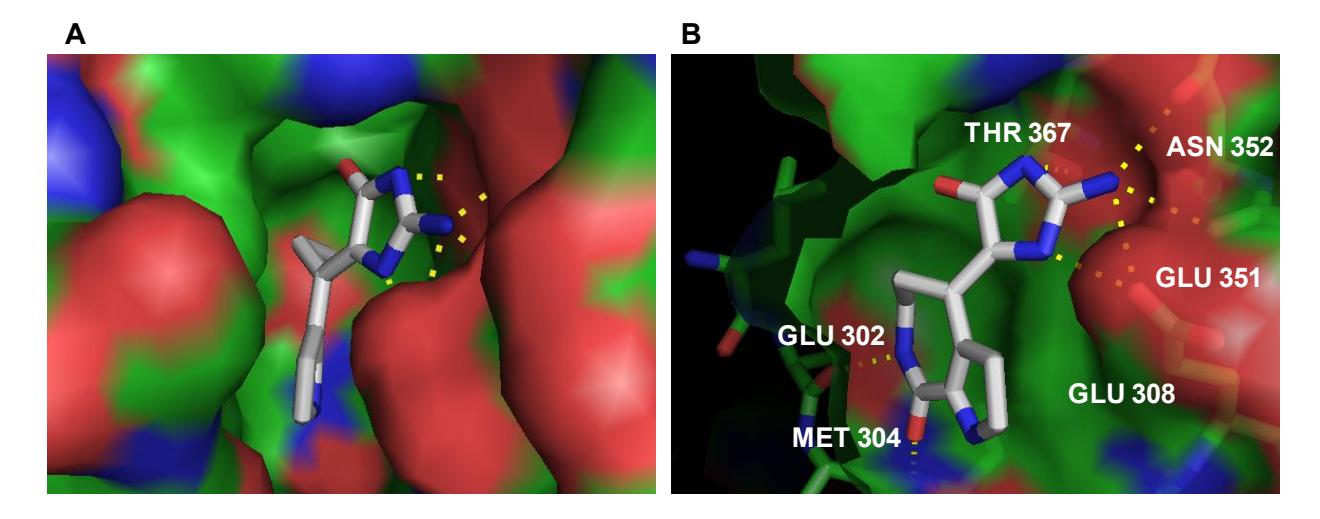


Figure III-5. Natural product hymenialdisine in Chk2 catalytic site. A) Hymenialdisine pictured with surface interactions. B) Hymenialdisine pictured with surface interactions as well as with hydrogen bonds to residues. Green regions represent hydrophobic areas, blue indicates electropositive areas and red areas are electronegative. ²⁰

bonding could also contribute to the change in the way **III-1** fits in the active site when the glycocyamidine ring is aligned with glycocyamidine ring of hymenialdisine (Figure III-6b). As anticipated, phenyl pyrrole **III-2**, was capable of inhibiting Chk2 effectively, but unfortunately displayed a reduced activity and selectivity compared to indoloazepine **II-70**. The hydrophobic phenyl ring may have steric interactions with an electronegative area instead of fitting into the hydrophobic region of the catalytic site.

A radio-labeled filter mat experiments demonstrate that II-70, III-1 and III-2 are inhibitors of Chk1 and Chk2. The structural similarities of the glycocyamidine ring of these analogs compared to the natural product hymenialdisine can explain the ability of these analogs to inhibit Chk1 and Chk2. As noted above, analogs II-84 and II-99 are poor inhibitors of both of these kinases due to their lack of hydrogen bond donors and steric methyl groups.

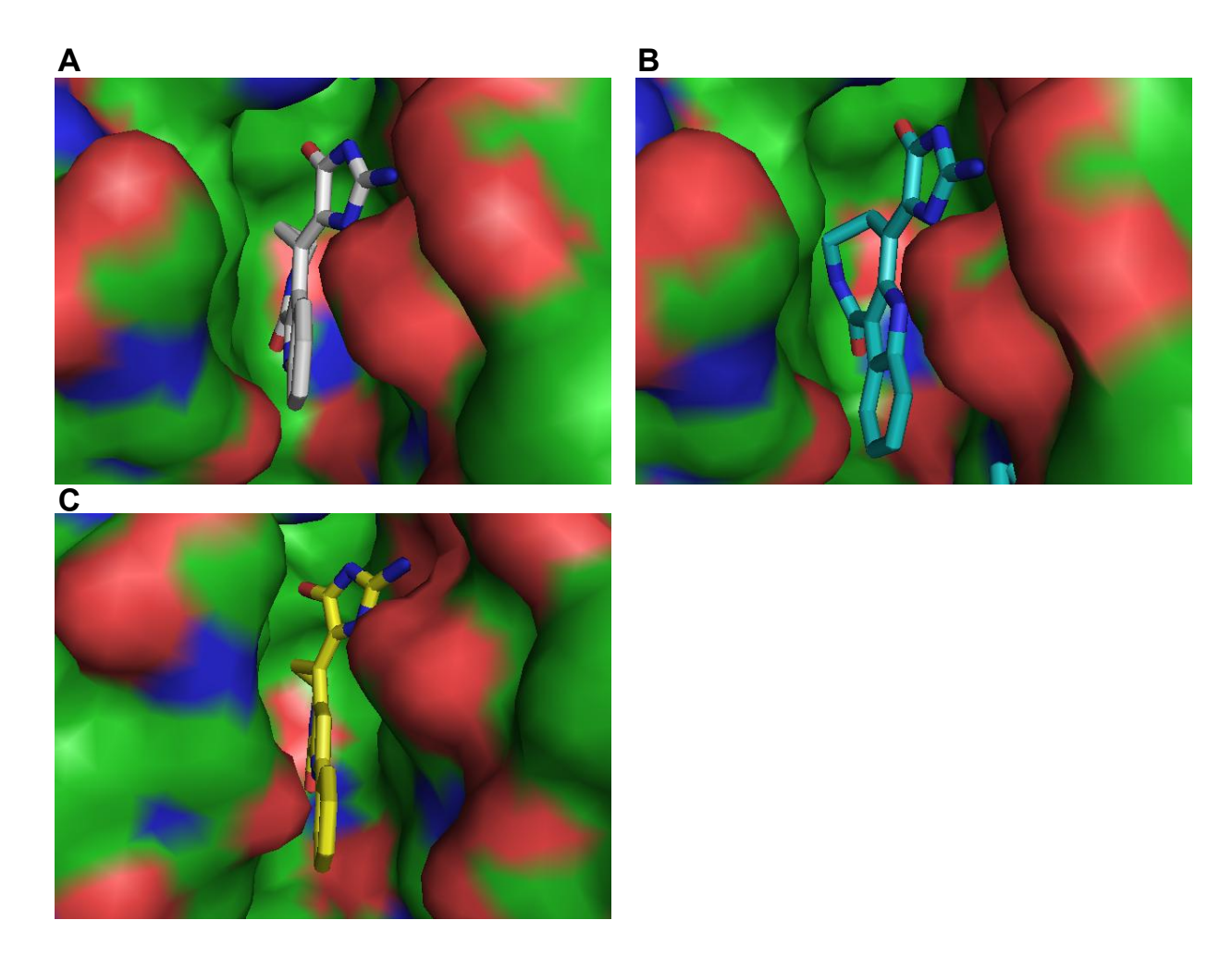


Figure III-6. Compounds **II-70**, **III-1** and **III-2** modeled in the Chk2 catalytic site with PyMol.²¹ A) **II-70** pictured with surface interactions. B) **III-1** pictured with surface interactions. C) **III-2** pictured with surface interactions. Green regions represent hydrophobic areas, blue indicates electropositive areas and red areas are electronegative.²⁰

III.C In vitro evaluation of the effect of indoloazepine in the DNA pathway

In order to determine support for cellular inhibition of Chk2 by **II-70**, Chk2 levels (total protein levels) were evaluated, in addition to Chk2 Th68 and Chk2 autophosphorylation at Ser516. A normal breast cell line, 184B5 was untreated or pretreated for 2 hours prior to IR with vehicle (DMSO), the positive control Chk2 inhibitor **ABI** (Chapter 1, Figure I-16A, 30 μ M), the negative control Chk2-inactive indoloazepine

II-99 (30 µM), and the Chk2 inhibitor II-70 (30 µM). The cells were irradiated (10 Gy) and treated with fresh media and vehicle or 30 µM ABI, II-99 or II-70 for 4 hours at which time whole cell extracts were collected. Whole cell extracts were then evaluated by Western blot for cellular inhibition of Chk2. Total Chk2 levels were probed with anti-Chk2 antibody. No changes in the level of Chk2 were observed upon exposure to low $(0.1 \mu M)$ and high $(30 \mu M)$ concentrations of **II-70** (Figure III-7A). **ABI** $(30 \mu M)$ also did not have an effect on the total levels of Chk2. The IR-induced activation of Chk2 was confirmed by observing phosphorylation of Chk2 at Thr68, which occurred when cells were exposed to IR (Figure III-7A, Lanes 3, 5-8, 10, and 12).²² As anticipated, inhibition of Chk2 by II-70 or ABI did not affect phosphorylation of Thr68 by ATM (Figure III-7A, Lanes 5 and 12), indicating that the ATM function was not affected by compound **II-70**. However, there was a dose-dependent effect of II-70 on IR-induced Chk2 autophosphorylation at Ser516 shown in 184B5 cells (Figure III-7A and B, lanes 5-8). As expected, Chk2 autophosphorylation at Ser516 was also seen with ABI (Figure III-7A and B, lane 12), a known Chk2 inhibitor²³. Figure III-7B shows the relative levels of phosphorylated forms of Chk2 pSer516 after normalization for total β-actin levels as determined by densitometry. This further illustrates the dose dependent inhibition of autophosphorylation by II-70. ABI also showed a comparable level of Chk2 inhibition at 30 µM compared to that seen with II-70. There was no inhibition of Chk2 phosphorylation of Thr68 or Ser516 with the inactive Chk2 agent II-99 (IC₅₀ > 10 μ M), which was used in the assay as a negative control (Figure III-7A, Lane 10).

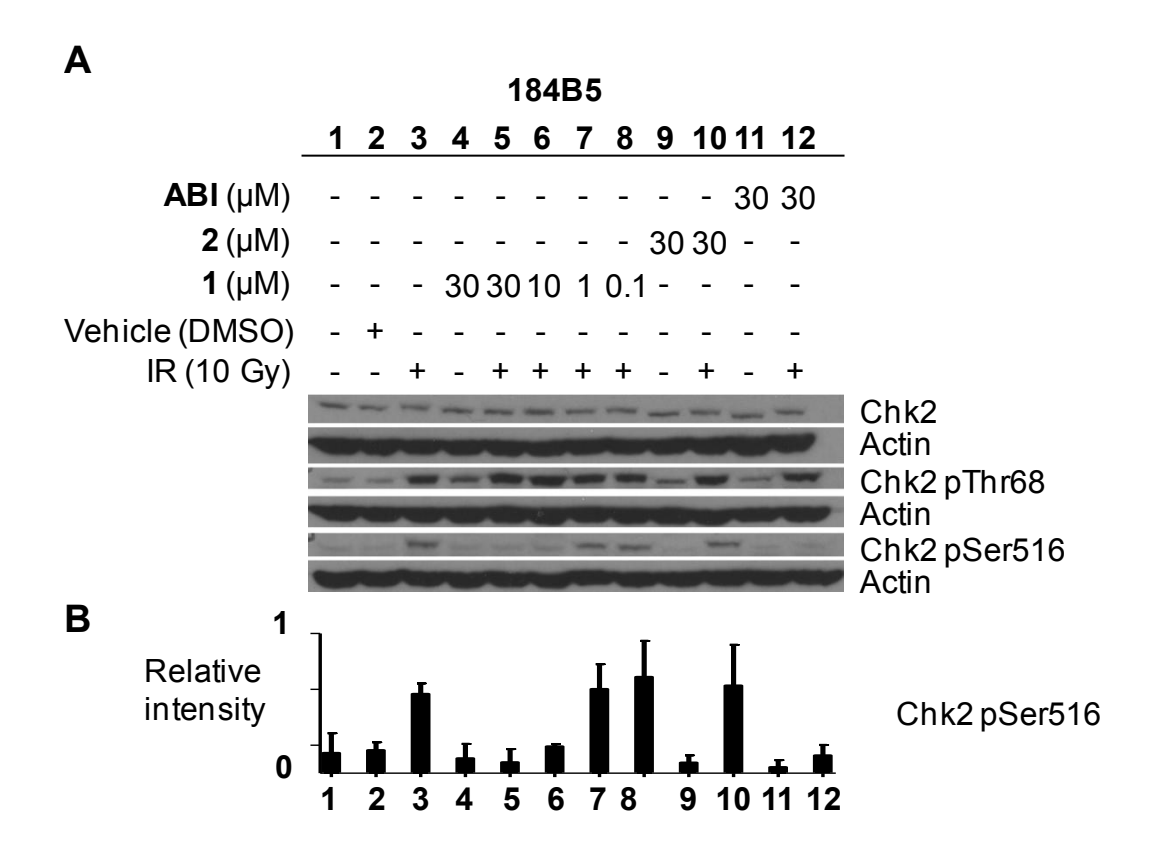


Figure III-7. Western blot analysis of 184B5 (normal, p53 WT) whole cell extracts. A) Cells were untreated (control) or treated with vehicle or with compounds **ABI**, **II-99**, and **II-70** for 2 hours prior to IR (10 Gy). Cells were incubated for 4 hours after IR when extracts were collected. The western blot was evaluated with Chk2 antibodies. B) Quantification of relative densities of bands for pSer516. These blots and data are representative of 3 independent experiments.

To further investigate the effect of **II-70** on Chk2 inhibition, we evaluated **II-70** in a breast cancer cell line, MDA-MB-231 with a mutated p53. DNA damage was induced with IR in MDA-MB-231 cells and inhibition of Chk2 phosphorylation was evaluated (Figure III-8A). As in the normal breast cell line, levels of total Chk2 in MDA-MB-231 remain unchanged when treated with IR, **ABI**, **II-99** or **II-70**. Chk2 Thr68 was phosphorylated following treatment with IR and remained unchanged when pretreated with **ABI**, **II-99** or **II-70** (Figure III-8A, Lanes 3, 5-8, 10, 12). Chk2 inhibition with **II-70** inhibited autophosphorylation at Ser516 in a dose dependent manner following IR (Figure III-8A, Lanes 5-8). Figure III-8B shows the relative levels of phosphorylated

forms of Chk2 pSer516 after normalization for total β-actin levels as determined by densitometry. This further illustrates the dose dependent inhibition of autophosphorylation by II-70. Levels of Chk2 inhibition were again compared to ABI, which also inhibited *cis*-autophosphorylation of Chk2 at Ser516 (Figure III-8A, Lane 12). As anticipated, inactive analog II-99 did not inhibit Chk2 autophosphorylation (Figure III-8A, Lane 10). This data illustrates that the cellular inhibition of Chk2 by II-70 is independent of the p53 status of the cell lines and that Chk2 is inhibited in both the normal breast line, 184B5 as well as the breast tumor cell line, MDA-MB-231.

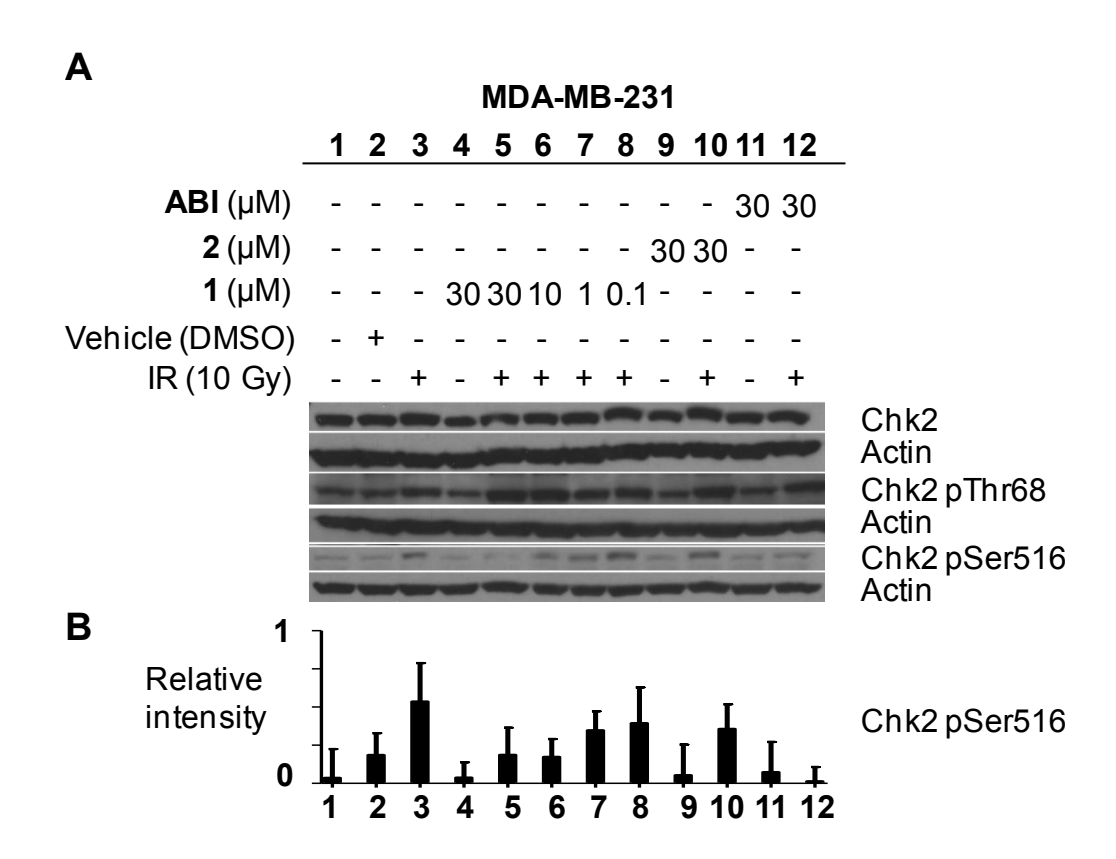


Figure III-8. Western blot analysis of MDA-MB-231 (tumor, p53 mut) whole cell extracts. Cells untreated (control) or treated with vehicle or with compounds **ABI**, **II-99**, and **II-70** for 2 hours prior to IR (10 Gy). Cells were incubated for 4 hours after IR when extracts were collected. The western blot was evaluated with Chk2 antibodies. B) Quantification of relative densities of bands for pSer516. These blots and data are representative of 3 independent experiments.

Two other hymenialdisine derived analogs **III-1** (IC₅₀ =68.8 nM) and **III-2** (IC₅₀ = 43.9 nM), were evaluated as cellular inhibitors of autophosphorylation of Chk2 at Ser516 (Figure III-9). Both analogs **III-1** and **III-2** demonstrated a dose dependent effect on inhibition of Chk2 Ser516, supporting cellular inhibition of Chk2 by **III-1** and **III-2**.

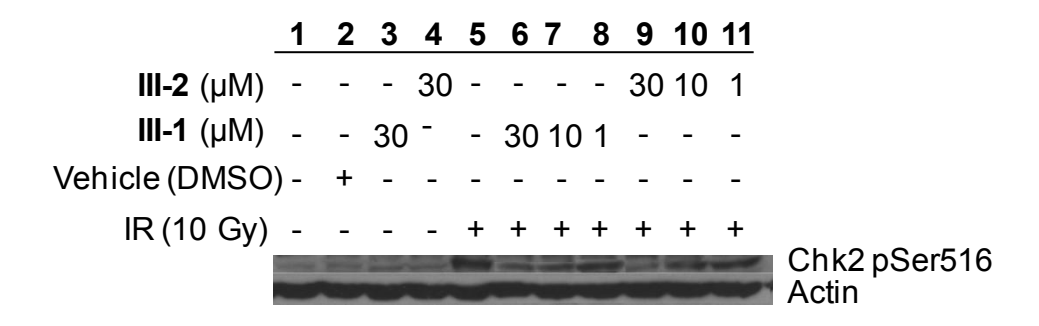


Figure III-9. Western blot analysis of 184B5 whole cell untreated (control) or treated with vehicle or with compounds **III-1** and **III-1** for 2 hours prior to IR (10 Gy). Cells were incubated for 4 hours after IR when extracts were collected. The western blot was evaluated with Chk2 antibodies. These blots are representative of 3 independent experiments.

Thus, this data indicates that the *in vitro* activity of inhibitor **II-70**, **III-1** and **III-2**, translates in cell culture. In addition, the more potent and selective Chk2 inhibitor **II-70** abrogates Chk2 activity in both the normal breast cell line, 184B5 as well as the breast tumor cell line MDA-MB-231.

III.D In vitro evaluation of the cell cycle with indoloazepine

Checkpoint signaling pathways are activated following DNA double strand breaks and result in the arrest of cells at the G_1/S , S or G_2/M transitions, which allows cells time to repair the damage or execute apoptosis. ²⁴ In response to IR, the activated ATM-Chk2 pathway phosphorylates their downstream substrates resulting in a G_2 arrest. To determine whether inhibition of Chk2 by **II-70** would modulate the G_2 checkpoint, we monitored the cell cycle using single parameter flow cytometry. We utiliazed two

HCT116 cell lines which were either a Chk2 +/+ or Chk2 -/- genotype. This allowed us to further verify that Chk2 is the target of **II-70**. We hypothesized that inhibiting Chk2 with **II-70** would yield similar cell cycle effects as the Chk2 -/- cells following IR-induced DNA damage.

HCT116 Chk2 +/+ cells were pretreated with nothing, vehicle or II-70 (30 µM) for 2 hours, and then the cells were irradiated with various doses of IR. HCT116 Chk2 -/remained untreated or were irradiated at the same doses of IR as HCT116 Chk2 +/+ cells (Figure III-10, Figure III-11). The cells were allowed to incubate for 0-22 hours at which point cells were harvested and fixed. Consistent with the early and temporary activation of the ATM-Chk2 pathway, 5, 6, 25 untreated HCT116 Chk2 +/+ cells resulted in G₂ arrest 22 hours after IR, relative to the control cells (Figure III-10B; Figure III-11E). HCT116 Chk2 +/+ cells treated with Chk2 inhibitor II-70, displayed a significant (**P < 0.0071) decrease at the G2 checkpoint (Figure III-10, Figure III-11) compared to the untreated control. A similar abrogation of the G2 checkpoint was demonstrated in the Chk2 -/- cell line (Figure III-11E, **P < 0.0012), again, compared to the Chk2 +/+ untreated cells. Table III-4 summarizes the values of significance between the untreated Chk2 +/+ and II-70 treated cells as well as the untreated Chk2 +/+ and Chk2 -/- cells. The inhibition of the IR-induced G₂ checkpoint in the Chk2 -/- cell line clearly indicates that **II-70** inhibits Chk2. Abrogation of the IR-induced G₂ arrest with Chk2 inhibitor **II-70**, allows normal cells to progress to the G1 checkpoint where DNA replication is initiated and carried out.

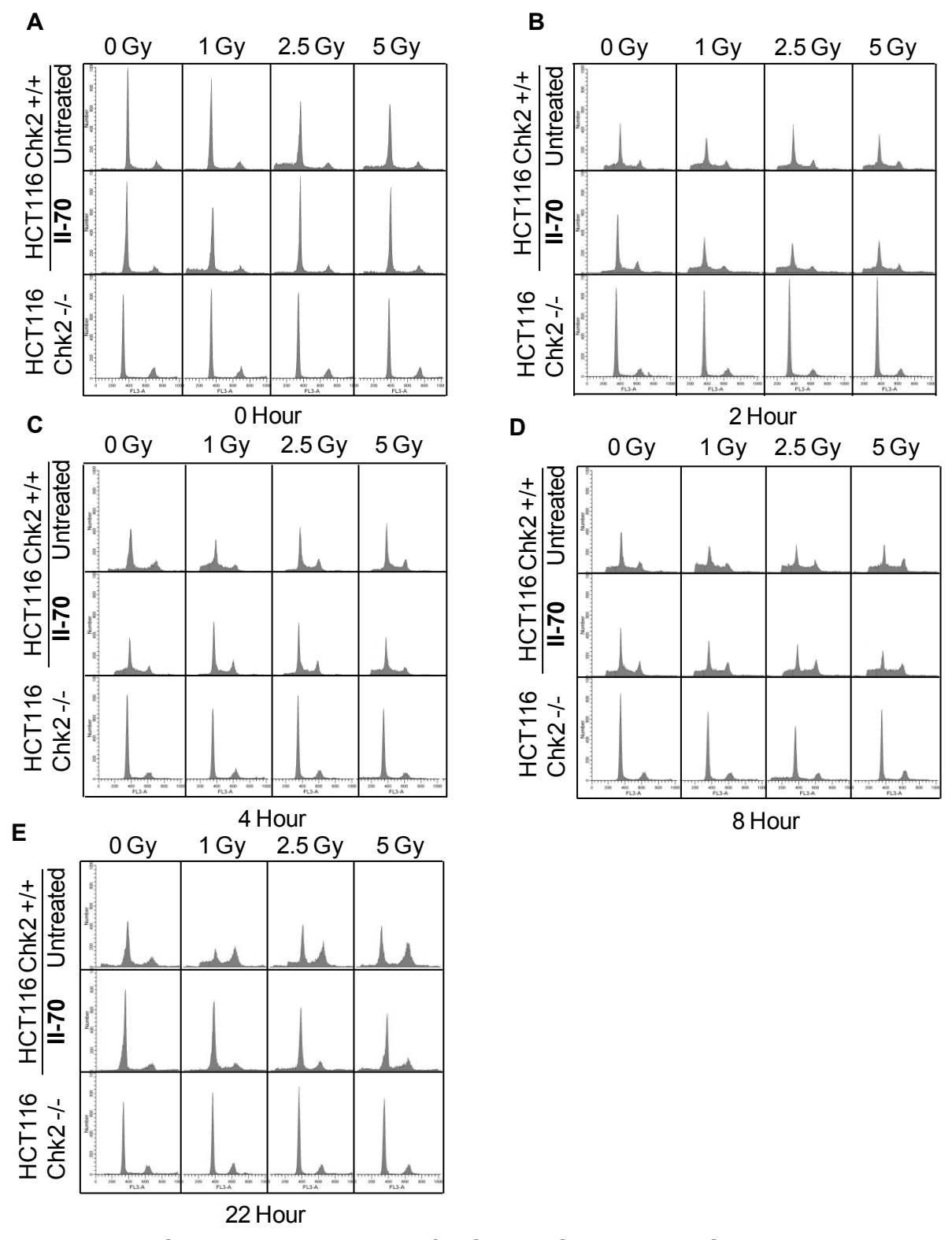


Figure III-10. Cell cycle histograms of HCT116 Chk2 +/+ or Chk2 -/- cells untreated (control) or pretreated for 2 hours with **II-70** (30 μ M) followed by IR (0-5 Gy). Cells were fixed at indicated times after IR. A) 0 hr; B) 2 hr. C) 4 hr; D) 8 hr; E) 22 hr. These histograms are representative of 3 independent experiments.

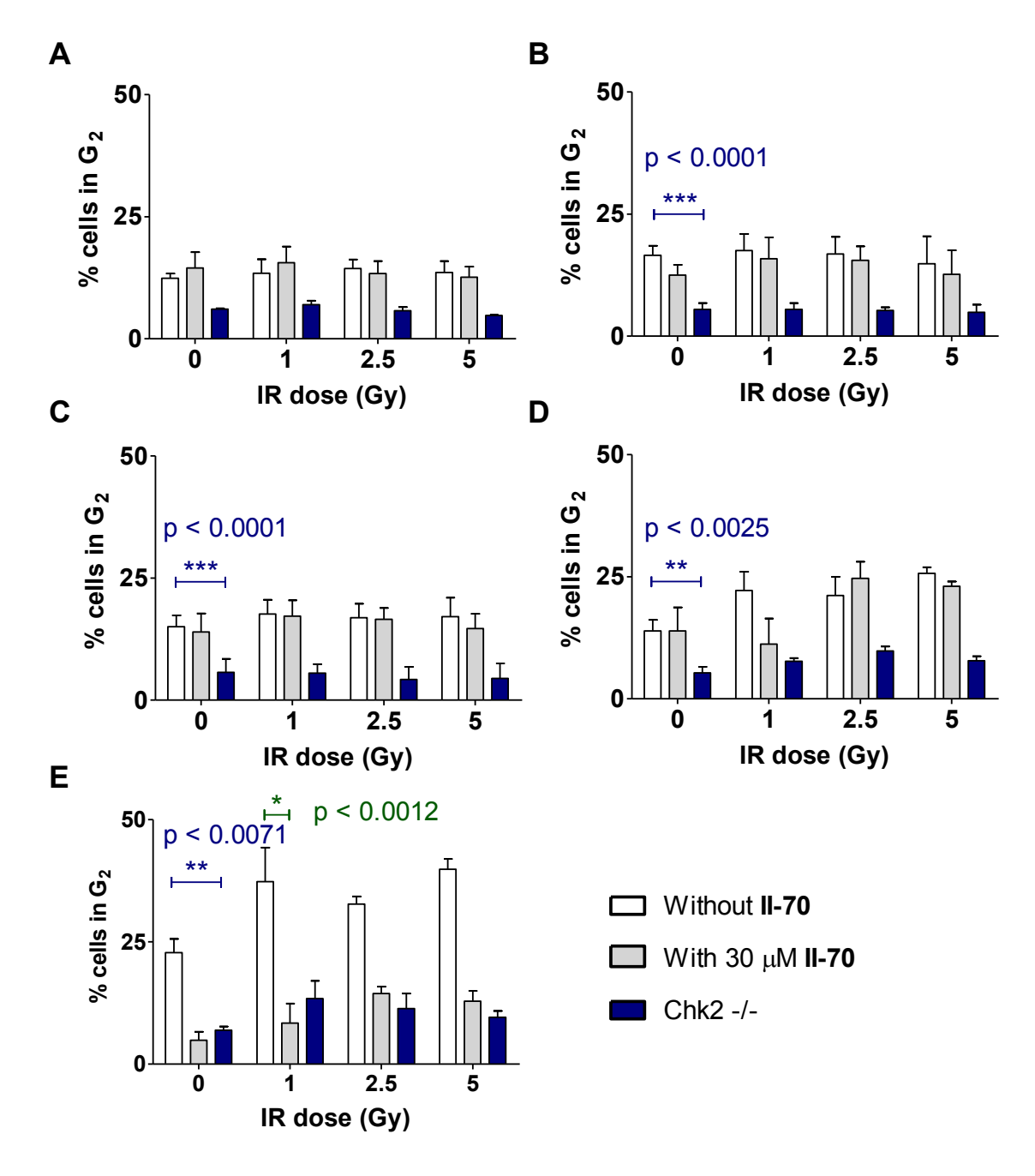


Figure III-11. DNA frequency histograms of HCT116 Chk2 +/+ or Chk2 -/- cells in G_2 . Cells were either untreated (control) or pretreated for 2 hours with **II-70** (30 μ M) followed by IR (0-5 Gy). A) Cells at time 0. B) Cells 2 hours after IR. C) Cells 4 hours after IR. D) Cells 8 hours after IR. E) Cells 22 hours after IR. Data for G_2 were expressed as mean \pm SEM from 3 independent experiments.

After IR-induced DNA damage, the ATM-ATR pathway is activated and can trigger a checkpoint at both G_1 and G_2 (Figure III-12). When Chk2 is activated normally, it phosphorylates p53 which can activate p21, resulting in arrest at both G_1 and G_2 . When Chk2 is inhibited, G_2 checkpoint arrest can only occur if it is going through the Chk1 pathway (Figure III-12). Because Chk1 tends to be activated later, inhibition of Chk2 also inhibits the G_2 arrest and leads to a buildup of cells at G_1 .

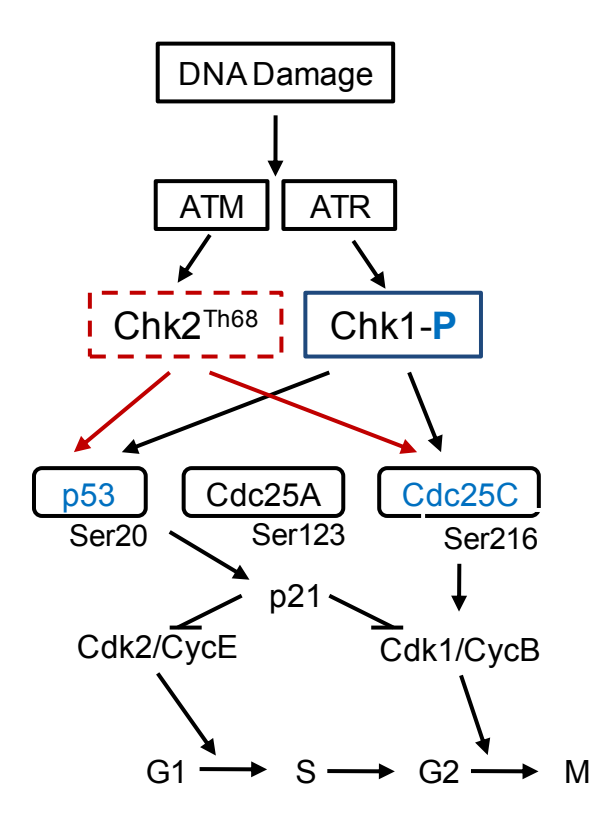


Figure III-12. The abbreviated G1/S and G2/M checkpoint regulation network following upstream ATM/ATR activation.

In response to IR-induced cellular damage, the G_1 arrest has been established in response to a signal transmitted via ATM and p53. The increase in G_1 arrest has been observed in wild-type, but not mutant p53. Transgenic p53 knockout mice have demonstrated that G_1 arrest in response to radiation requires p53. Because Chk2 has

been implicated in the G₁ cell cycle checkpoint and predicted to act as a downstream substrate of ATM, the role of Chk2 was evaluated in this capacity.

Table III-3. Statistically significant differences in cell cycle distribution of untreated Chk2 +/+ versus **II-70** treated cells, and untreated Chk2 +/+ versus Chk2 -/- cells.

G ₂					
Time (hr)	II-70	Chk2 -/-			
0					
2		***P < 0.0001			
4		***P < 0.0001			
8		**P < 0.0025			
22	*P < 0.0071	**P < 0.0012			
G ₁					
Time (hr)	II-70	Chk2 -/-			
0		***P < 0.0005			
2		***P < 0.0001			
4		***P < 0.0001			
8		***P < 0.0001			
22	**P < 0.0053	***P < 0.0001			

In response to treatment with IR, untreated HCT116 Chk2 +/+ cells demonstrated a G_1 arrest comparable to those cells treated with II-70 up to 8 hours following 1 Gy IR (Figure III-13A-C). At 8 hours after IR, the cells treated with II-70 and IR started to demonstrate a slightly higher percentage of cells in G_1 compared to the untreated control. At 22 hours, there is a significant (Table III-4) increase in the amount of cells in G_1 when treated with II-70 and 1 Gy IR. However, inhibition of Chk2 by compound II-70 did not have a statistically significant effect on IR-induced change in the G_1 arrest when compared to the no-IR treated controls (Figure III-13E). The difference in G_1 is less noticeable and statistically insignificant following 2.5 and 5 Gy IR. It is unclear if the

increase in G1 population is due to the combination of IR and inhibition of Chk2 with II-

70. Chk2 +/+ cells that were treated with II-70 alone for 22 hours demonstrated a G₁

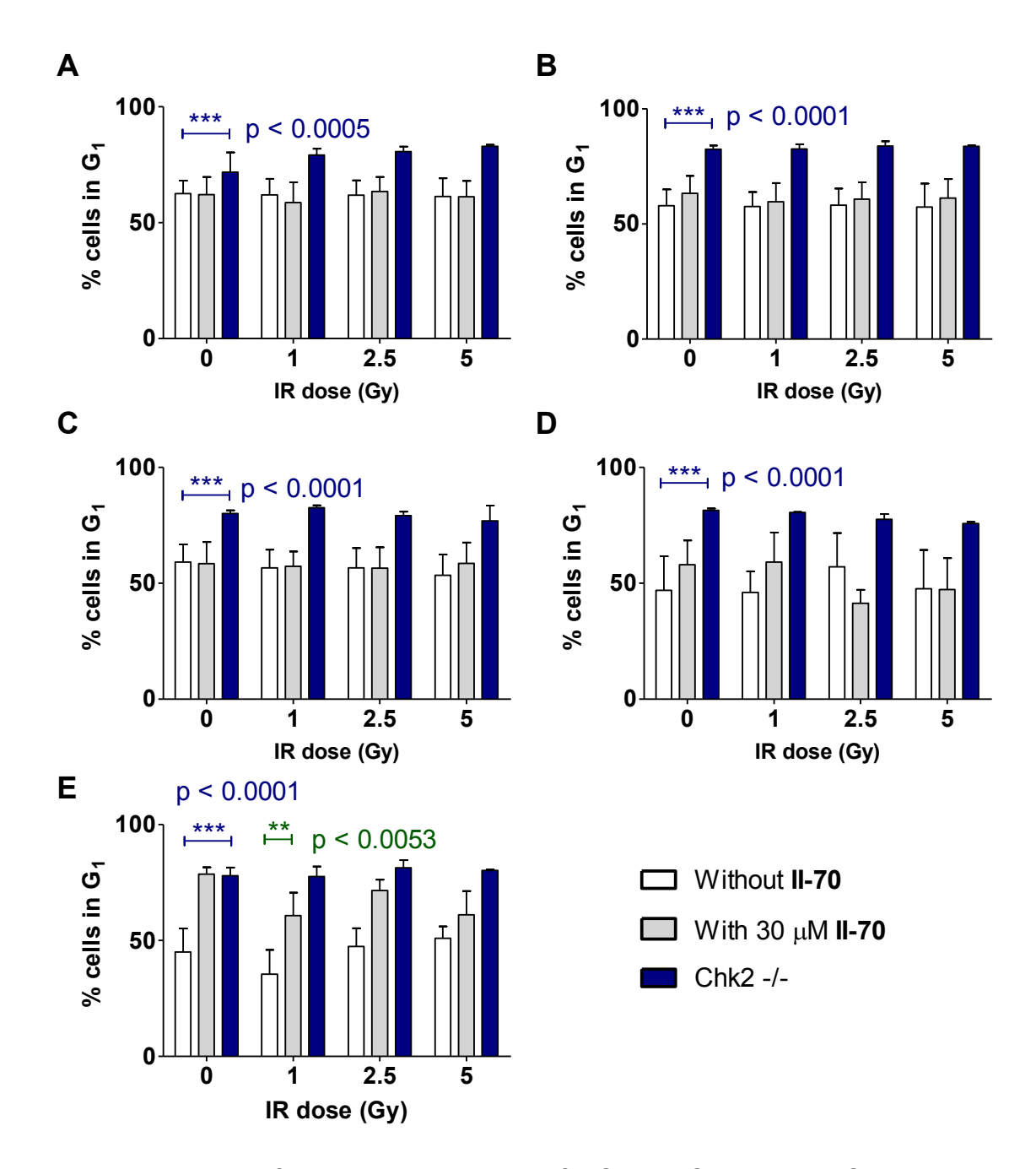


Figure III-13. DNA frequency histograms of HCT116 Chk2 +/+ or Chk2 -/- cells in G_1 . Cells were either untreated (control) or pretreated for 2 hours with **1** (30 μ M) followed by IR (0-5 Gy). A) Cells at time 0. B) Cells 2 hours after IR. C) Cells 4 hours after IR. D) Cells 8 hours after IR. E) Cells 22 hours after IR. Data for G_1 were expressed as mean \pm SEM from 3 independent experiments.

arrest without the induction of DNA damage. The Chk2 -/- cells had an increased percentage of cells present in G₁ compared to the Chk2 +/+ cells at all times following no IR and with IR.

The cell cycle experiments indicate that inhibition of Chk2 allows the abrogation of the G_2 checkpoint, which could result in the prevention of replication of cancer cells. This effect was also confirmed with the Chk2 -/- cells. Additionally, these experiments also indicated that inhibition Chk2 does not have a significant effect in the arrest of G_1 following IR.

III.E Cellular evaluation of indoloazepine

With the knowledge that **II-70** inhibited Chk2 at nanomolar levels *in vitro*, it was necessary to determine if those results translated into cell culture. Before cellular inhibition of Chk2 was examined, the affect of **II-70** on cell proliferation and cytotoxicity was determined in normal and tumor cell lines using a trypan blue exclusion assay of cell viability. Cells were treated with vehicle (final DMSO concentration, < 0.1%) or **II-70** (various concentrations) continuously for up to 60 hours. At each time point, cells were trypsanized and counted with the diazo dye, trypan blue, which passes through the membranes of dead cells. Figure III-7 shows the results of this assay in breast cell lines. It is clear that **II-70** is not toxic to these cell lines in the concentrations that were tested.

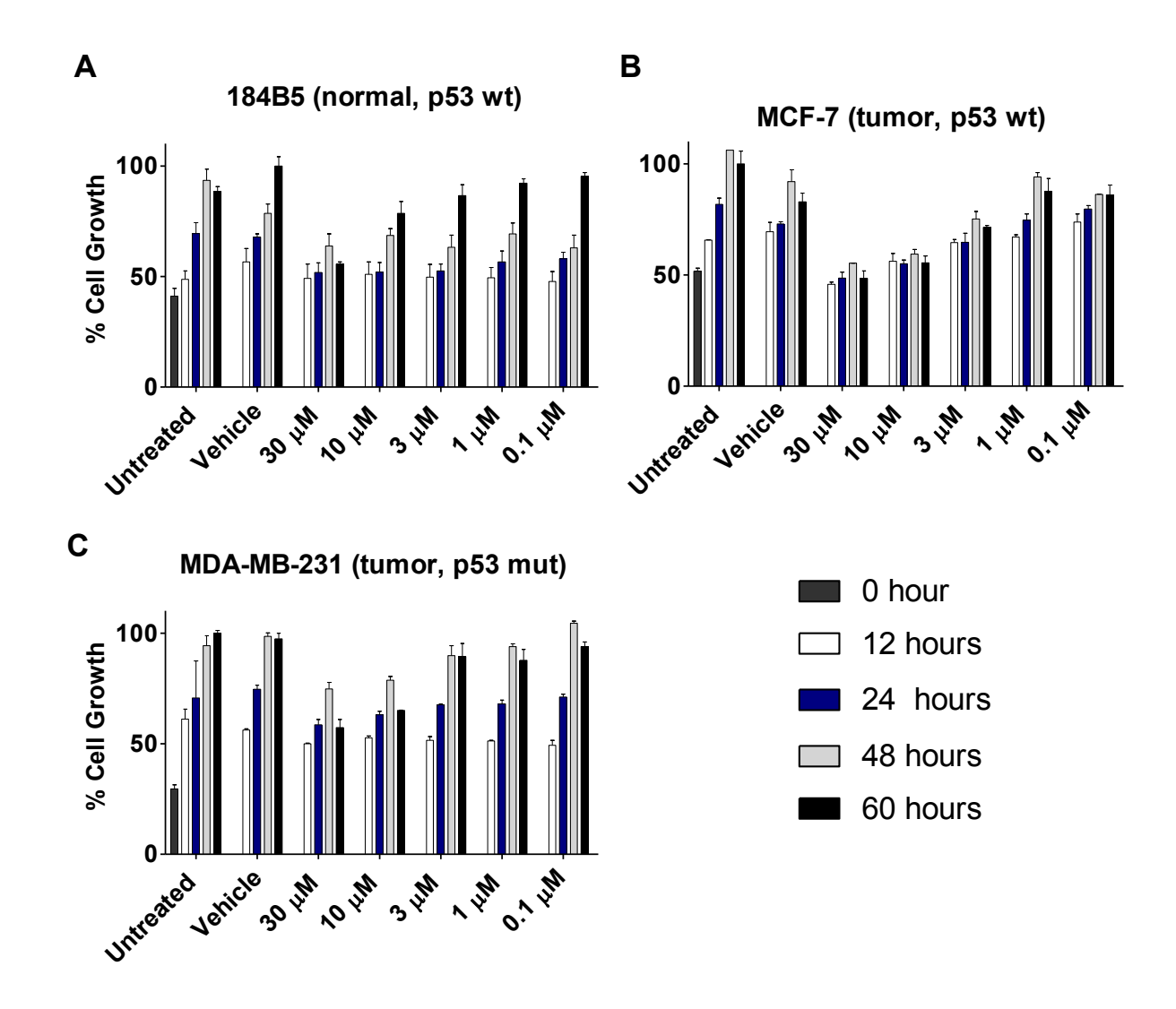


Figure III-14. Results of trypan blue exclusion test in breast cell lines. A) 184B5 cells, normal, breast, p53 wt; B) MCF-7 cells, tumor, breast, p53 wt; C) MDA-MB-231 cells, tumor, breast, p53 mutant.

In the normal breast cell line 184B5 (Figure III-14A), a cytostatic effect (or no growth compared to untreated 12 hour control) was observed at the highest concentration tested (30 μ M), after 12 hours of continuous exposure. The cells grew very slowly following 48 hours exposure, and **II-70** became slightly cytotoxic following 60 hours of exposure. At 10 μ M of **II-70**, a similar cytostatic effect was observed, but to a lesser degree, and did not seem to be cytotoxic after 60 hours. Concentrations less

than 10 μ M did not significantly hinder cell growth in the normal cell line. MCF-7 tumor breast cells (p53 wt) displayed a cytostatic effect following continuous treatment with **II-70** (30 μ M and 10 μ M), and as with the normal cells, growth was not significantly inhibited at concentrations below 10 μ M (Figure III-14B). The MDA-MB-231 cells (tumor, breast, p53 mutant) also experienced cytostatic growth with continuous exposure to **II-70** and slight cytotoxicity after 60 hours (Figure III-14C). From these data, it was concluded that experiments can be performed in breast cell lines with continuous exposure to **II-70** for 48 hours without the cells being affected by cytotoxicity.

There was an interest in performing experiments in the HCT116 colon cell lines due to the availability of Chk2 +/+, Chk2 -/-, p53 +/+, p53 +/- and p53 -/- phenotypes. HCT116 colon cell lines were also evaluated with the trypan blue exclusion assay (Figure III-15). If II-70 inhibits Chk2 in cell culture, these cell lines would theoretically mimic the results seen in the Chk2 -/- cell line. All of these colon cell lines displayed cytotoxicity after 24 hours when exposed to a high concentration (100 µM) of II-70. Growth inhibition was observed at 30 µM concentrations after 12 hours. No significant growth inhibition was observed at concentrations below 10 µM. The physiological effects of II-70 (100 µM, 30 µM) on the cell lines following 24 hours of exposure is illustrated in Figure III-16. An enlargement was observed in the cytosol in the cells treated with **II-70**, as compared to untreated cells. In the HCT116 parent cells (p53 wt, Chk2 p53), a cytostatic effect was observed at 24 and 48 hours and cytotoxic effect after 60 hours of continuous exposure (Figure 15A). A cytostatic effect was also observed with 10 µM treatment in the HCT116-40-16 (p53 wt) for up to 60 hours (Figure III-15B).

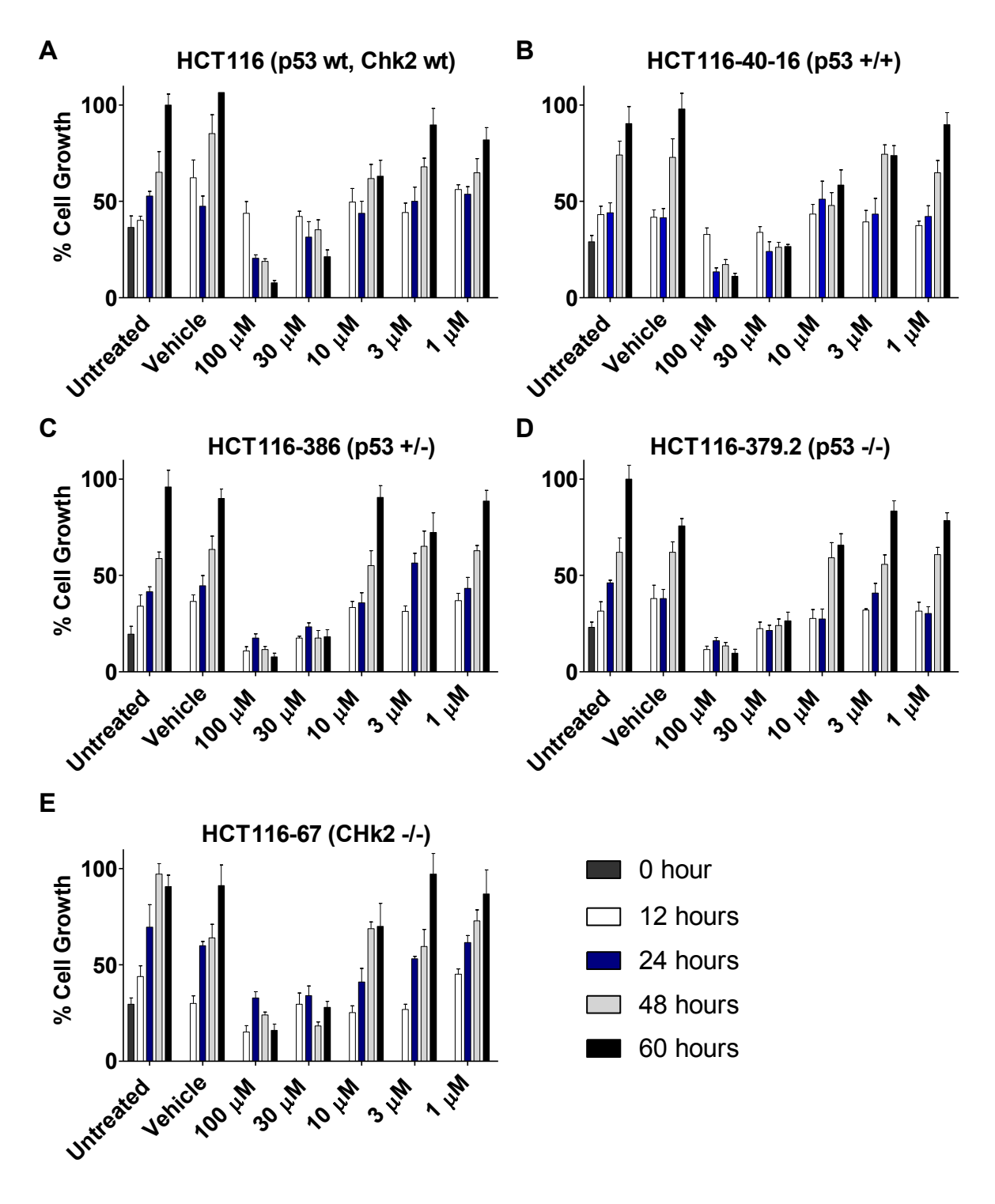


Figure III-15. Results of trypan blue exclusion test in colon cancer cell lines. A) HCT116-parent cells (p53 wt, Chk2 wt); B) HCT116-40-16 cells (p53 +/+); C) HCT116-386 cells (p53 +/-); D) HCT116-379.2 cells (p53 -/-); HCT116-67 cells (Chk2 -/-).

The cell lines in which p53 (Figure III-15C, HCT116-386 (p53 +/-); Figure III-15D, HCT116-379.2 (p53 -/-)) or Chk2 (Figure III-15D, HCT116-67 (Chk2 -/-) were modified and treated with 10 µM of **II-70** did not grow during the first 24 hours, and demonstrated slowed growth following that time. Therefore, additional experiments on the effect of cells with **II-70** will be limited to exposures that are not cytotoxic to cells.

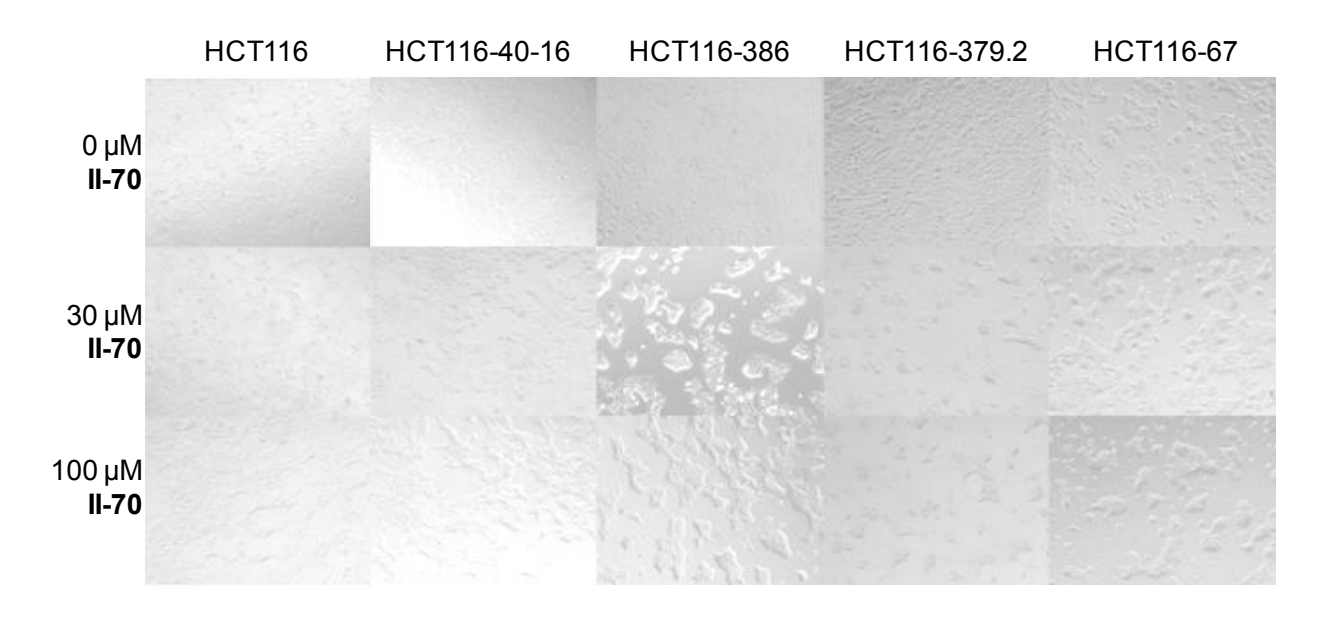


Figure III-16. Microscopic cell images of HCT116 cell lines following treatment with **II-70** for 24 hours of continuous exposure.

Indoloazepine II-70 was sent to the National Cancer Institute and screened in the NCI-60 Developmental Therapeutics Program Human Tumor Cell line screen.²⁸ Cytotoxicity of particular tumor cell lines were evaluated using a sulforhodamide B (SRB) colorimetric assay. SRB is an aminoxanthene dye with two sulfonic groups that can bind to basic amino-acid residues under mild acid conditions, and dissociate under basic conditions.²⁹ Human tumor cells are incubated with drug (II-70, 10 µM) for 48 hours at which point cells are fixed to the plate with trichloroacetic acid and stained with SRB. Cells are washed, removing the excess dye. Protein-bound dyes is dissolved and

Table III-4. Results of NCI-60 cell line screen with II-70.

Panel/Cell Line	Growth Percent	Panel/Cell Line	Growth Percent
Leukemia		Melanoma	
CCRF-CEM	83.50	LOX IMVI	72.71
HL-60 (TB)	82.28	MALME-3M	88.29
K-562	92.42	M14	72.12
MOLT-4	85.50	MDA-MB-435	87.62
RPMI-8226	93.48	SK-MEL-2	52.87
SR	51.05	SK-MEL-28	121.55
Non-Small Lung Ca	ancer	SK-MEL-5	98.22
A549/ATCC	98.73	UACC-257	118.75
EKVX	15.24	UACC-62	91.46
HOP-62	118.10	Ovarian Cancer	
HOP-92	119.60	IGROV1	80.66
NCI-H226	89.39	OVCAR-3	118.4
NCI-H23	103.46	OVCAR-4	89.16
NCI-H322M	87.93	OVCAR-5	107.96
NCI-H460	97.28	OVCAR-8	93.84
NCI-H522	44.82	NCI/ADR-RES	118.14
Colon Cancer		SK-OV-3	51.55
COLO-205	89.02	Renal Cancer	
HCC-2998	92.05	786-0	69.6
HCT-116	54.43	ACHN	70.27
HCT-15	85.80	CAKI-1	57.46
HT29	65.75	RXF 393	83.5
KM12	91.48	SN12C	104.43
SW-620	106.59	TK-10	59.85
CNS Cancer		UO-31	93.35
SF-268	102.62	Prostate Cancer	
SF-295	106.10	PC-3	100.4
SF-539	81.69	DU-145	101.88
SNB-19	116.40	Breast Cancer	
SNB-75	79.23	MCF7	104.39
U251	102.46	MDA-MB-231/ATCC	115.29
		HS 578T	77.73
		BT-549	88.73
		T-47D	114.9
		MDA-MB-468	78.2

Optical density is determined with a microplate reader.²⁹ The amount of dye in the cells is directly proportional to the cell mass.²⁹ The results of the NCI-60 cell line screen are listed in Table III-3. Compound **II-70** did not demonstrate any significant inhibition of growth in the majority of the cell lines screened. The handful of cell lines which were inhibited by **II-70** did exhibit growth inhibition. The growth percentage was reported as 44.52% in a non-small lung cancer cell line, NCI-H522, the cell line most affected by **II-70**.

III.F Indoloazepine as a radioprotecting agent

Chk2 inhibition has been indicated to elicit radio- or chemoprotection of normal tissue via inhibition of p53-dependent apoptosis. ^{11, 12} Therefore, we wanted to perform a clonogenic survival assay to determine if pretreatment of normal breast cells (184B5 cells, p53 wt) with Chk2 inhibitor **II-70** (30 µM) was capable of protecting only the normal cells from the cytotoxic effects of various doses of IR (0-7.5Gy). Conversely, we hypothesized that the inhibition of Chk2 would have an insignificant effect on cell survival in p53 mutant cancer cells (MDA-MB-231 cells), compared to the vehicle control.

In order to evaluate this hypothesis, 184B5 and MDA-MB-231 cells were pretreated with nothing, vehicle (DSMO), or **1** (30 μ M) for 30 minutes. The cells were irradiated in suspension (0-7.5 Gy) and seeded at cloning density. Cells were allowed to incubate for 7 days at which point fresh media was given to the clones. After 10-14 days, clones were fixed and stained with crystal violet. Surviving clones were scored (ie, colonies containing > 50 cells) and viability of the cells was determined (Figure III-17).

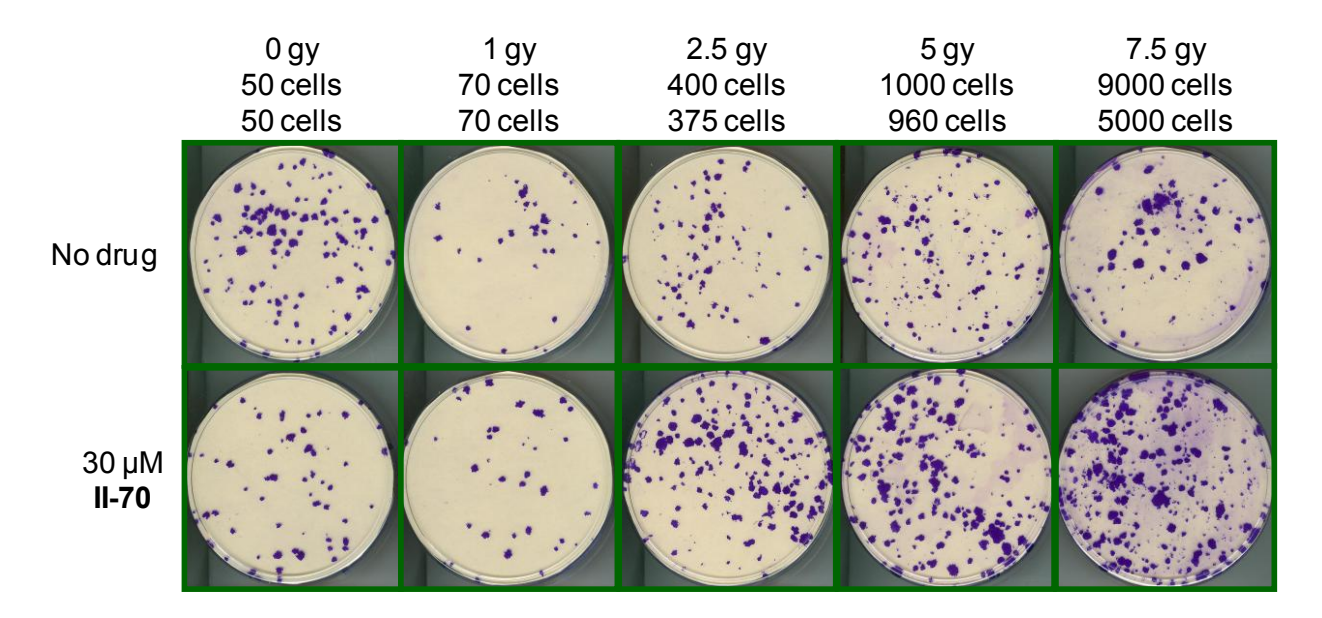


Figure III-17. Clones of184B5 (normal) cells untreated (top panel) or pretreated with **II-70** for 30 minutes (bottom panel) followed by IR (0-7.5 Gy) and seeded at the indicated cloning density.

The results of the clonogenic assay revealed that the control treatment (IR and vehicle only) resulted in a decrease in the number of viable cells with increasing doses of IR (Figure 18a) as anticipated. However, treatment with Chk2 inhibitor II-70 protected cells from IR-induced cell death in the normal cell line (p53 wt), as compared to the vehicle control treatments with nearly 75% survival at doses up to 5 Gy IR, or compared to the untreated control. The radio-protective effect was also evaluated at concentrations below 30 μ M (Figure III-18B). Decreased cell death was observed 10 and 3 μ M II-70, with less radioprotection at the lower dose. A radioprotective effect was not demonstrated with 1 μ M at IR doses of 1-5 Gy. However, a very slight effect was observed at 7.5 Gy.

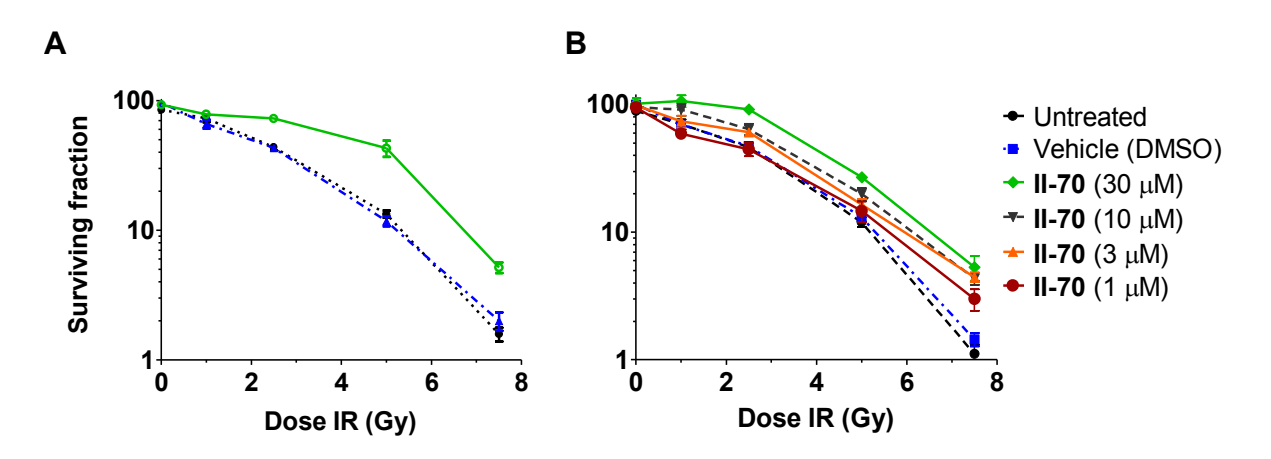


Figure III-18. Cloning survival of 184B5 (normal) cells untreated or pretreated with **II-70** for 30 minutes followed by IR (0-7.5 Gy). A) Cells treated with 30 μ M **II-70** followed by IR (0-7.5 Gy); B) Cells treated with 10, 3, or 1 μ M **II-70** followed by IR (0-7.5 Gy).

A closer look at the colonies illustrates the physiological differences in the normal cells treated with II-70 and those that remained untreated prior to IR (Figure III-19). The morphology of the normal cells that were treated with II-70 had an enlarged cytoplasm, making the cell appear larger than those that were exposed to IR alone. This was also observed above in the HCT116 cells that were not exposed to IR (Figure III-19). However, those cells were continuously treated with II-70 for a period of 24 hours. The normal cells (184B5) were treated for only 30 minutes before IR, and still demonstrated a slight, but noticeable change in morphology. The exact reason why II-70 causes this expansion in cell cytoplasm is unclear.

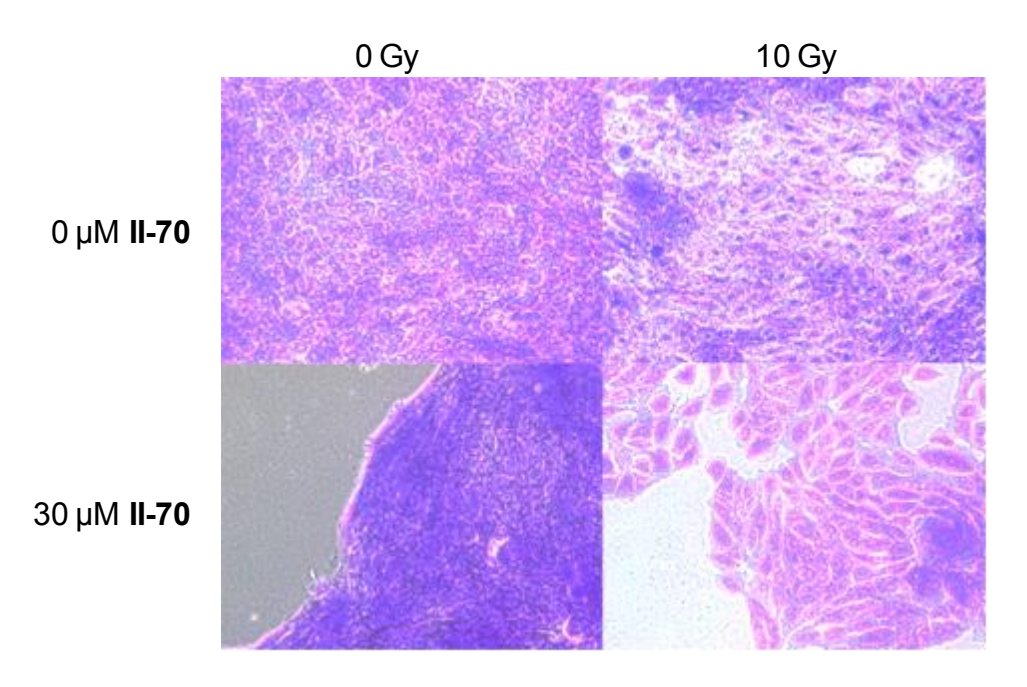


Figure III-19. Microscopic images (20X) of normal cell colonies (184B5) treated with **II-70** followed by 0 or 10 Gy IR.

With just a 30 minute pretreatment of **II-70**, a decrease in cell death was observed. There was a question of whether modifying the order of treatment and modifying the length of time would change the radioprotective effect. Figure III-20A shows the cloning survival of normal breast cells treated with **II-70** (30 µM) 30 minutes after IR. Although there was radioprotective effect observed with this treatment, the percentage of survival was less with a 30 minute post-treatment (69.2% at 2.5 Gy, 24.5% at 5 Gy) than with a 30 minute pretreatment (72.8% at 2.5 Gy, 43.0% at 5 Gy) as seen in Figure III-20A. **II-70** is slightly less effective when treated after IR.

Normal cells were then pretreated with vehicle or **II-70** (30 µM) for 2 hours followed by IR and post-treated for 4 hours (Figure III-20B). These cells were exposed to the Chk2 inhibitor **II-70** for a total of 6 hours. It was anticipated that increased exposure time to **II-70** would strengthen the radioprotection. However, the decrease in cell death (67.9% at 2.5 Gy, 43.1% at 5 Gy) was very similar to that of cells pretreated

for only 30 minute indicating that increased exposure time before and after IR did not further radioprotect normal cells as compared to the 30 minute pretreatment.

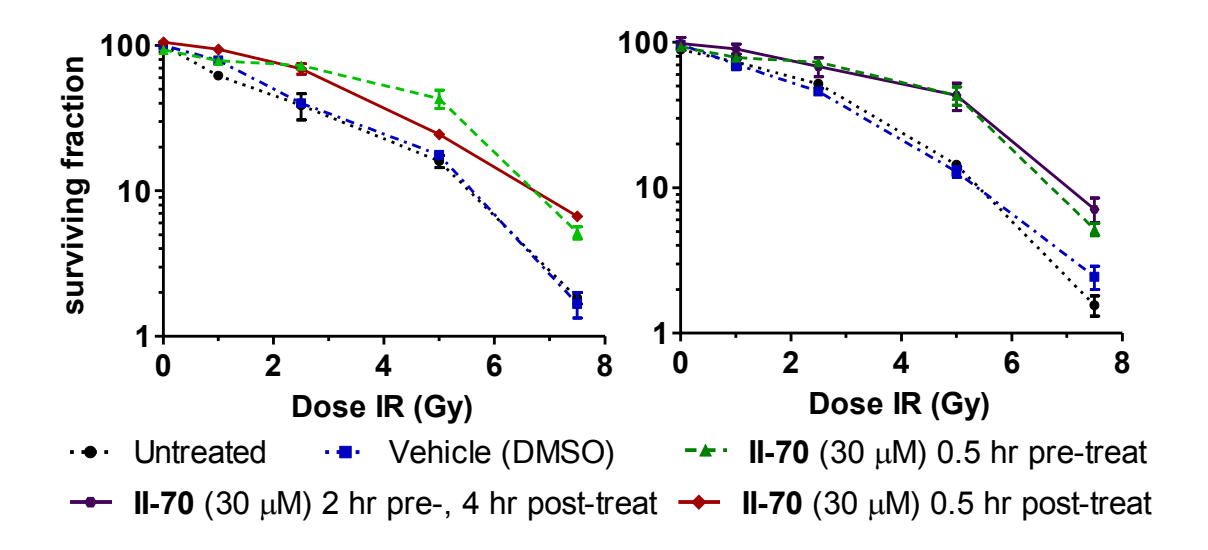


Figure III-20. Cloning survival of 184B5 normal cells with various treatment times. A) Cells post-treated 30 minutes following IR (0-7.5 Gy); B) Cells pretreated for 2 hours and post-treated for 4 hours after IR (0-7.5 Gy).

As a negative control, analog **II-99** was evaluated to make sure that a compound lacking *in vitro* Chk2 inhibition activity could not enhance survival following radiation. The negative control, inactive Chk2 inhibitor analog **II-99** did not exhibit any radioprotective effects in the IR challenged 184B5 cells (Figure III-21A). This data strongly indicates that the enhanced survival seen in this cell line is due to the abrogation of Chk2 activity by Chk2 inhibitor **II-70**.

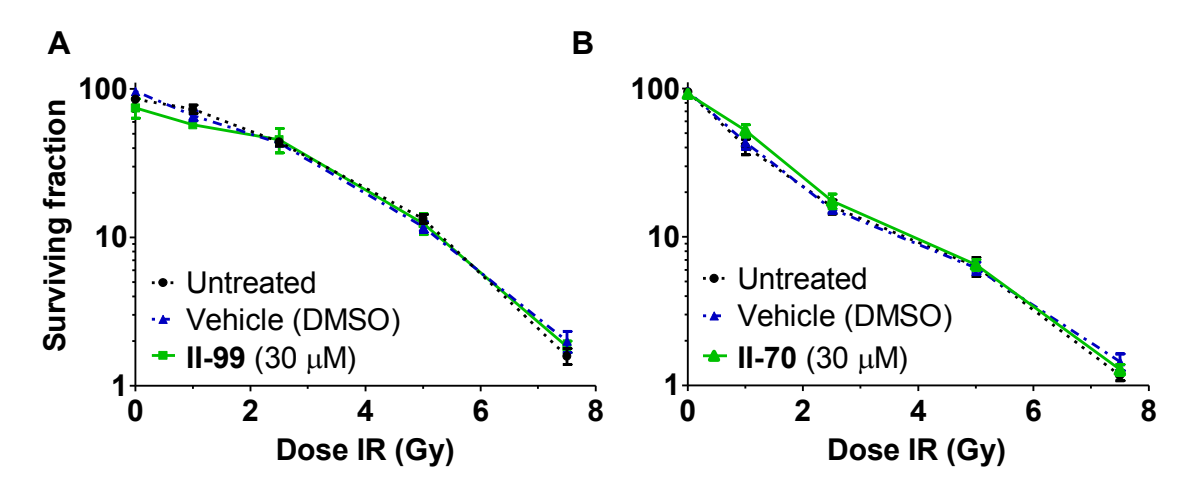


Figure III-21. Cloning survival of 184B5 and MDA-MB-231 cells. A) 184B5 cells pretreated with **II-99** (30 μ M) for 30 minutes, followed by various doses of IR (0-7.5 Gy); B) MDA-MB-231 cells pretreated with **II-70** (30 μ M) for 30 minutes, followed by various doses of IR (0-7.5 Gy).

Importantly, pretreatment of the p53 mutant MDA-MB-231 cells for 30 minutes with nothing, vehicle (DMSO) or II-70 (30 μM) followed by the same doses of IR (0-7.5 Gy) did not show a decrease in cell death in the presence of Chk2 inhibitor II-70 (Figure III-22). Figure III-21B clearly indicates that there was no detectable induction of cell survival as the untreated, vehicle and treated cells showed statistically identical survival curves. These results in the two cell lines implicate the p53 pathway in the survival mechanism of Chk2 inhibitor II-70, in cells treated with IR.

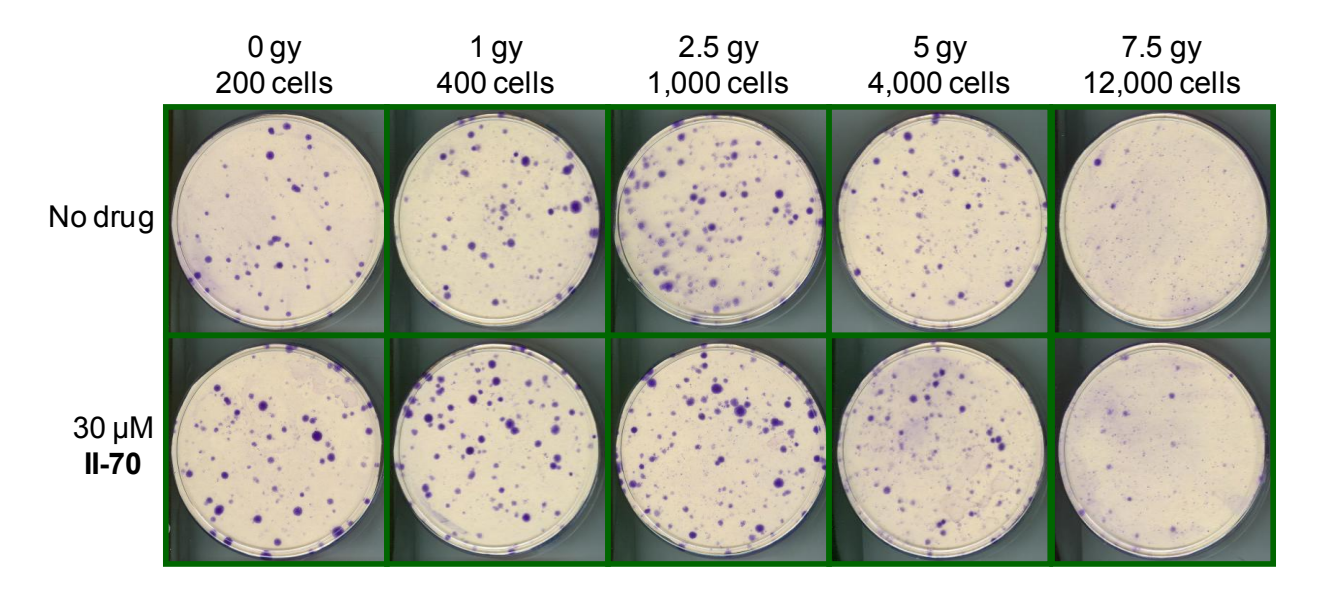


Figure III-22. Clones of MDA-MB-231 (tumor, p53 mutant) cells untreated (top panel) or pretreated with **II-70** for 30 minutes (bottom panel) followed by IR (0-7.5 Gy) and seeded at the indicated cloning density.

The morphological differences in the tumor cell line, MDA-MB-231 are more obvious in the cells receiving both 30 minute pretreatment of **II-70** and IR (Figure III-23). These cells are grossly enlarged as is illustrated in the lower right panel. There are approximately 5-6 cells in this window and each cell's nucleus and cytoplasm are larger than cells that did not receive the pretreatment of **II-70**. The cell morphology was affected here, however, survival remained unaffected.

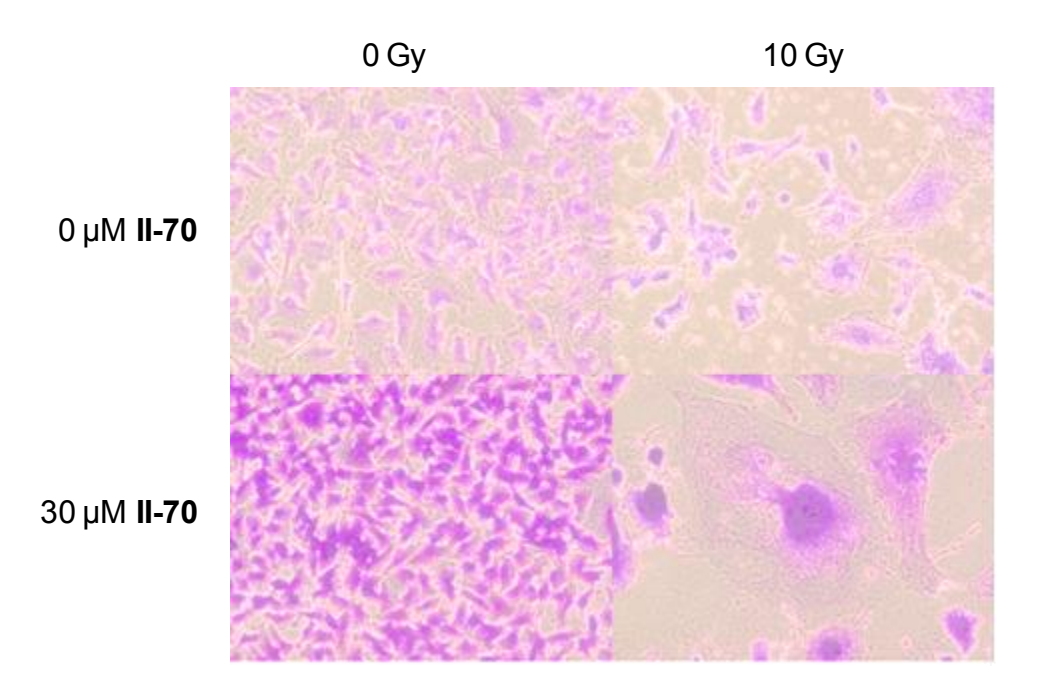


Figure III-23. Microscopic images (20X) of tumor cell colonies (MDA-MB-231) treated with **II-70** followed by 0 or 10 Gy IR.

The HCT116 tumor colon cell lines were also evaluated using the clonogenic survival assay (Figure III-24). The HCT116 parent cell line demonstrated a very slight decrease in cell death when pretreated with **II-70** for 30 minutes (Figure III-24A). The radioprotection in the tumor cell line was less than the protection observed in normal cells (Figure III-18A). The p53 wild type (Figure III-24B), p53 +/- (Figure III-24C), and p53 -/- (Figure 24D) had no detectable radioprotection when treated with the Chk2 inhibitor **II-70**. Interestingly, the two untreated p53 mutant cell lines (Figure III-24C,D) had survival curves that were slightly higher than those seen for the p53 wild type cell lines (Figure III-24,B). These results may further support the p53 pathway in the survival mechanism in cells treated with IR.

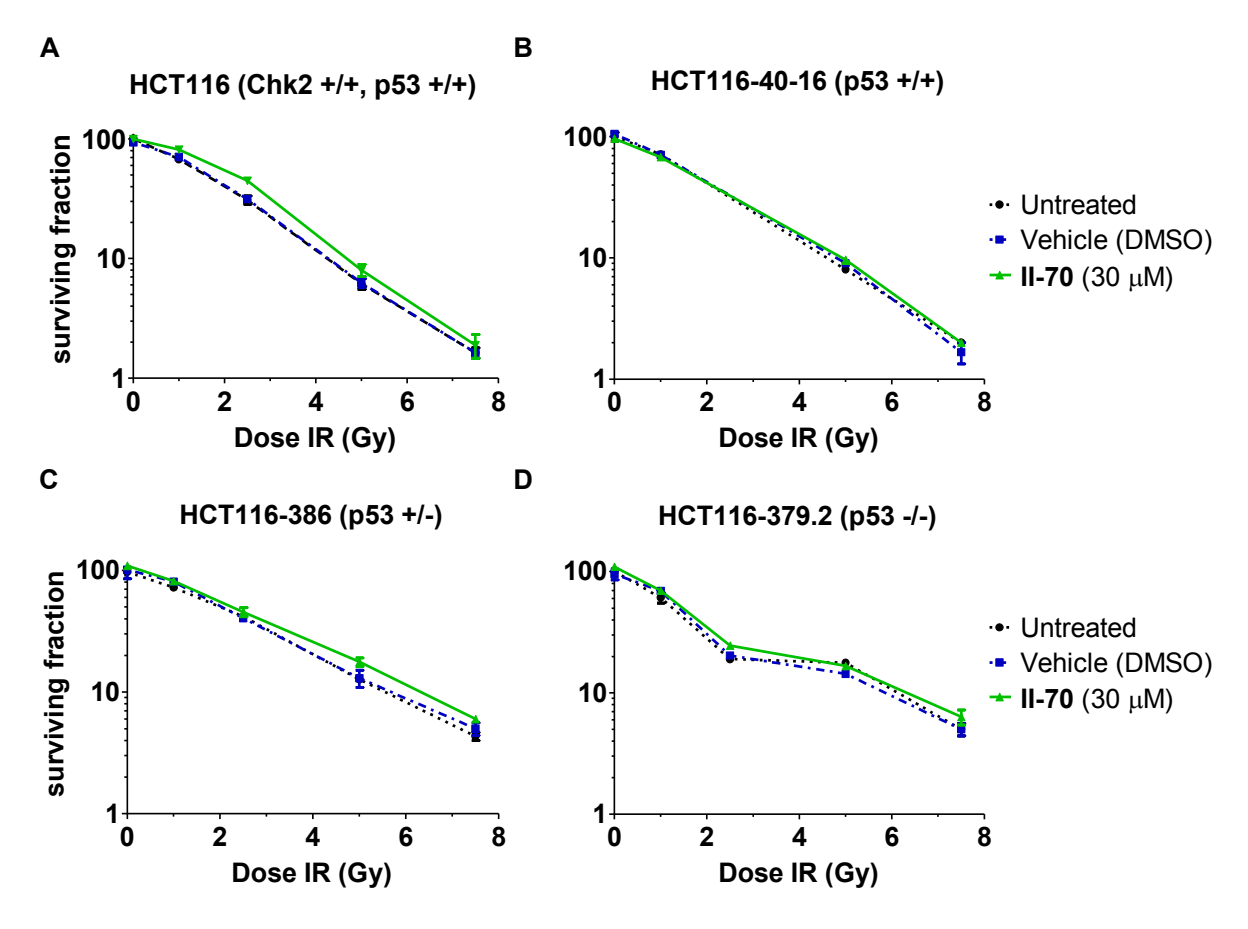


Figure III-24. Cloning survival of HCT116 cell lines. A) HCT116 (Chk2 +/+, p53 +/+) pretreated for 30 minutes with **II-70** (30 μM) followed by various doses of IR (0-7.5 Gy); B) HCT116-40-16 (p53 +/+) pretreated for 30 minutes with **II-70** (30 μM) followed by various doses of IR (0-7.5 Gy); C) HCT116-386 (p53 +/-) pretreated for 30 minutes with **II-70** (30 μM) followed by various doses of IR (0-7.5 Gy); D) HCT116-379.2 (p53 -/-) pretreated for 30 minutes with **II-70** (30 μM) followed by various doses of IR (0-7.5 Gy).

To further understand the role of Chk2 inhibition in cell survival, the cloning survival assay was performed in the Chk2 -/- cell line and compared to the HCT116 parent cell line (Figure III-25). There was a slight increase in survival in HCT116 cells treated with II-70 (44.7% at 2.5 Gy, 8.0% at 5 Gy) as compared to the untreated HCT116 cells (30.9% at 2.5 Gy, 6.1% at 5 Gy). It was anticipated that the Chk2 -/- cell line would show a greater protective effect or one similar to that observed in the normal cell line treated with II-70 (Figure III-18A). However, the Chk2 -/- demonstrated a very

little radioprotection when compared to Chk2 +/+ cells treated with II-70 (Figure III-24A). It is not clear why removing Chk2 completely from the cell line did not protect the cells from IR. The tumor status of the colon cells versus the normal cell status of the breast cells may contribute to these results. Additionally, another explanation could be due to the redundant functions of the checkpoint present in normal cells that could mask any checkpoint defects. Increases in cell apoptosis immediately following IR have been observed between the Chk2 +/+ cell line versus the Chk2 -/-. 30, 31 Cloning survival has been increased in Chk2 siRNA studies as compared to Chk2 wild type cell lines following IR-induced DNA damage, 30 however these differences have not yet been demonstrated in the HCT116 Chk2 -/- cell line. Additionally, this protective effect in cloning survival has also been observed in Chk2 -/- mouse embryonic fibroblasts (MEFs). 31 However, the cloning assay performed here with the Chk2 +/+ and Chk2 -/- cell lines have not indicated differences in long term survival as observed in the MEFs. 31

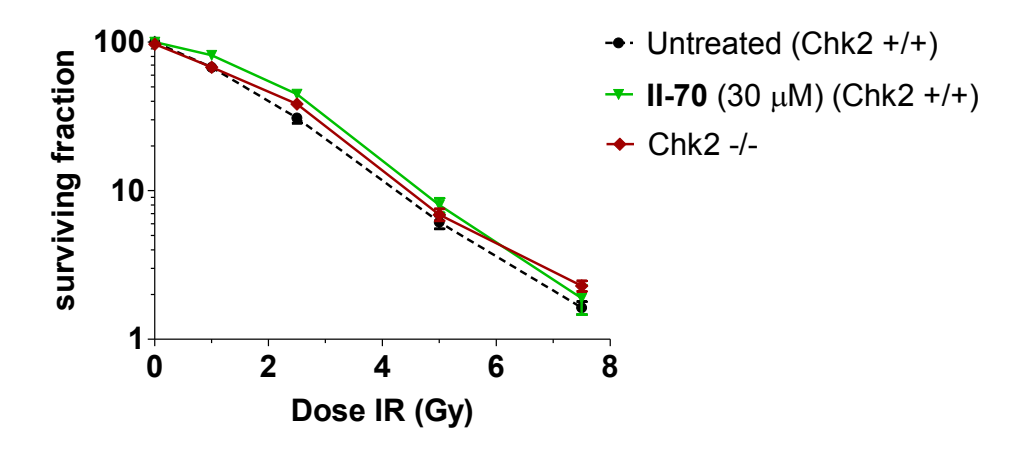


Figure III-25. Comparison of cloning survival of HCT116 treated with **II-70** versus HCT116 Chk2 -/- cells following IR.

The clonogenic survival assays in the normal and tumor cell lines demonstrated that inhibition of Chk2 in p53 mutant cells did not have any cellular effect on cell survival, whereas Chk2 inhibition by **II-70** increased cell survival following IR-induced DNA damage in the normal breast p53 wt cell line. The graphs in Figure III-18A clearly indicate the difference in IR protection by **II-70** in the normal p53 wt cells over the p53 mutant cells (Figure III-21b).

III.G In vivo evaluation of indoloazepine

With cloning survival demonstrating the radioprotective effect of **II-70**, and western blot data supporting cellular inhibition of Chk2, we wanted to evaluate the protective effect of **II-70** in a mouse model. We were interested in mimicking the results of the Chk2 -/- mice exposed to whole body IR. The hypothesis was that treatment of Balb C mice with Chk2 inhibitor **II-70** 30 minutes prior to whole body IR would allow mice to survive longer than those mice not receiving the inhibitor. Mouse handling and studies were performed by Dr. Sandra O'Reilly of Osteopathic Medicine and Research with my assistance.

In order to evaluate the mice exposed to IR and II-70, it was important to monitor the mice for acute radiation syndrome (ARS). There are three syndromes associated with ARS: the central nervous system (neurovascular) syndrome (CNS), the gastrointestinal syndrome (GI) and the hematopoietic syndrome (BM). These syndromes can occur after whole body or partial body IR. The effects may appear within minutes of IR exposure, or may present symptoms years after exposure, depending on the type, dose and dose-rate of the irradiation. Cells that are proliferating are sensitive to the effects of whole body IR. These effects are mainly associated with changes in the

germinal epithelium, gastrointestinal epithelium and the bone marrow progenitor cells. The gastrointestinal epithelium and the bone marrow progenitor cells are pivotal for the maintenance of life. 33 Damage to either of these cell types can have an adverse effect on survival due to the drastic disruption of normal physiological mechanisms. 33 Although the bone marrow progenitor cells are more sensitive to the damaging effects of whole body IR compared to the gastrointestinal epithelium, the effects on the GI system are expressed more rapidly compared to the effects on the hematopoietic system due to the rapid transit time of the cells in the GI tract. 33 In mice receiving whole body IR the lethal (death) effects are seen within 10 days post-irradiation for the gastrointestinal system whereas changes in the hematopoietic system are seen between days 11 to 30 post-irradiation. 33

Before subjecting mice to whole body IR, it was necessary to first determine if **II-70** was observed in the blood stream. Mice were initially given **II-70** dissolved in 30% propylene glycol/water by oral gavage. Blood from the mice was collected at various time points. The serum from the mice was then analyzed by Liquid Chromatography Mass Spectrometry (LC/MS). It was concluded that **II-70** was not orally available in mice.

Mice were then given an intraperitoneal (IP) injection of varying doses (100, 10, 1 mg/kg) of II-70 dissolved in a 33% propylene glycol/water solution. Males and females were treated with II-70 (100 mg/kg, Figure III-26A,B) or vehicle (data not shown, II-70 was not observed in vehicle mice) to determine if there was a difference in absorption between the two sexes. Figure III-26A illustrates that there is not a statistical significance in the amount of II-70 that is absorbed in the blood. There was

approximately 8 mg/kg, or ~800 μ M of **II-70** remaining in the blood 30 minutes after the injection, and was still detected 12 hours after injection (Figure III-26A,B). Because the differences in absorption in the blood were not significant, there was no preference to which group (male or female) would undergo IR treatment. Mice that were injected IP with 10 mg/kg had ~ 80 μ M of **II-70**, (Figure III-26C) present 30 minutes after injection. Mice injected with 1 mg/kg had ~8 μ M of **II-70** remaining in the blood after 30 minutes (Figure III-26D). Indoloazepine **II-70** was not present at detectable levels past 4 and 2 hours when injected with 10 mg/kg and 1 mg/kg doses, respectively. However, the concentrations of Chk2 inhibitor **II-70** present 30 minutes after the injection time well above the Chk2 *in vitro* IC₅₀ (10 nM).

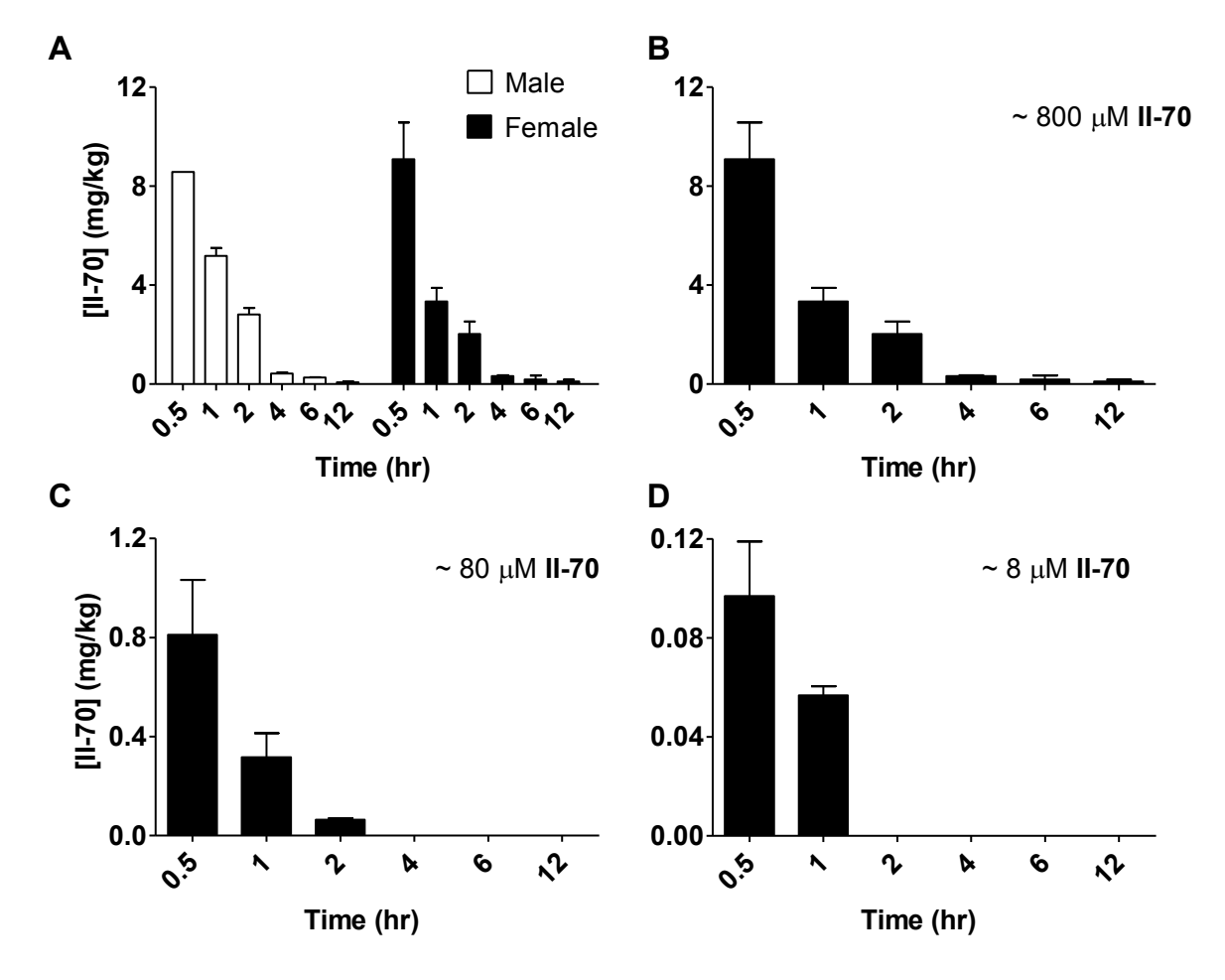


Figure III-26. LC/MS quantification of biologically available **II-70** in mice. n = 2 for each time point. A) Male and female mice injected IP with 100 mg/kg **II-70**; B) Females injected IP with 100 mg/kg **II-70**; C) Female mice injected with 10 mg/kg **II-70**; D) Female mice injected with 1 mg/kg **II-70**.

Following the bioavailability experiment, a toxicity study with the mice was performed next to evaluate the long term affects of mice treated with II-70 (Figure III-27). Mice were treated with various concentrations of II-70 and were monitored over 30 days. At the highest concentration (100 mg/kg), two mice died within the first two days of the study, this may have been in part due to an injection to a vital organ. Nevertheless, the majority of the mice survived out to 30 days, in addition to the mice treated with 50, 10 and 1 mg/kg. There were no cytotoxic effects observed the mice

treated with **II-70** as compared to those treated with vehicle only (30% propylene glycol/water).

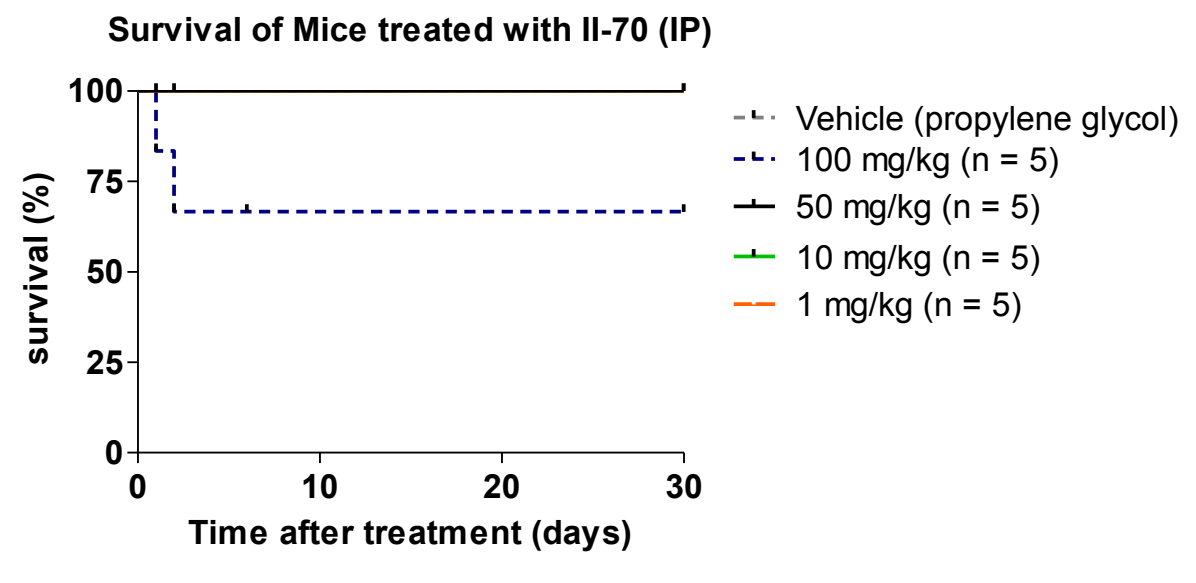


Figure III-27. Cytotoxicity of mice treated with varying doses of II-70 by IP.

The bioavailability data and cytotoxicity studies encouraged us to move forward with mouse whole body irradiations in order to investigate the protective effect of II-70. The radioprotective effect of II-70 was determined not by using death as an end point, but instead evaluation of how well II-70 alleviated symptoms associated with the GI and BM syndromes. The animals were monitored for physical changes that would indicate changes in the GI and BM syndromes including: ruffled fur coat, loss of body weight, labored breathing, lethargy, lack of curiosity, dehydration, evidence of diarrhea, hunched posture, closed eyes, or discharge around eyes, change in color of tails, and ears or any obvious hematomas. Mice showing several or all severe symptoms were sacrificed and removed from the study. The spleens and intestines of mice dosed with II-70 and those receiving IR only were compared following necropsies of the mice.

Initially, mice aged 6-8 weeks, were pretreated with **II-70**, then given averting (2,2,2-tribromoethanol) an anesthetic drug, before being transferred in an irradiation chamber, to the veterinary oncology clinic at MSU. Irradiations were performed by Dr. Elizabeth McNeil, of the College of Veterinary Medicine. The mice were then irradiated using a 6 MV linear accelerator between a 1.5 cm sheet of bolus material. Mice were returned to a pathogen free room before they awoke from the anesthetic. In some experiments, the avertin did not successfully anesthetize the mice. In others, the mice were already deceased upon returning from IR, or died shortly after IR. It was later discovered that avertin can degrade in the presence of heat, light or changes in pH, leading to degradation products that can be nephrotoxic and hepatotoxic.³⁴ In order to avoid these unnecessary and sometimes lethal side effects, a new chamber was designed that was made with polystyrene which could be autoclaved. This new chamber did not require the use of anesthesia (Figure III-28). The lid of the chamber was capable of rotating and also contained a sliding wedge in which the mice could be put in and taken out of each of the sections of the chamber.



Figure III-28. Mouse irradiation chamber used for whole body IR.

Although Motoyama et al used a sub lethal irradiation dose of 8 Gy,³² this dose was too toxic to see any improvement in survival of the mice when we performed the experiment with the same dosage. The mice suffered from the effects of damage to the BM and GI systems before any radioprotection could be observed (~10 days). The intestines of mice treated with II-70 were yellow in appearance instead of the normal pale green/whitish color. Some of the pretreated mice intestines were observed to be empty, indicating a depletion of the epithelial layer and damage to tissue that was not replenished by the stem cells.

A slightly lower dose of 7.3 Gy allowed the IR-only mice to survive for more than 15 days, past the initial stages of GI syndrome effects (Figure III-29). Mice that were pretreated for 30 minutes with 10 mg/kg II-70 were observed to starting at 8 days, likely from the beginning stages of GI syndrome. At day 13, ~50% of the II-70-IR mice and about 80% of the vehicle-IR mice were still alive, indicating that II-70 was having a negative effect on the survival of the mice, contrary to the radioprotective effect seen in

the cloning assay with normal cells. Statistical analysis was performed on the vehicle mice as compared to the **II-70** mice and there was no significant difference in the two curves (Table

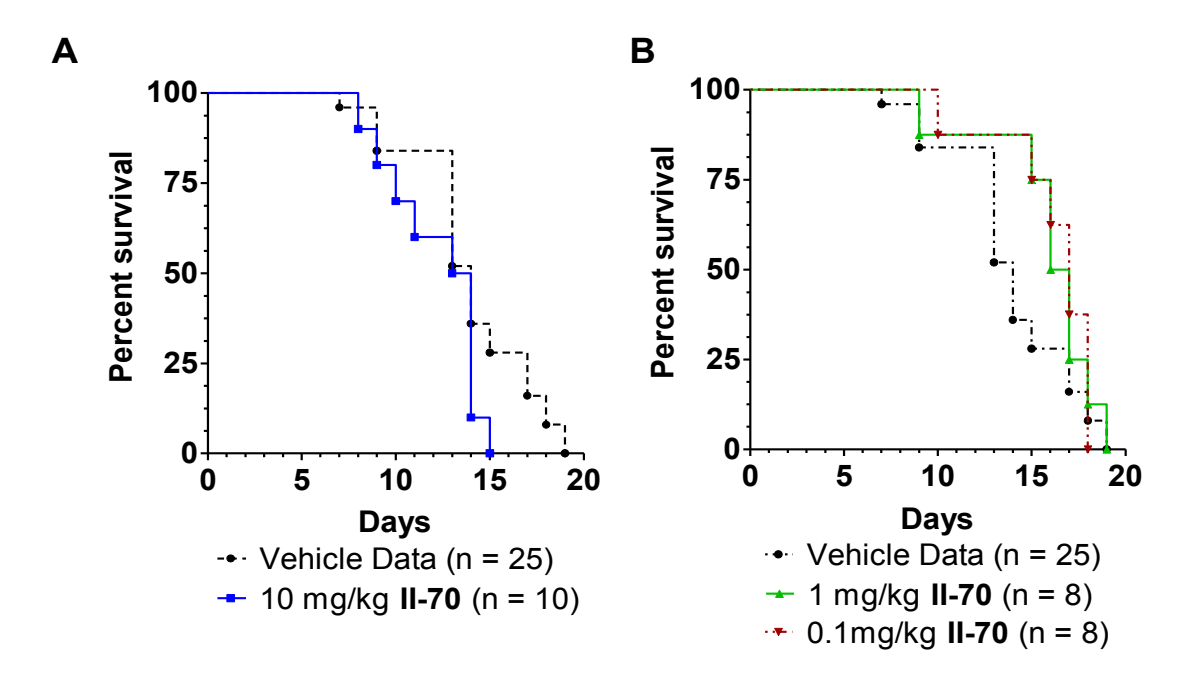


Figure III-29. Effect of pre-treatment with **II-70** (10, 1 or 0.1mg/kg) for 30 minutes prior to whole body IR with 7.3 Gy on survival of male Balb-C mice.

Mice that received lower concentrations of 1 mg/kg or 0.1 mg/kg saw an increase in survival between days 13-17 (Figure III-29) showing some protection or delay in the effects of the GI syndrome. These slight increases in mouse survival between days 13-17 were not statistically significantly different from the vehicle treated mice (Table III-5). By day 20, it is likely that both the GI and BM syndromes have affected the II-70 treated and vehicle treated mice. Necropsies of sacrificed mice treated with II-70 revealed the same yellowed intestines that were observed in the mice irradiated with 8.3 Gy IR.

Table III-5. Statistically analysis of vehicle compared to **II-70** whole body irradiated Balb-C mice.

Comparison of survival curves	Vehicle vs 10 mg/kg II-70	Vehicle vs 1.0 mg/kg II-70		
Log-rank (Mantel-Cox) Test				
Chi square	2.872	1.475	1.466	
df	1	1	1	
P value	0.0901	0.2245	0.226	
P value summary	ns	ns	ns	
Significant?	No	No No		
Gehan-Breslow-Wilcoxon Test				
Chi square	1.565	2.722	3.198	
df	1	1	1	
P value	0.211	0.099	0.0737	
P value summary	ns	ns	ns	
Significant?	No	No	No	

These results were puzzling, to say the least. It was anticipated that inhibiting Chk2 with II-70 would increase the survival of the mice following IR. However, in some cases (10 mg/kg, Figure III-29A), treatment with II-70 sensitized the mice to IR. II-70 is also an inhibitor of Chk1 (IC $_{50}$ = 220 nM), as well as NF- $_{\rm K}$ B (IC $_{50}$ = 10 $_{\rm H}$ M, Chapter IV). Inhibiting either of these proteins *in vitro* can result in sensitization of cells to DNA damage, leading to cell death. With a treatment of 10 mg/kg II-70, there is approximately 80 $_{\rm H}$ M, which is well above the IC $_{50}$ values. It is possible that at this dose in the mice, II-70 is inhibiting Chk1 and/or NF- $_{\rm K}$ B and therefore sensitizing mice to cell death following IR-induced DNA damage.

The lower doses (1 mg/kg, 0.1 mg/kg, Figure III-29B) did not completely increase survival of mice over the 20 day period. The protective effect was observed between days 13-17 (Figure III-29B), however, it is unclear why all of the mice in this study died

at the same time as the vehicle mice. It is possible that the mice treated with **II-70** started to suffer from side effects of whole body irradiation.

Although these results are promising, it is important to note that the whole body irradiation experiments with mice and **II-70** were not optimized, and that many more experiments need to be performed. These include optimal pretreatment time for dosage, concentration administered, multiple administrations of drug, IR dose rate, or multiple low IR doses over a period of time, etc.

III.H Inhibition of Chk2 as a strategy for chemosensitization

The radiosensitization results of the mouse irradiation (Figure III-30A) prompted an investigation of using Chk2 inhibition as a means for sensitizing cells to DNA damage. Many human tumors have increased levels of activated Chk2.³⁵ It is conceivable that the human tumor cells with increased levels of Chk2 have become dependent on Chk2 in order to survive.³⁵ Consequently, inhibition of Chk2 in these cells would result in cell death. Jobson et al demonstrated a sensitization to a chemotherapeutic (topotecan) in colon and ovarian cancer cell lines having increased levels of Chk2 when treated with PV1019 (Chapter I, Figure I-13).³⁵ PV1019 alone was also able to inhibit growth in the Chk2-overexpressing cells.³⁵

Chk2 inhibitor **II-70** was evaluated in one of the ovarian cancer cell lines with increased levels of Chk2 to determine if it was cytotoxic to these cells alone, or if it had a synergistic effect with the cytotoxic agent topotecan. The trypan blue exclusion assay was first performed in the ovarian cancer cell line, OVCAR-3, with **II-70** (Figure III-30). It is evident from the cell counts that after 24 hours of continuous exposure, the cells

treated with 30 μ M of **II-70** begin to display cytotoxic effects (Figure III-30). Cytotoxicity at 10 μ M is also observed following 72 hours of exposure.

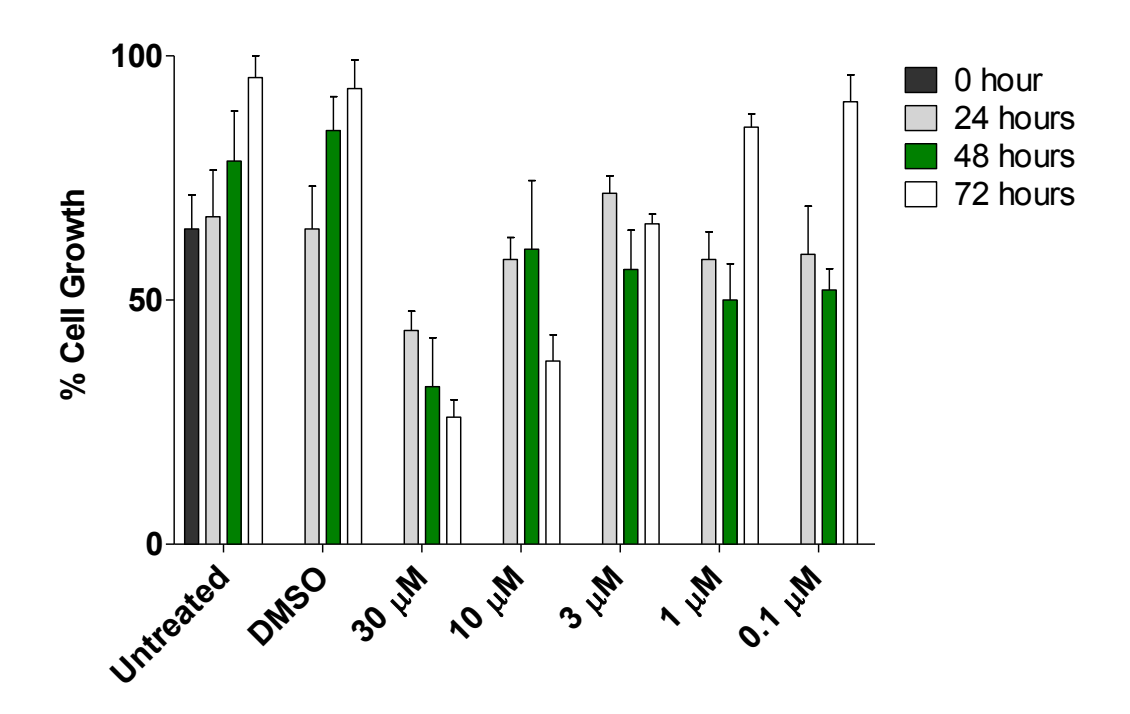


Figure III-30. Trypan blue exclusion assay of OVCAR-3 cells treated with **II-70**. OVCAR-3 cells treated with **II-70** only. B) OVCAR-3 cells treated in combination with 0.5 μ M Topotecan.

Topotecan alone demonstrates a cytotoxic effect at 48 and 72 hours of continuous exposure (Figure III-31). Compound **II-70** (30 μ M) seems to be slightly more toxic alone than topotecan (0.5 μ M). However, when topotecan is combined with **II-70** for 48 hours, **II-70** increases the cell cytotoxicity compared to topotecan alone (Figure III-31). The combination of topotecan and **II-70** in OVCAR-3 cells also demonstrates cell death at doses as low as 0.1 μ M. These data provide evidence as to the capabilities of Chk2 inhibitor **II-70** for sensitization of human tumor cells with increased levels of activated Chk2. This increased cell cytotoxicity was only evaluated in one ovarian cancer cell line with increased expression of Chk2 and would of course need to be

repeated in other cell lines with similar Chk2 properties in order to support the use of **II-70** as a sensitization drug for human tumor cells.

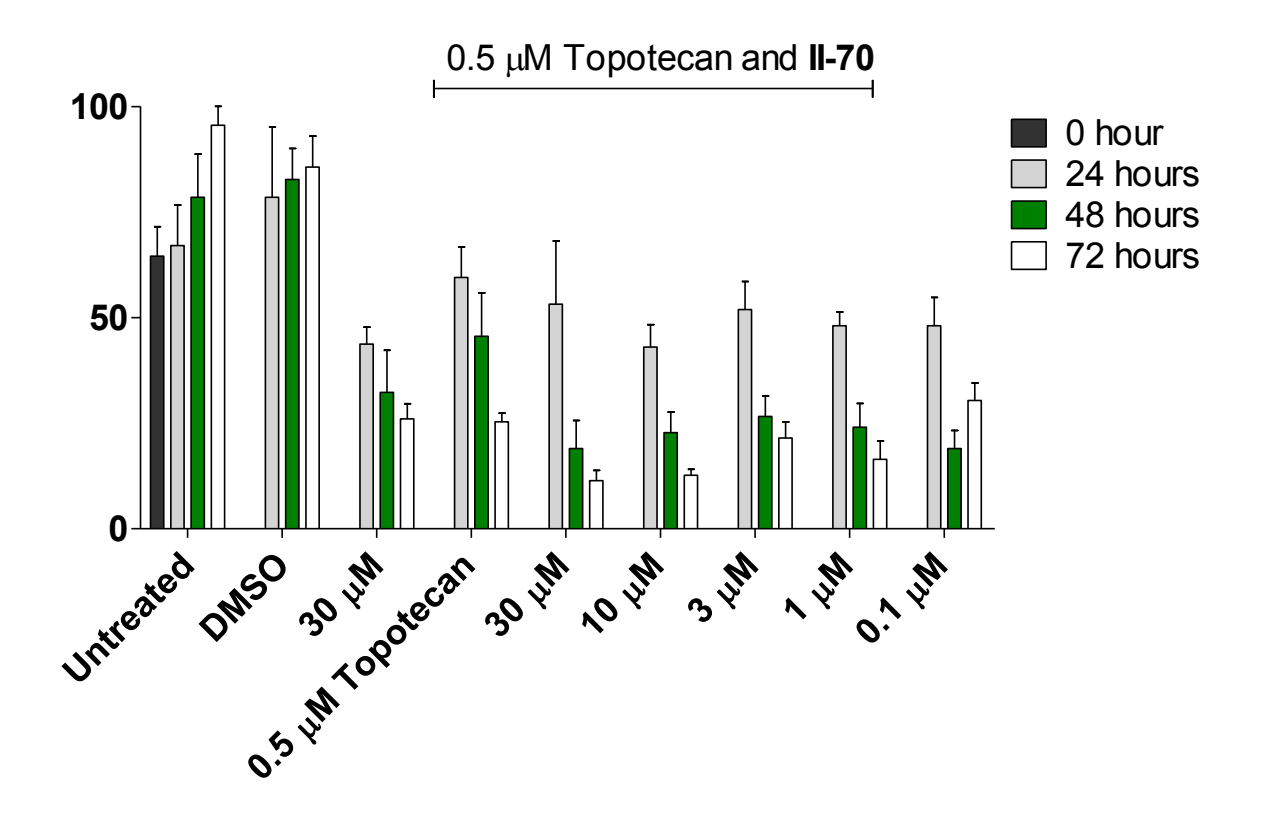


Figure III-31. Trypan blue exclusion assay of OVCAR-3 cells treated with **II-70** in combination with $0.5 \mu M$ Topotecan.

III.I Conclusions

The inhibition of Chk2 by **II-70** has been demonstrated at nanomolar levels in a radioactive filter-based kinase assay. Additionally, **II-70** inhibited cisautophosphorylation at Ser516 of Chk2 *in vitro* demonstrating direct cellular inhibition of Chk2. Chk2 inhibitor **II-70** also demonstrated inhibition of G₂ arrest following treatment with IR and HCT116 Chk2 +/+ cells, which was confirmed with Chk2 -/- cells. Inhibition of Chk2 did not have an effect on IR-induced arrest of G₁. Modifications of the glycocyamidine moiety in compounds **II-99** and **II-100** indicated the potential importance

of the free amine for inhibition of Chk2, which corresponds to the previously reported binding motive of the structurally related natural product debromohymenialdisine. Indoloazepine II-70 was found to increase survival in normal cells exposed to IR, however tumor cells having mutated p53 had no noticeable enhancements in survival. II-70 was also able to sensitize human ovarian cancer cells having overexpression of Chk2 to cell death induced by topotecan.

Chk2 inhibitor II-70 has demonstrated its potential as an adjuvant drug for cancer therapy. However, several questions have yet to be probed concerning the mechanism of inhibition of II-70. II-70 also inhibits other kinases at nanomolar concentrations which have possibly affected its ability to protect the mice from the toxic effects of IR. It will become important to determine the preferred mode of inhibition and possibly use that information to create more effective inhibitors for radio-protection.

III.J General experimental information and procedures

All cell lines were cultured at 37° C with 5% bone dry CO_2 atmosphere, 97% humidity and ambient O_2 in a Napco water-jacketed incubator. Adherent cells were routinely passaged by 0.25% trypsin-EDTA (Invitrogen, Fredrick, MD) using sterile technique and materials in a Nuaire biological safety cabinet Class II type A2. For all lysate and whole cell experiments, the inhibitors were dissolved in DMSO and the final DMSO concentration of the experiments was maintained at $\leq 0.1\%$ in the reaction buffer or culture medium. Cells were observed using a 1200CMI series spectrum inverted microscope. Cells were counted with a hemacytometer or using the Beckman Coulter Z1 Coulter® Particle Counter. Centrifugation was performed using the Beckman Coulter Allegra X-15R Centrifuge or Spectrafuge 16M microcentrifuge. Buffers, solutions and

media were made with water purified with the Millipore Quantum® Ex filtration system. Buffers requiring pH adjustments were monitored with a Mettler Toledo SevenEasy pH meter. Protein assays were read using the Molecular Devices SpectraMax M5^e plate reader. Western blots were run on hand-poured SDS PAGE gels using the BioRad mini protean pouring and electrophoresis system with the BioRad PowerPac HC. Gels were transferred to polyvinylidene fluoride membrane (BioRad) with the BioRad Criterion blotter wet transfer system. Blots and gels were quantified using the BioRad Molecular Imager FX. Luminescence in the luciferase assays were monitored and quantified using the Turner Biosystems Veritas Microplate Luminometer. Cells in the cloning survival assay and western blots were irradiated with a ⁶⁰Co source providing 1.93 Gy/min. Cells used in the cell cycle analysis were irradiated using a 6 MV linear accelerator (Clinac 2100 C, Varian Inc) at a dose rate of 300 cGy/minute. The quantity of incorporated [γ-³³P]-ATP on the P30 filter mat was detected using a Wallac 1450 Microbeta Plus Liquid Scintillation counter. Cell cycle analysis was performed using a Vantage TurboSort SE cytometer (Becton Dickinson, San Jose, CA).

Cell Culture Methods. The 184B5 and MDA-MB-231 cell lines were cultured in Dulbecco's Modified Essential Medium (DMEM) supplemented with 5% heat inactivated bovine calf serum with supplemented with 100 U/ml penicillin, 100 μg/mL streptomycin, 1 mM sodium pyruvate, 0.2 mM L-glutamine, and 100 mM MEM non-essential amino acids. HCT116 cells were cultured in McCoy's 5A with 5% bovine calf serum and supplemented with 100 U/ml penicillin, 100 μg/mL streptomycin. The HCT116 cell lines were a generous gift from Bert Vogelstein (Howard Hughes Medical Institute, Chevy Chase, MD). OVCAR-3 cells were cultured in RPMI-8226 media supplemented with 5%

heat inactivated bovine calf serum with 100 U/ml penicillin, 100 μ g/mL streptomycin, 1 mM sodium pyruvate, and 0.2 mM L-glutamine. For all lysate and whole cell experiments, the inhibitors were dissolved in DMSO and the final DMSO concentration of the experiments was maintained at \leq 0.1% in the reaction buffer or culture medium. Cells were cultured at 37° in a 5% CO₂ incubator. Cells in the cloning survival assay and western blots were irradiated with a 60 Co source providing 1.93 Gy/min. Cells used in the cell cycle analysis were irradiated using a 6 MV linear accelerator (Clinac 2100 C, Varian Inc) at a dose rate of 300 cGy/minute. The quantity of incorporated [γ - 33 P]-ATP on the P30 filter mat was detected using a Wallac 1450 Microbeta Plus Liquid Scintillation counter. Cell cycle analysis was performed using a FACS-Calibur-Vantage cytometer (Becton Dickinson, San Jose, CA).

In vitro kinase assay. In a final reaction volume of 25 μ L, Chk1 (h) or Chk2 (h) (Millipore) (5-10 mU) was incubated with 8 mM MOPS pH 7.0, 0.2 mM EDTA, 100 μ M CHKtide (KKKVSRSGLYRSPSMPENLNRPR) (Millipore), [γ -33P-ATP] (Perkin Elmer) (approximately 1 μ Ci diluted in 25 mM MgAcetate and 0.25 mM ATP) and inhibitor. The reaction was initiated by the addition of the MgATP mix. After incubation for 10 minutes at 30°C, the reaction was stopped by addition of 5 μ L of a 3% phosphoric acid solution. 10 μ L of the reaction was spotted onto a p30 filtermat and washed three times for 5 minutes in 75 mM phosphoric acid and once in methanol for 2 minutes before the addition of scintillation cocktail. The filtermat was read in a scintillation counter.

Table III-6. Log values, standard error of log values and IC_{50} values.

Compound	Chk1 Log IC ₅₀ ^a	Chk1 Std. Error Log IC ₅₀ ^b	Chk1 Std. IC ₅₀ ^c (μΜ)	Chk2 Log IC ₅₀ ^d	Chk2 Std. Error Log IC ₅₀ e	Chk2 Std. IC ₅₀ ^f (μΜ)
II-70	-0.6594	0.1412	0.2204	-1.893	0.06599	0.0135
II-84	NA	NA	> 1,000	NA	NA	> 1,000
II-99	NA	NA	> 1,000	NA	NA	> 1,000
III-1	-0.2540	0.08176	0.5814	-1.194	0.08455	0.06589
III-2	-0.2024	0.09818	0.6268	-1.347	0.08789	0.05393

^aLog EC₅₀ values for inhibition of phosphorylation of purified active Chk1 by $[\gamma^{-33}P]$ -ATP. ^bStandard error of log EC50 values inhibition of phosphorylation of purified active Chk1 by $[\gamma^{-33}P]$ -ATP. ^cEC₅₀ values calculated from the log EC₅₀ values for of phosphorylation of purified active Chk1 by $[\gamma^{-33}P]$ -ATP. ^dLog EC₅₀ values for inhibition of phosphorylation of purified active Chk1 by $[\gamma^{-33}P]$ -ATP. ^eStandard error of log EC50 values inhibition of phosphorylation of purified active Chk1 by $[\gamma^{-33}P]$ -ATP. ^fEC₅₀ values calculated from the log EC₅₀ values for of phosphorylation of purified active Chk1 by $[\gamma^{-33}P]$ -ATP. NA: Not available.

Table III-7. Mean and standard deviation of IC₅₀ values of Chk1 and Chk2.

Compound	Chk1 Experiment #	Chk1 EC ₅₀ (nM)	Chk2 Experiment #	Chk2 EC ₅₀ (nM)
	1	354.9	1	21.3
II-70	2	83.8	2	7.7
	3	222.6	3	11.6
	Mean	220.43	Mean	13.53
	Std Dev	135.56	Std Dev	7.00
	1	> 10,000	1	> 10,000
	2	> 10,000	2	> 10,000
II-84	3	> 10,000	3	> 10,000
	Mean	>10,000	Mean	>10,000
	Std Dev		Std Dev	
II-99	1	> 10,000	1	> 10,000
	2	> 10,000	2	> 10,000
	3	> 10,000	3	> 10,000
	Mean	>10,000	Mean	>10,000
	Std Dev		Std Dev	
III-1	1	358.1	1	100.5
	2	629.7	2	27.07
	3	756.4	3	70.1
	Mean	581.40	Mean	65.89
	Std Dev	203.50	Std Dev	36.90
	1	819.5	1	79.2
III-2	2	434.4	2	15.7
	3	626.5	3	66.9
	Mean	626.80	Mean	53.93
	Std Dev	192.55	Std Dev	33.68

Kinase Profile Assay. The Kinase profile was performed by the Millipore Kinase ProfilingServices (Millipore, Billerica, MA). This technology is a radioisotope-based P30 filter-binding assay. **1** was dissolved in pure DMSO to make a 10 mM stock. **1** was then diluted in pure DMSO to make serial dilutions based on the IC₅₀ ranges. The purified enzyme (e.g., Chk2) was diluted with 20 mM MOPS/NaOH pH7.0, 1 mM EDTA, 0.01% Triton-X-100, 5% glycerol, 0.1% 2-mercaptoethanol, 1 mg/ml BSA and incubated with 8

mM MOPS pH 7.0, 0.2 mM EDTA, substrate [e.g., Chktide (100 μ M in H₂0) (KKKVSRSGLYRSPSMPENLNRPR)] and 10 mM MgAcetate and [γ -³³P-ATP] (specific activity approx. 500 cpm/pmol, concentration as required). The reaction was initiated by the addition of the MgATP mix. After incubation for 40 minutes at room temperature, the reaction was stopped by the addition of 3% phosphoric acid solution. 10 μ L of the reaction was then spotted onto a P30 filtermat and washed three times for 5 minutes in 75 mM phosphoric acid and once in methanol prior to drying and scintillation counting.

Trypan blue exclusion assay: Cells were seeded at 2.5×10^5 cells/ml in a 24-well plate the day before treatment. Cells were then treated with vehicle or II-70 in varying concentrations. At the appropriate time points, media was removed and cells were washed with PBS. Cells were then removed from the wells with 0.25% Trypsin/EDTA (50 μ l) and diluted with complete media (200 μ l). 10 μ l of this mixture was then mixed with 10 μ l of Trypan blue. Cells were then counted with a hemacytometer.

Table III-8. Summary of Gl₅₀ values of cells treated with **II-70**.

Cell Line	Gl ₅₀ (μΜ)	Std Error LogGl ₅₀	Cell Line	Gl ₅₀ (μM)	Std Error LogGl ₅₀
184B5	> 30		HCT116	> 30	0.09771
MCF-7	~ 30		HCT116-40-16	20.63	0.08592
MDA-MB-231	> 30		HCT116.386	22.84	0.07148
			HCT116-379.2	28.58	0.07945
			HCT116-67	8.19	0.1262

Western Blot analysis whole cell extracts of cells treated with Chk2 inhibitor. 184B5 (or MDA-MB-231) cells in T25 flasks were 80% confluent when incubated with **II-70** (in DMSO) for 2 hours, then activated in situ with 10 Gy of IR. Cells were given fresh media and inhibitor and incubated for 4 hours. Media was then removed from the plates and cells were washed two times with ice-cold PBS. Whole cell lysis buffer (20 mM Tris HCl (pH =7.5), 150 mM NaCl, 1mM Na₂EDTA, 1 mM EGTA, 1% Triton X 100, 20 μ M DTT, 2 μ M NaVO₄, 2 μ M NaF, 2 μ M PMSF, 2 μ M β glycerophosphate, 0.02 µg/ml Aprotinin, 0.02 µg/ml Leupeptin) was then added to the plates which were then rocked for 10 minutes at 4°C. Cells were then scraped and transferred to a tube followed by brief sonication. Cells were centrifuged at 500 x g for 3 min. 50 µg of protein (quantified with Bradford assay) was diluted with 6X SDS-PAGE buffer. Equal amounts of denatured protein were electrophoresed on SDSpolyacrylamide gels and transferred to PVDF membranes using wet transfer. Membranes were blocked with 4% blocking grade non-fat dairy milk (NFDM) for 1 hour at room temperature and washed with Tris-buffered saline-Tween 20 (TBS-T) containing 10X Tris Buffer and 0.1% Tween 20 for 10 minutes. Blots were then probed with primary AB 1:1000 in 5% BSA TBS-T (overnight, 4°C) and were washed with TBS-T (3 x 5 minutes). They were then incubated with horse radish peroxidase conjugated to secondary antibody. Actin antibody (1:10,000 dilution) (Amersham) was incubated in 4% NFDM in TBS-T, washed and incubated with horse radish peroxidase conjugated to secondary antibody mouse. Complexes detected by enhanced were chemiluminescence (ECL) technique according to manufacturer's directions (Amersham) on XAR film.

Cloning Survival Assay: 184B5 cells were cultured and when 80% confluent, cells were treated with II-80 for 30 minutes and irradiated in suspension with varying doses (0-7.5 Gy) of irradiation (Cobalt60) on ice. Cells were diluted and were plated at cloning density in triplicate, and were allowed to incubate at 37°C with 5% CO₂ and ambient oxygen. Medium was replaced at 7 days and clones were incubated another 3-7 days at which point clones were fixed with 0.9% saline and stained with 3% crystal violet in 70% ethanol.

Flow Cytometry: The distribution of HCT116 cells at different stages of the cell cycle was estimated using flow cytometric DNA analyses. 5 x 10⁵ cells were incubated overnight in McCoy 5A medium containing 5% BCS, then treated with or without compound for 2 hours in 6-well plates. Tissue culture plates were placed on a 1.5 cm sheet of tissue equivalent bolus material, to provide for dose build up on the radiation treatment couch. The linac gantry was positioned at 180 degrees to irradiate the plates using a single portal from below. Dose was calculated to the bottom of the tissue culture plates. Cells were irradiated with 1.0, 2.5, or 5.0 cGy at a dose rate of 3.0 Gy/min. Cell were allowed to incubate for varying lengths of time (0, 2, 4, 8, 22 hours) postirradiation. Cells were then harvested and washed with phosphate-buffered saline (PBS; pH 7.4) containing 5% BCS, fixed with 70% ethanol/30% water at 4°C. The cells were washed with 5%BCS/PBS twice and the pellet was resuspended in a solution containing RNAse (20µg/ml) and propidium iodide (Invitrogen) and incubated for 15 minutes in the dark at 37°C. For each sample, at least 10,000 events were analyzed using a Vantage TurboSort SE cytometer (Becton Dickinson, San Jose, CA) with 488 nM excitation, fluorescence at 630/22 bandpass filter. The percentage of cells in each cell cycle phase

was calculated using CellQuest Ver3.3, and the WinList6 and ModFITLT software packages (Becton Dickinson).

REFERENCES

III.K References

- 1. Bartkova, J.; Horejsi, Z.; Koed, K.; Kramer, A.; Tort, F.; Zieger, K.; Guldberg, P.; Sehested, M.; Nesland, J. M.; Lukas, C.; Orntoft, T.; Lukas, J.; Bartek, J., DNA damage response as a candidate anti-cancer barrier in early human tumorigenesis. *Nature* **2005**, *434* (7035), 864-70.
- 2. Gorgoulis, V. G.; Vassiliou, L. V. F.; Karakaidos, P.; Zacharatos, P.; Kotsinas, A.; Liloglou, T.; Venere, M.; DiTullio, R. A.; Kastrinakis, N. G.; Levy, B.; Kletsas, D.; Yoneta, A.; Herlyn, M.; Kittas, C.; Halazonetis, T. D., Activation of the DNA damage checkpoint and genomic instability in human precancerous lesions. *Nature* **2005**, *434* (7035), 907-913.
- 3. Clarke, D. J.; Gimenez-Abian, J. F., Checkpoints controlling mitosis. *BioEssays* **2000**, *22* (4), 351-63.
- 4. Iliakis, G.; Wang, Y.; Guan, J.; Wang, H. C., DNA damage checkpoint control in cells exposed to ionizing radiation. *Oncogene* **2003**, *22* (37), 5834-5847.
- 5. Bernhard, E. J.; Maity, A.; Muschel, R. J.; McKenna, W. G., Effects of ionizing-radiation on cell-cycle progression A review. *Radiat. Environ. Biophys.* **1995**, *34* (2), 79-83.
- 6. Iliakis, G., Cell cycle regulation in irradiated and nonirradiated cells. *Semin. Oncol.* **1997**, *24* (6), 602-615.
- 7. Lowndes, N. F.; Murguia, J. R., Sensing and responding to DNA damage. *Curr. Opin. Genet. Dev.* **2000**, *10* (1), 17-25.
- 8. Zhou, B. B.; Elledge, S. J., The DNA damage response: putting checkpoints in perspective. *Nature* **2000**, *408* (6811), 433-9.
- 9. Maity, A.; McKenna, W. G.; Muschel, R. J., The molecular-basis for cell-cycle delays following ionizing-radiation A review. *Radiotherapy and Oncology* **1994**, 31 (1), 1-13.
- 10. Pommier, Y.; Weinstein, J. N.; Aladjem, M. I.; Kohn, K. W., Chk2 molecular interaction map and rationale for Chk2 inhibitors. *Clin. Cancer Res.* **2006**, *12* (9), 2657-61.

- 11. Antoni, L.; Sodha, N.; Collins, I.; Garrett, M. D., CHK2 kinase: cancer susceptibility and cancer therapy two sides of the same coin? *Nat. Rev. Cancer* **2007**, *7*, 925-936.
- 12. Pommier, Y.; Sordet, O.; Rao, V. A.; Zhang, H. L.; Kohn, K. W., Targeting Chk2 kinase: Molecular interaction maps and therapeutic rationale. *Curr. Pharm. Des.* **2005**, *11* (22), 2855-2872.
- 13. Carlessi, L.; Buscemi, G.; Larson, G.; Hong, Z.; Wu, J. Z.; Delia, D., Biochemical and cellular characterization of VRX0466617, a novel and selective inhibitor for the checkpoint kinase Chk2. *Mol. Cancer Ther.* **2007**, *6* (3), 935-44.
- Curman, D.; Cinel, B.; Williams, D. E.; Rundle, N.; Block, W. D.; Goodarzi, A. A.; Hutchins, J. R.; Clarke, P. R.; Zhou, B. B.; Lees-Miller, S. P.; Andersen, R. J.; Roberge, M., Inhibition of the G2 DNA damage checkpoint and of protein kinases Chk1 and Chk2 by the marine sponge alkaloid debromohymenialdisine. *J. Biol. Chem.* 2001, 276 (21), 17914-9.
- 15. Wan, Y.; Hur, W.; Cho, C. Y.; Liu, Y.; Adrian, F. J.; Lozach, O.; Bach, S.; Mayer, T.; Fabbro, D.; Meijer, L.; Gray, N. S., Synthesis and target identification of hymenialdisine analogs. *Chem. Biol.* **2004**, *11* (2), 247-59.
- 16. Meijer, L.; Thunnissen, A. M. W. H.; White, A. W.; Garnier, M.; Nikolic, M.; Tsai, L. H.; Walter, J.; Cleverley, K. E.; Salinas, P. C.; Wu, Y. Z.; Biernat, J.; Mandelkow, E. M.; Kim, S. H.; Pettit, G. R., Inhibition of cyclin-dependent kinases, GSK-3 beta and CK1 by hymenialdisine, a marine sponge constituent. *Chem. Biol.* **2000**, *7* (1), 51-63.
- 17. Sharma, V.; Tepe, J. J., Potent inhibition of checkpoint kinase activity by a hymenialdisine-derived indoloazepine. *Bioorg. Med. Chem. Lett.* **2004,** *14* (16), 4319-4321.
- 18. Tasdemir, D.; Mallon, R.; Greenstein, M.; Feldberg, L. R.; Kim, S. C.; Collins, K.; Wojciechowicz, D.; Mangalindan, G. C.; Concepcion, G. P.; Harper, M. K.; Ireland, C. M., Aldisine alkaloids from the Philippine sponge Stylissa massa are potent inhibitors of mitogen-activated protein kinase kinase-1 (MEK-1). *J. Med. Chem.* **2002**, *45* (2), 529-32.
- 19. Sharma, V.; Lansdell, T. A.; Jin, G.; Tepe, J. J., Inhibition of Cytokine Production by Hymenialdisine Derivatives. *J. Med. Chem.* **2004,** *47* (14), 3700-3703.

- 20. Oliver, A. W.; Paul, A.; Boxall, K. J.; Barrie, S. E.; Aherne, G. W.; Garrett, M. D.; Mittnacht, S.; Pearl, L. H., Trans-activation of the DNA-damage signalling protein kinase Chk2 by T-loop exchange. *EMBO J.* **2006**, *25* (13), 3179-90.
- 21. DeLano, W. L. The PyMol Molecular Graphics System., 2009.
- 22. Ahn, J. Y.; Schwarz, J. K.; Piwnica-Worms, H.; Canman, C. E., Threonine 68 phosphorylation by ataxia telangiectasia mutated is required for efficient activation of Chk2 in response to ionizing radiation. *Cancer Res.* **2000**, *60* (21), 5934-5936.
- 23. Arienti, K. L.; Brunmark, A.; Axe, F. U.; McClure, K.; Lee, A.; Blevitt, J.; Neff, D. K.; Huang, L.; Crawford, S.; Pandit, C. R.; Karlsson, L.; Breitenbucher, J. G., Checkpoint kinase inhibitors: SAR and radioprotective properties of a series of 2-arylbenzimidazoles. *J. Med. Chem.* **2005**, *48* (6), 1873-85.
- 24. Yang, J.; Yu, Y. N.; Hamrick, H. E.; Duerksen-Hughes, P. J., ATM, ATR and DNA-PK: initiators of the cellular genotoxic stress responses. *Carcinogenesis* **2003**, *24* (10), 1571-1580.
- 25. Bernhard, E. J.; McKenna, W. G.; Muschel, R. J., Radiosensitivity and the cell cycle. *Cancer J. Sci. Amer.* **1999,** *5* (4), 194-204.
- 26. Kastan, M. B.; Onyekwere, O.; Sidransky, D.; Vogelstein, B.; Craig, R. W., Participation of p53 protein in the cellular-response to DNA damage. *Cancer Res.* **1991**, *51* (23), 6304-6311.
- 27. Kuerbitz, S. J.; Plunkett, B. S.; Walsh, W. V.; Kastan, M. B., Wild-type p53 is a cell-cycle checkpoint determinant following irradiation. *Proc. Natl. Acad. Sci. U. S. A.* **1992**, *89* (16), 7491-7495.
- 28. Shoemaker, R. H., The NCI60 human tumour cell line anticancer drug screen. *Nat. Rev. Cancer* **2006**, *6* (10), 813-823.
- 29. Vichai, V.; Kirtikara, K., Sulforhodamine B colorimetric assay for cytotoxicity screening. *Nat. Protocols* **2006**, *1* (3), 1112-1116.

- 30. Solier, S.; Sordet, O.; Kohn, K. W.; Pommier, Y., Death Receptor-Induced Activation of the Chk2-and Histone H2AX-Associated DNA Damage Response Pathways. *Mol. Cell. Biol.* **2009**, *29* (1), 68-82.
- 31. MacLaren, A.; Slavin, D.; McGowan, C. H., Chk2 Protects against Radiation-Induced Genomic Instability. *Radiat. Res.* **2009**, *172* (4), 463-472.
- 32. Takai, H.; Naka, K.; Okada, Y.; Watanabe, M.; Harada, N.; Saito, S.; Anderson, C. W.; Appella, E.; Nakanishi, M.; Suzuki, H.; Nagashima, K.; Sawa, H.; Ikeda, K.; Motoyama, N., Chk2-deficient mice exhibit radioresistance and defective p53-mediated transcription. *EMBO J.* **2002**, *21* (19), 5195-205.
- 33. Hall, E. J.; Giaccia, A. J., *Radiobiology for the radiologist*. Lippincott Williams & Wilkins: Philadelphia, 2006; p 546.
- 34. Meyer, R. E.; Fish, R. E., A review of tribromoethanol anesthesia for production of genetically engineered mice and rats. *Lab Animal* **2005**, *34* (10), 47-52.
- Jobson, A. G.; Lountos, G. T.; Lorenzi, P. L.; Llamas, J.; Connelly, J.; Cerna, D.; Tropea, J. E.; Onda, A.; Zoppoli, G.; Kondapaka, S.; Zhang, G. T.; Caplen, N. J.; Cardellina, J. H.; Yoo, S. S.; Monks, A.; Self, C.; Waugh, D. S.; Shoemaker, R. H.; Pommier, Y., Cellular Inhibition of Checkpoint Kinase 2 (Chk2) and Potentiation of Camptothecins and Radiation by the Novel Chk2 Inhibitor PV1019 [7-Nitro-1H-indole-2-carboxylic acid {4-[1-(guanidinohydrazone)-ethyl]-phenyl}-amide]. J. Pharmacol. Exp. Ther. 2009, 331 (3), 816-826.

CHAPTER IV

EVALUATION OF INDOLOAZEPINE AS AN INHIBITOR OF NF-KB

IV.A Introduction to the NF-кВ pathway

Nuclear transcription factor kappa B (NF-κB) is a mammalian nuclear transcription factor involved in many cellular processes including inflammation, immune responses, cell proliferation and cell death. 1-6 NF-kB is believed to be a cell death suppressor and plays an important role in regulating the inducible activation of antiapoptotic signaling pathways. NF-κB is made up of five distinct subunits found in mammalian cells including NF-kB1 (p105/50), NF-kB2 (p100/p52), RelA (p65), RelB and c-Rel.⁸ The subunits can form a variety of homo- or heterodimers that are used to control the specificity and selectivity of specific DNA control elements. 9, 10 In its inactive form, NF-κB is sequestered in the cytoplasm by the inhibitory protein IκB-α. 11 These IκBα-NF-κB complexes constantly shuttle between the cytoplasm and the nucleus in cells that have not been activated. The back and forth transport between the nucleus and cytoplasm is regulated by a nuclear export signal (NES) located near the amino terminus of IκB-α and also by an unmasked nuclear localization signal (NLS) of the p50 proteins that is likely masked. 12 IκB-β does not have the NES and can provide a more effective mask of the NLS due to the exclusive presence of the IκB-β-NF-κB complexes in the cytoplasm. 13

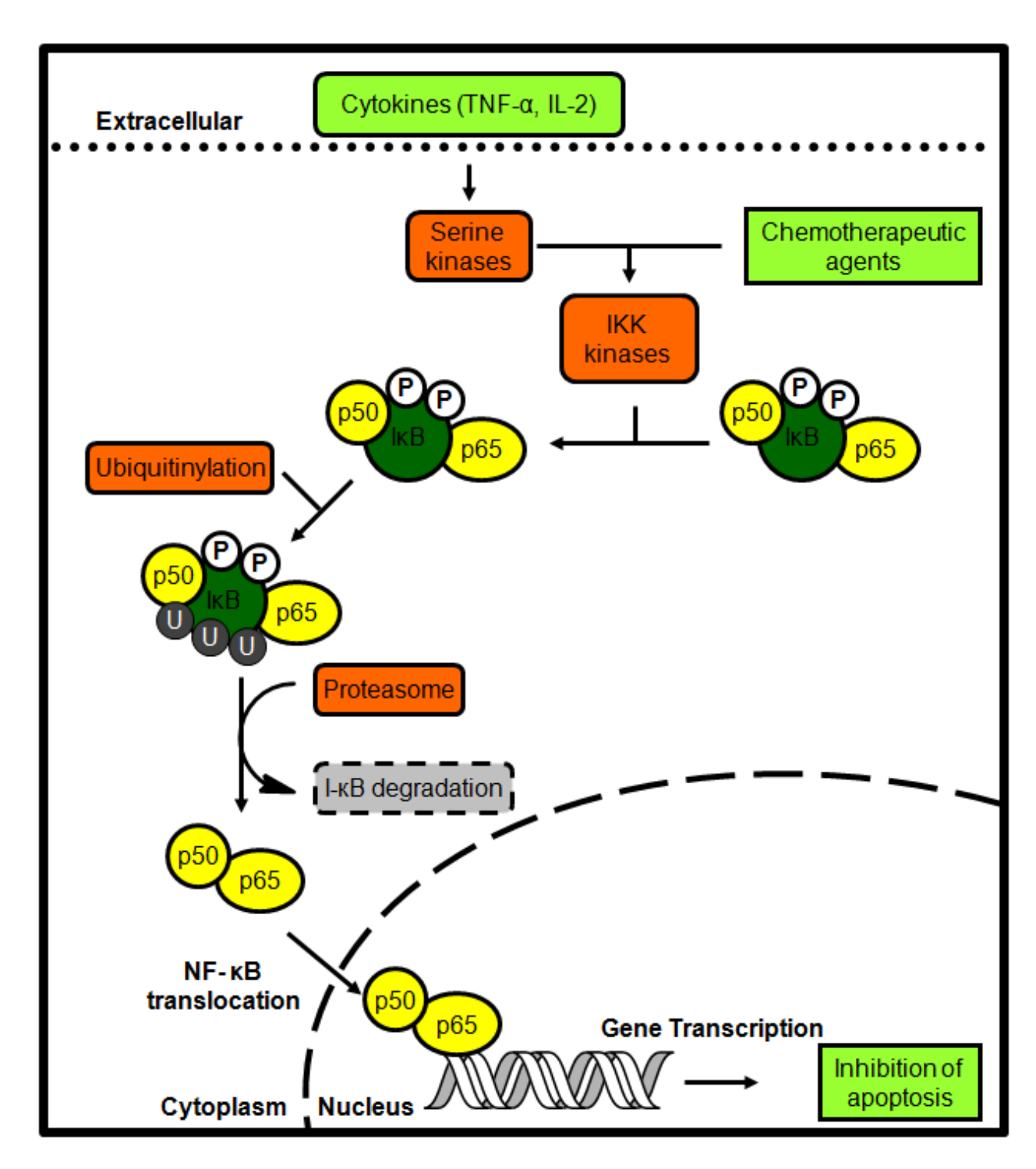


Figure IV-1. NF-кВ signal cascade.

The IKK complex regulates IkB phosphorylation and is activated by extracellular stimuli including pro-inflammatory cytokines such as tumor necrosis factor alpha (TNF- α) and IL-1 β (Figure IV-1). Signal-induced ubiquitinylation and proteasomal

degradation of IκBα by the 26S proteasome allows the irreversible release of NF-κB which translocates into the nucleus following degradation of IκB. ^{7, 14-18} After NF-κB is released, it translocates into the nucleus where the subunits are able to bind with specific DNA control elements, initiating the transcription of several immune and proinflammatory signaling genes. ^{14, 19} In most cells, NF-κB bypasses apoptosis by inducing survival genes. However, there are special conditions in which NF-κB can mediate antiapoptotic responses including responses induced by cellular DNA repair mechanism. ^{20, 21}

Transactivation of NF-κB has recently received attention. ²²⁻²⁴ The Rel proteins share a Rel homology domain (RHD), which controls DNA-binding activity. p65, RelB and c-Rel have COOH-terminal transactivation domains (TADs). ^{11, 25} Only TAD in the p65 can regulate the transcriptional activity of the p65/p50 NF-κB complex. Studies have suggested that phosphorylation of the p65 subunit plays a key role in the transcriptional activation after stimulus-induced nuclear translocation. ²⁶⁻³⁰ Ser276 was reported in RHD, ^{26, 28} while Ser529/Ser536 are in TAD. ³¹⁻³³ Protein kinase A and mitogen- and stress-activated protein kinase-1 (MSK1) have been identified as proteins that phosphorylate Ser276. ^{26, 34} IKK has been reported as the source of phosphorylation for Ser536. ³² TNF-α has been shown to induce phosphorylation by IKK of p65 on Ser536. ³²

NF-κB regulates genes directly involved in the pathogenesis of inflammatory diseases including rheumatoid arthritis (RA),^{35, 36} inflammatory bowel disease,³⁷⁻³⁹ helicobacter pylori-associated gastritis,⁴⁰ atheroscelerosis,⁴¹ multiple sclerosis⁴² and

asthma.⁴³ NF-кВ plays a significant role in cytokine responses making it an attractive target for therapy of these inflammatory diseases.⁴⁴⁻⁴⁶

Additionally, constitutively active NF-κB has been observed in cancer cell lines, as well as in human tumor tissues stemming from patients with multiple myeloma, ⁴⁷ acute myelogenous leukemia, ⁴⁸ acute lymphocyte leukemia, ⁴⁹ chronic myelogenous leukemia, ⁵⁰ prostate, ⁵¹ breast ⁵² and pancreatic cancers. ⁵³

NF-κB mediated chemoresistance has been shown via activation by many clinically used chemotherapeutic agents. Effectiveness of treatment with chemotherapeutic agents often is reduced due to a NF-κB mediated double stimulus, which causes chemoresistance leading to uncontrolled cell growth. All Inhibition of NF-κB with a mutated form of IκB-α, a natural inhibitor, was shown to control inducible chemoresistance. Overexpression of IκB, in combination with camptothecin had an increased cytotoxicity when compared to camptothecin alone. Inhibition of NF-κB has become an attractive strategy in combination chemotherapy that has been proven to improve efficacy of anticancer treatment.

Inhibition of NF-κB through the IKK complex regulates IκB phosphorylation and is activated by extracellular stimuli including pro-inflammatory cytokines such as tumor necrosis factor alpha (TNF-α) and IL-1β (Figure IV-1). Signal-induced ubiquitinylation and proteasomal degradation of IκBα by the 26S proteasome allows the irreversible release of NF-κB which translocates into the nucleus following degradation of IκB. After NF-κB is released, it translocates into the nucleus where the subunits are able to

bind with specific DNA control elements, initiating the transcription of several immune and pro-inflammatory signaling genes. ^{14, 19} In most cells, NF-κB bypasses apoptosis by inducing survival genes. However, there are special conditions in which NF-κB can mediate antiapoptotic responses including responses induced by cellular DNA repair mechanism. ^{20, 21}

Inhibition of NF-κB by genetic or chemical inhibitors induces the apoptotic response of various tumor cells and/or inhibits the anti-apoptotic response following treatment with ionizing radiations or other chemotherapeutic agents. This, in turn reverses any NF-κB-linked radioresistance or chemoresistance in many models. ^{67, 70-74} These and other studies have made developing inhibitors of NF-κB activity an attractive target for chemotherapy.

IV.B Targets for inhibition of NF-кВ

As mentioned above, in order for NF- κ B to become activated, a phosphorylation event must occur on $I\kappa$ B- α followed by subsequent ubiquitinylation and degradation. Inhibition of $I\kappa$ B- α would eventually lead to the inhibition of the transcriptional activity of NF- κ B. The group of kinases involved in phosphorylation of $I\kappa$ B are also known as the IKK complex. The group of kinases involved in phosphorylation of $I\kappa$ B are also known as the IKK complex.

There are several subunits that make up the IKK complex including the kinase subunits IKK α and IKK β , and the regulatory subunit IKK γ (NEMO). The classical pathway of the activation of NF- κ B involves phosphorylation of the p50/p65 heterodimer

by the IKKβ subunit. ⁷⁵ Many lymphoid or myeloid tumors including multiple myeloma, Hodgkin diseases, and various solid tumors, including breast cancers and glioblastomas have constitutively activated NF-κB. ^{70, 71, 76, 78, 79} The constitutive activity is often linked to genetic rearrangements which can lead to abnormal gene expression of NF-κB and consequently mutations of the IκB-α inhibitor or to increased IKK activity. ^{71, 80-82} Animal models demonstrated that developments of cancers due to chronic inflammations was dependent on IKK activity and activation of NF-κB. ^{83, 84} The combination of this with inducing the anti-apoptotic gene expression provide potentially useful anticancer therapy by inhibiting IKKβ mediated NF-κB activation. ⁸⁰ The lack of selective kinase inhibitors of IKK have made this potential therapeutic strategy limited, despite the many examples in literature. ⁸⁰

Evodiamine is an indole alkaloid that is a major constituent of the Chinese herb *Evodiae fructus* having significant antitumor activity (Figure IV-2). Although it is effective as a single agent, it more importantly has a more additive cytotoxic effect when used in combination with chemotherapeutics. Evodiamine was found to inhibit NF- κ B activation in the induced as well as constitutive form in a variety of cell lines. Mechanistic studies have demonstrated that Evodiamine functions by inhibiting I κ B- α phosphorylation via inhibiting TNF- α induced IKK activation. Evodiamine decreased the expression of anti-apoptotic genes as well as enhanced the cytotoxicity of TNF- α and chemotherapeutics including taxol and cis-platin. 87

Parthenolide, a sesquiterpene lactone was initially isolated from *Tanacetum* parthenium and is a potent inhibitor of the covalent binding of the IKK complex (Figure

IV-2). ⁸⁸⁻⁹⁰ An increase in apoptosis was observed when parthenolide was used in combination with roscovitine, a Cdk2 and Cdk5 kinase inhibitor. ⁹¹ This affect was not observed when used in combination with paclitaxel. ⁹²

MLN120B is a highly selective inhibitor of IKK β (IC $_{50}$ = 60 nM) over IKK α (IC $_{50}$ = >100,000 nM) (Figure IV-2). ⁹³ This compound was able to decrease paw swelling in a dose-dependent manner with an ED $_{50}$ = 7 mg/kg and 12 mg/kg, respectively when dosed orally twice daily in either prophylactic or therapeutic adjuvant induced arthritis models in rats. ^{94, 95} LPS-induced TNF- α production was also inhibited in rats by MLN120B with a similar EC $_{50}$. A significant protection against bone and cartilage destruction was observed in the diseased controls when monitored by histology and micro-CT (computerized tomography) imaging. When compared to the diseased controls, NF- κ B regulated gene expression in the joints was significantly decreased. A dose-dependent decrease in clinical symptoms compared to control animals in a collagen antibody-induced BALBc model of arthritis was observed. ^{94, 96}

Thienopyridine (Figure IV-2), another potent inhibitor of IKK β (IC₅₀ = 26 nM) was evaluated in a rat collagen induced arthritis model. P4, P7 Rats were dosed orally at 10 mg/kg and demonstrated a 44% decrease in paw weight when compared to control animals.

Figure IV-2. IkB Kinase inhibitors.

Several other classes of IKK β inhibitors have also been identified including benzamides and thiophenes (Figure IV-3). An increasing number of IKK β inhibitors continue to be discovered with various scaffolds using SAR studies. 4

$$S \longrightarrow NH_2$$
 NH_2 $NH_$

Figure IV-3. IKKβ inhibitors.

In addition to inhibiting IKK, glycogen synthase-3 (GSK-3) has also been targeted for inhibition. GSK-3 exists in two homologous isoforms that are encoded by different genes, GSK-3α and GSK-3β. Research has suggested that GSK-3 could be positively regulating NF-κB. Inhibition of GSK-3 has also significantly decreased proinflammatory

responses. ⁹⁹ Hoeflich et al. ¹⁰⁰ demonstrated the necessary role of GSK-3 β , and not GSK-3 α , in the NF- κ B-mediated survival response after TNF- α stimulation. ¹⁰⁰⁻¹⁰² It was also discovered that GSK-3 played a role in suppressing apoptosis induced by TNF- α . ¹⁰⁰

Inhibition of GSK-3β with a known inhibitor, lithium chloride caused a decrease in NF-кB-dependent gene transcription. The same treatment, however, did not interfere with the degradation of IκB-α or activity of IKK. The translocation of the NF-κB heterodimer into the nucleus and its binding to DNA were also unaffected. 103 Another study knocked down GSK-3β resulting in a suppression of TNF-α-induced IKK activation, IκB-α phosphorylation, and IκB-α ubiquitinylation. 104 GSK-3β was again shown to inhibit NF-kB-dependent transcription and DNA binding activity by inhibiting the phosphorylation and degradation of IkB- α following TNF- α induction. ¹⁰⁵ As evidence indicates that GSK-3β plays a part in NF-κB activation, the site of phosphorylation on the p65 subunit has not been determined. Several protein kinases have demonstrated phosphorylation of p65 at Ser276, 27 Ser 311, 106 Ser529, 31 and Ser 536. 32 The total number of phosphorylation sites of p65 has yet to be determined. The Ser468 of p65 was proposed as a site of phosphorylation for GSK-3β and is believed to negatively control NF-κB. 25 When GSK-3β was inhibited with increasing amounts of LiCl, 107 decreased levels of phosphorylation of Ser468 was observed in a dose-dependent manner.²⁵

Following inhibition of GSK-3 β , high levels of β -catenin have been observed, resulting in inhibition NF- κ B activity at the level of DNA binding, though the mechanism

is unclear. $^{108, 109}$ When β -catenin is phosphorylated by GSK-3, it is subsequently targeted for ubiquitin-mediated proteasomal degradation, which limits the accumulation of free β -catenin in the nucleus. $^{110, 111}$ MEFs and non-transformed rat intestinal epithelial cells did not exhibit increased levels of β -catenin when decreased levels of GSK-3 were observed when compared to control cells. 15 These cell lines also demonstrated the importance of GSK-3 β for efficient localization of p65 to the promoter region of NF- κ B-regulated genes during cytokine stimulation. $^{15, 112}$

Lithium selectively inhibits the activity of purified GSK-3 α and GSK-3 β as well as their functions in intact cells. ^{113, 114} Its selectively has been used to evaluate the role of GSK-3 in pharmacological cellular processes. ¹¹⁵ Valproic acid is a dose-dependent inhibitor of GSK-3 α and GSK-3 β . ¹¹⁶⁻¹¹⁸ ATP-competitive inhibitors of GSK-3 have been identified during screenings of other protein kinase inhibitors including: paullones, hymenialdisine and staurosporine derivatives. Nanomolar IC₅₀ values were observed with these inhibitors. ^{119, 120} Two maleimides, SB216763 and SB415286 (Figure IV-4) were identified as selective, ATP-competitive inhibitors of both GSK-3 α and GSK-3 β . ¹²¹

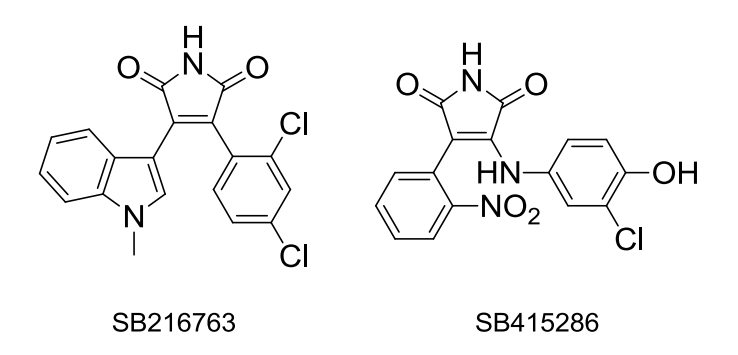


Figure IV-4. Structures of GSK-3 Inhibitors.

IV.C Evaluation of II-70 and analogs as an inhibitor of NF-κB-mediated gene transcription.

Previous biological evaluation of **II-70** demonstrated inhibition effects against IL-2 and TNF-α production. This was an indication that it could also be an inhibitor of NF-κB. Compounds **II-70**, **II-84**, and **II-99** were evaluated for their ability to inhibit NF-κB-mediated gene transcription (Figure IV-5).

Figure IV-5. Structures of II-70, II-84, II-100.

The marine alkaloid **IV-8** from the tunicate *Dendrodoa grossularia* was synthesized in addition to a few analogues (Figure IV-6). ^{123, 124} Compounds **IV-1** – **IV-4** have similarities to the analogues discussed above, however lack the azepine ring that is present in **II-2** and **II-70**. In addition, the glycocyamidine ring is bonded to indole via an sp³ hybridized quaternary center. This differs from the azepine ring of **II-2** and **II-70** which are bonded to the glycocyamidine ring by an sp² bond. The synthesis of **IV-1** – **IV-4** were described previously, and will not be discussed here. ^{123, 124}

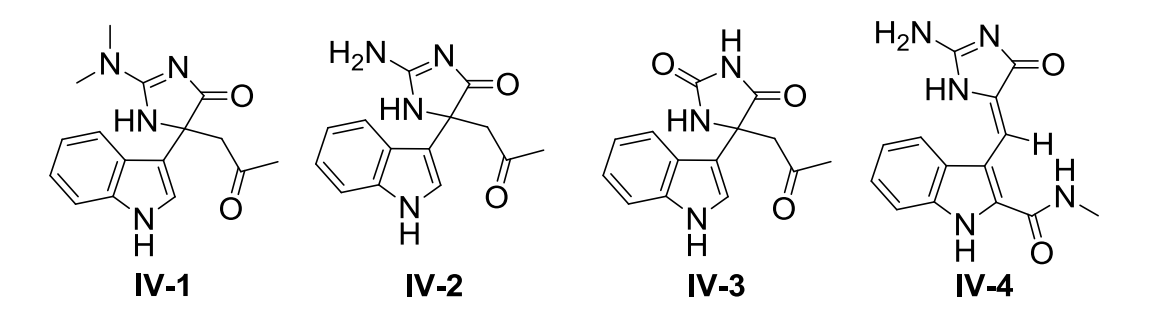


Figure IV-6. Structures of IV-1 – IV-4.

NF-кB-mediated gene transcription was evaluated by using a luciferase reporter assay in human cervical epithelial (HeLa) cells containing a stably transfected NF-kB-luc gene (Figure IV-7). The cells were pretreated for thirty minutes with II-70, II-84, or II-99 followed by activation with TNF- α (25 ng/mL). The proteasome inhibitor MG-132 125 was used as a positive control, and DMSO (vehicle) was used as a negative control. After 8 hours of incubation, luciferase production was evaluated. The samples were normalized to the TNF-α activation control. The results of the luciferase assay are summarized in Table IV-1. HeLa-NF-κB-luc cells pretreated with the analogs without activation by TNF-α did not induce a significant amount of luciferase activity. This was an indication that these compounds did not stimulate the NF-kB pathway alone. Compounds II-84, II-99 and IV-1 - IV-4 (Table IV-1) resulted in EC₅₀ values greater than 80 μM for NF-κB mediated gene transcription. Compound IV-4 showed a slight inhibition with an EC₅₀ value of 51.5 μM. **II-70** displayed inhibition of NF-κB mediated gene transcription with an EC₅₀ of 6.88 μM . **II-2** showed potent inhibition of NF-κB-mediated gene transcription with an EC50 of 0.64 µM. The related analogues were screened for inhibition of the kinases listed in Table IV-1.Compounds II-70, II-84, II-99, IV-1 - IV-4 were also evaluated for inhibition of other kinases involved in the NF-kB pathway. None of these

compounds showed significant inhibition of the kinases tested with most IC $_{50}$ values > 10,000 nM. In addition to inhibition of gene transcription compound **II-70** also inhibited GSK-3 β (86 nM).

Table IV-1. Kinase inhibition by hymenialdisine-derived analogs.

	II-2	II-70	II-84	II-99	IV-1	IV-2	IV-3	IV-4
HeLa NF-кВ-luc (µМ)	0.64	6.88	> 80	> 80	> 80	> 80	> 80	51.5
GSK-3β (μM)	0.073 ^{120, 126}	0.086	NA	NA	> 50	> 50	> 50	NA
Chk1 (µM)	1.950 ¹²⁷	0.237	> 10	> 10	> 10	> 10	> 10	> 10
Chk2 (µM)	0.042 ¹²⁷	0.008	> 10	> 10	> 10	> 10	> 10	> 10
CK1δ(h) (μM)	0.035 ^{120, 126}	1.352	> 10	> 10	> 10	> 10	> 10	> 10
CK2 (h) (µM)	7 ^{120, 126}	> 10	> 10	> 10	> 10	> 10	> 10	> 10
IKKα(h) (μM)	> 10 ^{120, 126}	> 10	> 10	> 10	> 10	> 10	> 10	> 10
IKKβ(h) (μM)	> 5 ^{120, 126}	> 10	> 10	> 10	> 10	> 10	> 10	> 10
MEK1(h) (µM)	0.006 ¹²⁸	0.089	NA	NA	NA	NA	NA	NA
PKCα(h) (μM)	0.7 ^{120, 126}	2.539	NA	NA	NA	NA	NA	NA
PKCβII(h) (nM)	1200 ^{120, 126}	3,381	NA	NA	NA	NA	NA	NA

The lack of inhibition with compounds II-84, II-99, IV-1 – IV-4 could give an indication of key structural requirements for biological activity. II-84 has a hydantoin ring lacking a hydrogen donor for hydrogen bonding. II-99 contains a dimethyl amine that may prevent efficient binding due to the bulky steric interactions resulting in a poor inhibitor of NF-κB. II-70 possesses a free amine on the glycocyamidine ring offering a hydrogen donor and possibly contributing to the inhibitor activity. IV-1 – IV-4 were also unable to inhibit any of the kinases evaluated in Table IV-1. The azepine ring present in II-70 was absent in IV-1 – IV-4 suggesting the importance of the amide in the binding

pocket. Although compound **IV-2** contained the glycocyamidine ring, no inhibition of kinase activity was found. This could indicate that the free amine is not the only requirement for binding and activity. Compound **IV-4** has the glycocyamidine ring as well as an amide nitrogen at the 2-indole position. With the free amine on the glycocyamidine ring and the methyl amide, **IV-4** gains back some inhibition activity for NF-κB-mediated gene transcription with an EC_{50} of 51.5μM.

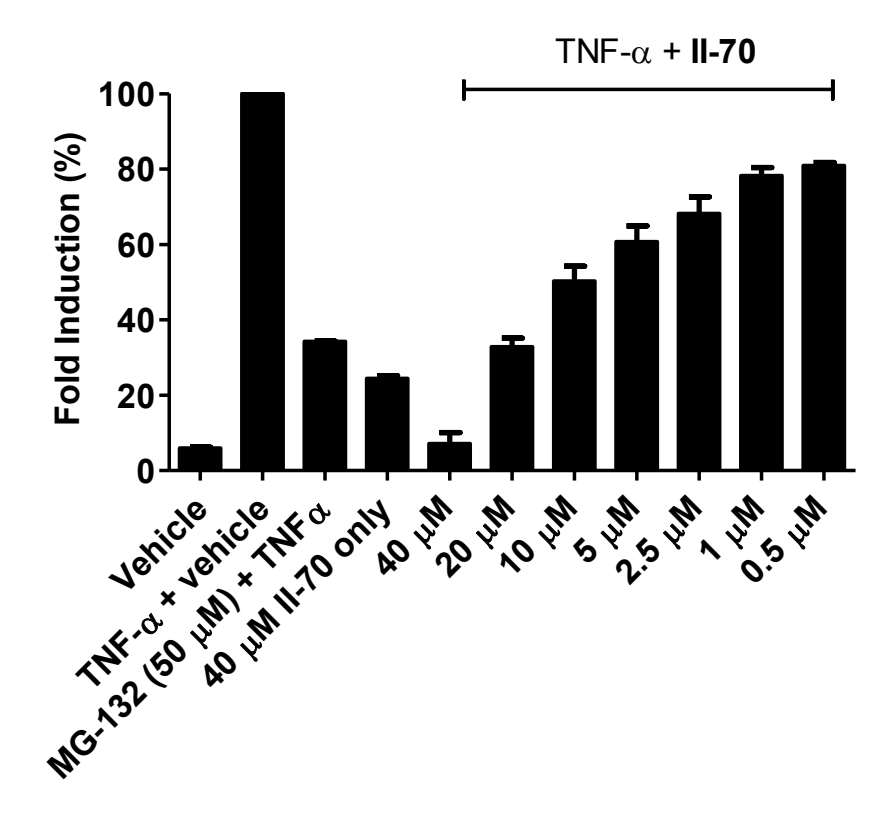


Figure IV-7. Dose-response activity of **II-70** in inhibition of luciferase production in HeLa-NF-κB-luc cells.

IV.D Evaluation of II-70 as an inhibitor of IL-1 β induced TNF- α production in human whole blood

The results of the luciferase reporter assay lead to further analysis of **II-70** for its anti-inflammatory potential in human whole blood. **II-70** was evaluated for its ability to

inhibit an NF-κB mediated cytokine response in IL-1 β stimulated human blood (Theresa Landsell). Human whole blood was pretreated with II-70 for 2 hours and was stimulated by IL-1 β . Plasma was harvested 22 hours after stimulation. IL-1 β induced TNF- α production was measured using a human TNF- α ELISA assay. The amount of IL-1 β induced TNF- α production was significantly higher than the level of TNF- α in the unstimulated vehicle treated blood (Figure IV-8). Dexamethasone (dex) is an anti-inflammatory drug known to inhibit TNF- α production 129 and was used here as a positive control. II-70 inhibited TNF- α production in a dose-dependent manner (EC₅₀ = 4 μM) as compared to the vehicle treated control. Due to the lack of inhibition against any kinases examined in Table IV-1, II-84, II-99, IV-1 – IV-4 were not evaluated in human whole blood.

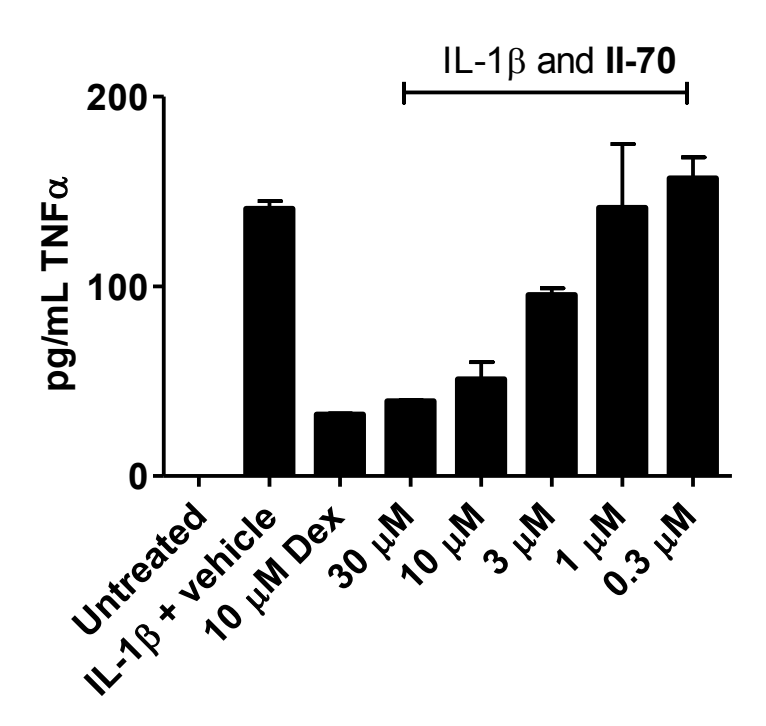


Figure IV-8. Dose-response activity of **II-70** in inhibition of TNF- α production in IL-1 β stimulated human blood.

IV.E Evaluation of II-70 as an inhibitor of NF-kB in vitro.

II-70 demonstrated inhibition of NF-κB mediated gene transcription and TNF-α production. The mechanism of action of II-70 in the NF-κB pathway remained unclear. *In vitro* evaluation of NF-κB translocation of the p65 subunit followed. HeLa-NF-κB-luc cells were pretreated with II-70, DMSO or MG-132 for 30 minutes at varying concentrations. The cells were then activated with TNF-α (10 ng/mL) for 30 minutes. Nuclear extracts were collected and western blot analysis ensued as seen in Figure IV-9. Samples that were not activated with TNF-α did not show increased basal levels of p65. II-70 alone did not increase levels of p65 indicating that it is not an activator of NF-κB. The combination of TNF-α and II-70 at high (30 μM) and low (3 μM) doses did not show any decrease in levels of activated p65. Levels of induced p65 were inhibited by the proteasome inhibitor MG-132 (Figure IV-9), the positive control. This illustrates that II-70 is not inhibiting nuclear translocation of the p65 subunit of NF-κB.

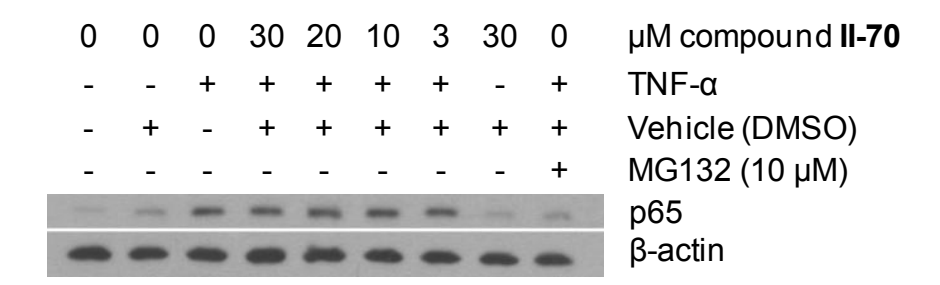


Figure IV-9. Western blot of TNF- α induced p65 after 30 minutes in HeLa-NF- κ B-luc cells.

II-70 was then evaluated for its ability to inhibit phosphorylation of p65. The nuclear extracts collected above were analyzed with Western blot and probed for p-p65 at phosphorylation sites S276, S468 and S536. GSK-3β is known to phosphorylate p65 at S468 as mentioned above, ¹⁰³ Although **II-70** inhibits GSK-3β at 86 nM, there was no

evidence of inhibition of phosphorylation of S468 (Figure IV-10). **II-70** did not inhibit phosphorylation at S276 or at S536 at any concentration.

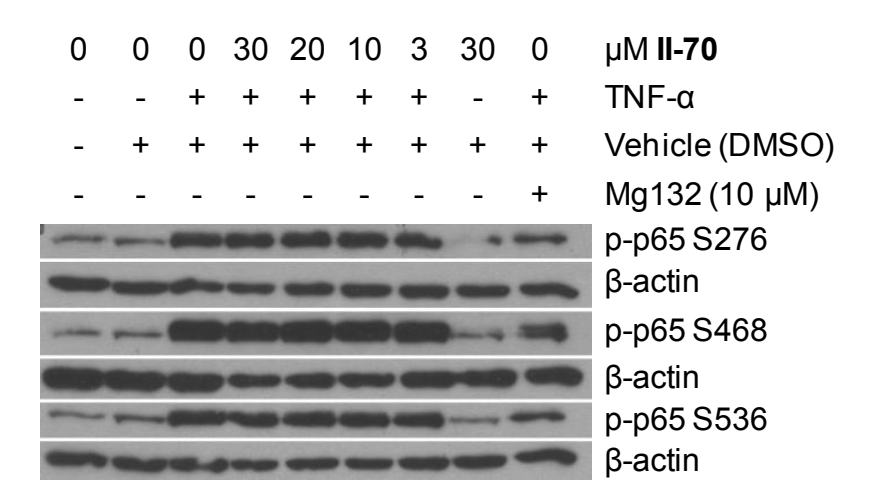


Figure IV-10. Western blot of HeLa cells with TNF-α induced p-p65 after 30 minutes.

Inhibition of NF-κB-DNA binding was evaluated next with II-70. The cellular nuclei were isolated and evaluated for NF-κB-DNA binding utilizing the fluorescent-labeled NF-κB-DNA consensus sequence (Figure IV-11). Nuclear extracts stimulated with TNF-α and the NF-κB consensus oligo resulted in DNA binding to NF-κB (Figure IV-11, lanes 3-7). As a negative control, cells were left unactivated and were also exposed to the NF-κB consensus sequence, resulting in background NF-κB/DNA binding (Figure IV-11, lanes 1-2). Treatment of cells with II-70 followed by TNF-α did not result in inhibition of NF-κB/DNA (Figure IV-11, lanes 4-7). II-70, at 30 μM without TNF-α stimulation did not accumulate NF-κB/DNA binding (Figure IV-11, lane 8). NF-κB-mediated gene transcription *in vitro* in addition to TNF-α production in whole human blood was inhibited by II-70. Cellular studies indicated that II-70 was did not inhibit translocation of p65 into the nucleus. The EMSA assay shows that NF-κB/DNA binding is also not inhibited by II-70.

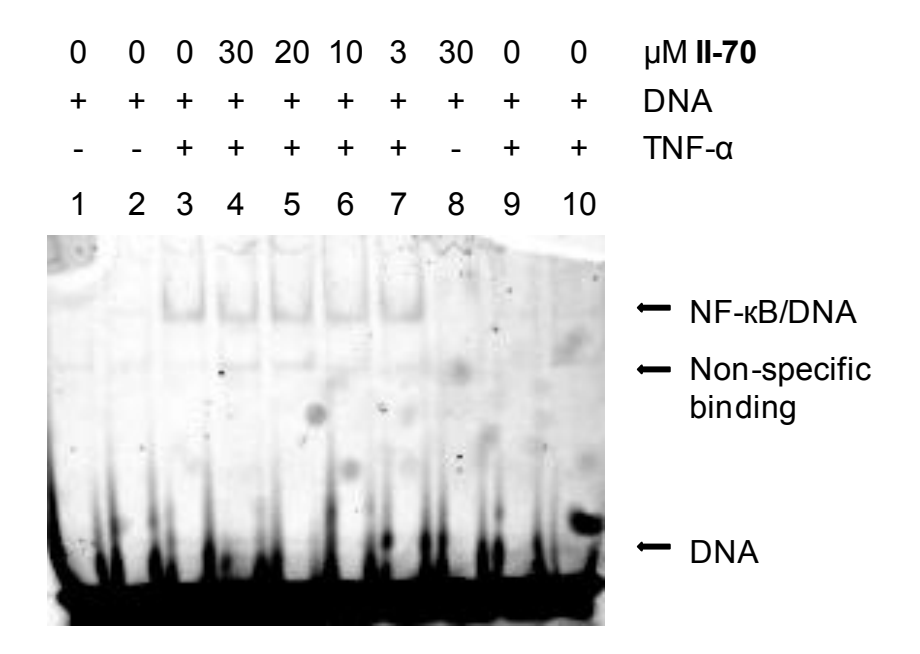


Figure IV-11. EMSA Assay for NF- κ B Activation by TNF- α (10 ng/mL).

In summary, a series of indole analogs inspired by hymenialdisine and the marine alkaloid from *Dendrodoa grossularia* were prepared and evaluated for their biological activity. Most of the synthesized compounds were not biologically active with the exception of **II-70**. A kinase inhibition panel revealed that **II-70** inhibited GSK-3β (86 nM). Further evaluation of **II-70** demonstrated its ability to inhibit NF-κB mediated gene transcription (6.88 μM) as well as TNF-α production in human whole blood (4 μM). The analogs synthesized (**II-84** and **II-99**) lost activity when the free amine was replaced with dimethyls or an oxygen.. Further cellular studies concluded that **II-70** does not inhibit p65 translocation into the nucleus, nor does it inhibit phosphorylation of p65. An EMSA binding assay revealed that **II-70** does not inhibit NF-κB/DNA binding.

IV.F General experimental information

All cell lines were cultured at 37°C with 5% bone dry CO2 atmosphere, 97% humidity and ambient O2 in a Napco water-jacketed incubaor. Adherent cells were routinely passaged by 0.25% trypsin-EDTA (Invitrogen, Fredrick, MD) using sterile technique and materials in a Nuaire biological safety cabinet Class II type A2. For all lysate and whole cell experiments, the inhibitors were dissolved in DMSO and the final DMSO concentration of the experiments was maintained at $\leq 0.1\%$ in the reaction buffer or culture medium. Cells were observed using a 1200CMI series spectrum inverted microscope. Cells were counted with a hemacytometer or using the Beckman Coulter Z1 Coulter® Particle Counter. Centrifugation was performed using the Beckman Coulter Allegra X-15R Centrifuge or Spectrafuge 16M microcentrifuge. Buffers, solutions and media were made with water purified with the Millipore Quantum® Ex filtration system. Buffers requiring pH adjustments were monitored with a Mettler Toledo SevenEasy pH meter. Protein assays were read using the Molecular Devices SpectraMax M5^e plate reader. Western blots were run on hand-poured SDS PAGE gels using the BioRad mini protean pouring and electrophoresis system with the BioRad PowerPac HC. Gels were transferred to polyvinylidene fluoride membrane (BioRad) with the BioRad Criterion blotter wet transfer system. Blots and gels were quantified using the BioRad Molecular Imager FX. Luminescence in the luciferase assays were monitored and quantified using the Turner Biosystems Veritas Microplate Luminometer.

Cell Culture. The human cell line HeLa-NF-κB-luc was purchased from Panomics, Inc. (Fremont, CA). the cells were maintained in Dulbecco's Modified Eagle's Medium (DMEM, Invitrogen, Fredrick, MD) containing 4.5 g/L glucose, 3.7 g/L

bicarbonate, and supplemented with 5% fetal bovine serum, 100 U/ml penicillin, 100 μg/mL streptomycin, 1 mM sodium pyruvate, 0.2 mM L-glutamine, and 100 μg/mL of hygromycin B. Cells were cultured at 37°C, 5% CO₂ atmosphere, 97% relative humidity and were routinely passaged by 0.25% trypsin-EDTA (Invitrogen, Fredrick, MD) treatment according to ATCC protocol.

NF-kB-luc reporter assay. HeLa NF-κB-luc cells (5.0 x 10⁵ cells/ml) were seeded into a 96-well white opaque plate using DMEM medium supplemented with 5% fetal bovine serum, 100 U/ml penicillin, 100 µg/mL streptomycin, 1 mM sodium pyruvate. 0.2 mM L-glutamine, and 100 µg/mL of hygromycin B (Roche). After 24 h the cell culture medium was replaced with DMEM medium supplemented with 100 U/ml penicillin, 100 µg/mL streptomycin, 1 mM sodium pyruvate, and 0.2 mM L-glutamine. Cell cultures were pretreated with vehicle (1% DMSO), 50 µM Mg132 (EMD Biosciences, San Diego, CA) or analogues II-70, II-84, and II-99 (final concentrations were 40, 20, 10, 5, 2.5, 1, 0.5 µM (II-70) and 80, 40, 20, 10, 5, 2,5, 1.25 μ M (II-84, and II-99) for 30 min at 37°C in 5% CO₂. TNF-α (Invitrogen Cytokines & Signaling, Camarillo, CA) was added to a final concentration of 25 ng/mL and the samples were further incubated for 8 hours at 37°C in 5% CO₂. The plate and Steady-Glo assay reagent (Promega Corporation, Madison, WI) were equilibrated to room temperature. An equal volume of Steady-Glo assay reagent was added to each well. The contents of the plate were gently mixed for 5 min and the luminescence of each well was measured using a Veritas microplate luminometer (Turner Biosystems, CA). All reported data are the average of two independent experiments. The data were analyzed using GraphPad Prism 5.0. The data was

normalized to TNF- α activation and the EC₅₀ values were calculated using the equation for the sigmoidal curve for variable slope.

GSK-3β, Chk1, Chk2, CK1δ, CK2, IKKα, IKKβ, MEK1, PKCα, PKCβ in vitro kinase assay. Compounds evaluated were tested in vitro against the kinases indicated by Millipore UK limited, Dundee, UK using a Kinase Profiler Assay according to the manufacture's protocol. Briefly, in a final volume of 25 μL, the kinase was incubated with the desired buffer and the required polypeptide substrate, in presence of 10 mM magnesium acetate and γ -³³P-ATP (10 μM). After incubation for 40 min at room temperature, the reaction was stopped by the addition of 3% H₃PO₄ (5μL). A 10μL aliquot of the reaction was then spotted on a P30 filtermat and washed 3 X in 75 mM H₃PO₄ and finally in methanol. Samples were then dried and signals counted on a scintillation counter.

Human whole blood IL-1β challenge. After obtaining the appropriate approval for de-identified human cell lines, human whole blood was obtained through the Jasper Research Clinic, Kalamazoo, MI, from a single healthy, fasted human volunteer and was collected in glass citrated tubes by venipuncture. Only samples with a white blood count falling within normal range (4,800-10,800 white blood cells per liter) were used. To support the viability of white blood cells, blood was diluted 1:10 in RPMI-1640 media supplemented with 10% fetal bovine serum, 100 U/mL penicillin, and 100 μg/mL streptomycin. Aliquots of diluted blood (1 mL) were preincubated with vehicle (0.1% DMSO, final concentration) or II-70 (final concentrations were 30, 10, 3, 1, 0.3 μM) for 2 hours at 37°C in 5% CO₂. IL-1β (Roche) was added to a final concentration of 200 U/mL and the samples were further incubated for 18 hours at 37°C in 5% CO₂. At the end of

the incubation period, the blood samples were centrifuged at 3000 rpm for 5 min. The plasma was removed, snap frozen and stored at -80°C.

Western blot analysis. Cells were cultured in 100 mm plates until ~80% confluence. Cells were pre-treated with II-70 (in DMSO) for 30 minutes, then activated with TNF-α (10 ng/ml) for 30 minutes. Cells were then with ice cold PBS (2 ml) twice. PBS was then removed and lysis buffer (10 mM HEPES (pH =7.9), 1% Igepal-630, 1.5 mM MgCl₂, 10 mM KCl₂, 20 μ M DTT, 2 μ M NaVO₄, 2 μ M NaF, 2 μ M PMSF, 0.02 μ g/ml Aprotinin, 0.02 µg/ml Leupeptin) was added and rocked at 4°C for 10 minutes. Samples were vortexed and centrifuged at 3000 RPM for 3 minutes. Cytosolic extracts were removed and nuclear extracts were lysed open with high salt buffer (3.4 M glycerol, 2 0mM HEPES (pH=7.9), 1.5 mM MgCl₂, 0.42 M NaCl, 0.1 M EDTA, 20 μM DTT, 2 μM NaVO₄, 2 μM NaF, 2 μM PMSF, 0.02 μg/ml Aprotinin, 0.02 μg/ml Leupeptin). The samples were vortex at 2,000 RPM for 20 minutes and centrifuged at 3000 RPM for 15 minutes. 25 µg of protein (quantified with Bradford assay (BioRad, Hercules, CA)) was diluted with 2X SDS-PAGE buffer and water to bring to equal volumes, and boiled for 3 minutes. Equal volumes of boiled protein were electrophoresed on SDS-polyacrylamide gels and transferred to PVDF membranes using wet transfer. Membranes were blocked with 4% blocking grade non-fat dairy milk (NFDM) for 1 hour at room temperature and washed with Tris-buffered saline-Tween 20 (TBS-T) containing 10X Tris Buffer and 0.1% Tween 20 for 10 minutes. Blots were then probed with primary AB NF-kB p65 (Santa Cruz Biotechnology, CA) 1:1000 dilution in 4% NFDM (1 hour room temperature) and were washed with TBS-T (3 x 10 minutes). AB NF-kB Phospho-p65 S276, S468, S536 (Cell Signaling Technology, MA) were diluted (1:1000) in TBS-T containing 5% w/v bovine serum albumin (Sigma, WI). They were then incubated with horse radish peroxidase conjugated to secondary antibody goat anti-rabbit (Cell Signaling Technology) diluted 1:2000 in TBS-T containing 5% BSA. Actin antibody (1:10,000 dilution) (Amersham) was incubated in 4% NFDM in TBS-T, washed and incubated with horse radish peroxidase conjugated to secondary antibody mouse (1:3,000 dilution in 4% NFDM). Complexes were detected by enhanced chemiluminescence (ECL) technique according to manufacturer's directions (Denville) on XAR film.

EMSA Assay for NF-κB-DNA binding. HeLa-NF-κB-luc cells were cultured in 100 mm plates until ~80% confluence. Cells were pre-treated with II-70 (in DMSO) for 30 minutes, then activated with TNF-α (10 ng/ml) for 30 minutes. Nuclear extracts were collected as previously described. Nuclear extracts (20 μg total protein) were incubated for 20 min at room temperature with a double-stranded Cy3-labelled NF-κB consensus oligonucleotide, 5'-AGTTGAGGGGACTTTC CCAGGC-3' (0.16 pmol). The binding mixture (40 μL) contained 500 mM KCl, 25 mM DTT, 0.5% Igepal CA-630, 1 μg/μL herring sperm DNA. The mixture was loaded on a 5% TBE gel prepared in 1 X Tris borate/EDTA buffer and electrophoresed at 120V for 30 min. After electrophoresis, the gel was analyzed using a phosphorimager (Biorad FX plus) for detection of NF-κB-DNA binding.

REFERENCES

IV.H References

- 1. Sakurai, H.; Suzuki, S.; Kawasaki, N.; Nakano, H.; Okazaki, T.; Chino, A.; Doi, T.; Saiki, I., Tumor necrosis factor-alpha-induced IKK phosphorylation of NF-kappaB p65 on serine 536 is mediated through the TRAF2, TRAF5, and TAK1 signaling pathway. *J. Biol. Chem.* **2003**, 278 (38), 36916-23.
- 2. Silverman, N.; Maniatis, T., NF-kappaB signaling pathways in mammalian and insect innate immunity. *Genes Dev.* **2001**, *15* (18), 2321-42.
- 3. Baldwin, A. S., Jr., Series introduction: the transcription factor NF-kappaB and human disease. *J. Clin. Invest.* **2001**, *107* (1), 3-6.
- 4. Tak, P. P.; Firestein, G. S., NF-kappaB: a key role in inflammatory diseases. *J. Clin. Invest.* **2001**, *107* (1), 7-11.
- 5. Baldwin, A. S., Control of oncogenesis and cancer therapy resistance by the transcription factor NF-kappaB. *J. Clin. Invest.* **2001**, *107* (3), 241-6.
- 6. Ghosh, S.; Karin, M., Missing pieces in the NF-kappaB puzzle. *Cell* **2002**, *109 Suppl*, S81-96.
- 7. Baeuerle, P. A.; Henkel, T., Function and activation of NF-kappa B in the immune system. *Annu. Rev. Immunol.* **1994,** *12*, 141-79.
- 8. Baldwin, A. S., Jr., The NF-kappa B and I kappa B proteins: new discoveries and insights. *Annu. Rev. Immunol.* **1996,** *14*, 649-83.
- 9. Perkins, N. D., Achieving transcriptional specificity with NF-kappa B. *Int. J. Biochem. Cell Biol.* **1997**, *29* (12), 1433-1448.
- 10. Webster, G. A.; Perkins, N. D., Transcriptional cross talk between NF-kappa B and p53. *Mol. Cell. Biol.* **1999**, *19* (5), 3485-3495.
- 11. Karin, M.; Ben-Neriah, Y., Phosphorylation meets ubiquitination: the control of NF-[kappa]B activity. *Annu. Rev. Immunol.* **2000**, *18*, 621-63.

- 12. Malek, S.; Chen, Y.; Huxford, T.; Ghosh, G., I kappa B beta but not I kappa B alpha, functions as a classical cytoplasmic inhibitor of NF-kappa B dimers by masking both NF-kappa B nuclear localization sequences in resting cells. *J. Biol. Chem.* **2001**, *276* (48), 45225-45235.
- 13. Huang, T. T.; Miyamoto, S., Postrepression activation of NF-kappa B requires the amino-terminal nuclear export signal specific to I kappa B alpha. *Mol. Cell. Biol.* **2001**, *21* (14), 4737-4747.
- 14. Hayden, M. S.; Ghosh, S., Signaling to NF-kappaB. *Genes Dev.* **2004,** *18* (18), 2195-224.
- 15. Steinbrecher, K. A.; Wilson, W., 3rd; Cogswell, P. C.; Baldwin, A. S., Glycogen synthase kinase 3beta functions to specify gene-specific, NF-kappaB-dependent transcription. *Mol. Cell Biol.* **2005**, *25* (19), 8444-55.
- 16. Liu, S. X.; Yu, Y. Z.; Zhang, M. H.; Wang, W. Y.; Cao, X. T., The involvement of TNF-alpha-related apoptosis-inducing ligand in the enhanced cytotoxicity of IFN-beta-stimulated human dendritic cells to tumor cells. *J. Immunol.* **2001,** *166* (9), 5407-5415.
- 17. Lin, Y. C.; Brown, K.; Siebenlist, U., Activation of NF-kappa-B requires proteolysis of the inhibitor I-kappa-alpha signal induced phosphorylation of I-kappa-B-alpha alone does not release active NF-kappa-B. *Proc. Natl. Acad. Sci. U. S. A.* **1995,** *92* (2), 552-556.
- 18. Palombella, V. J.; Rando, O. J.; Goldberg, A. L.; Maniatis, T., The ubiquitin-proteasome pathway is required for processing the NF-kappa-B1 precursor protein and the activation of NF-kappa-B. *Cell* **1994**, *78* (5), 773-785.
- 19. Janssens, S.; Tschopp, J., Signals from within: the DNA-damage-induced NF-kappa B response. *Cell Death Differ.* **2006**, *13* (5), 773-784.
- 20. Boland, M. P., DNA damage signalling and NF-kappa B: implications for survival and death in mammalian cells. *Biochem. Soc. Trans.* **2001**, 29, 674-678.
- 21. Baichwal, V. R.; Baeuerle, P. A., Apoptosis: Activate NF-kappa B or die? *Curr. Biol.* **1997**, *7* (2), R94-R96.

- 22. Sakurai, H.; Suzuki, S.; Kawasaki, N.; Nakano, H.; Okazaki, T.; Chino, A.; Doi, T.; Saiki, I., Tumor necrosis factor-alpha-induced IKK phosphorylation of NF-kappaB p65 on serine 536 is mediated through the TRAF2, TRAF5, and TAK1 signaling pathway. *J. Biol. Chem.* **2003**, *278* (38), 36916-23.
- 23. Vermeulen, L.; De Wilde, G.; Notebaert, S.; Vanden Berghe, W.; Haegeman, G., Regulation of the transcriptional activity of the nuclear factor-kappa B p65 subunit. *Biochem. Pharmacol.* **2002**, *64* (5-6), 963-970.
- 24. Richmond, A., NF-kappa B, chemokine gene transcription and tumour growth. *Nat. Rev. Immunol.* **2002**, *2* (9), 664-674.
- 25. Buss, H.; Dorrie, A.; Schmitz, M. L.; Frank, R.; Livingstone, M.; Resch, K.; Kracht, M., Phosphorylation of serine 468 by GSK-3beta negatively regulates basal p65 NF-kappaB activity. *J. Biol. Chem.* **2004**, *279* (48), 49571-4.
- 26. Zhong, H.; Voll, R. E.; Ghosh, S., Phosphorylation of NF-kappa B p65 by PKA stimulates transcriptional activity by promoting a novel bivalent interaction with the coactivator CBP/p300. *Mol. Cell* **1998**, *1* (5), 661-71.
- 27. Zhong, H.; May, M. J.; Jimi, E.; Ghosh, S., The phosphorylation status of nuclear NF-kappa B determines its association with CBP/p300 or HDAC-1. *Mol. Cell* **2002**, *9* (3), 625-36.
- 28. Okazaki, T.; Sakon, S.; Sasazuki, T.; Sakurai, H.; Doi, T.; Yagita, H.; Okumura, K.; Nakano, H., Phosphorylation of serine 276 is essential for p65 NF-kappaB subunit-dependent cellular responses. *Biochem. Biophys. Res. Commun.* **2003**, 300 (4), 807-12.
- 29. Madrid, L. V.; Mayo, M. W.; Reuther, J. Y.; Baldwin, A. S., Akt stimulates the transactivation potential of the RelA/p65 subunit of NF-kappa B through utilization of the I kappa B kinase and activation of the mitogen-activated protein kinase p38. *J. Biol. Chem.* **2001,** 276 (22), 18934-18940.
- 30. Jiang, X.; Takahashi, N.; Matsui, N.; Tetsuka, T.; Okamoto, T., The NF-kappa B activation in lymphotoxin beta receptor signaling depends on the phosphorylation of p65 at serine 536. *J. Biol. Chem.* **2003**, *278* (2), 919-926.

- 31. Wang, D.; Westerheide, S. D.; Hanson, J. L.; Baldwin, A. S., Tumor necrosis factor alpha-induced phosphorylation of RelA/p65 on Ser(529) is controlled by casein kinase II. *J. Biol. Chem.* **2000**, *275* (42), 32592-32597.
- 32. Sakurai, H.; Chiba, H.; Miyoshi, H.; Sugita, T.; Toriumi, W., IkappaB kinases phosphorylate NF-kappaB p65 subunit on serine 536 in the transactivation domain. *J. Biol. Chem.* **1999**, *274* (43), 30353-6.
- 33. Wang, D.; Baldwin, A. S., Activation of nuclear factor-kappa B-dependent transcription by tumor necrosis factor-alpha is mediated through phosphorylation of RelA/p65 on serine 529. *J. Biol. Chem.* **1998**, *273* (45), 29411-29416.
- 34. Vermeulen, L.; De Wilde, G.; Van Damme, P.; Vanden Berghe, W.; Haegeman, G., Transcriptional activation of the NF-kappa B p65 subunit by mitogen- and stress-activated protein kinase-1 (MSK1). *EMBO J.* **2003**, *22* (6), 1313-1324.
- 35. Makarov, S. S., NF-kappa B in rheumatoid arthritis: a pivotal regulator of inflammation, hyperplasia, and tissue destruction. *Arthritis Res.* **2001**, *3* (4), 200-6.
- 36. Okazaki, Y.; Sawada, T.; Nagatani, K.; Komagata, Y.; Inoue, T.; Muto, S.; Itai, A.; Yamamoto, K., Effect of nuclear factor-kappaB inhibition on rheumatoid fibroblast-like synoviocytes and collagen induced arthritis. *J. Rheumatol.* **2005**, 32 (8), 1440-7.
- 37. Ardizzone, S.; Bianchi Porro, G., Biologic therapy for inflammatory bowel disease. *Drugs* **2005**, *65* (16), 2253-86.
- 38. Boone, D. L.; Lee, E. G.; Libby, S.; Gibson, P. J.; Chien, M.; Chan, F.; Madonia, M.; Burkett, P. R.; Ma, A., Recent advances in understanding NF-kappaB regulation. *Inflamm. Bowel Dis.* **2002**, *8* (3), 201-12.
- 39. Schreiber, S.; Nikolaus, S.; Hampe, J., Activation of nuclear factor kappa B inflammatory bowel disease. *Gut* **1998**, *42* (4), 477-84.
- 40. van Den Brink, G. R.; ten Kate, F. J.; Ponsioen, C. Y.; Rive, M. M.; Tytgat, G. N.; van Deventer, S. J.; Peppelenbosch, M. P., Expression and activation of NF-kappa B in the antrum of the human stomach. *J. Immunol.* **2000**, *164* (6), 3353-9.

- 41. de Winther, M. P.; Kanters, E.; Kraal, G.; Hofker, M. H., Nuclear factor kappaB signaling in atherogenesis. *Arterioscler. Thromb. Vasc. Biol.* **2005**, *25* (5), 904-14.
- 42. Eggert, M.; Goertsches, R.; Seeck, U.; Dilk, S.; Neeck, G.; Zettl, U. K., Changes in the activation level of NF-kappa B in lymphocytes of MS patients during glucocorticoid pulse therapy. *J. Neurol. Sci.* **2008**, *264* (1-2), 145-150.
- 43. Hart, L. A.; Krishnan, V. L.; Adcock, I. M.; Barnes, P. J.; Chung, K. F., Activation and localization of transcription factor, nuclear factor-kappaB, in asthma. *Am. J. Respir. Crit. Care Med.* **1998**, *158* (5 Pt 1), 1585-92.
- 44. D'Acquisto, F.; May, M. J.; Ghosh, S., Inhibition of nuclear factor kappa B (NF-B): an emerging theme in anti-inflammatory therapies. *Mol. Interv.* **2002**, *2* (1), 22-35.
- 45. Renard, P.; Raes, M., The proinflammatory transcription factor NFkappaB: a potential target for novel therapeutical strategies. *Cell Biol. Toxicol.* **1999**, *15* (6), 341-4.
- 46. Sharma, V.; Hupp, C. D.; Tepe, J. J., Enhancement of chemotherapeutic efficacy by small molecule inhibition of NF-kappaB and checkpoint kinases. *Curr. Med. Chem.* **2007**, *14* (10), 1061-74.
- 47. Feinman, R.; Koury, J.; Thames, M.; Barlogie, B.; Epstein, J.; Siegel, D. S., Role of NF-kappa B in the rescue of multiple myeloma cells from glucocorticoid-induced apoptosis by bcl-2. *Blood* **1999**, 93 (9), 3044-3052.
- 48. Griffin, J. D., Leukemia stem cells and constitutive activation of NF-kappa B. *Blood* **2001**, *98* (8), 2291-2291.
- 49. Kordes, U.; Krappmann, D.; Heissmeyer, V.; Ludwig, W. D.; Scheidereit, C., Transcription factor NF-kappa B is constitutively activated in acute lymphoblastic leukemia cells. *Leukemia* **2000**, *14* (3), 399-402.
- 50. Baron, F.; Turhan, A. G.; Giron-Michel, J.; Azzarone, B.; Bentires-Alj, M.; Bours, V.; Bourhis, J. H.; Chouaib, S.; Caignard, A., Leukemic target susceptibility to natural killer cytotoxicity: relationship with BCR-ABL expression. *Blood* **2002**, *99* (6), 2107-2113.

- 51. Palayoor, S. T.; Youmell, M. Y.; Calderwood, S. K.; Coleman, C. N.; Price, B. D., Constitutive activation of I kappa B kinase alpha and NF-kappa B in prostate cancer cells is inhibited by ibuprofen. *Oncogene* **1999**, *18* (51), 7389-7394.
- 52. Nakshatri, H.; BhatNakshatri, P.; Martin, D. A.; Goulet, R. J.; Sledge, G. W., Constitutive activation of NF-kappa B during progression of breast cancer to hormone-independent growth. *Mol. Cell. Biol.* **1997**, *17* (7), 3629-3639.
- 53. Wang, W. X.; Abbruzzese, J. L.; Evans, D. B.; Larry, L.; Cleary, K. R.; Chiao, P. J., The nuclear factor-kappa B RelA transcription factor is constitutively activated in human pancreatic adenocarcinoma cells. *Clin. Cancer Res.* **1999**, *5* (1), 119-127.
- 54. Takai, H.; Tominaga, K.; Motoyama, N.; Minamishima, Y. A.; Nagahama, H.; Tsukiyama, T.; Ikeda, K.; Nakayama, K.; Nakanishi, M.; Nakayama, K., Aberrant cell cycle checkpoint function and early embryonic death in Chk1(-/-) mice. *Genes Dev.* **2000**, *14* (12), 1439-47.
- 55. Bottero, V.; Busuttil, V.; Loubat, A.; Magne, N.; Fischel, J. L.; Milano, G.; Peyron, J. F., Activation of nuclear factor kappa B through the IKK complex by the topoisomerase poisons SN38 and doxorubicin: A brake to apoptosis in HeLa human carcinoma cells. *Cancer Res.* **2001**, *61* (21), 7785-7791.
- 56. Piret, B.; Piette, J., Topoisomerase poisons activate the transcription factor NF-kappa B in ACH-2 and CEM cells. *Nucleic Acids Res.* **1996**, *24* (21), 4242-4248.
- 57. Sodhi, A.; Singh, R. A. K., Mechanism of NF-kappa B translocation in macrophages treated in vitro with cisplatin. *Immunol. Lett.* **1998,** *63* (1), 9-17.
- 58. Chen, J. S.; Lin, S. Y.; Tso, W. L.; Yeh, G. C.; Lee, W. S.; Tseng, H.; Chen, L. C.; Ho, Y. S., Checkpoint kinase 1-mediated phosphorylation of Cdc25C and bad proteins are involved in antitumor effects of loratedine-induced G(2)/M phase cell-cycle arrest and apoptosis. *Mol. Carcinog.* **2006**, *45* (7), 461-478.
- 59. Eichholtz-Wirth, H.; Sagan, D., I kappa B/NF-kappa B mediated cisplatin resistance in HeLa cells after low-dose gamma-irradiation is associated with altered SODD expression. *Apoptosis* **2000**, *5* (3), 255-263.

- 60. Maldonado, V.; MelendezZajgla, J.; Ortega, A., Modulation of NF-kappa B, p53 and Bcl-2 in apoptosis induced by cisplatin in HeLa cells. *Mut. Res. Fund. Mol. Mech. Mutag.***1997**, *381* (1), 67-75.
- 61. Salvatore, C.; Camarda, G.; Maggi, C. A.; Goso, C.; Manzini, S.; Binaschi, M., NF-kappa B activation contributes to anthracycline resistance pathway in human ovarian carcinoma cell line A2780. *Int. J. Oncol.* **2005**, *27* (3), 799-806.
- 62. Wang, Q. Z.; Fan, S. J.; Eastman, A.; Worland, P. J.; Sausville, E. A.; Oconnor, P. M., UCN-01, a potent abrogator of G(2) checkpoint function in cancer cells with disrupted p53. *J. Nat. Cancer Inst.* **1996**, *88* (14), 956-965.
- 63. Cusack, J. C., Jr.; Liu, R.; Baldwin, A. S., Jr., Inducible chemoresistance to 7-ethyl-10-[4-(1-piperidino)-1-piperidino]-carbonyloxycamptothe cin (CPT-11) in colorectal cancer cells and a xenograft model is overcome by inhibition of nuclear factor-kappaB activation. *Cancer Res.* **2000**, *60* (9), 2323-30.
- 64. Habraken, Y.; Piret, B.; Piette, J., S phase dependence and involvement of NF-kappaB activating kinase to NF-kappaB activation by camptothecin. *Biochem. Pharmacol.* **2001**, *62* (5), 603-16.
- 65. Jones, D. R.; Broad, R. M.; Madrid, L. V.; Baldwin, A. S., Jr.; Mayo, M. W., Inhibition of NF-kappaB sensitizes non-small cell lung cancer cells to chemotherapy-induced apoptosis. *Ann. Thorac. Surg.* **2000**, *70* (3), 930-6; discussion 936-7.
- 66. Weaver, K. D.; Yeyeodu, S.; Cusack, J. C., Jr.; Baldwin, A. S., Jr.; Ewend, M. G., Potentiation of chemotherapeutic agents following antagonism of nuclear factor kappa B in human gliomas. *J. Neurooncol.* **2003**, *61* (3), 187-96.
- 67. Wang, C. Y.; Cusack, J. C., Jr.; Liu, R.; Baldwin, A. S., Jr., Control of inducible chemoresistance: enhanced anti-tumor therapy through increased apoptosis by inhibition of NF-kappaB. *Nat. Med.* **1999**, *5* (4), 412-7.
- 68. Cusack, J. C., Jr.; Liu, R.; Houston, M.; Abendroth, K.; Elliott, P. J.; Adams, J.; Baldwin, A. S., Jr., Enhanced chemosensitivity to CPT-11 with proteasome inhibitor PS-341: implications for systemic nuclear factor-kappaB inhibition. *Cancer Res.* **2001**, *61* (9), 3535-40.

- 69. Sharma, V.; Peddibhotla, S.; Tepe, J. J., Sensitization of cancer cells to DNA damaging agents by imidazolines. *J. Am. Chem. Soc.* **2006**, *128* (28), 9137-9143.
- 70. Sovak, M. A.; Bellas, R. E.; Kim, D. W.; Zanieski, G. J.; Rogers, A. E.; Traish, A. M.; Sonenshein, G. E., Aberrant nuclear factor-kappa B/Rel expression and the pathogenesis of breast cancer. *J. Clin. Invest.* **1997**, *100* (12), 2952-2960.
- 71. Olivier, S.; Robe, P.; Bours, V., Can NF-kappa B be a target for novel and efficient anti-cancer agents? *Biochem. Pharmacol.* **2006**, 72 (9), 1054-1068.
- 72. Wang, C. Y.; Mayo, M. W.; Baldwin, A. S., Jr., TNF- and cancer therapy-induced apoptosis: potentiation by inhibition of NF-kappaB. *Science* **1996**, *274* (5288), 784-7.
- 73. Frelin, C.; Imbert, V.; Griessinger, E.; Peyron, A. C.; Rochet, N.; Philip, P.; Dageville, C.; Sirvent, A.; Hummelsberger, M.; Berard, E.; Dreano, M.; Sirvent, N.; Peyron, J. F., Targeting NF-kappa B activation via pharmacologic inhibition of IKK2-induced apoptosis of human acute myeloid leukemia cells. *Blood* **2005**, *105* (2), 804-811.
- 74. Bentires-Alj, M.; Barbu, V.; Fillet, M.; Chariot, A.; Relic, B.; Jacobs, N.; Gielen, J.; Merville, M. P.; Bours, V., NF-kappa B transcription factor induces drug resistance through MDR1 expression in cancer cells. *Oncogene* **2003**, *22* (1), 90-97.
- 75. Liu, Q. H.; Guntuku, S.; Cui, X. S.; Matsuoka, S.; Cortez, D.; Tamai, K.; Luo, G. B.; Carattini-Rivera, S.; DeMayo, F.; Bradley, A.; Donehower, L. A.; Elledge, S. J., Chk1 is an essential kinase that is regulated by Atr and required for the G(2)/M DNA damage checkpoint. *Genes Dev.* **2000**, *14* (12), 1448-1459.
- 76. Karin, M.; Lin, A., NF-kappaB at the crossroads of life and death. *Nat. Immunol.* **2002**, 3 (3), 221-7.
- 77. Zandi, E.; Karin, M., Bridging the gap: Composition, regulation, and physiological function of the I kappa B kinase complex. *Mol. Cell. Biol.* **1999**, *19* (7), 4547-4551.
- 78. Loercher, A.; Lee, T. L.; Ricker, J. L.; Howard, A.; Geoghegen, J.; Chen, Z.; Sunwoo, J. B.; Sitcheran, R.; Chuang, E. Y.; Mitchell, J. B.; Baldwin, A. S.; Van

- Waes, C., Nuclear factor-kappa B is an important modulator of the altered gene expression profile and malignant phenotype in squamous cell carcinoma. *Cancer Res.* **2004**, *64* (18), 6511-6523.
- 79. Robe, P. A.; Bentires-Alj, M.; Bonif, M.; Rogister, B.; Deprez, M.; Haddada, H.; Khac, M. T. N.; Jolois, O.; Erkmen, K.; Merville, M. P.; Black, P. M.; Bours, V., In vitro and in vivo activity of the nuclear factor-kappa B inhibitor sulfasalazine in human glioblastomas. *Clin. Cancer Res.* **2004**, *10* (16), 5595-5603.
- 80. Kim, H. J.; Hawke, N.; Baldwin, A. S., NF-kappa B and IKK as therapeutic targets in cancer. *Cell Death Differ.* **2006**, *13* (5), 738-747.
- 81. Pikarsky, E.; Ben-Neriah, Y., NF-kappa B inhibition: A double-edged sword in cancer? *Eur. J. Cancer* **2006**, *42* (6), 779-784.
- 82. Rayet, B.; Gelinas, C., Aberrant rel/nfkb genes and activity in human cancer. *Oncogene* **1999**, *18* (49), 6938-6947.
- 83. Greten, F. R.; Eckmann, L.; Greten, T. F.; Park, J. M.; Li, Z. W.; Egan, L. J.; Kagnoff, M. F.; Karin, M., IKK beta links inflammation and tumorigenesis in a mouse model of colitis-associated cancer. *Cell* **2004**, *118* (3), 285-296.
- 84. Pikarsky, E.; Porat, R. M.; Stein, I.; Abramovitch, R.; Amit, S.; Kasem, S.; Gutkovich-Pyest, E.; Urieli-Shoval, S.; Galun, E.; Ben-Neriah, Y., NF-kappa B functions as a tumour promoter in inflammation-associated cancer. *Nature* **2004**, *431* (7007), 461-466.
- 85. Liao, C. H.; Pan, S. L.; Guh, J. H.; Chang, Y. L.; Pai, H. C.; Lin, C. H.; Teng, C. M., Antitumor mechanism of evodiamine, a constituent from Chinese herb Evodiae fructus, in human multiple-drug resistant breast cancer NCI/ADR-RES cells in vitro and in vivo. *Carcinogenesis* **2005**, *26* (5), 968-975.
- 86. Huang, Y. C.; Guh, J. H.; Teng, C. M., Induction of mitotic arrest and apoptosis by evodiamine in human leukemic T-lymphocytes. *Life Sci.* **2004,** *75* (1), 35-49.
- 87. Takada, Y.; Kobayashi, Y.; Aggarwal, B. B., Evodiamine abolishes constitutive and inducible NF-kappa B activation by inhibiting I kappa B alpha kinase activation, thereby suppressing NF-kappa B-regulated antiapoptotic and metastatic gene expression, up-regulating apoptosis, and inhibiting invasion. *J. Biol. Chem.* **2005**, *280* (17), 17203-17212.

- 88. Kwok, B. H.; Koh, B. D.; Ndubuisi, M. I.; Elofsson, M.; Crews, C. M., The sesquiterpene lactone parthenolide binds and inhibits IKK beta. *Mol. Biol. Cell* **2001**, *12*, 1479.
- 89. Kwok, B. H. B.; Koh, B.; Ndubuisi, M. I.; Elofsson, M.; Crews, C. M., The antiinflammatory natural product parthenolide from the medicinal herb Feverfew directly binds to and inhibits I kappa B kinase. *Chem. Biol.* **2001**, *8* (8), 759-766.
- 90. Hehner, S. P.; Hofmann, T. G.; Droge, W.; Schmitz, M. L., The antiinflammatory sesquiterpene lactone parthenolide inhibits NF-kappa B by targeting the I kappa B kinase complex. *J. Immunol.* **1999**, *163* (10), 5617-5623.
- 91. Cory, A. H.; Cory, J. G., Augmentation of apoptosis responses in p53-deficient L1210 cells by compounds directed at blocking NFkappaB activation. *Anticancer Res.* **2001**, *21* (6A), 3807-3811.
- 92. Bellarosa, D.; Binaschi, M.; Maggi, C. A.; Goso, C., Sabarubicin- (MEN 10755) and paclitaxel show different kinetics in nuclear factor-KappaB (NF-kB) activation: Effect of parthenolide on their cytotoxicity. *Anticancer Res.* **2005**, *25* (3B), 2119-2128.
- 93. Wen, D. Y.; Nong, Y. H.; Morgan, J. G.; Gangurde, P.; Bielecki, A.; DaSilva, J.; Keaveney, M.; Cheng, H.; Fraser, C.; Schopf, L.; Hepperle, M.; Harriman, G.; Jaffee, B. D.; Ocain, T. D.; Xu, Y. J., A selective small molecule I kappa B kinase beta inhibitor blocks nuclear factor kappa B- mediated inflammatory responses in human fibroblast-like synoviocytes, chondrocytes, and mast cells. *J. Pharmacol. Exp. Ther.* **2006**, *317* (3), 989-1001.
- 94. Pitts, W. J.; Kempson, J., Advances in the Discovery of I kappa B Kinase Inhibitors. *Annu. Rep. Med. Chem.*, Vol 43 **2008**, 43, 155-170.
- 95. Schopf, L.; Savinainen, A.; Anderson, K.; Kujawa, J.; DuPont, M.; Silva, M.; Siebert, E.; Chandra, S.; Morgan, J.; Gangurde, P.; Wen, D. Y.; Lane, J.; Xu, Y. J.; Hepperle, M.; Harriman, G.; Ocain, T.; Jaffee, B., IKK beta inhibition protects against bone and cartilage destruction in a rat model of rheumatoid arthritis. *Arthritis and Rheum.* **2006**, *54* (10), 3163-3173.
- 96. Izmailova, E. S.; Paz, N.; Alencar, H.; Chun, M. Y.; Schopf, L.; Hepperle, M.; Lane, J. H.; Harriman, G.; Xu, Y. J.; Ocain, T.; Weissleder, R.; Mahmood, U.; Healy, A. M.; Jaffee, B., Use of molecular Imaging to quantify response to IKK-2 inhibitor treatment in murine arthritis. *Arthritis and Rheum.* **2007**, *56* (1), 117-128.

- 97. Ginn, J. D. S., Ronald John; Turner, Michael Robert; Young, Erick Richard Roush. Preparation of substituted 3-amino-thieno[2,3-b]pyridine-2-carboxylic acid amide compounds and processes for preparing and their uses. 20071220, 2007.
- 98. Doble, B. W.; Woodgett, J. R., GSK-3: tricks of the trade for a multi-tasking kinase. *J. Cell Sci.* **2003**, *116* (7), 1175-1186.
- 99. Martin, M.; Rehani, K.; Jope, R. S.; Michalek, S. M., Toll-like receptor-mediated cytokine production is differentially regulated by glycogen synthase kinase 3. *Nat. Immunol.* **2005**, *6* (8), 777-784.
- 100. Hoeflich, K. P.; Luo, J.; Rubie, E. A.; Tsao, M. S.; Jin, O.; Woodgett, J. R., Requirement for glycogen synthase kinase-3beta in cell survival and NF-kappaB activation. *Nature* **2000**, *406* (6791), 86-90.
- Li, Q. T.; Van Antwerp, D.; Mercurio, F.; Lee, K. F.; Verma, I. M., Severe liver degeneration in mice lacking the I kappa B kinase 2 gene. Science 1999, 284 (5412), 321-325.
- 102. Beg, A. A.; Sha, W. C.; Bronson, R. T.; Ghosh, S.; Baltimore, D., Embryonic lethality and liver degeneration in mice lacking the RelA component of NF-kappa-B. *Nature* **1995**, *376* (6536), 167-170.
- 103. Schwabe, R. F.; Brenner, D. A., Role of glycogen synthase kinase-3 in TNF-alpha-induced NF-kappaB activation and apoptosis in hepatocytes. *Am. J. Physiol. Gastrointest. Liver Physiol.* **2002**, 283 (1), G204-11.
- 104. Takada, Y.; Fang, X. J.; Jamaluddin, M. S.; Boyd, D. D.; Aggarwal, B. B., Genetic deletion of glycogen synthase kinase-3 beta abrogates activation of I kappa B alpha kinase, JNK, Akt, and p44/p42 MAPK but potentiates apoptosis induced by tumor necrosis factor. *J. Biol. Chem.* **2004**, *279* (38), 39541-39554.
- 105. Sanchez, J. F.; Sniderhan, L. F.; Williamson, A. L.; Fan, S. S.; Chakraborty-Sett, S.; Maggirwar, S. B., Glycogen synthase kinase 3 beta-mediated apoptosis of primary cortical astrocytes involves inhibition of nuclear factor kappa B signaling. *Mol. Cell. Biol.* 2003, 23 (13), 4649-4662.

- 106. Duran, A.; Diaz-Meco, M. T.; Moscat, J., Essential role of RelA Ser311 phosphorylation by zeta PKC in NF-kappa B transcriptional activation. *EMBO J.* **2003**, *22* (15), 3910-3918.
- 107. Zhang, F.; Phiel, C. J.; Spece, L.; Gurvich, N.; Klein, P. S., Inhibitory phosphorylation of glycogen synthase kinase-3 (GSK-3) in response to lithium Evidence for autoregulation of GSK-3. *J. Biol. Chem.* **2003**, *278* (35), 33067-33077.
- 108. Deng, J.; Miller, S. A.; Wang, H. Y.; Xia, W.; Wen, Y.; Zhou, B. P.; Li, Y.; Lin, S. Y.; Hung, M. C., beta-catenin interacts with and inhibits NF-kappa B in human colon and breast cancer. *Cancer Cell* 2002, 2 (4), 323-34.
- 109. Deng, J.; Xia, W. Y.; Miller, S. A.; Wen, Y.; Wang, H. Y.; Hung, M. C., Crossregulation of NF-kappa B by the APC/GSK-3 beta/beta-catenin pathway. *Mol. Carcinog.* **2004**, *39* (3), 139-146.
- 110. Ougolkov, A. V.; Billadeau, D. D., Targeting GSK-3: a promising approach for cancer therapy? *Future oncology (London, England)* **2006**, *2* (1), 91-100.
- 111. Polakis, P., Wnt signaling and cancer. Genes Dev. 2000, 14 (15), 1837-1851.
- 112. Dugo, L.; Collin, M.; Thiemermann, C., Glycogen synthase kinase 3[beta] as a target for the therapy of shock and inflammation *Shock* **2007**, *27* (2), 113-123 10.1097/01.shk.0000238059.23837.68.
- 113. Klein, P. S.; Melton, D. A., A molecular mechanism for the effect of lithium on development. *Proc. Natl. Acad. Sci. U. S. A.* **1996,** 93 (16), 8455-8459.
- 114. Stambolic, V.; Ruel, L.; Woodgett, J. R., Lithium inhibits glycogen synthase kinase-3 activity and mimics Wingless signalling in intact cells. *Curr. Biol.* **1996**, *6* (12), 1664-1668.
- 115. Chalecka-Franaszek, E.; Chuang, D. M., Lithium activates the serine/threonine kinase Akt-1 and suppresses glutamate-induced inhibition of Akt-1 activity in neurons. *Proc. Natl. Acad. Sci. U. S. A.* **1999**, *96* (15), 8745-8750.
- 116. Fink, M. P., What do insulin, estrogen, valproic acid, and TDZD-8 have in common? *Crit.Care Med.* **2005**, 33 (9), 2115-2117.

- 117. De Sarno, P.; Li, X. H.; Jope, R. S., Regulation of Akt and glycogen synthase kinase-3 beta phosphorylation by sodium valproate and lithium. *Neuropharmacology* **2002**, *43* (7), 1158-1164.
- 118. Chen, G.; Huang, L. D.; Jiang, Y. M.; Manji, H. K., The mood-stabilizing agent valproate inhibits the activity of glycogen synthase kinase-3. *J. Neurochem.* **1999,** *72* (3), 1327-1330.
- 119. Van Wauwe, J.; Haefner, B., Glycogen synthase kinase-3 as drug target: From wallflower to center of attention. *Drug News & Perspectives* **2003**, *16* (9), 557-565.
- 120. Meijer, L.; Thunnissen, A. M. W. H.; White, A. W.; Garnier, M.; Nikolic, M.; Tsai, L. H.; Walter, J.; Cleverley, K. E.; Salinas, P. C.; Wu, Y. Z.; Biernat, J.; Mandelkow, E. M.; Kim, S. H.; Pettit, G. R., Inhibition of cyclin-dependent kinases, GSK-3 beta and CK1 by hymenialdisine, a marine sponge constituent. *Chem. Biol.* **2000**, *7* (1), 51-63.
- 121. Coghlan, M. P.; Culbert, A. A.; Cross, D. A. E.; Corcoran, S. L.; Yates, J. W.; Pearce, N. J.; Rausch, O. L.; Murphy, G. J.; Carter, P. S.; Cox, L. R.; Mills, D.; Brown, M. J.; Haigh, D.; Ward, R. W.; Smith, D. G.; Murray, K. J.; Reith, A. D.; Holder, J. C., Selective small molecule inhibitors of glycogen synthase kinase-3 modulate glycogen metabolism and gene transcription. *Chem. Biol.* 2000, 7 (10), 793-803.
- 122. Sharma, V.; Lansdell, T. A.; Jin, G.; Tepe, J. J., Inhibition of Cytokine Production by Hymenialdisine Derivatives. *J. Med. Chem.* **2004**, *47* (14), 3700-3703.
- 123. Hupp, C. D.; Tepe, J. J., Total synthesis of a marine alkaloid from the tunicate Dendrodoa grossularia. *Org. Lett.* **2008,** *10* (17), 3737-3739.
- 124. Hupp, C. D.; Tepe, J. J., 1-Ethyl-3-(3-dimethylaminopropyl)carbodiimide Hydrochloride-Mediated Oxazole Rearrangement: Gaining Access to a Unique Marine Alkaloid Scaffold. *J. Org. Chem.* **2009**, *74* (9), 3406-3413.
- 125. Fiedler, M. A.; Wernke-Dollries, K.; Stark, J. M., Inhibition of TNF-alpha-induced NF-kappaB activation and IL-8 release in A549 cells with the proteasome inhibitor MG-132. *Am. J. Respir. Cell Mol. Biol.* **1998**, *19* (2), 259-68.

- 126. Wan, Y.; Hur, W.; Cho, C. Y.; Liu, Y.; Adrian, F. J.; Lozach, O.; Bach, S.; Mayer, T.; Fabbro, D.; Meijer, L.; Gray, N. S., Synthesis and target identification of hymenialdisine analogs. *Chem. Biol.* **2004,** *11* (2), 247-59.
- 127. Sharma, V.; Tepe, J. J., Potent inhibition of checkpoint kinase activity by a hymenialdisine-derived indoloazepine. *Bioorg. Med. Chem. Lett.* **2004,** *14* (16), 4319-4321.
- 128. Tasdemir, D.; Mallon, R.; Greenstein, M.; Feldberg, L. R.; Kim, S. C.; Collins, K.; Wojciechowicz, D.; Mangalindan, G. C.; Concepcion, G. P.; Harper, M. K.; Ireland, C. M., Aldisine alkaloids from the Philippine sponge Stylissa massa are potent inhibitors of mitogen-activated protein kinase kinase-1 (MEK-1). *J. Med. Chem.* **2002**, *45* (2), 529-32.
- 129. Martinez, V.; Mitjans, M.; Vinardell, M. P., TNF alpha measurement in rat and human whole blood as an in vitro method to assay pyrogens and its inhibition by dexamethasone and erythromycin. *J. Pharm. Sci.* **2004**, *93* (11), 2718-23.